NORTHWEST GEOLOGY

The Journal of The Tobacco Root Geological Society

Volume 46, July 2017

42nd Annual Field Conference

Geology of the Leadore Area and Other Papers

July 27–30, 2017

View south of Yellow Lake in the central Lemhi Range—type locality of the Yellow Lake Formation. Photo by Jeff Lonn.

Published by The Tobacco Root Geological Society, Inc.

P.O. Box 118
Butte, Montana 59703

http://trgs.org

Edited by: Bruce Cox, Phyllis A. Hargrave, and Katie McDonald

The Tobacco Root Geological Society, Inc.

P.O. Box 118
Butte, Montana 59703

Officers, 2017:

President: Jesse Mosolf, Montana Bureau of Mines and Geology, Butte, MT
Vice-President: William M. Phillips, Idaho Geological Survey, Moscow, ID
Treasurer: Katie McDonald, Montana Bureau of Mines and Geology, Butte, MT
Secretary: Emily Geraghty Ward, Rocky Mountain College, Billings, MT
Corresponding Secretary: Lara Strickland, Columbus, MT
Webmasters: Skye Cooley (Missoula, MT) and Petr Yakovlev (Butte, MT)

Board of Directors, 2017:

Ted Antonioli, Geologist, Missoula, MT
Bruce E. Cox, Geologist (semi-retired), Missoula, MT
Larry Johnson, Consultant, Missoula, MT
Larry N. Smith, Dept. of Geological Engineering, Montana Tech, Butte, MT
Mike Stickney, Montana Bureau of Mines and Geology, Butte, MT
Robert C. Thomas, Dept. of Environmental Sciences, U. of Montana-Western, Dillon, MT
Emily Geraghty Ward, Geology Dept., Rocky Mountain College, Billings, MT

2017 Conference Organizers:

Bruce Cox, Geologist, Missoula, Montana

Editors: Bruce Cox, Phyllis A. Hargrave (MBMG), and Katie McDonald (MBMG)

Layout and Editing: Susan Barth (MBMG)

Printed by Insty-Prints, Butte, Montana

ISSN: 0096-7769

http://trgs.org

NORTHWEST GEOLOGY

The Journal of The Tobacco Root Geological Society

Volume 46, July 2017

Geology of the Leadore Area and Other Papers

TABLE OF CONTENTS

TRGS 2017 SCHOLARSHIP AWARD WINNERS

- Andrew Canada (TRGS) University of Idaho
  The Eocene Elko Formation: A Paleogeographic Record of High-Elevation Lake Basin Formation and Topographic Evolution in the North American Cordilleran Hinterland

- Philip Dalhof (Foster) Colorado State University
  Mapping of hydrothermal alterations in the Boulder Batholith and related igneous rocks using a pXRF

- Garrett Hill (Harrison) Montana Tech
  Using fluid inclusions and C, O, H, and Sr isotopes to understand the genesis of dolomite-hosted talc mineralization in Montana

- Erin Lathrop (Harrison) Utah State University
  Capturing changes in the Mesoproterozoic carbon cycle: C-isotope stratigraphy of the 1255 Ma Bass Formation, Grand Canyon Supergroup, AZ

- Zachary Lettenga (Foster) Montana Tech
  Prospecting Placer Gold in Libby Creek

- Jacob McCane (Foster) Colorado State University
  The Petrogenesis of Lamprophyric Rocks of the Absaroka Volcanic Province and their Association with Gold Mineralization

- William Moynihan (TRGS) Idaho State University
  Paleontology and sequence stratigraphy of the near-shore facies of the Permian Phosphoria Formation in the Teton, Gros Ventre, and Wind River ranges, Wyoming

- Ashely Provow (Skipp) Utah State University
  Reconstructing paleofluidrock interactions using electron microprobe dating of authigenic monazite in Neoproterozoic sandstones

- Jacob Thacker (TRGS) University of New Mexico
  Regional tectonic analysis of Laramide orogenesis using field studies, apatite fission track, and (U-Th)/He thermochronology

- Richard Trippe (Harrison) University of Montana
  Geology of a structurally inverted graben of possible Cambrian age, southern Pioneer Mountains, southwestern Montana

- Matthew Wanker (TRGS) Indiana University
  Tracking sediment through a river bifurcation on the Jefferson River, MT

- Mike Zawaski (TRGS) University of Colorado, Boulder
  Stromatolites as chemical and isotopic probes of paleoenvironmental conditions during the Permian-Triassic extinction event

TRGS CHARTER MEMBERS

Stanley W. Anderson
Clyde Cody
William S. Cordua
Lanny H. Fisk
Richard I. Gibson†
Thomas Hanley
Stephen W. Henderson
Thomas E. Hendrix
Mac R. Hooton
Inda Immega
Steven W. Koehler
Marian Millen Lankston†
Robert W. Lankston†
J. David Lazor
Joe J. Liteheiser, Jr.
Judson Mead*
Marvin R. Miller
Vicki M. Miller*
Allen H. Nelson
Alfred H. Pekarek
Patricia Price*
Donald L. Rasmussen
Raymond M. Rene

TRGS LIFETIME MEMBERS

John Childs
Rob Foster
Joan (Mrs. Jack) Harrison*
Karen Keefer
Layaka Mann
Chris Pool

† = co-founder
* = deceased

TRGS HAMMER AWARD RECIPIENTS

Awarded for distinguished achievement in the study of the geology of the Northern Rocky Mountains

1993: Ed Ruppel*
1994: Dick Berg
2003: Don Winston
2004: Dean Kleinkopf*
2009: Betty Skipp
2010: Jim Sears
2011: John Childs
2012: J. Michael O'Neill
2013: Paul Karl Link
2014: Reed Lewis
2015: Jeff Lonn
2016: Bruce Cox

TRGS HONORARY MEMBERS

1980: Charles J. Vitaliano*
2008: Elizabeth Younggren
(also honorary Board member)
2010: Dick Berg
2010: Bruce Cox
2010: Dean Kleinkopf*
2010: Dave Lageson
2011: Marie Marshall Garsjo
2011: Paul Link
2011: Rob Thomas
2012: Jeff Lonn
2012: Mitch Reynolds
2013: Reed Lewis
2015: Don Winston

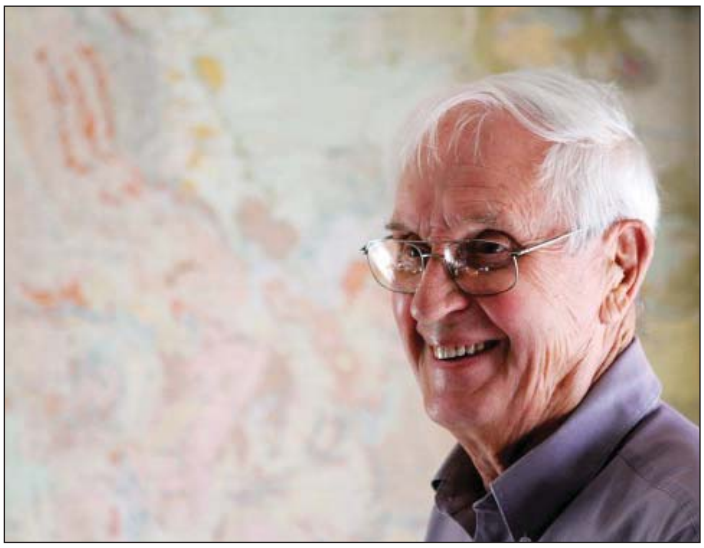

EDWARD T. RUPPEL (1925–2014)

The Tobacco Root Mountains were the backdrop for many years of Ed Ruppel's life–first his birth, childhood, and youth in Twin Bridges, Montana, and then full-circle to his retirement years. During the intervening period, Leadore, Idaho became a second special place for Ed and his family as he worked many years in the Lemhi Range. Ed was a faithful Tobacco Root Geological Society member and received the TRGS's first award for Excellence in Field Work. He authored more than 50 significant geologic maps and geologic research publications in western Montana and eastern Idaho. Colleagues admired Ed for many decades as a quintessential field geologist. It is most appropriate that we dedicate this volume to Ed!

Ed left Twin Bridges after high school to serve in the U.S. Navy, and then obtained degrees from University of Montana, University of Wyoming, and a Ph.D. from Yale University. His subsequent 30-year career with the U.S. Geological Survey produced numerous classic publications on the geology of western Montana, eastern Idaho, and Yellowstone National Park. He served as Chief of the USGS Central Environmental Geology Branch, supervising 70 earth scientists in the 13-state Central Region of the Rocky Mountains and High Plains.

After his retirement from the USGS, Ed became the Director of the Montana Bureau of Mines and Geology (MBMG), and Montana State Geologist in 1986. In addition to his administrative demands, he continued his dedicated geologic research in Montana, publishing papers and maps on many diverse geologic topics from the gold mines of the Virginia City district to Cenozoic valley formation in southwestern Montana. Even after his retirement from the MBMG in 1994, Ed continued many years of field research in the high country of southwestern Montana; on occasion he conducted it by horseback. Some of this retirement field work resulted in his popular guide "Along the Great Divide: The rocks and their history along the Continental Divide Trail between Montana and Idaho." In his final months, he produced a revised map of the Montana part of the Leadore quadrangle. He and two co-authors had nearly completed a USGS Professional Paper that he was still working on near the time of his death.

Ed's professional life was devoted to the geology of western Montana and eastern Idaho. The Tobacco Root Mountains near Twin Bridges were the bookends of his life, and the Lemhi Range near Leadore was a major chapter.

DEDICATIONS

VICTORIA E. MITCHELL (1954–2017)

Victoria E. Mitchell passed away in April after over 30 years' service with the Idaho Bureau of Mines and the Idaho Geological Survey. She assisted with the 250,000-scale geologic map compilation project in the late 1970s and later established the IGS Mines and Prospects Database, which contains information on over 8,000 Idaho mines and prospects. Vicki wrote histories for 57 Idaho mines and co-authored numerous site inspection reports for abandoned and inactive mines. These reports give mine production data and concise descriptions of mineral deposit geology compiled from previous investigators. The reports are available as Staff Reports in the Idaho Geological Survey website. Two of Vicki's reports are of particular interest to this years' TRGS field conference: "History of Mines in the Texas Mining District near Gilmore, Idaho, 1997" and "History of the Leadville, Kimmel and Baby Joe Mines, Lemhi County, Idaho, 2004." Vicki received an Esto Perpetua award from the Idaho State Historical Society in 2006 for her work on Idaho's mining history. Esto Pertpetua is the highest award given for historical research in Idaho. In addition to her professional career, Vicki enjoyed, and successfully wrote, science fiction novels and short stories and participated in science fiction conventions. According to her obituary, she died peacefully at home surrounded by her dogs.

PAPERS

DEVELOPMENT OF GEOLOGIC THOUGHT ON THE LEMHI AND BEAVERHEAD RANGES

Paul K. Link[1] and Bruce Cox[2]

[1]Department of Geosciences, Idaho State University, Pocatello, ID 83209, linkpaul@isu.edu
[2]Geologist/Consultant, Missoula, Montana, bcox737@gmail.com

INTRODUCTION

The Beaverhead Range has been historically important for over 200 years, since the first Euro-American exploration of the area. In 1806, Lewis and Clark used Lemhi Pass to get over the Beaverhead Range. In the early 20th century, discovery of silver–lead deposits at Gilmore and Leadore motivated the construction of the Gilmore and Pittsburgh railroad, the last constructed and first dismantled of railroads in the northern Rockies.

Several important geologic relations exist in the Beaverhead and Lemhi Ranges, and these have been documented by important figures in the history of Idaho and Montana Geology. In the past 40 years, most of these geologists have been active in the Tobacco Root Geological Society.

PALEOZOIC STRATIGRAPHY

Larry Sloss (1953) observed that lower Paleozoic strata thinned from southwest Montana into Idaho over what he called the Lemhi Arch. This observation grew into the recognition of North American cratonic sequences, which are the framework for regional stratigraphic studies (Sloss, 1988). C. Ross (1962) and colleagues established the Paleozoic stratigraphy of east-central Idaho.

Rob Scholten and colleagues (Scholten, 1957a, 1957b; Scholten and Ramspott, 1968) documented the Lemhi Arch as manifested by the Skull Canyon disturbance and developed the concept of a thrust belt in southwest Montana. In the Lemhi Arch, Mesoproterozoic Belt Supergroup country rock is intruded by alkalic plutons of the Neoproterozoic and Cambrian Big Creek–Beaverhead Belt (Evans and Zartman, 1988, 1990; Lund and others, 2010). Locally, the latest Neoproterozoic Wilbert Formation crops out above the Belt Supergroup (Skipp and Link, 1992), but in most places on the arch the Middle Ordovician Kinnikinic Quartzite unconformably lies on Belt Supergroup strata.

Charlie Sandberg and colleagues (Poole and Sandberg, 1991) studied Mississippian carbonate bank facies in southwest Montana and adjacent Idaho. They used conodonts to establish a framework for both early Mississippian and late Mississippian carbonate banks that can be recognized from the craton on the east across thrust sheets to the Copper Basin Antler flysch trough in the Pioneer Mountains on the west (Skipp and others, 1979; Beranek and others, 2016).

Decades of mapping by Glenn Embree and colleagues (Embree and others, 1975, 1983; Price and others, 1999) has contributed a wealth of stratigraphic data for the southern Beaverhead Mountains.

DETRITAL ZIRCON STUDIES

Deciphering the age and provenance of sandstones of the Beaverhead and Lemhi Ranges was frustrating before the advent of geochronological techniques based around isotopic analysis of individual grains of the mineral zircon (Gehrels and others, 2008). The use of analyses of detrital zircons from these sandstones began with G. Ross and others (1992) and today is essential to understanding the rocks (Link and others, 2007, 2016; Lewis and others, 2010).

Detrital zircon studies have allowed us to answer questions that previously we could not even ask about the age and derivation of quartzose sandstones. Detrital zircon studies allow us to determine the maximum possible age for a sandstone, and for tuffaceous rocks, allow us to estimate a depositional age. Further, the comparison of detrital zircon age-populations allows us to make inferences about source areas and continuity of depositional basins. Geslin and others (1999) used the presence of 480 Ma detrital zircons to fingerprint input of sands from Birch Creek, draining plutons of the southern Beaverhead Mountains.

BELT SUPERGROUP

Based on sedimentary facies, Don Winston and colleagues (Winston and Link, 1993; Winston and others, 1999) proposed that east-central Idaho Lemhi

Group quartzites were indeed part of the Belt Supergroup, rather than from a separate depositional basin. Work by Tydsal (2003) confirmed this conclusion. Continuing on this premise, and using detrital zircon data, Burmester and others (2016) defined new stratigraphic units of upper Belt Supergroup strata exposed in the Beaverhead Range. The geologic map of Lewis and others (2016) uses this stratigraphic framework.

Detrital zircons from many of these rocks contain the same provenance, with a 1,740 to 1,720 Ma age peak (Link and others, 2016). This provenance is attributed to the Big White arc, a huge magmatic arc to the south.

BEAVERHEAD IMPACT

Shattercones found in Belt Supergroup strata in a wide area of the southeastern Beaverhead Mountains indicate that a large meteorite impact, the Beaverhead Impact, occurred at or after 900 Ma (Hargraves and others, 1990; Kellogg and others, 2003).

CORDILLERAN THRUST BELT

Betty Skipp (1987, 1988) also mapped in the southern Beaverheads and defined the Cabin thrust as a major compressional structure that includes bits of crystalline basement along its leading edge. On the west side of the Beaverhead Range, the Hawley Creek thrust has been proposed to be part of the Cabin system.

The steep northern Beaverhead Range and much of the Lemhi Range were mapped by Ed Ruppel (1968), who established that Belt Supergroup underlies much of the area (Ruppel, 1975). Ruppel and Lopez (1988) summarized the geology of the Lemhi Range and the mineral deposits of the Gilmore area, related to the Eocene Challis magmatic episode (M'Gonigle and Dalrymple, 1996) and host rock Paleozoic carbonates.

EXTENSIONAL DEFORMATION

Susanne Janecke and students (Janecke, 1992; Janecke and others, 1998, 2003) mapped in the Salmon basin and Horse Prairie areas and described the Salmon Basin detachment, an Eocene to Miocene, pre-Basin and Range detachment system, which preceded the late Miocene to Recent high-angle Basin and Range normal faults (Bennett, 1988) of the area.

SNAKE RIVER PLAIN-YELLOWSTONE PROVINCE

In the last 17 m.y., rhyolite magmatism of the Snake River Plain province has migrated northeastward across southern Idaho concomitant with Basin and Range normal faulting (Pierce and Morgan, 1992). Some of the rhyolite ignimbrites reach into the Birch Creek and Lemhi Valleys.

GEOLOGIC MAPS

Early geologic maps of the Lemhi and Beaverhead area include Umpleby (1913) and Anderson (1956, 1961). The U.S. Geological Survey produced a geologic map of the northern Lemhi and Beaverhead Ranges (Evans and Green, 2003) that serves as a starting point for ongoing studies (Lewis and others, 2016).

MINERAL DEPOSITS

From 1880 to the late 20th century, metallic mineral deposits were discovered and developed in Lemhi County and Cassia County, especially along the rangefront foothills adjacent to the Lemhi and Birch Creek Valleys. Chemically and texturally receptive host rocks and long-lived structural features provided favorable sites for deposition of economic concentrations of silver, base metals, and gold. Permian phosphate deposits and thorium/rare earth deposits of Lemhi County have received intense exploration scrutiny in the past 50 years.

With few exceptions, mining and mineral exploration have been dormant in southern Lemhi County for several decades. However, the volume of historic and geologic literature on the subject is considerable. Several previous authors supplemented their field investigation reports with data supplied by the mine operators, most notably Umpleby (1913), Ruppel and Lopez (1988), and Mitchell (2004). Similar effort has been made to document industrial minerals occurrences and exploration (Scholten, 1957a; Gillerman and others, 2003). There is probably an equal or greater volume of unpublished mineral exploration and mine production data for these Lemhi County and Clark County mining districts. In aggregate, the data can build 4-dimensional pictures of ore controls for the deposits that have been historically exploited and help construct models for deposits yet to be discovered.

Several advancements in exploration theory and technology have occurred since area mines were in their heyday. Foremost is development of the porphyry copper ore deposit model. Porphyry copper deposits commonly exhibit predictable alteration assemblages, metal zoning, structural control, and mid-Tertiary (Eocene) age. These features are evident along the eastern margin of the Lemhi Range and provide rationale for continued exploration. The western margins of the Beaverhead Range display similar but more subtle intrusive porphyry features.

REFERENCES CITED

Anderson, A.L., 1956, Geology and mineral resources of the Salmon quadrangle, Lemhi County, Idaho: Idaho Bureau of Mines and Geology Pamphlet 106, 102 p.

Anderson, A.L., 1961, Geology and mineral resources of the Lemhi quadrangle, Lemhi County, Idaho: Idaho Bureau of Mines and Geology Pamphlet 124, 111 p.

Bennett, E.H., 1986, Relationship of the Trans-Challis fault system in central Idaho to Eocene and Basin-and-Range extensions: Geology, v. 14, p. 481–484.

Beranek, L.P., Link, P.K., and Fanning, C.M., 2016, Detrital zircon record of mid-Paleozoic convergent margin activity in the northern U.S. Rocky Mountains: Implications for the Antler orogeny and early evolution of the North American Cordillera: Lithosphere: doi: 10.1130/L557.

Burmester, R.F., Lonn, J.D., Lewis, R.S., and McFaddan, M.D., 2016, Stratigraphy of the Lemhi subbasin of the Belt Supergroup, *in* MacLean, J.S., and Sears, J.W., Belt Basin: Window to Mesoproterozoic Earth: Geological Society of America Special Paper, v. 522, p. 121–137.

Embree, G.F., Hoggan, R.D., Williams, E.J., and Skipp, Betty, 1975, Stratigraphy of southern Beaverhead Range, Clark and Lemhi Counties, Idaho: Geological Society of America Abstracts with Programs, v. 7, no. 5, p. 607.

Embree, G.F., Hoggan, R.D., and Williams, E.J., 1983, Preliminary reconnaissance geologic map of the Copper Mountain quadrangle, Lemhi County, Idaho: U.S. Geological Survey Open-File Report 83-599, 1:24,000.

Evans, K.V., and Green, G.G., compilers, 2003, Geologic map of the Salmon National Forest and vicinity, east-central Idaho: U.S. Geological Survey Geologic Investigations Series Map I-2765, 2 sheets, scale 1:100,000.

Evans, K.V., and Zartman, R.E., 1988, Early Paleozoic alkalic plutonism in east-central Idaho: Geological Society of America Bulletin 100, p. 1981–1987.

Evans, K.V., and Zartman, R.E., 1990, U-Th-Pb and Rb-Sr geochronology of Middle Proterozoic granite and augen gneiss, Salmon River Mountains, east-central Idaho: Geological Society of America Bulletin, v. 102, p. 63–73.

Gehrels, G.E., Valencia, V.A., and Ruiz, J., 2008, Enhanced precision, accuracy, efficiency, and spatial resolution of U-Pb ages by laser ablation-multicollector-inductively coupled plasma-mass spectrometry: Geochemistry, Geophysics, Geosystems, v. 9, no. 3, Z03017, doi: 10.1029/2007GC001805

Geslin, J.K., Link, P.K., and Fanning, C.M., 1999, High-precision provenance determination using detrital-zircon ages and petrography of Quaternary sands on the eastern Snake River Plain, Idaho: Geology, v. 27, p. 295–298.

Gillerman, V.S., Lund, K., and Evans, K.V., 2003, Stratigraphy, structure, and mineral deposits of the Lemhi Pass area, central Beaverhead Mountains, eastern Idaho: Northwest Geology, v. 32, p. 134–146.

Hargraves, R.B., Cullicott, C.E., Deffeyes, K.S., Hougen, S.B., Christiansen, P.P., and Fiske, P.S., 1990, Shatter cones and shocked rocks in southwestern Montana: The Beaverhead impact structure: Geology, v. 18, p. 832–834.

Janecke, S.U., 1992, Kinematics and timing of three superposed extensional systems, east central Idaho: Evidence for an Eocene tectonic transition: Tectonics, v. 11, p. 1121–1138.

Janecke, S.U., and Blankenau, J.J., 2003, Extensional folds associated with Paleogene detachment faults in SE part of the Salmon Basin: Northwest Geology, v. 32, p. 51–73.

Janecke, S.U., Vandenburg, C.J., and Blankenau, J.J., 1998, Geometry, mechanisms and significance of extensional folds from examples in the Rocky

Mountain Basin-and-Range province, U.S.A., Journal of Structural Geology, v. 20, no. 7, p. 841–856.

Kellogg, K.S., Snee, L.W., and Unruh, D.M., 2003, The Mesoproterozoic Beaverhead impact structure and its tectonic setting: $^{40}Ar/^{39}Ar$ and U/Pb isotopic constraints: Journal of Geology, v. 222, p. 639–652.

Lewis, R.S., Vervoort, J.D., Burmester, R.F., and Oswald, P.J., 2010, Detrital zircon analysis of Mesoproterozoic and Neoproterozoic metasedimentary rocks of northcentral Idaho: Implications for development of the Belt-Purcell Basin: Canadian Journal of Earth Sciences, v. 47, no. 11, p. 1383–1404, doi:10.1139/E10-049.

Lewis, R.S., Othberg, K.L., Stanford, L.R., and McFadden, M.D., 2016, Geologic map of the western part of the Salmon 30' x 60' quadrangle, Idaho and Montana: Idaho Geological Survey Geologic Map GM-52, scale 1:75,000.

Link, P.K., Fanning, C.M., Lund, K.I., and Aleinikoff, J.N., 2007, Detrital zircons, correlation and provenance of Mesoproterozoic Belt Supergroup and correlative strata of east-central Idaho and southwest Montana, *in* Link, P.K., and Lewis, R.S., eds., SEPM Special Publication 86, Proterozoic geology of western North America and Siberia, p. 101–128.

Link, P.K., Stewart, E.D., Steel, T., Sherwin, J.-A., Hess, L.T., and McDonald, C., 2016, Detrital zircons in the Mesoproterozoic upper Belt Supergroup in the Pioneer, Beaverhead and Lemhi Ranges, Montana and Idaho: The Big White arc, *in* MacLean, J.S, and Sears, J.W., eds., Belt Basin: Window to Mesoproterozoic Earth: Geological Society of America Special Paper 522, p. 163–183, doi:10.1130/2016.2522(03)

Lund, K., Aleinikoff, J.N., Evans, K.V., duBray, E.A., Dewitt, E.H., and Unruh, D.M., 2010, SHRIMP U-Pb dating of recurrent Cryogenian and Late Cambrian-Early Ordovician alkalic magmatism in central Idaho: Implications for Rodinian rift tectonics: Geological Society of America Bulletin, v. 122, no. 3/4, p. 430–453.

Mitchell, V.E., 2004, History of the Leadville, Kimmel, and Baby Joe mines, Lemhi County, Idaho: Idaho Geological Survey Staff Report 04-1, 35 p.

M'Gonigle, J.W., and Dalrymple, G.B., 1996, $^{40}Ar/^{39}Ar$ ages of Challis volcanic rocks and the initiation of Tertiary sedimentary basins in southwestern Montana: U.S. Geological Survey Bulletin 2132, 17 p.

Pierce, K.L., and Morgan, L.A., 1992, The track of the Yellowstone hot spot: Volcanism, faulting, and uplift, *in* Link, P.K., Kuntz, M.A., and Platt, L.B., eds., Regional geology of eastern Idaho and western Wyoming: Geological Society of America Memoir 179, p. 1–53.

Poole, F.G., and Sandberg, C.A., 1991, Mississippian paleogeography and conodont biostratigraphy of the Western United States, *in* Cooper, J.D., and Stevens, C.H., eds., Paleozoic Paleogeography of the Western United States-II: Pacific Section Society of Economic Paleontologists and Mineralogists, Book 67, v. 1, p. 107–136.

Price, K.B., Embree, G., Hoggan, R., and Hansen, S., 1999, Field guide along the northern edge of the eastern Snake River Plain, and the Lemhi and Beaverhead Mountain Ranges bordering Birch Creek Valley, Idaho, *in* Hughes, S.S., and Thackray, G.D., eds., Guidebook to the geology of eastern Idaho: Idaho Museum of Natural History, p. 335–342.

Ross, C.P., 1962, Stratified rocks in south-central Idaho: Idaho Bureau of Mines and Geology Pamphlet 125, 126 p.

Ross, G.M., Parrish, R.R., and Winston, D., 1992, Provenance and U-Pb geochronology of the Mesoproterozoic Belt Supergroup (northwestern United States): Implications for age of deposition and pre-Panthalassa plate reconstructions: Earth and Planetary Science Letters, v. 113, p. 57–76.

Ruppel, E.T., 1968, Geologic map of the Leadore quadrangle, Lemhi County, Idaho: U.S. Geological Survey Geological Quadrangle Map GQ-733, scale 1:62,500.

Ruppel, E.T., 1975, Precambrian Y sedimentary rocks in east-central Idaho: U.S. Geological Survey Professional Paper 889-A, 23 p.

Ruppel, E.T., and Lopez, D.A., 1988, Regional geology and mineral deposits in and near the central part of the Lemhi Range, Lemhi County, Idaho: U.S. Geological Survey Professional Paper 1480, 122 p.

Scholten, R., 1957a, Paleozoic evolution of the geosynclinal margin north of the Snake River Plain, Idaho–Montana: Geological Society of America Bulletin, v. 68, p. 151–170.

Scholten, R., 1957b, Preliminary interpretation of Permo-Carboniferous stratigraphy in east-central Idaho–Montana: Geological Society of America Bulletin v. 68, no. 12, p. 1794.

Scholten, R., and Ramspott, L.D., 1968, Tectonic mechanisms indicated by structural framework of central Beaverhead Range, Idaho–Montana: Geological Society of America Special Paper 104, 71 p., map scale 1:62,500.

Skipp, Betty, 1987, Basement thrust sheets in the Clearwater orogenic zone, central Idaho and western Montana: Geology, v. 15, p. 220–224.

Skipp, Betty, 1988, Cordilleran thrust belt and faulted foreland in the Beaverhead Mountains, Idaho and Montana, *in* Schmidt, C.J., and Perry, W.R, Jr., eds., Interaction of the Rocky Mountain foreland and Cordilleran thrust belt: Geological Society of America Memoir 171, p. 237–266, scale 1:250,000.

Skipp, Betty, and Link, P.K., 1992, Middle and Late Proterozoic rocks and Later Proterozoic tectonics in the southern Beaverhead Mountains, Idaho and Montana: A preliminary report, *in* Link, P.K., Kuntz, M.A., and Platt, L.B., eds., Regional Geology of Eastern Idaho and Western Wyoming: Geological Society of America Memoir 179, p.141–154.

Skipp, Betty, Sando, W.J., and Hall, W.E., 1979, The Mississippian and Pennsylvanian (Carboniferous) systems in the United States-Idaho: U.S. Geological Survey Professional Paper 1110-AA, p. AA1–AA42.

Sloss, L.L., 1963, Sequences in the Cratonic Interior of North America: Geological Society of America Bulletin, v. 74, p. 93–114.

Sloss, L.L., 1988, Tectonic evolution of the craton in Phanerozoic time, *in* Sloss, L.L., ed., Sedimentary Cover–North American Craton, U.S.: Boulder, Colorado, Geological Society of America, The Geology of North America, v. D-2, p. 25–51.

Tysdal, R.G., 2003, Correlation, sedimentology, and structural setting, upper strata of Mesoproterozoic Apple Creek Formation and lower strata of Gunsight Formation, Lemhi Range to Salmon River Mountains, east-central Idaho: U.S. Geological Survey Professional Paper 1668-A, p. 1–22.

Umpleby, J.B., 1913, Geology and ore deposits of Lemhi County, Idaho: U.S. Geological Survey Bulletin 528, 182 p.

Winston, Don, and Link, P.K., 1993, Middle Proterozoic rocks of Montana, Idaho and Eastern Washington: The Belt Supergroup, *in* Reed, J.C., Jr., Bickford, M.E., Houston, R.S., Link, P.K., Rankin, D.W., Sims, P.K., and Van Schmus, W.R., eds., Precambrian: Conterminous U.S.: Boulder, Colorado, Geological Society of America, The Geology of North America, v. C-2, p. 487–517.

Winston, Don, Link, P.K., and Hathaway, Nate, 1999, The Yellowjacket is not the Prichard and other heresies: Belt Supergroup Correlations, Structure and Paleogeography, east-central Idaho, *in* Hughes, S.S., and Thackray, G.D., eds., Guidebook to the Geology of Eastern Idaho: Pocatello, Idaho Museum of Natural History, p. 3–20.

WERE WE WRONG? SECOND THOUGHTS ON GEOLOGY OF THE LEMHI SUBBASIN

Russell F. Burmester,[1,3] Reed S. Lewis,[1] and Jeffrey D. Lonn[2]

[1]Idaho Geological Survey, University of Idaho, Moscow, Idaho 83844-3014

[2]Montana Bureau of Mines and Geology, Montana Tech, Butte, Montana 59701, jlonn@mtech.edu

[3]Geology, Western Washington University, Bellingham, Washington 98225-9080, russb@wwu.edu

ABSTRACT

Work on the stratigraphy and structure of the Lemhi subbasin continues to yield surprises. This is partly because the units are incredibly thick, vary laterally, are faulted, and have non-unique characteristics. Even the Swauger Formation, which we had proposed 2 years ago was a regional marker, seems to vary across the basin, although it is still (so far) the closest to a unique unit in the basin. Where Swauger is not exposed, determining whether a section is Lemhi Group below the Swauger or Lawson Creek–Apple Creek Formations above is difficult. Compounded by lack of time (is money), our inability to map the whole basin in a short spell spawned a scenario reminiscent of the blind men and elephant parable. When we mapped beyond the Salmon 30' x 60' quadrangle, we saw different parts of the Lemhi subbasin elephant than we had before. This led to doubts about some parts of the Salmon map and a pressing need to look both farther and in more detail outside that quadrangle.

INTRODUCTION

TRGS organizers (aka Bruce Cox) suggested that we summarize the state of research into Mesoproterozoic quartzites of Idaho and Montana, and discuss in particular (1) the stratigraphic problems, (2) what is known (or suspected) regarding the structural control of the Lemhi subbasin, (3) what field observations and field methods most directly address the problems, and (4) what questions remain. The brief answer to #1 is that some units appear to vary laterally within the mountain ranges in which they are exposed, the many faults within ranges make assembling complete sections challenging, and several units appear to share lithologic and sedimentary structure (sediment type) characteristics. These complications make correlation between ranges difficult to support. For instance, see Lonn (this volume) for new ideas about the Lemhi Group type sections. Variation in appearance due to different metamorphism and deformation across the exposures clouds recognition of sedimentary characteristics that might be useful for recognition. For #2, we have no new data or thoughts to revise the current consensus that the Lemhi subbasin got a much later start and then subsided much more rapidly than the main Belt basin. The most recent speculation of how the Lemhi subbasin is related to the main Belt basin is Lonn and others (2016a). For #3, mapping and sampling in more detail probably is the only way to go, unless Don Winston could measure a few more sections. For this, we would need to find the fountain of youth, or some youths willing to better their elders. For #4, the main question is where to get the money to support more intensive field work as well as petrography, geochemistry, and detrital zircon (DZ) analyses. More on some of these below, along with comments on our recently released map of the western part of the Salmon 30' x 60' quadrangle (Burmester and others, 2016a).

Previous Truths

Money for our work in the Salmon area over the past decade came mostly from the USGS Statemap program, the Idaho Geological Survey, and the Montana Bureau of Mines and Geology. Statemap is focused on producing quadrangle maps, so we started with the stratigraphy that had been developed in the Lemhi Range. The stratigraphy accepted into the 21st century, built on regional and detailed mapping mostly in the Lemhi Range by earlier geologists (e.g., Anderson, Staatz, Ruppel, Tysdal, Evans, and Lund), consisted of Lemhi Group topped by the Swauger Formation and, in turn, a very thin Lawson Creek Formation. We started applying that stratigraphy to the Beaverhead Mountains as others had done (Evans and Green, 2003). What got the ball rolling for us to revise that stratigraphy (Burmester and others, 2013, 2016b) was recognition that east of the Beaverhead Divide, a thick section of feldspathic quartzite (meta-arkose if you prefer) was stratigraphically above a thick section of anomalously feldspar-poor and coarse-grained

strata, which we correlated with the Swauger Formation. Between them are thinner and finer strata correlative of the Lawson Creek. The next step was that we disentangled the Apple Creek Formation from broadly similar strata farther south in the Lemhi Range that Ruppel (1975) had correlated with it. This rejuvenated the real Apple Creek to be younger than the Lawson Creek. This led to identification of the feldspathic quartzite east of the Beaverhead Divide as Apple Creek. Although there are variations within this unit that could be used to subdivide it into multiple members, its poor exposure and our lack of time led to it being simply the Jahnke Lake member of the Apple Creek Formation (fig 1a). Missing from it are finer

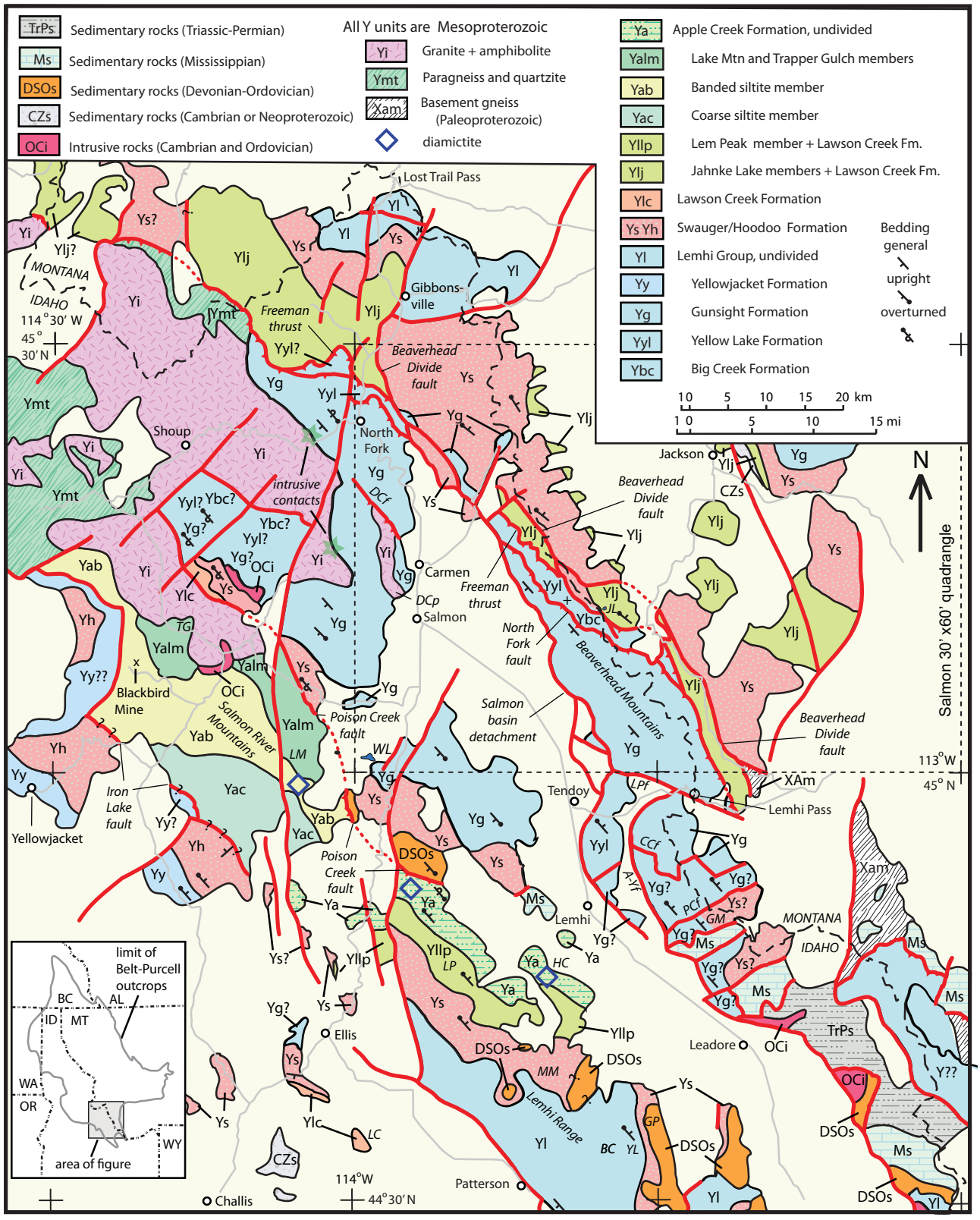

Figure 1. (a) Full caption on opposite page.

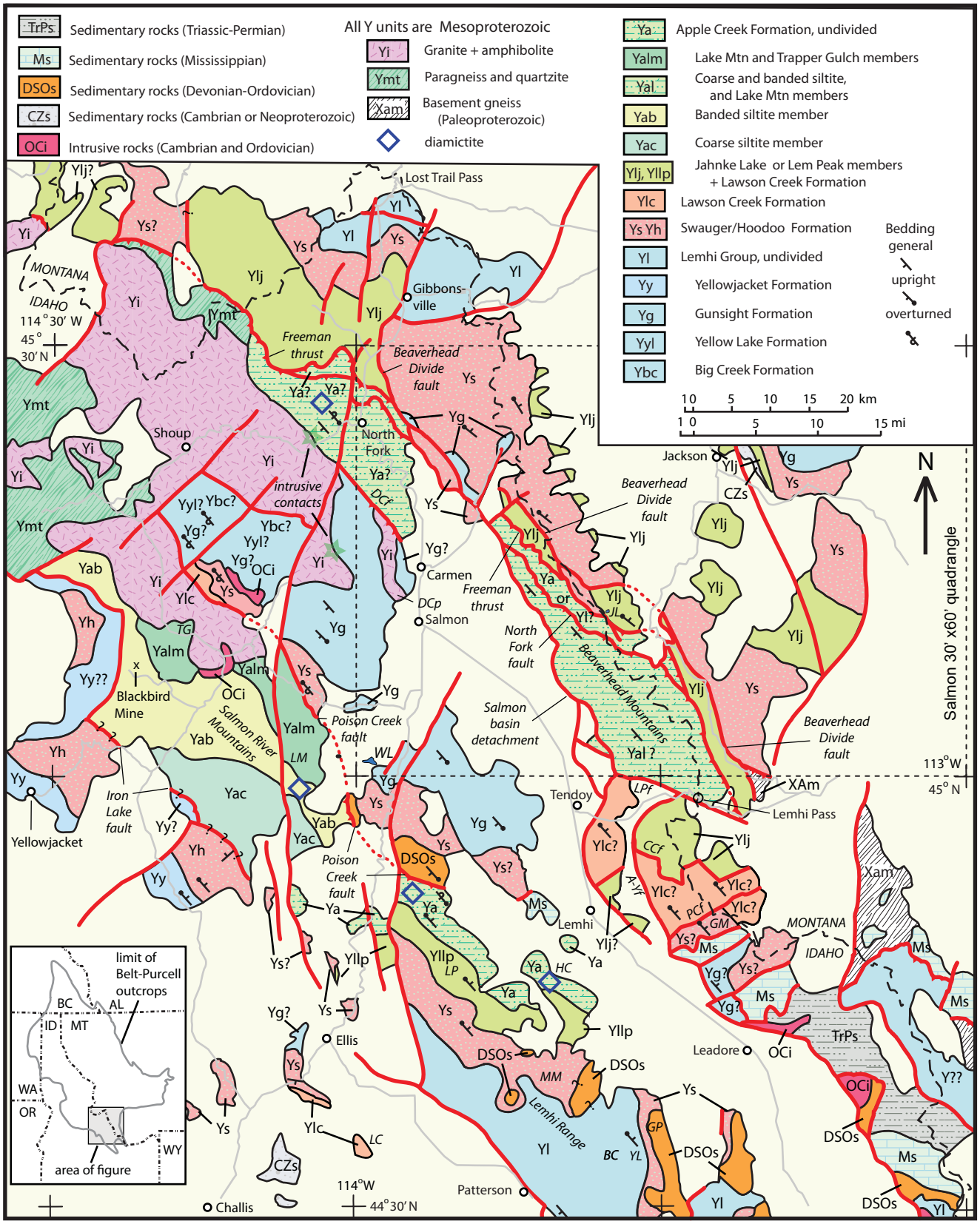

Figure 1. Regional geology around Salmon, Idaho. (a) Consensus as of 2015. (b) Alternative interpretation as of 2017. Some Apple Creek Formation member labels on map omit "a" to save space. For type or reference sections, units are in parentheses after location letter codes: A-Yf—Agency-Yearian fault; BC—Big Creek (Ybc); CCf—Cow Creek fault; DC—Diamond Creek fault; DC—Diamond Creek pluton; GM—Goat Mountain; GP—Gunsight Peak (Yg); HC—Hayden Creek (Ya); JL—Jahnke Lake (Yajl); LC—Lawson Creek (Ylc); LM—Lake Mountain (Yalm); LP—Lem Peak (Yalp); MM—Mogg Mountain (Ys); PCf—Peterson Creek fault; TG—Trapper Gulch (Yatg); YL—Yellow Lake (Yyl). Stars mark known intrusive contacts of Mesoproterozoic granite with Gunsight and possible Apple Creek Formation strata. Diamonds approximate diamictite locations that we have visited.

grained and thinner bedded units of the Apple Creek type section. These are the fine siltite, diamictite, coarse siltite, and banded siltite members (Tysdal, 2000). The fine siltite and diamictite members don't continue very far northwest across the Salmon River into the Salmon River Mountains, but the coarse siltite is very thick there, and curiously, diamictite appears in the banded siltite in several places. Above the banded siltite are two other units, the quartzitic Lake Mountain member and the finer Trapper Gulch member (fig. 2).

While we were learning the stratigraphy above the Swauger, we continued to think in terms of Lemhi Group stratigraphy for correlation of map units west of the Beaverhead Divide. Thus we extended the Gunsight Formation from the Salmon River Mountains across the Salmon River and into the Beaverhead Mountains despite a change in lithology from type Gunsight in the Lemhi Range, and crossing the Diamond Creek fault (fig. 1a). This led to the concept that the Beaverhead Divide fault system was within a complete, although folded and faulted, section of Lemhi subbasin strata from the Lemhi Group through the Apple Creek Formation (Lonn and others, 2013a, 2016b).

Alternative Facts

Thoughts of changing our story from our 2016 map grew when we resumed mapping outside of the Salmon 30' x 60' quadrangle and two major revelations that came from looking outside that box. First was recognition of a very thick mixed unit of cracked and uncracked, even and lenticular siltite and argillite couplets and quartzite south of the Lemhi Pass

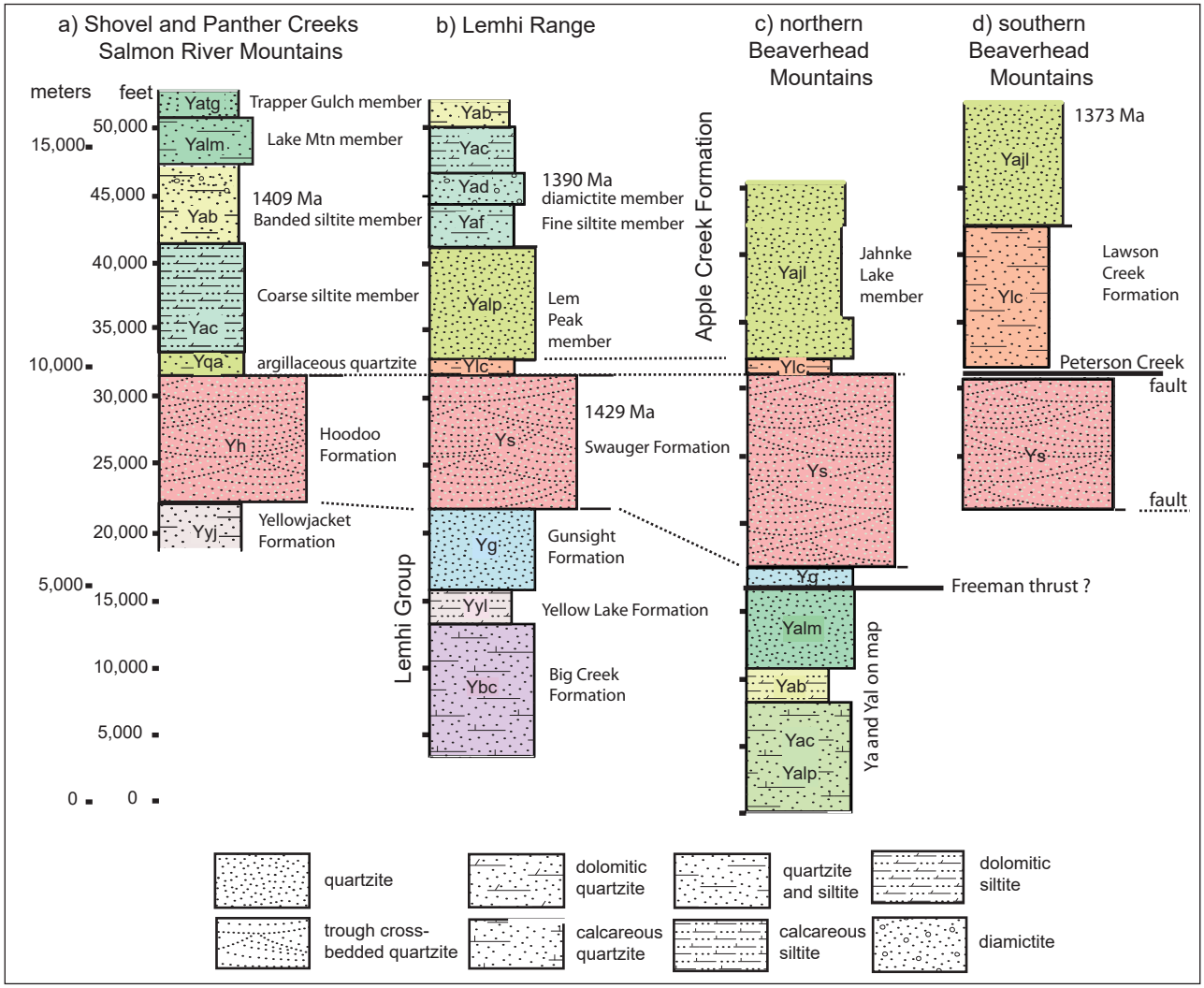

Figure 2. Stratigraphic columns for (a) Salmon River Mountains, (b) Lemhi Range, (c) Beaverhead Mountains north, and (d) south of the Lemhi Pass fault. For (a), backsliding on the Iron Lake fault is assumed to make net stratigraphic throw negligible. Both (a) and (b) are south of the Poison Creek fault (fig. 1), so lack of lateral continuity of the Lem Peak, fine siltite, and diamictite members of the Apple Creek Formation and the Gunsight Formation may reflect locally restricted environments of deposition. Mean ages of youngest grains are for banded siltite (Yab) from Aleinikoff and others (2012), for diamictite (Yad) and Swauger (Ys) from Link and others (2016), and for Jahnke Lake (Yajl) from Gillerman (2008).

fault in the Agency Creek and Lemhi Pass quadrangles. Most quartzite is fine-grained and feldspathic. However, spherical medium quartz grains form lags with mud chips (fig. 3), small channels, and rare thicker beds. Chert is rare but present in several localities. Elsewhere chert is diagnostic of McNamara–Lawson Creek strata, and spherical medium quartz grains are much more common in the Swauger and higher strata than below, making correlation of this unit with the Lawson Creek Formation attractive. One caution is this unit's great thickness (fig. 2, column d), which is a bit worrisome. A thick alternative, the coarse siltite member of the Apple Creek Formation in the Salmon River Mountains, could have the anomalously large quartz grains here if they were sourced from the east, and chert because it is above the Lawson Creek. South of that unit is a crossbedded quartzite unit with spherical, medium to coarse quartz grains (fig. 4) and more potassium feldspar than plagioclase, consistent with it being Swauger Formation (Burmester and others, 2015). If those correlations are correct, the Peterson Creek fault between those units (PCf, fig 1a) would have minor throw down to the north.

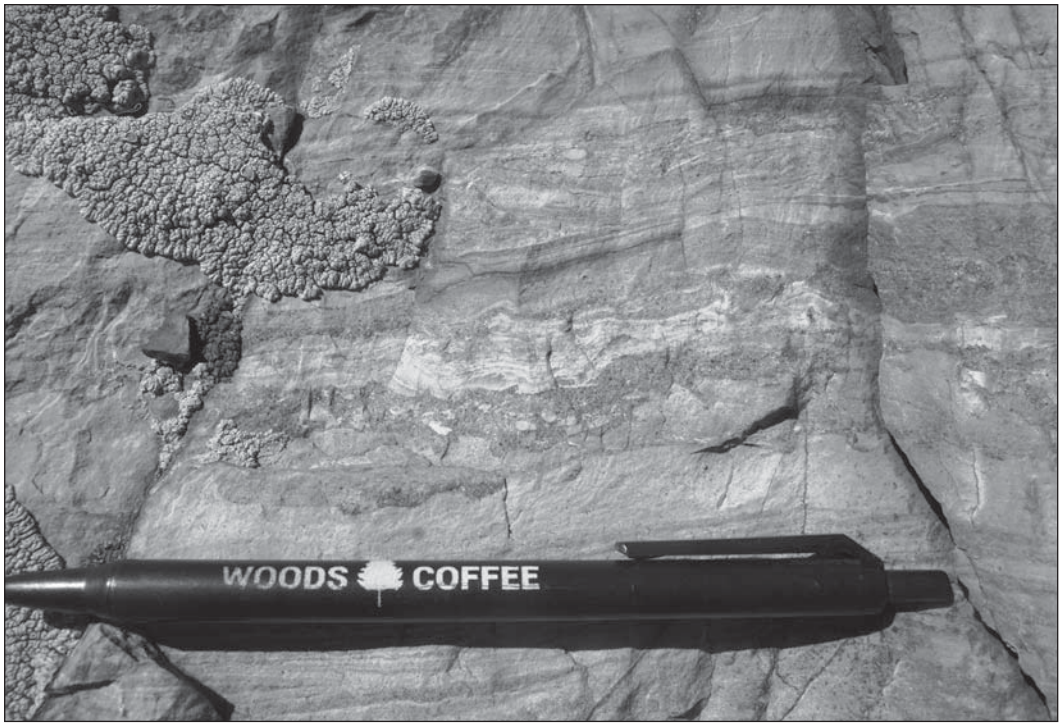

Figure 3. Example of medium to coarse quartz lenses, and mud chips in siltite and argillite of the unit south of the Lemhi Pass fault (fig. 1b) that correlates best with the Lawson Creek Formation. Width of letters on pen is about 1 mm.

Figure 4. Blocks of fine- to coarse-grained quartzite on Goat Mountain (GM, fig. 1b). Crossbedding is visible near the middle and toward the bottom of the largest block. Darker siltite and argillite encountered on lower western and eastern parts of mountain are absent along the highest part. Nine of 10 samples had potassium feldspar exclusively or in excess of plagioclase. The exception had the lowest quartz content. Width of pencil tip for 0.5 mm lead is about 1 mm.

The second discovery that altered our views was confirmation of Noranda's observations of diamictite west of North Fork (fig. 5). This was disturbing because to the east on the Salmon map we had called those rocks Yellow Lake or Gunsight Formation (fig. 1a; Burmester and

Figure 5. Diamictite from west of North Fork. Clasts in other exposures include fine-grained material, similar to what dominates diamictite unit of Apple Creek Formation (Yad) along Hayden Creek (HC, fig. 1), and laminated quartzite as found in the banded siltite member of the Apple Creek Formation south of Lake Mountain (LM, fig. 1). Width of hammer handle below head is about 2 cm.

others, 2016a). To date, diamictite has been reported only in the diamictite and banded siltite members of the Apple Creek Formation (Tietbohl, 1986; Connor and Evans, 1986; Tysdal, 2000). Note that the diamictite is carbonate-free and the Apple Creek is stratigraphically above the Swauger (Bonner) Formation. Thus, although the banded siltite member has some pinch and swell sediment type complete with crinkle cracks and has been correlated with the Wallace by Winston and others (1999), the diamictite cannot be Wallace breccia. This underscores one of the problems working out the stratigraphy—no sediment type appears unique to any single unit. To make matters more interesting, this unit bears garnets, and parts west of North Fork are severely overturned. North of North Fork, kinematic indicators of top-east motion consistent with shear above the Freeman thrust, presumably in the Cretaceous, involve those garnets (Lonn and others, 2013b). However, they formed at about 1,100 Ma (Jeff Vervoort, pers. comm. in Burmester and others, 2016a). Well, if this unit is Apple Creek and not Yellow Lake Formation as mapped, could neighboring strata that we had called Gunsight Formation also be Apple Creek? The two revelations suggest that not all rocks west of the continental divide in the Beaverhead Mountains are necessarily Lemhi Group.

A regional geologic map (fig. 1b) and section (fig. 2) show a possible revision to our previous map that would accommodate the speculative correlations above. All strata from the Diamond Creek fault (DCf, fig. 1b) and intrusions on the west, to the Beaverhead Divide fault system on the east, are shown as being above the Swauger instead of below. An intermediate version would have rocks east of Salmon between the North Fork and Beaverhead faults below the Swauger. The Diamond Creek fault is imagined as the west contact because it is mylonitic and juxtaposes Mesoproterozoic granite and a Gunsight–Swauger section in its hanging wall against possibly younger metasedimentary rocks. However, metasedimentary rocks on opposite sides are so similar that we had discounted it as a major fault. Furthermore, we have not been able to follow it to the northwest. Its trace on the map beyond the Diamond Creek pluton (DCp, fig. 1b) is artistic. Note that there are intrusive contacts of the Mesoproterozoic granite with both the rocks west of North Fork (Ya?) and west of Carmen (Yg).

What Questions Remain?

Clearly, the foremost question is: What is the real stratigraphy of the Lemhi subbasin and how does it relate to that of the main Belt Basin? To answer this, a multi-prong approach might be necessary. More detailed field work combining field observations and sample collection would be a start to test the alternate correlations suggested above, or reveal others. Suitable petrography and chemistry should help. Ideally, something quantitative, such as detrital zircon age spectra, might provide “fingerprints” for the units. However, DZ age spectra have yet to confirm

lithostratigraphic correlations. Kolmogorov–Smirnov (K-S) statistics, which test whether age spectra could have been derived from the same parent population, support close genetic relations among most subbasin samples (Link and others, 2016). However, they also show greater similarity between some different units than within each. Is this because some unit assignments are incorrect, or because mixing proportions of sediment from different sources was repeated at different times and places? Perhaps DZ ages would be more useful by counting more grains per sample (Gehrels and others, 2012) and more samples per unit at each of more sections to define each unit's signature better, if any.

A specific question to answer is whether diamictite is unique to the Apple Creek Formation. If not, and diamictite is found to exist in Yellow Lake Formation strata, the simple solution is to stay with the 2015 story in the north. However, if rocks south of the Lemhi Pass fault are Swauger and higher strata, the Lemhi Pass fault must have a longer history (Gillerman, 2008) and much greater displacement than 1.0 km heave estimated for Tertiary motion by VanDenburg and others (1998).

The other broad question is: What is the whole sedimentary, magmatic, and structural history of the subbasin? If the strata on the west flank of the Beaverhead Mountains are Apple Creek and more similar to strata of the Salmon River Mountains than to the Jahnke Lake member east of the Divide, there is a fault with major translation between them. Is that the Freeman thrust, and is the Diamond Creek fault an out-of-sequence thrust with smaller displacement? Is the Lemhi Pass fault a left-lateral ramp of such a major thrust and the strata south of it also allochthonous relative to the Swauger–Lawson Creek–Jahnke Lake section east of the Beaverhead Divide fault? Or, does the north to south variation in the Swauger–Lawson Creek–Jahnke Lake stack document rapid lateral change in character? Maybe of wider interest, what deformation accompanied the episodic metamorphism and mineralization of the region? Episodes include Mesoproterozoic magmatism and migmatite generation, the Grenville orogeny (including garnet growth in the unit we thought was Yellow Lake Formation), Neoproterozoic faulting, Paleozoic intrusion (Doughty and Chamberlain, 1996; Gillerman, 2008; Aleinikoff and others, 2012, Saintilan and others, 2017), and Cretaceous–Tertiary faulting, folding, and magmatism. One specific question is whether contractional deformation preceded or accompanied Mesoproterozoic intrusion and accounts for some of the present juxtaposition of different units or their facies. As noted above, efforts to answer these questions will require continued field work as well as application of petrographic, geochemical, and geochronologic techniques.

ACKNOWLEDGMENTS

As always, we greatly appreciate the discussions with Don Winston, Paul Link, Dave Pearson, and others with an interest in these challenging rocks. We also acknowledge the efforts of TRGS to disseminate our current research thoughts in a format that provides both a timely release and a field-based forum for discussion.

REFERENCES CITED

Aleinikoff, J.N., Slack, J.F., Lund, Karen, Evans, K.V., Fanning, C.M., Mazdab, F.K., Wooden, J.L., and Pillers, R.M., 2012, Constraints on the timing of Co-Cu ± Au mineralization in the Blackbird District, Idaho, using SHRIMP U-Pb ages of monazite and xenotime plus zircon ages of related Mesoproterozoic orthogneisses and metasedimentary rocks: Economic Geology, v. 107, p. 1143–1175.

Burmester, R.F., Lonn, J.D., Lewis, R.S., and McFaddan, M.D., 2013, Toward a grand unified theory for stratigraphy of the Lemhi subbasin of the Belt Supergroup: Northwest Geology, v. 42, p. 73–88.

Burmester, R.F., Lewis, R.S., Lonn, J.D., and McFaddan, M.D., 2015, The Hoodoo is the Swauger and other heresies: Lemhi subbasin correlations and structures, East-Central Idaho: Northwest Geology, v. 44, p. 1–19.

Burmester, R.F., Lewis, R.S., Othberg, K.L., Stanford, L.R., Lonn, J.D., and McFaddan, M.D., 2016a, Geologic map of the western part of the Salmon 30' x 60' quadrangle, Idaho and Montana: Idaho Geological Survey Geologic Map 52, scale 1:75,000.

Burmester, R.F., Lonn, J.D., Lewis, R.S., and McFaddan, M.D., 2016b, Stratigraphy of the Lemhi subbasin of the Belt Supergroup, *in* MacLean, J.S., and Sears, J.W., eds., Belt Basin: Window to Mesoproterozoic Earth: Geological Society of America Special Paper 522, p. 121–137.

Connor, J.J., and Evans, K.V., 1986, Geologic map of

the Leesburg quadrangle, Idaho: U.S. Geological Survey Miscellaneous Field Studies Map MF-1880, scale 1:62,500.

Doughty, P.T., and Chamberlain, K.R., 1996, Salmon River arch revisited: New evidence for 1370 Ma rifting near the end of deposition in the Middle Proterozoic Belt basin: Canadian Journal of Earth Sciences, v. 33, p. 1037–1052.

Evans, K.V., and Green, G.N., 2003, Geologic map of the Salmon National Forest and vicinity, east-central Idaho: U.S. Geological Survey Geologic Investigations Series Map I-2765, scale 1:100,000, 2 sheets, 19 p. text.

Gehrels, G.E., Giesler, Dominique, and Pecha, Mark, 2012, Detrital zircon geochronology with N=1000: Geological Society of America Abstracts with Programs. v. 44, no. 7, p. 71.

Gillerman, V.S., 2008, Geochronology of iron oxide-copper-thorium-REE mineralization in Proterozoic rocks at Lemhi Pass, Idaho, and a comparison to copper-cobalt ores, Blackbird Mining District, Idaho: Final Technical Report to U.S. Geological Survey, Grant Award 06HQGR0170, 66 p.

Link, P.K., Stewart, E.S., Steele, Travis, Sherwin, Jo-Ann, Hess, L.T., and McDonald, Catherine, 2016, Detrital zircons in the Mesoproterozoic upper Belt Supergroup in the Pioneer, Beaverhead, and Lemhi Ranges, Montana and Idaho: The Big White arc, *in* MacLean, J.S., and Sears, J.W., eds., Belt Basin: Window to Mesoproterozoic Earth: Geological Society of America Special Paper 522, p. 163–183.

Lonn, J.D., 2017, The Lemhi Group type sections revisited and revised, east-central Idaho; Northwest Geology, v. 46, p. 15–28.

Lonn, J.D., Lewis, R.S., Burmester, R.F., and McFaddan, M.D., 2013a, The complex structural geology of the northern Beaverhead Mountains, Montana and Idaho: Northwest Geology, v. 42, p. 111–130.

Lonn, J.D., Othberg, K.L., Lewis, R.S., Burmester, R.F., Stanford, L.R., and Stewart, D.E., 2013b, Geologic map of the North Fork quadrangle, Lemhi County, Idaho: Idaho Geological Survey Digital Web Map 160, scale 1:24,000.

Lonn, J.D., Burmester, R.F., Lewis, R.S., and McFaddan, M.D., 2016a, Mesoproterozoic Lemhi strata represent immense alluvial aprons that prograded northwest into the Belt sea, Idaho and Montana: Geological Society of America Abstracts with Programs, v. 48, no. 6, doi: 10.1130/abs/2016RM-276082.

Lonn, J.D., Burmester, R.F., Lewis, R.S., and McFaddan, M.D., 2016b, Giant folds and complex faults in Mesoproterozoic Lemhi strata of the Belt Supergroup, northern Beaverhead Mountains, Montana and Idaho, *in* MacLean, J.S., and Sears, J.W., eds., Belt Basin: Window to Mesoproterozoic Earth: Geological Society of America Special Paper 522, p. 139–162.

Saintilan, N.J., Creaser, R.A., Bookstrom, A.A., 2017, Re-Os systematics and geochemistry of cobaltite (CoAsS) in the Idaho cobalt belt, Belt-Purcell Basin, USA: Evidence for middle Mesoproterozoic sediment-hosted Co-Cu sulfide mineralization with Grenvillian and Cretaceous remobilization: Ore Geology Reviews, v. 86, p. 509–525.

Tietbohl, D.R., 1986, Middle Proterozoic diamictite beds in the Lemhi Range, east-central Idaho, *in* Roberts, S.M., ed., Belt Supergroup; A guide to Proterozoic rocks of western Montana and adjacent areas: Montana Bureau of Mines and Geology Special Publication 94, p. 197–207.

Tysdal, R.G., 2000, Stratigraphy and depositional environments of Middle Proterozoic rocks, northern part of the Lemhi Range, Lemhi County, Idaho: U.S. Geological Survey Professional Paper 1600, 40 p.

Winston, Don, Link, P.K., and Hathaway, Nathan, 1999, The Yellowjacket is not the Prichard and other heresies–Belt Supergroup correlations, structure, and paleogeography, east-central Idaho, *in* S.S. Hughes and G.D. Thackray, eds., Guidebook to the Geology of Eastern Idaho: Pocatello, Idaho, Idaho Museum of Natural History, p. 3–20.

THE LEMHI GROUP TYPE SECTION REVISITED AND REVISED, EAST-CENTRAL IDAHO

Jeff Lonn

Montana Bureau of Mines and Geology, 1300 W. Park Street, Butte, MT 59701, jlonn@mtech.edu

ABSTRACT

New mapping of the area surrounding the type sections of Gunsight, Yellow Lake, Big Creek, West Fork, and Inyo Creek Formations, Lemhi Group, in the central Lemhi Range, suggests that previously unrecognized faults cut across the type section of the Big Creek Formation. These faults separate the Big Creek from the type Inyo Creek and West Fork sections that were originally described as lying stratigraphically beneath the Big Creek. This study suggests instead that the Inyo Creek and West Fork Formations lie stratigraphically above the Big Creek and are correlative with the Yellow Lake Formation. The Yellow Lake Formation is poorly known due to structural complications and difficult access to its type area. It may include thick intervals of calcareous siltite and very fine quartzite that have been previously mapped across the region as Big Creek Formation, and it may be much thicker than previously thought. The Big Creek Formation in its type section is comprised of very thick bedded, fine-grained sand that lacks disseminated carbonate, and its exposed thickness is much less than previously described.

INTRODUCTION

More than a century has passed since Mesoproterozoic sedimentary rocks were first recognized in the Leadore, Idaho, area and assigned to the Belt Series (Umpleby, 1913). However, deciphering the stratigraphy of these 1.4 Ga strata has been especially challenging to geologists, and the relationships between the Belt Supergroup and these Lemhi strata are still debated. Both stratigraphic successions are immensely thick (>15 km), lithologically monotonous, and non-fossiliferous. Identification and correlation of individual units is exceedingly difficult, often requiring the occurrence of thick (>3,000 m) intact sections where stratigraphic sequences can be viewed. Plutonic provinces, faults, and broad valleys filled with Cenozoic sediments isolate these exposures and further complicate correlation. In addition, many of the best exposures occur in remote and rugged wilderness. The Lemhi Group type sections (Ruppel, 1975) are located in one such isolated area, the roadless central Lemhi Range. This paper describes a recent traverse across the Lemhi Group type section that resulted in new structural, and therefore stratigraphic, interpretations.

HISTORY OF THE LEMHI GROUP

Ross (1947) identified and described the Lemhi and Swauger quartzites on the southwest flank of the Lemhi Range (fig. 1). He included gray and greenish impure (feldspathic) fine-grained quartzite and interbedded argillite in the Lemhi quartzite, and the stratigraphically overlying coarser and purer quartzite in the Swauger. Anderson (1961), mapping to the north on the east side of the range, defined the Apple Creek Phyllite as having a lower phyllitic quartzite and an upper phyllite. He did not map the Apple Creek in stratigraphic contact with Ross' (1947) units, but he speculated that it underlay the Lemhi quartzite. Ed

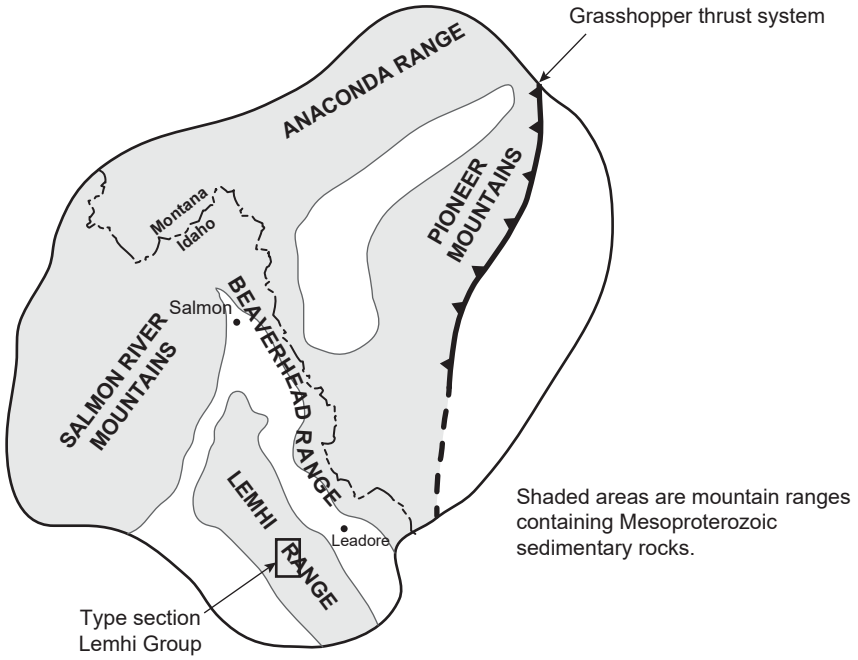

Figure 1. Location of the Lemhi Group type section.

Ruppel then mapped three 15' quadrangles (Ruppel, 1968, 1980; Ruppel and Lopez, 1981) that covered the rugged central Lemhi Range between the areas mapped by Ross and Anderson. There, he elevated the Lemhi quartzite to group status, subdivided it into five formations (fig. 2), and correlated the Apple Creek Phyllite with a fine-grained, thin-bedded interval within the newly defined Lemhi Group (Ruppel, 1975). He delineated reference/type sections for each formation (fig. 3) in a very remote and rugged part of the Lemhi Range on his Patterson quadrangle map (1980). As a result, only a very few determined geologists have revisited the area. McBean (1983) studied the type Gunsight section in an M.S. thesis. Winston and others (1999) measured key sections and correlated the Lemhi Group and overlying Swauger and Lawson Creek (Hobbs, 1980) Formations with both the Belt Supergroup strata of western Montana and Mesoproterozoic rocks of the Salmon River Mountains. Tysdal (2000) made reconnaissance traverses through the type Big Creek, Apple Creek, and Gunsight Formations. He named Ruppel's (1975) Apple Creek reference section the Yellow Lake unit of the Apple Creek Formation and perceptively noted that its lithofacies differed from those of the type Apple Creek farther northwest. He also pointed out a geochemical study by Conner (1991) that showed different chemical compositions for the Yellow Lake unit and the type Apple Creek.

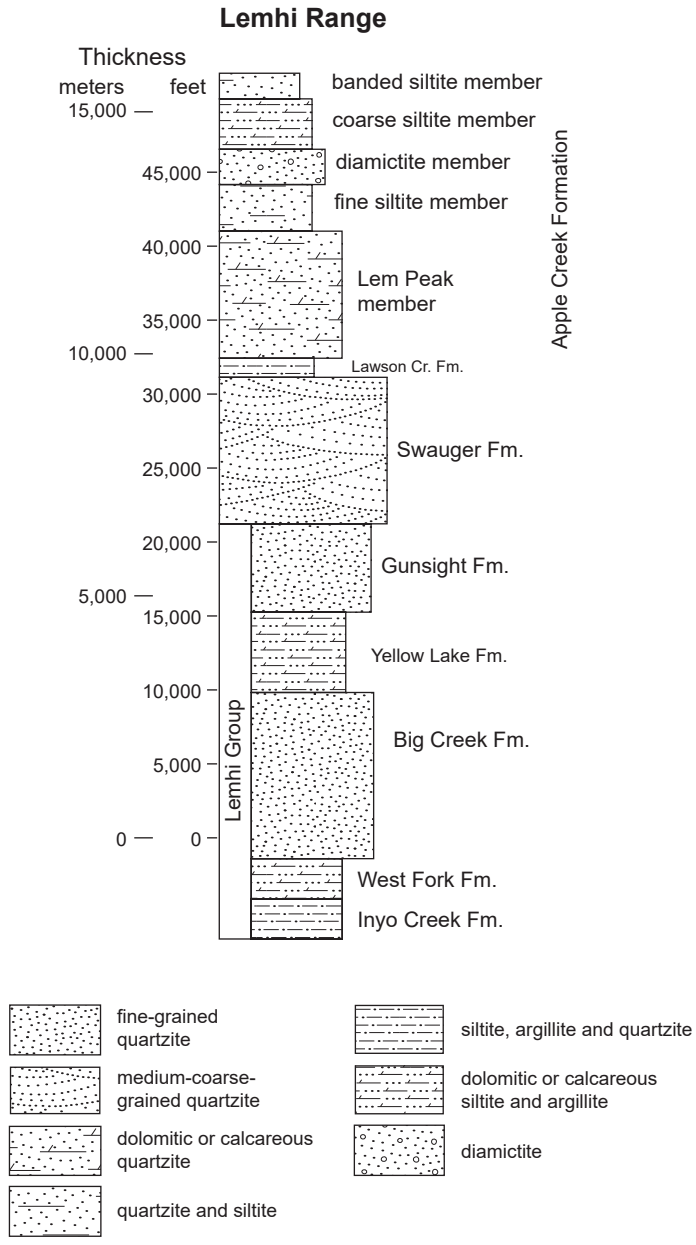

Figure 2. Lemhi Range stratigraphic column showing position of the original Lemhi Group (Ruppel, 1975). Modified from Burmester and others (2016a).

In 2007, a collaborative Idaho Geological Survey (IGS) and Montana Bureau of Mines and Geology (MBMG) team comprised of Reed Lewis, Russ Burmester, Mark McFaddan, and Jeff Lonn began 1:24,000-scale mapping in the Beaverhead Mountains along the Idaho–Montana border. Confused by the stratigraphy that was unfolding, they made reconnaissance trips into various parts of the Lemhi Range to view the strata. Surprisingly, they discovered that the type Apple Creek lay stratigraphically above the Lawson Creek and Swauger Formations, and thus well above the Lemhi Group. Therefore, Ruppel's (1975) Apple Creek reference section within the stratigraphically lower Lemhi Group is not part of the Apple Creek Formation. Following Tysdal's (2000) lead, the IGS–MBMG team renamed Ruppel's Apple Creek the Yellow Lake Formation, leaving the Apple Creek name attached to Anderson's (1961) Apple Creek Phyllite, now interpreted to lie well above the Lemhi Group (fig. 2). They also determined that the type Apple Creek Formation was as much as 4,500 m thick in the Beaverhead and Lemhi Ranges, and named the entire Idaho Mesoproterozoic stratigraphic column the Lemhi subbasin strata (Burmester and others, 2016a).

With this much stratigraphic confusion within just the Lemhi Range, it is no surprise that regional Belt–Lemhi correlations are still uncertain. Early workers speculated that the Mesoproterozoic rocks of the Lemhi region correlated with the Belt Supergroup, but provided few details (Umpleby, 1913; Ross, 1947; Anderson, 1961). Ruppel (1975) suggested that the lower part of the Lemhi Group might be equivalent to the Ravalli Group, the Apple Creek and Gunsight to the Helena and Wallace (Piegan Group), and the overlying Swauger to the Missoula Group. However, he

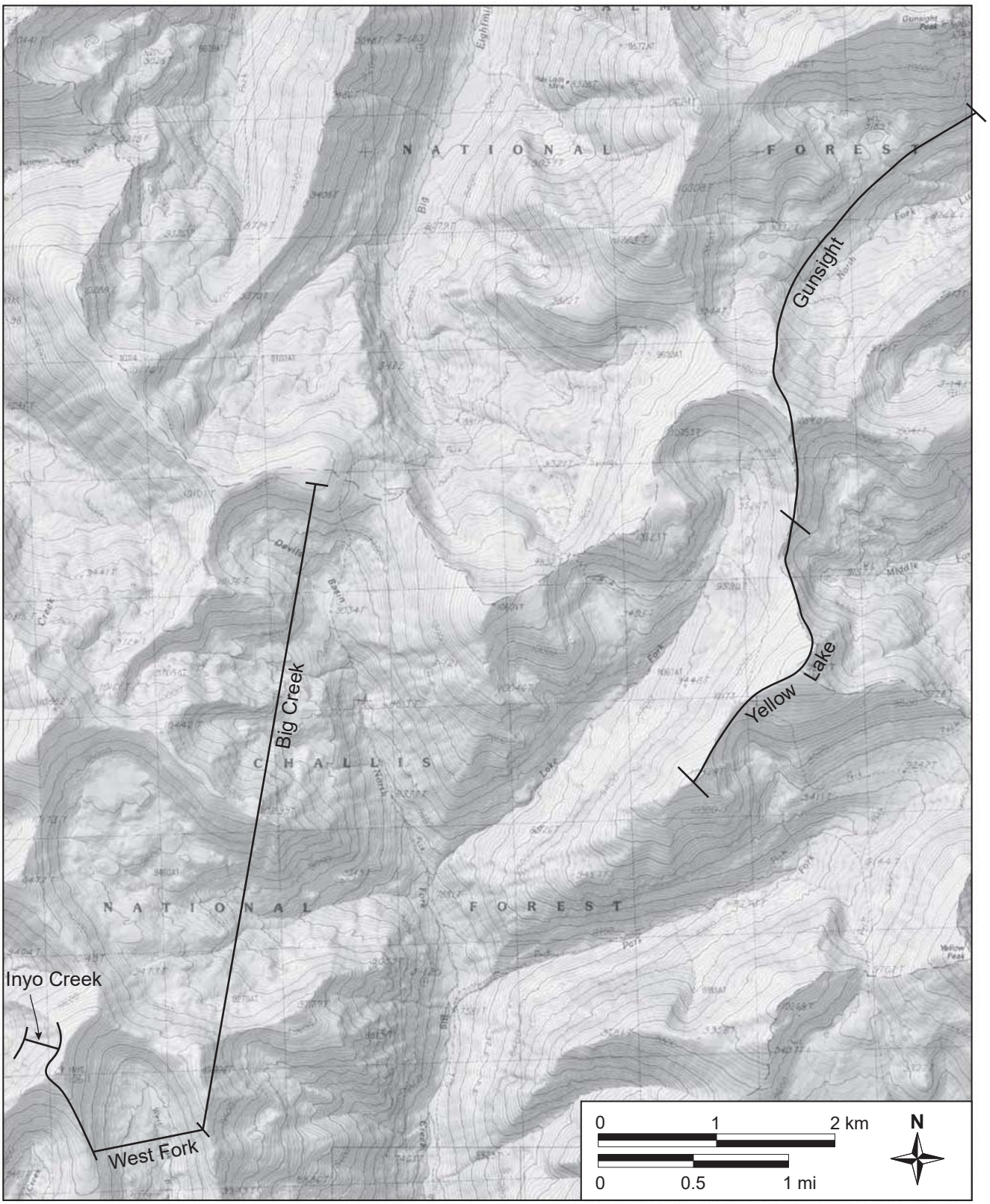

Figure 3. Location of the Lemhi Group type sections. From Ruppel (1975), superimposed on a caltopo.com topographic base.

did not conclude that these correlatives were deposited in the same basin, and later proposed that the Lemhi and Belt Basins were separated by the Lemhi Arch, which was also the sediment source for both basins (Ruppel, 1978, 1993). Still later, he and Mike O'Neill proposed that the two separate Lemhi and Belt Basins had been juxtaposed by a long-lived, continental-scale, left lateral fault, the Great Divide megashear (O'Neill and others, 2007), that lay roughly along the Montana–Idaho border. Meanwhile, Don Winston and Paul Link argued for deposition in a single basin and proposed direct specific correlations between not only the

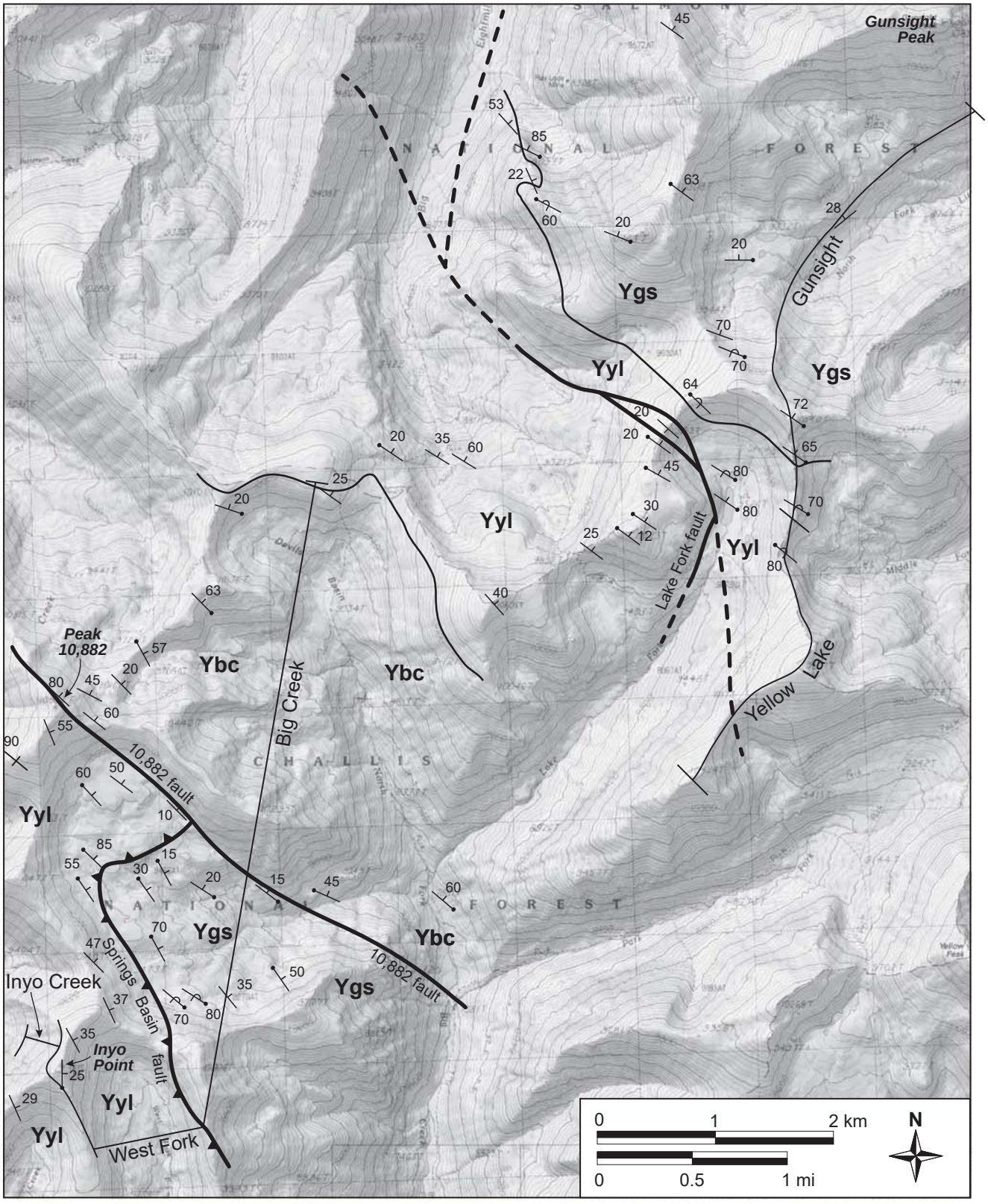

Figure 4. Geologic map of the area surrounding the Lemhi Group type sections. Data from this study superimposed on figure 3. Note that West Fork and Inyo Creek Fms are reinterpreted as Yellow Lake Fm. Ygs-Gunsight Fm; Yyl-Yellow Lake Fm; Ybc-Big Creek Fm.

Belt and Lemhi rocks, but also with the Mesoproterozoic rocks of the Salmon River Mountains (Winston and others, 1999). Evans and Green's (2003) map of Salmon National Forest shows fault zones along the Idaho–Montana border that juxtapose Lemhi and Belt rocks, but the map's text does not discuss relationships between the two groups. Tysdal and others (2005) applied Lemhi Group names on both sides of the Idaho–Montana border in the northern Beaverhead Mountains.

The IGS–MBMG mapping team concluded that, although significant structures do exist along the Idaho–Montana border in the northern Beaverhead Mountains, they are not terrane-bounding features separating different basins. Instead, the sandier Lemhi strata extend across the Beaverhead Mountains north and northeast into Montana. The cross-border mapping and examination of the Lemhi Range also gave the IGS–MBMG geologists the courage to propose that most of the Lemhi strata are correlative with, and facies of, the Missoula Group of the upper Belt Supergroup (Burmester and others, 2015, 2016a; Lonn, 2014; Lonn and others, 2016a, b). Detrital zircon data (Link and others, 2007, 2013, 2016; Stewart and others, 2010) support this correlation, as discussed in a later section.

This paper addresses only the type Lemhi Group (Ruppel, 1975), which is the lower part of the Lemhi subbasin section (fig. 2). Data and interpretations presented here result from three multi-day backpacking trips in 2014 and 2015 that traversed the type and reference sections of the Lemhi Group.

RESULTS

Figure 3 shows the locations of the type/reference sections for the Inyo Creek, West Fork, Big Creek, Yellow Lake (formerly Apple Creek), and Gunsight Formations of the Lemhi Group (Ruppel, 1975). Ruppel (1980) interpreted the Lemhi Group section as a northeast-facing homocline without significant faults, although he does show numerous flat thrusts atop the thick section.

The map produced by this study is shown on figure 4. On it, I eliminate Ruppel's flat thrusts and include new faults that cut the type sections. The 10,882 fault is of particular significance because it cuts across the Big Creek type section, disrupting the stratigraphic continuity between the West Fork and Big Creek Formations and calling into question the stratigraphic positions of the West Fork and Inyo Creek. This paper first discusses the Gunsight, Yellow Lake, and Big Creek Formations, which are in stratigraphic continuity, then discusses the complex geology southwest of the 10,882 fault.

Gunsight Formation

The type section of the Gunsight Formation is characterized by decimeter- to meter-thick beds of fine-grained feldspathic quartzite that is flat laminated, crossbedded, or massive. In the lower part, from 1- to 3-m-thick intervals of light gray, trough cross-bedded and flat-laminated, medium- to fine-grained quartzite alternate with darker intervals containing decimeter-thick beds of quartzite and siltite interbedded with siltite–argillite couplets (fig. 5). The lower contact with the Yellow Lake Formation is gradational and placed where the siltite–argillite couplets become dominant. McBean (1983) measured the type section as 1,700 m thick.

Figure 5. Lower part of the type Gunsight section. (a) Alternating light and dark intervals. "Up" is to the right. (b) Close-up showing thick beds of light-colored, fine-grained quartzite alternating with dark intervals of thinner bedded medium-grained quartzite, siltite, and argillite.

Yellow Lake Formation

I examined the Yellow Lake section on the ridge north and west of Yellow Lake about 1 km west of Ruppel's (1975) designated reference section. The upper part of the Yellow Lake section is characterized by non-dolomitic couplets of light gray, medium-grained quartzite or green siltite below dark purple argillite (fig. 6a). Lenticular and flaser bedding are common, and graded beds and mud chips are uncommon. A previously unrecognized curving, but generally north-striking, fault, labeled on figure 4 as the Lake Fork fault, cuts the Yellow Lake section approximately 220 m below its upper contact. The fault is marked by breccia, quartz veins, and a pronounced change in bedding attitudes. While magnitude and sense of movement are unknown, a thick interval of very fine-grained quartzite on the west side is not repeated on the east, and so stratigraphic section appears to be omitted rather than duplicated. Ruppel (1980) mapped a down-to-the-east fault to the north and approximately along strike with significant offset (Swauger against Yellow Lake). If this is the same fault, as shown on figure 4, it is possible that a large part of the Yellow Lake section has been omitted from the type area.

On the west side of the Lake Fork fault, downsection, are more strongly cleaved green siltite to purple argillite couplets with traces of carbonate. Farther

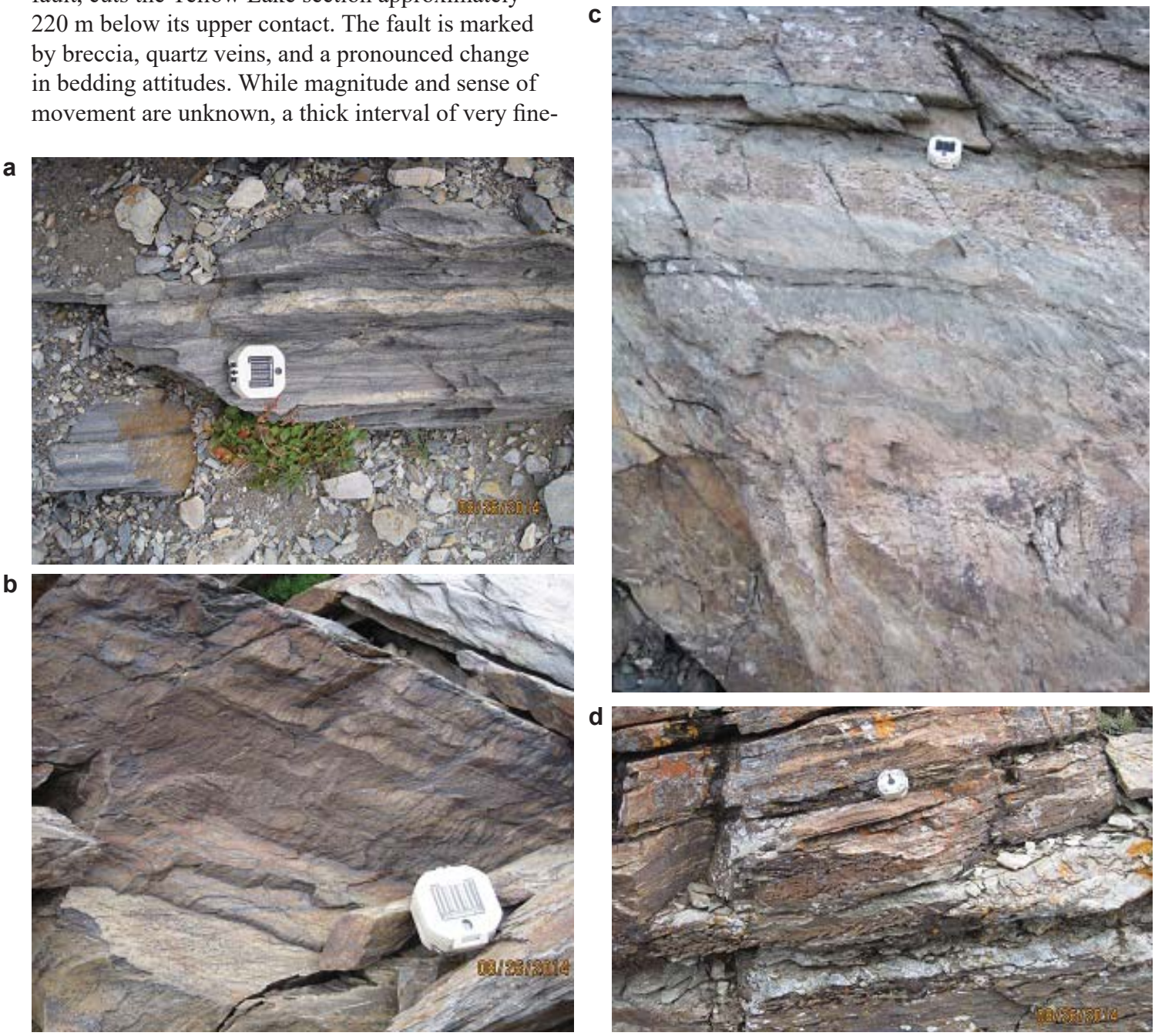

Figure 6. Type Yellow Lake section. (a) Upper part consists mostly of uncracked, non-dolomitic couplets of light-colored quartzite, darker siltite, and purple argillite. Lower part contains interbedded intervals of: (b) graded siltite–argillite couplets with abundant load structures, (c) decimeters-thick beds of calcareous fine-grained quartzite (bed below Brunton) and siltite, and (d) centimeters-thick beds of silty dolomite (darker beds).

downsection is a 100- to 200-m-thick interval of fine-grained quartzite followed by a mixture of dolomitic, graded green siltite to purple or black argillite couplets, decimeter- to meter-thick calcitic or dolomitic green siltite, and rusty-weathering very fine-grained dolomitic quartzite. Some pinch and swell structure and some load structures occur, as do 1- to 5-cm-thick lenses and beds of dolomite (fig. 6). The lower contact is gradational with the underlying Big Creek Formation, and placed where thick-bedded, fine-grained, carbonate-free quartzite begins to dominate. The Yellow Lake section here is estimated to be at least 1,500 m thick, considerably more than the 900 m estimated by Ruppel (1980).

Big Creek Formation

Very thick (as much as 2 m) beds of light gray, fine-grained quartzite with prominent black laminations that define cross beds, flat laminations, and soft sediment folds appear to be diagnostic of the Big Creek Formation (fig. 7). Decimeter-thick beds of siltite also occur, as do rare centimeter-scale argillite beds and rare mud chips up to 10 cm across. Although Ruppel (1975, 1980) and Tysdal (2000) reported disseminated calcite to be common, I only observed minor disseminated carbonate near the calcite-rich 10,882 fault. The 10,882 fault cuts across Ruppel's (1975) type Big Creek section (fig. 4), with lithologies on the other side assigned to the Yellow Lake and Gunsight Formations by this study. In this interpretation, about 1,300 m of Big Creek is exposed, in contrast to Ruppel's (1980) thickness estimate of 3,100 m.

The 10,882 Fault

A northwest-striking fault, evident from calcitic breccia and a profound change in lithology, is exposed at the summit of Peak 10,882, and labeled the 10,882 fault (fig. 4). Ruppel (1980) recognized this fault, but mapped it as a flat thrust placing a small klippe of Yellow Lake Formation over Big Creek. While I agree with his Yellow Lake Formation lithologic call, the Yellow Lake does not appear to be restricted to a small klippe. Instead, I interpret exposures south and west of Peak 10,882 as Yellow Lake Formation that grade downsection into calcareous very fine-grained quartzite and siltite and then into thin beds of dolomite and limestone mapped as West Fork Formation (Ruppel, 1980). The 10,882 fault continues southeast to the North Fork of Big Creek, and thus appears to be a northwest-striking high angle fault cutting through the type Big Creek section. In my interpretation, the southern half of the Big Creek type section, southeast of Peak 10,882, is Gunsight Formation (fig. 4). The Gunsight here can be distinguished from Big Creek by its thinner beds, common small-scale trough cross-beds, and abundant silt beds.

Figure 7. Type Big Creek section. (a) Beds of fine-grained quartzite are as much as 2 m thick. (b) Black laminations are common.

The Springs Basin Fault

A thrust fault marked by cataclasite, quartz veins, overturned strata, and a profound change in lithology occurs in the southwestern part of figure 4. Ruppel (1980) also mapped this thrust, although his trace diverges from mine. This thrust is named the Springs Basin fault after exposures in the unnamed basin with "springs" labeled on the topographic map (fig. 4). In its hanging wall, outcrop-scale isoclinal folds with gently southwest-dipping axial plane cleavage suggest the fault dips gently west (fig. 8a), although later high-angle faults appear to cut the thrust and complicate its trace. Northeast-overturned strata in the Springs Basin fault footwall indicate top-to-the-northeast reverse movement. The fault places hanging wall strata mapped as West Fork and Inyo Creek Formations by Ruppel (1980) over decimeter- to meter-thick beds of trough cross-bedded quartzite that I mapped as Gunsight and that Ruppel (1975, 1980) interpreted to be the lower part of the type Big Creek.

West Fork Formation

The type West Fork section appears to be characterized by dolomitic and non-dolomitic siltite–argillite couplets and couples (fig. 8). Mudcracks are common, and diagnostic lenses and beds of limestone and dolomite occur. Upward in the section, toward Peak 10,882, thicker beds of very fine-grained quartzite and green siltite with common disseminated calcite occur. Although these were previously assigned to the Big Creek Formation (Ruppel, 1980), this study suggests that they are stratigraphically continuous with both the type West Fork and the Yellow Lake mapped by Ruppel (1980) in a klippe at the summit of Peak 10,882.

Inyo Creek Formation

The West Fork Formation grades downward from carbonate-rich siltite–argillite couplets to thicker non-dolomitic siltite–argillite couplets and couples of the Inyo Creek Formation on the west face of Inyo Point (fig. 4). The lower part of the Inyo Creek Formation becomes coarser and thicker bedded, with decimeters-thick, very fine-grained, quartzite beds containing flat black laminations (fig. 8) reminiscent of the Big Creek Formation. Winston and others (1999, page 8) describe a similar coarsening-downward stratigraphy, and a lower Inyo Creek "principally composed of 20- to 80-cm-thick, tabular beds of flat-laminated, well-sorted, fine-grained feldspathic quartz arenite with climb-

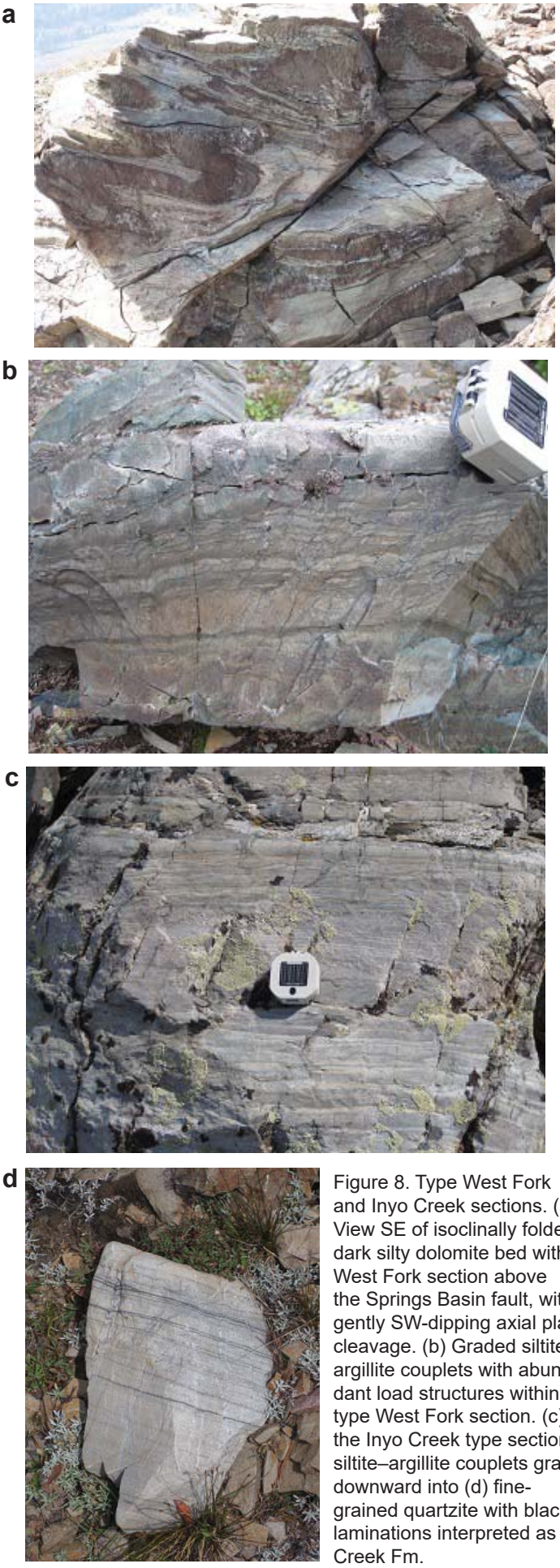

Figure 8. Type West Fork and Inyo Creek sections. (a) View SE of isoclinally folded dark silty dolomite bed within West Fork section above the Springs Basin fault, with gently SW-dipping axial plane cleavage. (b) Graded siltite–argillite couplets with abundant load structures within the type West Fork section. (c) In the Inyo Creek type section, siltite–argillite couplets grade downward into (d) fine-grained quartzite with black laminations interpreted as Big Creek Fm.

ing ripples at the tops of some beds." Although some faults intervene, as shown on Ruppel's (1980) map, it appears that just off the southwest corner of figure 4 the Inyo Creek Formation grades downward into thick bedded, fine-grained quartzite with black laminations similar to the lithologies characteristic of type Big Creek Formation. In fact, Ruppel (1980) maps this quartzite as Big Creek Formation, but he shows it in fault contact with his type Inyo Creek Formation.

Stratigraphic Positions of the Inyo Creek and West Fork Formations

Although I confirmed that the West Fork Formation grades downward into the Inyo Creek Formation, the 10,882 fault and Springs Basin fault separate them from the type Big Creek section. In no place can Big Creek be observed to grade downward into the West Fork. Therefore, the stratigraphic positions of the Inyo Creek and West Fork are uncertain. However, there are clues.

As described above, the Inyo Creek appears to grade downward into Big Creek on the west ridge of Inyo Point. Both the Inyo Creek and West Fork share lithologic similarities with the Yellow Lake: siltite–argillite couplets that are commonly dolomitic, decimeter- to meter-thick beds of calcareous silt and very fine sand, and thin lenses and beds of silty dolomite or limestone. The upper West Fork contact described as gradational into Big Creek (Ruppel, 1975) east of Inyo Point (fig. 3) is interpreted here as the Springs Basin fault that places West Fork against Gunsight (fig. 4). Therefore, I propose that the West Fork and Inyo Creek are correlative with the lower part of the Yellow Lake.

In addition, the calcareous silt and fine sand formerly assigned to the lower part of the Big Creek in Springs Basin (Ruppel, 1975, 1980) are interpreted to be part of the Yellow Lake Formation (fig. 4). At the type section, these lithologies are poorly exposed in the upper cirque of Big Eightmile Creek, west of Yellow Lake, and may be partly omitted by the Lake Fork fault. On a reconnaissance traverse of the ridge between Patterson Creek and its east fork (7 km west of this study), I found that the Big Creek mapped stratigraphically above West Fork (Ruppel, 1980) consists mostly of green siltite with common disseminated calcite – very different than the thick bedded, non-calcareous quartzite of type Big Creek described above. This Patterson Creek section is topped by green siltite–purple argillite couplets, similar to those of the upper Yellow Lake, that then grade up into Gunsight quartzite. I propose that the mapped Big Creek is really Yellow Lake, and, if this section is unfaulted, the Yellow Lake is more than 3,000 m thick. Other areas in east-central Idaho where geologists mapped calcareous siltite and quartzite as Big Creek may also be Yellow Lake Formation (e.g., in the Beaverhead Mountains: Burmester and others, 2016b; Evans and Green, 2003).

CORRELATIONS WITH THE BELT SUPERGROUP

Winston and others (1999) proposed that the Big Creek correlates with the Revett Formation of the Ravalli Group, the Yellow Lake with the Piegan Group, the Gunsight with the Snowslip, and the overlying Swauger with the Mt. Shields and possibly the Bonner. Lonn and others (2016a, b), observing that fine-grained sands directly overlie the Wallace Formation (upper Piegan Group) and grade up to Swauger Formation in the southern Sapphire Range, made similar correlations. They equated the Piegan Group with most of the Yellow Lake, the upper part of the Yellow Lake and the Gunsight with the Snowslip and Shepard, and the overlying Swauger with the Mount Shields and Bonner (fig. 9). The correspondence of chert and argillite abundance in the McNamara and Lawson Creek Formations is critical to these correlations. Lonn and others (2016a, b) noted that thick Gunsight–Swauger sands in the southern Sapphire Mountains thin and fine northward, with argillite-rich tongues in the Snowslip, Shepard, and Mount Shields Formations becoming prominent near Missoula. This large-scale facies change suggests that immense alluvial aprons or fans prograded north into the main Belt Basin, and that most of the Lemhi subbasin strata are relicts of the southeastern, upstream ends of these alluvial wedges. Finally, citing the thick-bedded but fine-grained character of the Revett quartzite in its closest exposures in the Anaconda Range, Lonn and others (2016b) proposed that the Big Creek correlates with the Revett of the Ravalli Group.

DETRITAL ZIRCON DATA

Using detrital zircon (DZ) data to support correlations is a tool only recently available. Link and others (2007, 2013, 2016) used DZ data to show that the

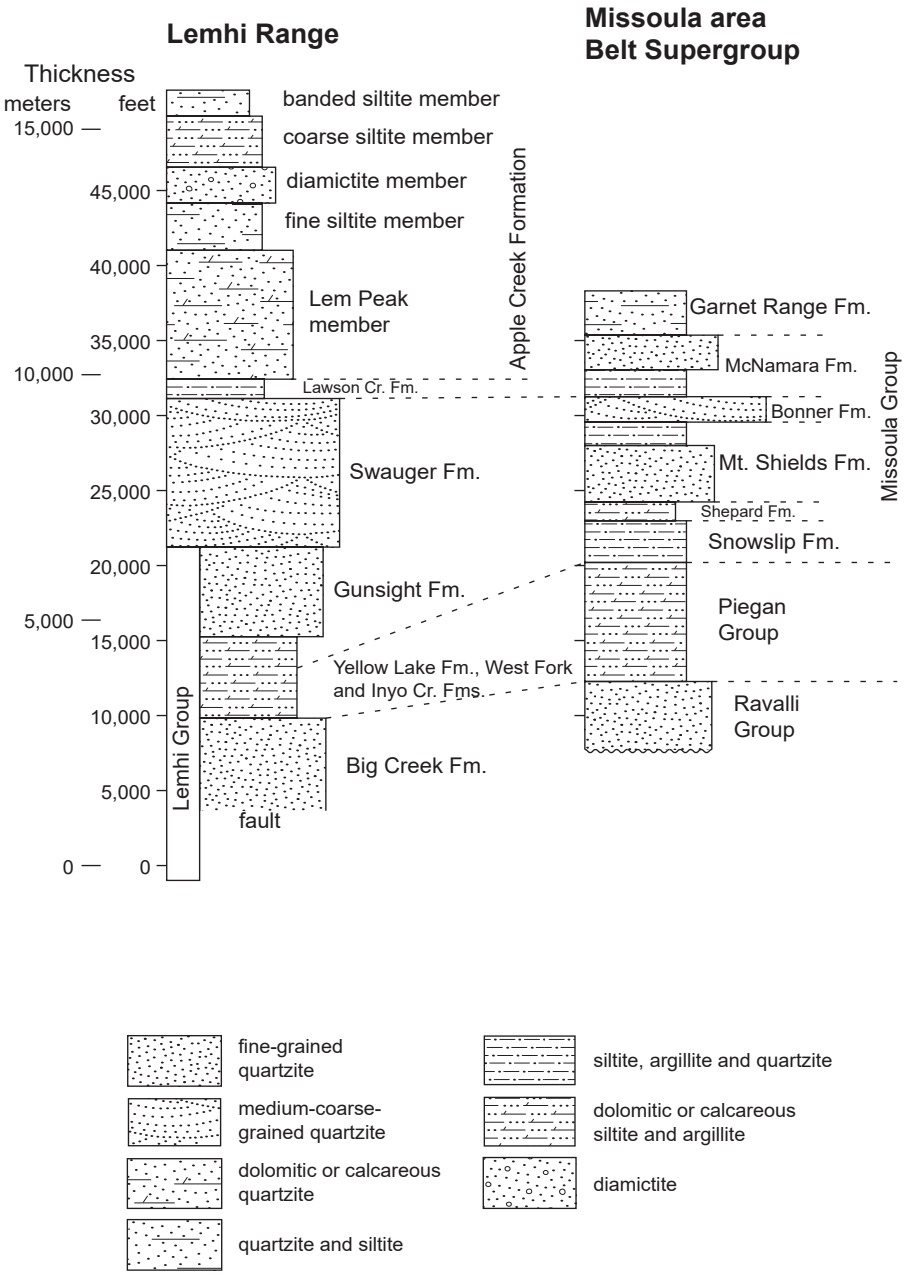

Figure 9. Revised Lemhi subbasin stratigraphic column and proposed correlations with the Belt Supergroup. From Lonn and others, 2016b.

upper Lemhi subbasin strata, above the Yellow Lake, have the same provenance as the Missoula Group of the upper Belt Supergroup, confirming at least the broad correlations proposed above. Upper Lemhi and Missoula Group strata lack significant "non-North American" 1510–1625 Ma detrital zircon grains, in contrast to the Prichard Formation and Ravalli Group of the lower Belt that have strong non-North American peaks (Ross and Villeneuve, 2003; Link and others, 2007). Only two samples of the Piegan Group have been analyzed, but they both contain about 20% non-North American grains (Ross and Villeneuve, 2003; Lewis and others, 2007), and so have zircon age distributions transitional between the Ravalli and Missoula Groups.

Only three analyses are available from the type Lemhi Group section. Figure 10 shows these results alongside all three plots available for the Ravalli and Piegan Groups. The Big Creek sample was taken "from lower part of the Big Creek type section" (Stewart and others, 2010) that is reinterpreted here as Gunsight Formation, which may explain its Missoula Group-like DZ signature with only 5% non-North American grains—probably statistically insignificant. The samples from the Inyo Creek and West Fork had 5% and less than 2% non-North American grains, respectively, which makes correlation with the Piegan Group–Yellow Lake proposed here uncertain. However, no samples from the type Yellow Lake have ever been collected or analyzed. The lack of non-North American grains in the Inyo Creek and West Fork samples does appear to preclude correlation with the Ravalli Group as previously proposed (Winston and others, 1999). Obviously, the rest of the type Lemhi Group section needs to be sampled and analyzed, and more samples need to be collected from the Ravalli and Piegan Groups in the central Belt Basin for comparison.

CONCLUSIONS

New mapping of the Lemhi Group type section suggests that previously unrecognized faults cut across the type section of the Big Creek Formation. These faults separate the Big Creek from the type Inyo Creek and West Fork sections, which were originally described as lying stratigraphically beneath the Big Creek. This study suggests that the Inyo Creek and West Fork Formations lie stratigraphically above the Big Creek and correlate with the Yellow Lake Formation. The Yellow Lake Formation is poorly known due to structural complications and difficult access to its type area. It may include thick intervals of calcareous siltite and very fine quartzite previously mapped across the region as Big Creek

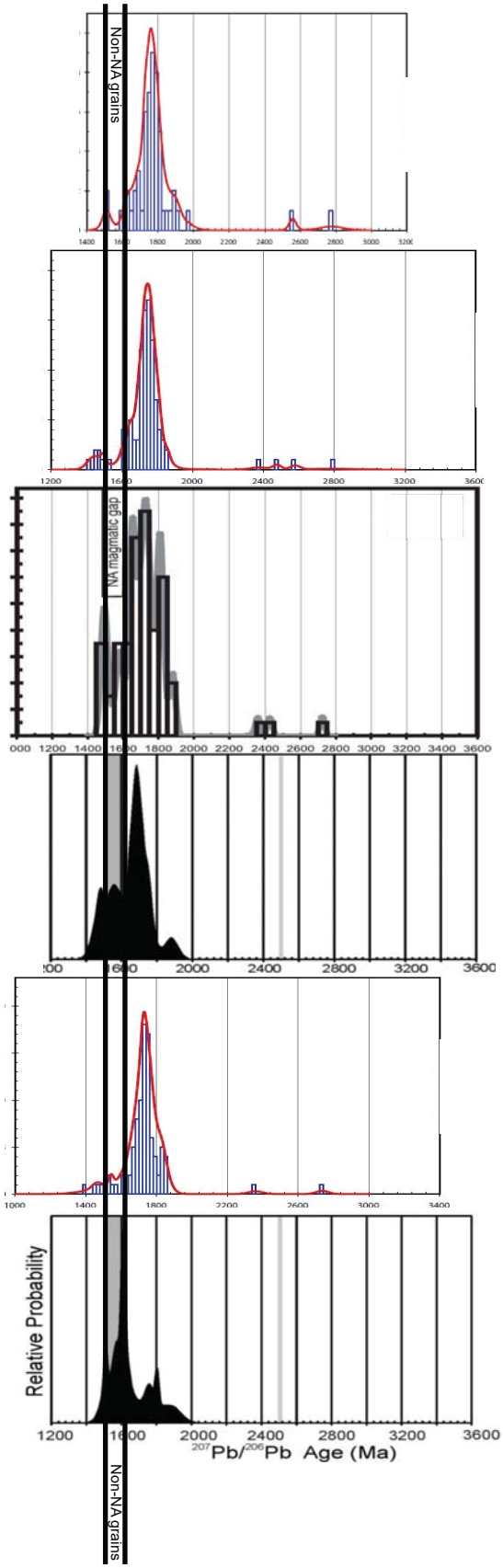

type West Fork Fm
n=58
Stewart and others, 2010

type Inyo Creek Fm
n=100
Stewart and others, 2010

Wallace Fm
Hoodoo Pass
n=83
Lewis and others, 2007

Wallace Fm
Lake Pend Oreille
n=27
Ross and Villeneuve, 2003

type Big Creek Fm
n=99
Stewart and others, 2010

Revett Fm
Coeur d'Alene district
n=24
Ross and Villeneuve, 2003

Figure 10. Stacked detrital zircon age plots from the Lemhi Group type sections compared with data from the Revett Formation of the Ravalli Group and the Wallace Formation of the Piegan Group. Note that the type Big Creek section plot is reinterpreted as Gunsight Formation in this paper.

Formation, and may be much thicker than previously thought. The Big Creek Formation in its type section is comprised of very thick bedded, fine-grained sand that lacks disseminated carbonate, and its exposed thickness is much less than previously described.

ACKNOWLEDGMENTS

This work would not have been possible without the late Ed Ruppel's pioneering work. After traversing some of his rugged territory and viewing some of his challenging rocks, I have the utmost respect for Ed. I shall also be forever indebted to him for hiring me at the MBMG 25 years ago. Thanks also to Don Winston for giving me my start mapping in tough rocks, to the MBMG for allowing me the freedom to follow these Belt rocks wherever they lead, even across the Idaho border, and to Reed Lewis, Russ Burmester, and Mark McFaddan for their expert guidance as we navigate the Belt Sea.

REFERENCES CITED

Anderson, A.L., 1961, Geology and mineral resources of the Lemhi quadrangle, Lemhi County, Idaho: Idaho Bureau of Mines and Geology Pamphlet 124, 111 p.

Burmester, R.F., Lewis, R.S., Lonn, J.D., and McFaddan, M.D., 2015, The Hoodoo is the Swauger and other heresies: Lemhi subbasin correlations and structures, east-central Idaho: Northwest Geology, v. 44, p. 73–88.

Burmester, R.F., Lonn, J.D., Lewis, R.S., and McFaddan, M.D., 2016a, Stratigraphy of the Lemhi subbasin of the Belt Supergroup, *in* MacLean, J.S., and Sears, J.W., eds., Belt Basin: Window to Mesoproterozoic Earth: Geological Society of America Special Paper 522, chapter 5, p. 121–138.

Burmester, R.F., Lewis, R.S., Othberg, K.L., Stanford, L.R., Lonn, J.D., and McFaddan, M.D., 2016b, Geologic map of the western part of the Salmon 30' x 60' quadrangle, Idaho and Montana, Idaho Geological Survey Geologic Map 52, scale 1:75,000.

Conner, J.J., 1991, Some geochemical features of the Blackbird and Jackass zones of the Yellowjacket Formation (middle Proterozoic) in east-central Idaho: U.S. Geological Survey Open-File Report 91-0259-A, 25 p.

Evans, K.V., and Green, G.N., 2003, Geologic map of the Salmon National Forest and vicinity, east-central Idaho: U.S. Geological Survey Geologic Investigations Series Map I-2765, 19 p., scale 1:100,000.

Hobbs, S.W., 1980, The Lawson Creek Formation of Middle Proterozoic age in east-central Idaho: U.S. Geological Survey Bulletin 1482-E, 12 p.

Lewis, R.S., Vervoort, J.D., Burmester, R.F., McClelland, W.C., and Chang, Z., 2007, Geochronological constraints on Mesoproterozoic and Neoproterozoic(?) high-grade metasedimentary rocks of north-central Idaho, U.S.A., *in* Link, P.K., and Lewis, R.S., eds., Proterozoic geology of Western North America and Siberia: Society for Sedimentary Geology Special Publication 86, p. 37–53, doi:10.2110/pec.07.86.0037.

Link, P.K., Fanning, C.M., Lund, K.I., and Aleinikoff, J.N., 2007, Detrital zircons, correlation and provenance of Mesoproterozoic Belt Supergroup and correlative strata of east-central Idaho and southwest Montana, *in* Link, P.K., and Lewis, R.S., eds., Proterozoic Geology of Western North America and Siberia: Society for Sedimentary Geology Special Publication 86, p. 101–128, doi:10.2110/pec.07.86.0101.

Link, P.K., Steele, Travis, Stewart, E.D., Sherwin, J-A., Hess, L.R., and McDonald, Catherine, 2013, Detrital zircons in the Mesoproterozoic upper Belt Supergroup in the Beaverhead and Lemhi Ranges, MT and ID: Northwest Geology, v. 42, p. 39–43.

Link, P.K., Stewart, E.D., Steel, Travis, Sherwin, J-A., Hess, L.T., and McDonald, Catherine, 2016, Detrital zircons in the Mesoproterozoic upper Belt Supergroup in the Pioneer, Beaverhead, and Lemhi Ranges, Montana and Idaho: The Big White arc, *in* MacLean, J.S., and Sears, J.W., eds., Belt Basin: Window to Mesoproterozoic Earth: Geological Society of America Special Paper 522, p. 163–183, doi:10.1130/2016.2522(07).

Lonn, J.D., 2014, The northern extent of the Mesoproterozoic Lemhi Group, Idaho and Montana, and stratigraphic and structural relations with Belt Supergroup strata: Geological Society of America Abstracts with Programs, v. 46, no. 5, p. 72.

Lonn, J.D., Burmester, R.F., Lewis, R.S., and McFaddan, M.D., 2016a, Giant folds and complex faults in Mesoproterozoic Lemhi strata of the Belt

Supergroup, northern Beaverhead Mountains, Montana and Idaho, *in* MacLean, J.S., and Sears, J.W., eds., Belt Basin: Window to Mesoproterozoic Earth: Geological Society of America Special Paper 522, chapter 6, p. 139–162.

Lonn, J.D., Lewis, R.S., Burmester, R.F., and McFaddan, M.D., 2016b, Mesoproterozoic Lemhi strata represent immense alluvial aprons that prograded northwest into the Belt Sea, Idaho and Montana: Geological Society of America Rocky Mountain Section Meeting, Moscow, Idaho: https://gsa.confex.com/gsa/2016RM/webprogram/Paper276082.html

McBean, A.J., II, 1983, The Proterozoic Gunsight Formation, Idaho-Montana: Stratigraphy, Sedimentology, and Paleotectonic Setting: State College, PA, The Pennsylvania State University, M.S. thesis, 235 p.

O'Neill, J.M., Ruppel, E.T., and Lopez, D.A., 2007, Great Divide megashear, Montana, Idaho, and Washington—An intraplate crustal-scale shear zone recurrently active since the Mesoproterozoic: U.S. Geological Survey Open-File Report 2007-1280-A, 10 p.

Ross, C.P., 1947, Geology of the Borah Peak quadrangle, Idaho: Geological Society of America Bulletin, v. 58, p. 1085–1160.

Ross, G.M., and Villeneuve, Mike, 2003, Provenance of the Mesoproterozoic (1.45 Ga) Belt Basin (western North America): Another piece in the pre-Rodinia paleogeographic puzzle: Geological Society of America Bulletin, v. 115, p. 1191–1217, doi:10.1130/B25209.1.

Ruppel, E.T., 1968, Geologic map of the Leadore quadrangle, Lemhi County, Idaho: U.S. Geological Survey Geologic Quadrangle Map GQ-733, scale 1:62,500.

Ruppel, E.T., 1975, Precambrian Y sedimentary rocks in east-central Idaho: U.S. Geological Survey Bulletin 889-A, 23 p.

Ruppel, E.T., 1978, Medicine Lodge thrust system, east-central Idaho and southwest Montana: U.S. Geological Survey Professional Paper 1031, 23 p.

Ruppel, E.T., 1980, Geologic map of the Patterson quadrangle, Lemhi County, Idaho: U.S. Geological Survey Geologic Quadrangle Map GQ-1529, scale 1:62,500.

Ruppel, E.T., 1993, Cenozoic tectonic evolution of southwest Montana and east-central Idaho: Montana Bureau of Mines and Geology Memoir 65, 62 p.

Ruppel, E.T., and Lopez, D.A., 1981, Geologic map of the Gilmore quadrangle, Lemhi County, Idaho: U.S. Geological Survey Geologic Quadrangle Map GQ-1543, scale 1:62,500.

Stewart, E.D., Link, P.K., Fanning, C.M., Frost, C.D., and McCurry, Michael, 2010, Paleogeographic implications of non-North American sediment in the Mesoproterozoic upper Belt Supergroup and Lemhi Group, Idaho and Montana, USA: Geology, v. 38, no. 10, p. 927–930, doi:10.1130/G31194.1. See GSA Data Repository for detailed data.

Tysdal, R.G., 2000, Stratigraphy and depositional environments of middle Proterozoic rocks, northern part of the Lemhi Range, Lemhi County, Idaho: U.S. Geological Survey Professional Paper 1600, 40 p.

Tysdal, R.G., Lindsey, D.A., Lund, K.I., and Winkler, G.R., 2005, Alluvial facies, paleocurrents, and source of the Mesoproterozoic Gunsight Formation, east-central Idaho and southwestern Montana, Chapter B, *in* J.M. O'Neill and R.G. Tysdal, eds., Stratigraphic studies in southwestern Montana and adjacent Idaho–Lower Tertiary Anaconda Conglomerate and Mesoproterozoic Gunsight Formation: U.S. Geological Survey Professional Paper 1700-B, p. 21–39.

Umpleby, J.B., 1913, Geology and ore deposits of Lemhi County, Idaho: U.S. Geological Survey Bulletin 528, 182 p.

Winston, Don, Link, P.K., and Hathaway, Nate, 1999, The Yellowjacket is not the Prichard and other heresies–Belt Supergroup correlations, structure, and paleogeography, east-central Idaho, *in* S.S. Hughes, and G.D. Thackray, eds., Guidebook to the geology of eastern Idaho: Pocatello, Idaho Museum of Natural History, p. 3–20.

ZIRCON U-PB AND LU-HF ANALYSIS OF BASEMENT ROCKS AT BLOODY DICK CREEK AND MAIDEN PEAK, SOUTHWESTERN MONTANA: A RECORD OF PALEO-PROTEROZOIC AND ARCHEAN PLUTONISM AND METAMORPHISM

David M. Pearson, Nathan D. Anderson, Paul K. Link

Idaho State University, Pocatello, Idaho

ABSTRACT

Zircon U-Pb analysis of three samples of quartzofeldspathic gneiss collected from near Maiden Peak in southwestern Montana found two distinct zircon age populations. Zircon cores from one sample yield an age of 2,790 ± 23 Ma, whereas metamorphic rims are 2,495 ± 20 Ma. Two other samples returned Paleoproterozoic (2,477 ± 25 Ma and 2,483 ± 23 Ma) U-Pb zircon crystallization ages with no apparent metamorphic overgrowths. Neoarchean zircon cores yield initial εHf values of 0 to -6 and Paleoproterozoic zircons yield initial εHf values of +2 to -3. Approximately 30 km to the northwest, southwest of Bloody Dick Creek, an additional quartzofeldspathic gneiss yielded 2,438 ± 20 Ma zircon cores and initial εHf values of +1 to -4, both of which are similar to Paleoproterozoic ages obtained from near Maiden Peak. However, U-Pb zircon analysis of the sample south of Bloody Dick Creek also identified 1,759 ± 15 Ma metamorphic rims. Felsic orthogneiss that crops out north of Bloody Dick Creek at the northern limit of basement exposure yielded a zircon U-Pb age of 1,802 ± 17 Ma with no apparent metamorphic rims. These zircons yielded initial εHf values of +3 to -3. Similarities in U-Pb ages and Lu-Hf isotopic composition (initial εHf values of +2 to -4) for the gneisses in the Bloody Dick and Maiden Peak areas suggests that they fundamentally belong to the same basement province. Ages of ~2,800 Ma, ~2,400–2,500 Ma, and ~1,800 Ma are also very similar to published ages from the Ruby Range ~70 km to the northeast, on the northwestern edge of the Wyoming craton.

INTRODUCTION

This work seeks to constrain the age and isotopic character of gneisses exposed adjacent to Bloody Dick Creek and near Maiden Peak in Beaverhead County, Montana (figs. 1 and 2). To this end, samples were collected in the context of field mapping for U-Pb and Lu-Hf isotopic analysis as a part of an M.S. thesis at Idaho State University (Anderson, 2017). Most previous workers have interpreted the Bloody Dick and Maiden Peak gneisses to be Archean in age (Geach, 1972; Coppinger, 1974; Hansen, 1983), possibly associated with other regional exposures of Archean basement rock of the Wyoming craton across southwestern Montana (VanDenburg and others, 1998). However, new U-Pb zircon results from rocks near Bloody Dick Creek indicate the presence of 1800–1900 Ma mag-

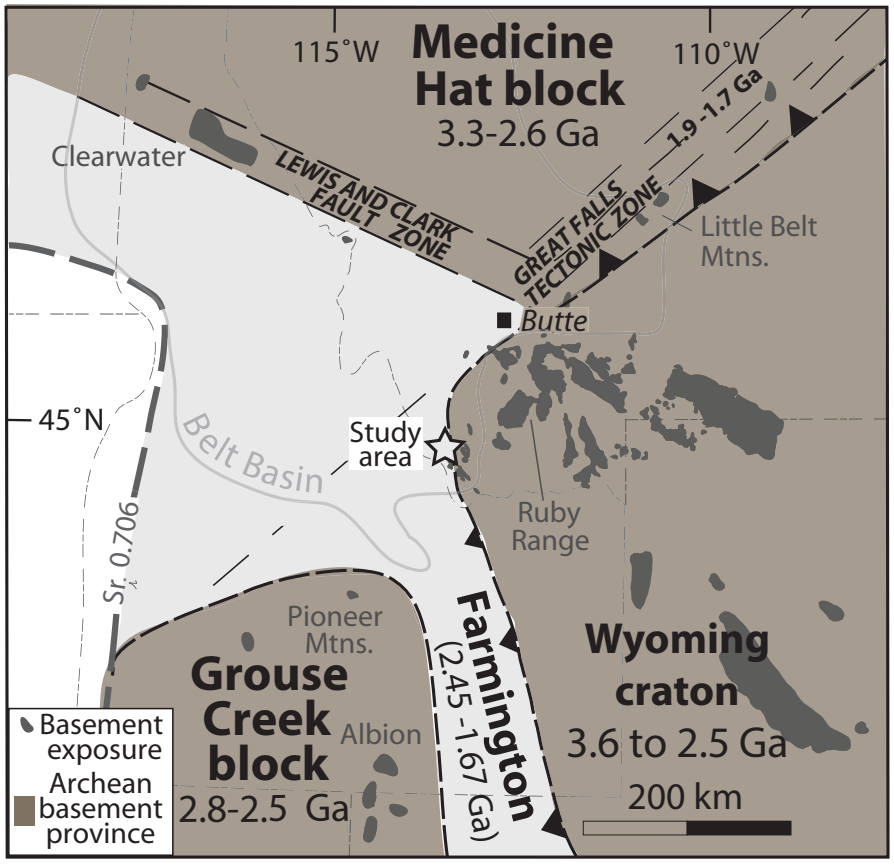

Figure 1. Study area in the context of the basement framework of the northern Rockies (modified from Link and others, in press).

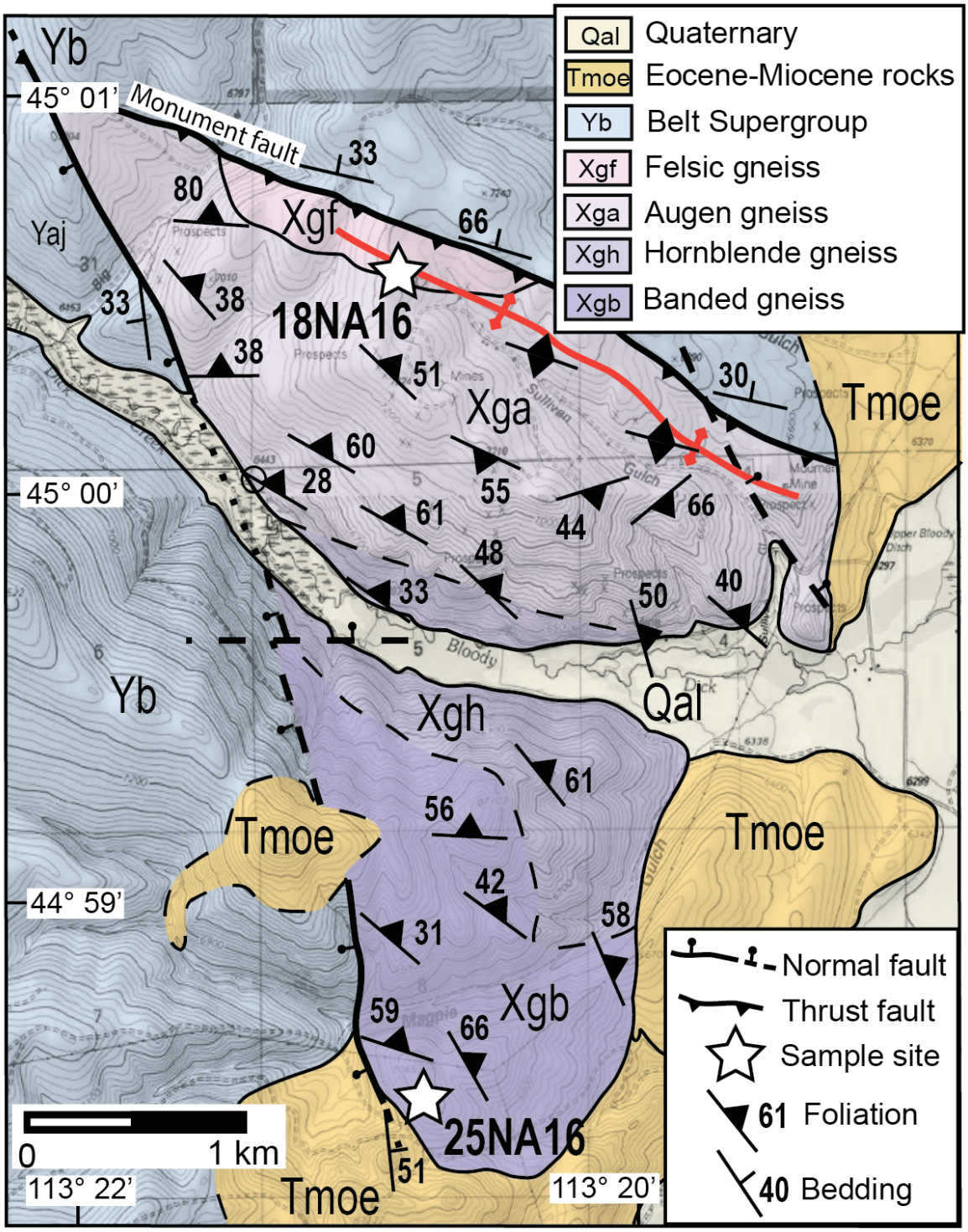

Figure 2. Geologic map of basement outcrop and surrounding area near Bloody Dick Creek in southwestern Montana (modified from Anderson, 2017).

matism and metamorphism (Mueller and others, 2016; Sherwin and others, 2016), which is similar to isotopically juvenile magmatism from ~1,860 to 1,790 Ma within the Great Falls tectonic zone, which culminated with the collision of the Wyoming craton with the Medicine Hat block to the north (Mueller and others, 2002; Harms and others, 2004; Foster and others, 2006; Mueller and others, 2016). However, the southwestern projection of the Great Falls tectonic zone into southwest Montana and eastern Idaho is limited by rare basement exposures. Thus, gneisses exposed near Bloody Dick Creek and Maiden Peak have the potential to further constrain the spatial distribution of the Great Falls tectonic zone and the greater basement framework of the northern Rocky Mountains.

GEOLOGIC SETTING

The Wyoming craton is an Archean crustal block discontinuously exposed in basement uplifts across southwest Montana and much of Wyoming (fig. 1). Prior high-temperature geo- and thermochronometry constrained several episodes of magmatism and high-grade metamorphism within the northwestern portion of the Wyoming craton, including the Beartooth orogeny at ~2,780 Ma (Wooden and Mueller, 1988) and the Tendoy/Beaverhead orogeny at 2,500–2,400 Ma (Kellogg and others, 2003; Jones, 2008; Cramer, 2015). This was followed by 1,860–1,790 Ma magmatism that defines the northeast-trending Great Falls tectonic zone of western Montana (fig. 1), which was hypothesized to result from arc-related magmatism on the southeastern margin of the Medicine Hat block above a northwest-dipping oceanic slab prior to collision with the northwestern Wyoming craton (Mueller and others, 2002; Harms and others, 2004; Foster and others, 2006; Mueller and others, 2016). Subsequent collision of the Medicine Hat block and Wyoming craton occurred at 1,790–1,720 Ma and resulted in high-grade metamorphism, deformation, and partial melting during the Big Sky orogeny (Harms and others, 2004; Jones, 2008; Cramer, 2015; Condit and others, 2015; Mueller and others, 2016). Though recent results from the Bloody Dick Creek area suggest that Paleoproterozoic magmatism and metamorphism is also reflected by basement rocks within extreme southwestern Montana (Mueller and others, 2016; Sherwin and others, 2016), the age of framework rocks and the relationship of these rocks to the existing basement framework of southwestern Montana are poorly constrained.

METHODS

A total of five samples from southwestern Montana were selected for U-Pb zircon dating and Lu-Hf isotopic analysis in the context of field mapping. Three samples were collected from near Maiden Peak in the northern Tendoy Range, and two others were collected near Bloody Dick Creek in the Beaverhead Mountains. The separation process was undertaken at Idaho State University using standard crushing techniques. U-Pb analysis was completed at the Arizona LaserChron Center at the University of Arizona by Laser Ablation-Inductively Coupled Plasma-Mass Spectrometry using methods described in Gehrels and others (2009). Lu-Hf analysis of four zircon samples followed procedures described by Cecil and others (2011). Target locations were selected for U-Pb and Lu-Hf analysis based on zoning observed in Back-Scattered Electron (BSE) images. $^{207}Pb/^{206}Pb$ ratios are reported here. Individual analyses that were more than 10% discordant were excluded from the results and not used in subsequent interpretations of U-Pb ages. Additional mineral separation procedures and analytical details can be found in Anderson (2017).

RESULTS AND DISCUSSION

U-Pb Zircon Geochronology

Textural observations and mineral abundances of the three samples of gneiss collected for U-Pb and Lu-Hf analysis from near Maiden Peak suggest igneous protoliths of the following compositions: (1) hornblende granodiorite (04NA16); (2) granite (03NA16); and (3) biotite–hornblende diorite (02NA16). Locations can be found in table 1. At Bloody Dick Creek, samples of two lithologies were collected for U-Pb and Lu-Hf analysis, and on the basis of textural and compositional criteria, both likely had igneous protoliths: (1) hornblende–biotite tonalite (25NA16; banded gneiss of fig. 2); and (2) porphyritic biotite tonalite (18NA16; felsic gneiss of fig. 2). For more detailed sample descriptions and BSE images, see Anderson (2017).

The samples collected from near Maiden Peak display the oldest U-Pb zircon ages obtained here (fig. 3). Sample 04NA16 displays a spread of U-Pb ages that are mostly concordant. The oldest ages come from zircon cores and are concordant at 2,790 ± 23 Ma (n=8; 2σ error including external error and analytical

Table 1. Location information for U-Pb and Lu-Hf samples.

Sample ID	UTM Easting (Z12)	UTM Northing (Z12)	Lat (north)	Long (West)	Elev (ft)
02NA16	32882	49717	44.8786	113.1673	7,885
03NA16	32902	49720	44.8818	113.1648	7,830
04NA16	32861	49754	44.9115	113.1712	8,195
18NA16	31500	49867	45.0102	113.3476	7,185
25NA16	31505	49829	44.9758	113.3456	7,003

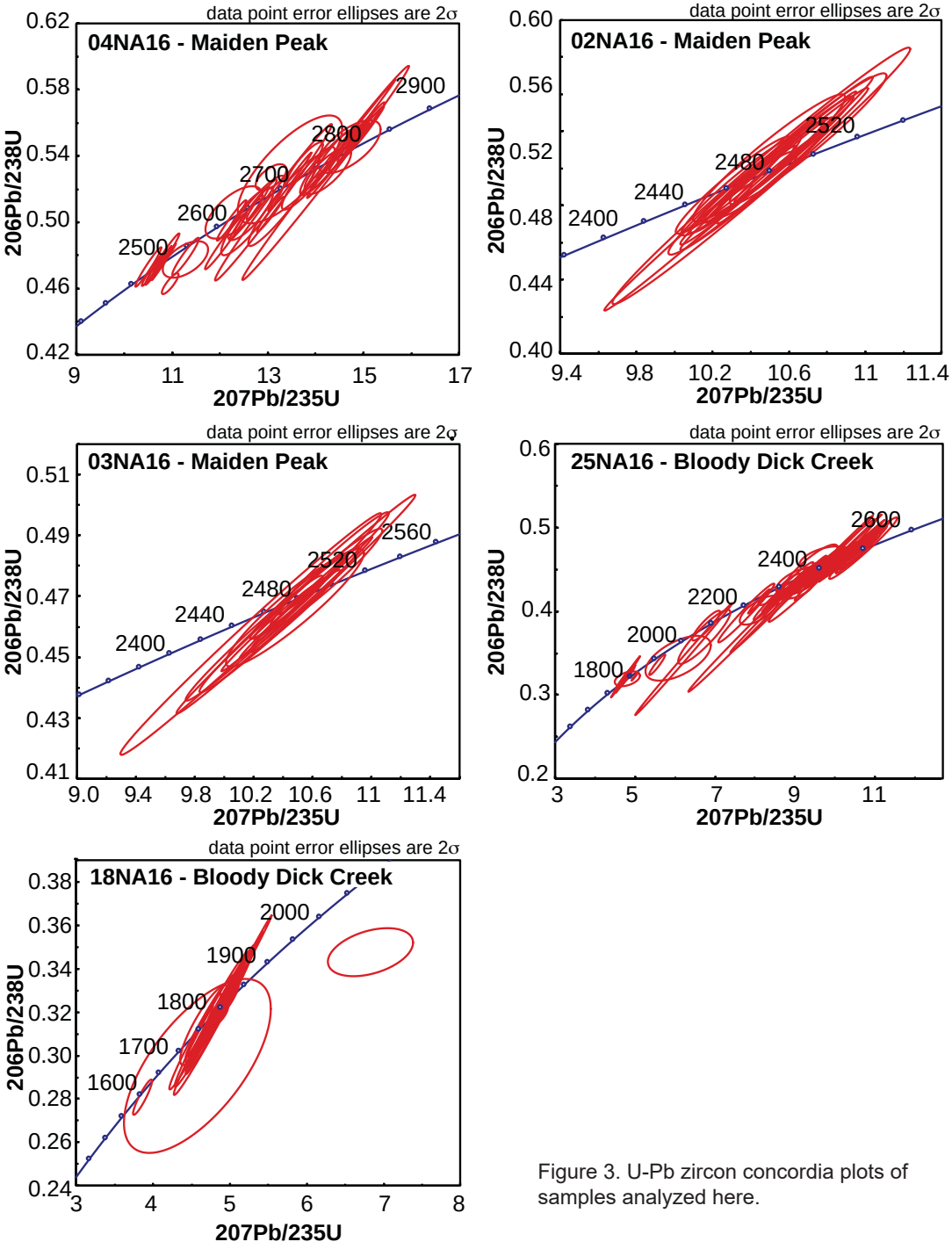

Figure 3. U-Pb zircon concordia plots of samples analyzed here.

uncertainty here and henceforth); the youngest analyses were obtained from zircon rims and are concordant at d (n=4). These ages appear to define lower and upper intercepts of a Pb-loss spectrum, with Pb-loss occurring at ~2,495 Ma. Seven of the rim analyses that yield the younger dates were also found to have U/Th ratios greater than 10, suggesting a metamorphic origin. Thus, these results suggest crystallization of the gneiss' protolith at ~2,790 Ma and metamorphism at ~2,495 Ma. Samples 03NA16 and 02NA16, also collected from near Maiden Peak, had indistinguishable zircon core and rim dates, yielding ages of 2,483 ± 23 Ma (n=29) and 2,477 ± 25 Ma (n=28), respectively. Thus, U-Pb zircon results from the Maiden Peak area suggest magmatism at ~2,790 Ma and magmatism and high-grade metamorphism at 2477-2495 Ma.

Sample 25NA16, collected south of Bloody Dick Creek (fig. 2), yielded a spread of ages with a coherent group of concordant ages defining an upper limit of 2,438 ± 20 Ma (n=73; fig. 3). This older population of ages was taken from zircon cores that display oscillatory zoning in BSE images. A lesser number of analyses (n=7), derived exclusively from zircon rims, yielded a weighted mean age of 1,759 ± 15 Ma and define an apparent lower intercept on the concordia plot. We interpret these results to reflect ~1,759 Ma high-grade metamorphism of an older ~2,438 Ma, Paleoproterozoic protolith. We note that the older zircon growth event at ~2,438 Ma is similar to the younger U-Pb zircon analyses from orthogneisses in the Maiden Peak area. The last sample analyzed here, which was collected from north of Bloody Dick Creek (18NA16), yielded a U-Pb zircon age of 1,802 ± 17 Ma (n=38). Zircons from this sample are euhedral, oscillatory-zoned, and lack any zircon core and rim morphologies.

Lu-Hf Isotopic Analysis

Lu-Hf analyses of Neoarchean zircons from sample 04NA16 from near Maiden Peak yield initial εHf values of 0 to -6 (fig. 4). These data yield a model age of ~3,260 Ma. In contrast, Paleoproterozoic zircons (samples 02NA16 and 03NA16) yield initial εHf values of +2 to -3 and a younger model age of uncertain significance. Initial εHf values of ~2,438 Ma gneisses south of Bloody Dick Creek (25NA16) are +1 to -4. Initial εHf values of the 1,802 ± 17 Ma orthogneiss north of Bloody Dick Creek are +3 to -3. Overall, these data are consistent with a model for petrogenesis of the rocks near Maiden Peak and Bloody Dick Creek with contributions of isotopically juvenile material at ~3,260 Ma, ~1,802 Ma, and possibly ~2,475 Ma (fig. 4).

Regional Implications

Current models of the Greats Falls orogeny constrain the timing of subduction-related arc magmatism to between ca. 1,860 Ma and 1,790 Ma (Harms and others, 2004; Mueller and others, 2016) and the initiation of continental collision to 1,790–1,780 Ma (Big Sky orogeny) (Cheney and others, 2004; Foster and others, 2006; Condit and others, 2015; Mueller and others, 2016). Given the hypothesized northwest dip to the subduction zone (Gorman and others, 2002; Harms and others, 2004), associated arc magmatism is thought to have been confined to the southeastern margin of the overriding Medicine Hat block (Foster and others, 2006).

Current U-Pb and Lu-Hf results indicate remobilization of older (~3,260 Ma) continental lithosphere during magmatism at ~2,790 Ma, as well as magmatism and metamorphism at ~2,480 Ma, and 1,700–1,800 Ma. Lu-Hf results obtained from one orthogneiss north of Bloody Dick Creek (sample 18NA16) suggest input of an isotopically juvenile component at ca. 1,802 Ma. Similar results from the Little Belt Mountains of the Great Falls tectonic zone also indicate that ca. 1,860 Ma plutons were derived from an isotopically juvenile source. The similarity of the current results to gneisses from the Little Belt Mountains of the Great Falls tectonic zone suggests that the Great Falls tectonic zone projects into southwest Montana at least as far as the Bloody Dick gneiss, 8 km east of the Idaho state line.

The Maiden Peak and Bloody Dick gneiss units contain U-Pb zircon ages and initial Hf isotopic values that suggest that several samples are part of the Archean Wyoming craton (affected by the 2,780 Ma Beartooth orogeny), Farmington zone (affected by the 2,550 to 2,455 Ma Tendoy orogeny), and the Great Falls tectonic zone (affected by 1,790 to 1,720 Ma Big Sky orogeny). Given these similarities (see Cramer, 2015 for a review), this suggests that if the Little Belt arc was indeed constructed on the southeastern margin

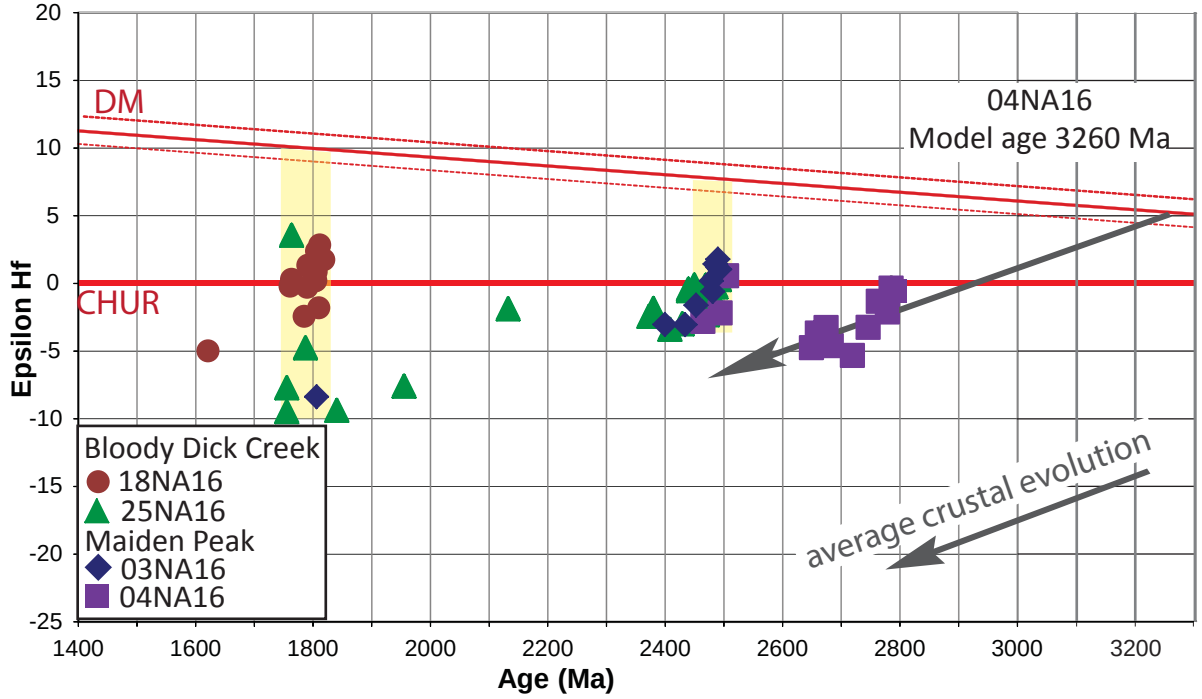

Figure 4. εHf values of samples analyzed in this study from near Bloody Dick Creek and Maiden Peak, southwestern Montana. Yellow boxes indicate likely episodes of juvenile isotopic input of material.

of the Medicine Hat block (e.g., Foster and others, 2006), this magmatic arc may have formed within a rifted fragment of the Wyoming craton (Harms and others, 2004).

CONCLUSIONS

Within the Tendoy Range of southwest Montana, U-Pb zircon analysis of quartzofeldspathic gneiss near Maiden Peak found two distinct zircon age populations. Within one sample (04NA16), the oldest zircons were dated to 2,790 ± 23 Ma (interpreted to have formed during the Beartooth orogeny), with 2,495 ± 20 Ma metamorphic rims attributed to plutonism and metamorphism during the Tendoy orogeny. Two other samples (02NA16 and 03NA16) of quartzofeldspathic gneiss from Maiden Peak returned unimodal U-Pb zircon crystallization ages of 2,477 ± 25 Ma and 2,483 ± 23 Ma. These two dates are encompassed in the ~2,495 Ma metamorphic age peak (rims) from sample 04NA16, which is interpreted to indicate that magmatism in samples 02NA16 and 03NA16 was concurrent with metamorphism during the Tendoy orogeny. All three of these gneisses are interpreted as being derived from an igneous protolith.

Several lines of evidence suggest original igneous protoliths for both gneiss samples from the Bloody Dick Creek area, including: unimodal zircon populations with younger, metamorphic overgrowths, the lack of pelitic minerals, and abundance of minerals indicative of an originally igneous protolith (e.g., abundant feldspar that is up to 1 cm). The oldest unit is the banded gneiss (25NA16), which contains 2,438 ± 20 Ma zircon cores and 1,759 ± 15 Ma metamorphic rims with high U/Th ratios. These rocks thus share similar U-Pb zircon ages of 2,400–2,500 Ma with some rocks studied from the Maiden Peak area. This is interpreted as evidence for correlation between the banded gneiss of the Bloody Dick unit and quartzofeldspathic gneiss in Maiden Peak. An additional sample at Bloody Dick Creek yielded a U-Pb zircon age of 1,802 ± 17 Ma; Lu-Hf isotopic analysis suggests input of isotopically juvenile material at that time.

Similarities in U-Pb and Lu-Hf isotopic values of ~2,400–2,500 Ma gneisses in the Bloody Dick gneiss and quartzofeldspathic gneiss from Maiden Peak suggests that they fundamentally belong to the same basement province. Younger felsic orthogneisses within the Bloody Dick gneiss are Paleoproterozoic in age and suggest contribution of isotopically juvenile material at crystallization (initial εHf values of +3 to -7), which is similar to rocks from the Little Belt Mountains. Those rocks were interpreted to have formed during arc magmatism above the northwest-dipping subduction of oceanic lithosphere beneath the Medicine Hat block during the 1,860 to 1,790 Ma Great Falls orogeny. This correlation of arc-related rocks between the Little Belt Mountains and the Bloody Dick gneiss suggests that the Great Falls tectonic zone projects into southwest Montana at least as far as the Bloody Dick gneiss. This work also establishes the basement framework into which some isotopically juvenile rocks of the Great Falls tectonic zone were intruded, which has strong affinities to the Wyoming craton.

REFERENCES CITED

Anderson, N.D., 2017, The Bloody Dick and Maiden Peak gneisses, southwest Montana: Implications for Archean and Paleoproterozoic basement framework: Pocatello, Idaho State University, M.S. thesis, 129 p., 1 plate.

Cecil, M.R., Gehrels, G., Ducea, M.N., and Patchett, P.J., 2011, U-Pb-Hf characterization of the central Coast Mountains batholith: Implications for petrogenesis and crustal architecture: Lithosphere, v. 3, no. 4, p. 247–260.

Cheney, J.T., Webb, A., Coath, C., and McKeegan, K., 2004, In situ ion micro-probe 207 Pb/ 206 Pb dating of monazite from Precambrian metamorphic rocks, Tobacco Root Mountains, Montana, *in* Brady, J.B., Burger, H.R., Cheney, J.T., and Harms, T.A., eds., Precambrian Geology of the Tobacco Root Mountains, Montana: Geological Society of America Special Paper 377, p. 151–179.

Condit, C.B., Mahan, K.H., Ault, A.K., and Flowers, R.M., 2015, Foreland-directed propagation of high-grade tectonism in the deep roots of a Paleoproterozoic collisional orogen, SW Montana, USA: Lithosphere, v. 7, p. 625–645.

Coppinger, W., 1974, Stratigraphy and structural study of Belt Supergroup and associated rocks in a portion of the Beaverhead Mountains, southwestern Montana and east-central Idaho: Oxford, Ohio, Miami University, Ph.D. dissertation, 224 p.

Cramer, M., 2015, Proterozoic tectonometamorphic evolution of the Ruby Range, SW Montana, USA:

Insights from phase equilibria modeling and in situ monazite petrochronology: University of Montana, Missoula, M.S. thesis, 120 p.

Foster, D.A., Mueller, P.A., Mogk, D.W., Wooden, J., and Vogl, J.J., 2006, Proterozoic evolution of the western margin of the Wyoming craton: Implications for the tectonic and magmatic evolution of the northern Rocky Mountains: Canadian Journal of Earth Sciences, v. 43, p. 1601–1619.

Geach, R.D., 1972, Mines and mineral deposits (except fuels) Beaverhead County, Montana: Montana Bureau of Mines and Geology Bulletin 85, 194 p.

Gehrels, G., Rusmore, M., Woodsworth, G., Crawford, M., Andronicos, C., Hollister, L., Patchett, J., Ducea, M., Butler, R., Klepeis, K., Davidson, C., Friedman, R., Haggart, J., Mahoney, B., Crawford, W., Pearson, D., and Girardi, J., 2009, U-Th-Pb geochronology of the Coast Mountains batholith in north-coastal British Columbia: Constraints on age and tectonic evolution: Geological Society of America Bulletin, v. 121, no. 9-10, p. 1341–1361.

Gorman, A.R., Clowes, R.M., Ellis, R.M., Henstock, T.J., Spence, G.D., Keller, G.R., Levander, A., Snelson, C.M., Burianyk, M.J.A., Kanasewich, E.R., Asudeh, I., Hajnal, Z., and Miller, K.C., 2002, Deep probe: Imaging the roots of western North America: Canadian Journal of Earth Sciences, v. 39, p. 375–398.

Hansen, P.M., 1983, Structure and stratigraphy of the Lemhi Pass area, Beaverhead Range, southwest Montana and east-central Idaho: University Park, Penn., The Pennsylvania State University, M.S. thesis, 112 p.

Harms, T.A., Brady, J.B., Burger, H.R., and Cheney, J.T., 2004, Advances in the geology of the Tobacco Root Mountains, Montana, and their implications for the history of the northern Wyoming Province, *in* Brady, J.B., Burger, H.R., Cheney, J.T., and Harms, T.A., eds., Precambrian geology of the Tobacco Root Mountains, Montana: Geological Society of America Special Paper 377, p. 227–243.

Jones, C., 2008, U-Pb geochronology of monazite and zircon in Precambrian metamorphic rocks from the Ruby Range, SW Montana: Deciphering geological events that shaped the NW Wyoming province: Kent State University, Ohio, M.S. thesis, 119 p.

Kellogg, K.S., Snee, L.W., and Unruh, D.M., 2003, The Mesoproterozoic Beaverhead Impact structure and its tectonic setting, Montana-Idaho: $^{40}Ar/^{39}Ar$ and U/Pb isotopic constraints: Journal of Geology, v. 111, p. 639–652.

Link, P.K., Autenrieth-Durk, K.M., Cameron, A., Fanning, C.M., Vogl, J.J., and Foster, D.A., in press, U-Pb zircon ages of Wildhorse Creek, Pioneer Mountains, south-central Idaho, and tectonic implications: Geosphere.

Mueller, P.A., Heatherington, A.L., Kelly, D.M., Wooden, J.L., and Mogk, D.W., 2002, Paleoproterozoic crust within the Great Falls tectonic zone: Implications for the assembly of southern Laurentia: Geology, v. 30, p. 127–130.

Mueller, P.A., Mogk, D.W., Wooden, J., and Spake, D., 2016, U-Pb ages of zircons from the Lower Belt Supergroup and proximal crystalline basement: Implications for the early evolution of the Belt Basin, *in* MacLean, J.S., and Sears, J.W., eds., Belt Basin: Window to Mesoproterozoic Earth: Geological Society of America Special Paper 522, p. 283–303.

Sherwin, J.A., Younggren, E.B., Link, P.K., and Gaschnig, R.M., 2016, Geologic map of the Coyote Creek 7.5' quadrangle, southwest Montana: Montana Bureau of Mines and Geology Geologic Map 67, scale 1:24,000.

Wooden, J., and Mueller, P.A, 1988. Pb, Sr, and Nd isotopic compositions of a suite of Late Archean, igneous rocks, eastern Beartooth Mountains: Implications for crust-mantle evolution, Earth and Planetary Sciences Letters, v. 87, p. 59–72.

A GEODYNAMIC MODEL FOR GRAVITY-DRIVEN EXTENSION—IMPLICATIONS FOR THE CENOZOIC EVOLUTION OF SOUTHWESTERN MONTANA

Kevin Lielke

Independent Geologist, Ennis, MT 59729

INTRODUCTION

The transition from Cretaceous compression to Cenozoic extension represents the most important tectonic event in the northern Rocky Mountains over the last 60 m.y. However, in southwestern Montana, many of the details of the initiation and evolution of Cenozoic extension remain poorly understood. The oldest theories posited an early Cenozoic beginning of extension within the boundaries of present-day intermontane basins (Fields and others, 1985; Hanneman, 1989; Hanneman and Wideman, 1991; Pardee, 1950). An alternative theory endorses a tectonically quiescent, largely featureless Paleogene "Renova basin" which was dissected by extension beginning in the middle Miocene (Sears and others, 1995; Sears and Fritz, 1998; Sears and Thomas, 2007). If this singular Paleogene Renova basin existed, it did so in a regional tectonic framework that included extensive contemporaneous volcanism and extension outside of its boundaries (Foster and others, 2010; Luedke, 1994). Recently, it has been suggested that relict Cretaceous paleotopography and Paleogene volcanic activity within the Renova basin, along with alterations to the physical properties of the underlying lithosphere, played an important role in the development of Cenozoic extension and sedimentation (Lielke, 2008, 2010; Rothfuss and others, 2012). Early Oligocene paleoelevation estimates suggest that the Renova basin may have been a relatively high (1.5–2.5 km) altitude sedimentary depocenter—possibly a remnant of an extensive Cretaceous altiplano (Lielke and others, 2012). The boundaries of this proposed Renova plateau are: in the north, the southwestern Montana transverse zone; to the west, the leading edge of the Sevier fold and thrust belt; the southern edge is obscured by younger volcanics; and the Beartooth plateau may represent its eastern extension. The purpose of this study is twofold: (1) to examine the viability of body forces internal to the lithosphere as the primary driving force of Cenozoic extension, and (2) to test the theory that alterations to the physical properties of the lithosphere are adequate to explain the existence of a stable, possibly high-elevation, Renova depocenter and its subsequent dismemberment owing to the destabilizing effects of the Yellowstone hotspot.

Southwestern Montana is underlain by the northwestern corner of the Archean Wyoming province craton. Cratons are generally characterized by stable, thick (>200 km) lithosphere largely undeformed since Precambrian time. However, the Wyoming province has been substantially modified by Cretaceous and Cenozoic aged orogenic and thermal events. From an analysis of passive source seismic data, Dave and Li (2016) calculated an average Wyoming province lithospheric thickness of only 150 km. Pervasive modification of the Wyoming province lithosphere is linked primarily to Cretaceous subduction and orogenesis and, on a smaller scale, to localized anomalies such as the Yellowstone hotspot currently situated beneath the northwestern corner of Wyoming (Jones and others, 2015). However, the effect of the middle Miocene outbreak of the Yellowstone hotspot on the physical properties of the Wyoming craton, and its tectonic implications, is not well understood. The middle Miocene (17–20 Ma) was a period of major tectonic reorganization throughout western North America, including Basin and Range extension, a widespread angular unconformity in western Montana, initiation of the Yellowstone hotspot and Snake River Plain volcanism, outbreak of the Columbia River and Steens Mountain flood basalts, emplacement of the Monument and Chief Joseph dike swarms, formation of the Oregon–Nevada lineament, and extension in the Rio Grande rift (Chapin and Cather, 1994; Liu and Shen, 1998; Sears and Thomas, 2007). In southwestern Montana, rapid extension occurred in a series of predominately N–NE-trending half-grabens, forming a prominent angular unconformity between Paleogene and Neogene sediments (Sears and Fritz, 1998; Sears and Thomas, 2007). It seems probable that the Yellowstone hotspot influenced the physical properties of the portion of the Wyoming province underlying southwestern Montana and that its initial outbreak served as a triggering event for the hypothesized middle Miocene breakup of the

previously stable Renova basin.

Sears and others (2009) attribute middle Miocene tectonism to radial extension across the top of a broad structural dome above the Yellowstone hotspot. However, the 400 to 500 km distance from southwestern Montana to the site of the initial outbreak in southeastern Oregon would appear to preclude a significant increase in elevation due to dynamic topography (Condie, 2001; Griffiths and Campbell, 1991). In the scenario expounded below, the driving mechanism for middle Miocene extension is stored gravitational potential energy (GPE) released by alteration of the physical properties of the Wyoming craton, specifically a decrease in the depth of isostatic compensation coupled with an increase in the geotherm. Heating accompanied by thermo-mechanical erosion of the cratonic mantle is an expected consequence of convection in the asthenosphere, especially along the boundaries associated with mantle heterogeneities (Davies, 1994; Liu and Shen, 1998; Moore and others, 1999; Wannamaker and others, 2001). Geodynamic analysis of lithosphere models can test the validity of this proposed driving mechanism and make testable predictions concerning the values of crustal thickness, paleoelevation, and geotherm parameters consistent with gravity-driven extension. The model developed below assumes that Cenozoic deformation in the northern Rockies was driven principally by gravitational body forces inherent to the lithosphere and attempts to replicate the pattern of deformation using the most conservative estimates of alterations to physical parameters.

GEODYNAMIC MODEL

Gravitational potential energy (GPE) can be defined as the depth integrated vertical stress from a topographic surface down to a common-depth reference level (Ghosh and others, 2009). Isostatic equilibrium between two lithospheric columns requires that the pressure at this reference level, generally assumed to correspond to the base of the lithosphere, be equal (Sonder and Jones, 1999). The difference in gravitational potential energy (ΔPE) between a lithospheric column and a reference column in isostatic equilibrium indicates the state of stress, compression or tension, acting upon the lithosphere (Sonder and Jones, 1999). In this study the asthenosphere geoid, the height the asthenosphere would rise to without an overlying lithosphere, is used for the reference column (Turcotte and others, 1977; Zoback and Mooney, 2003). This abstract standard was chosen in order to provide a single consistent basis of comparison that is not area or time specific. The ΔPE model used in this study consists of a two-layer lithosphere incorporating surface topography (fig. 1), coupled with a geotherm determined by two inputs: basal heat flow (Q) and radiogenic heat production (A). Since radiogenic minerals are disproportionately concentrated in the crust, mantle heat production is assumed to be zero. The density profile of this model is therefore the density due to lithology modified by thermal expansion. Given a set of initial parameters for the depth of isostatic compensation and the geotherm, ΔPE is calculated from the equation (modified from Jones, Sonder and Unruh, 1998):

$$\Delta PE = \int_{H0}^{z2} \rho_a\, g z dz - [\int_{-\varepsilon}^{z1} \rho_{c0}\,(1-(\alpha T_c\, z_1/2z_2))\, g\, zdz + \int_{z1}^{z2} \rho_{m0}\,(1-(\alpha T_m/2)-(\alpha T_m z_1/2z_2))\, g\, zdz], \quad (1)$$

where the crust and mantle components of the geotherm are determined by (Fowler, 1994):

$$T_c = A(\boldsymbol{\varepsilon^2} - \boldsymbol{z^2})/2\boldsymbol{k_1} + (Q/\boldsymbol{k_2} + Az/\boldsymbol{k_1})\,(z+\varepsilon). \quad (2)$$

$$T_m = Qz/\boldsymbol{k_2} + (A\,(\boldsymbol{\varepsilon^2} + \boldsymbol{z^2})/2\boldsymbol{k_1} + (Az/\boldsymbol{k_1} + Q/\boldsymbol{k_2})\,\varepsilon). \quad (3)$$

In the above equations, Ho = 2780 m and $\boldsymbol{\rho_a}$ = 3150 kg/m^3, the coefficient of thermal expansion α = 3.28 x 10^{-5}/°C, the gravitational constant g = 9.81 m/s^2, thermal conductivity is k_1 = 2.75 W/m°C for the crust and k_2 = 3.75 W/m°C for the mantle, and $\boldsymbol{\rho_{c0}}$ and $\boldsymbol{\rho_{m0}}$ are zero pressure average density for the crust (2780 kg/m^3) and top of the mantle average rock density (3350 kg/m^3), respectively.

The results of a ΔPE analysis can be illustrated by plots showing fields of tension and compression for each possible matched pair of crustal thickness and paleoelevation. The positive ΔPE field gives the range of these values for which extensional deformation is theoretically possible. The vertically averaged deviatoric stress ($\Delta\sigma_{xx}$) exerted by one lithospheric column upon the other can be calculated by dividing ΔPE by the total lithospheric thickness (Sonder and Jones, 1999). This stress represents the non-lithostatic force available to drive deformation (Turcotte and Schubert, 2002). Extension is predicted to occur if the tensional deviatoric stress exerted upon the lithosphere is of

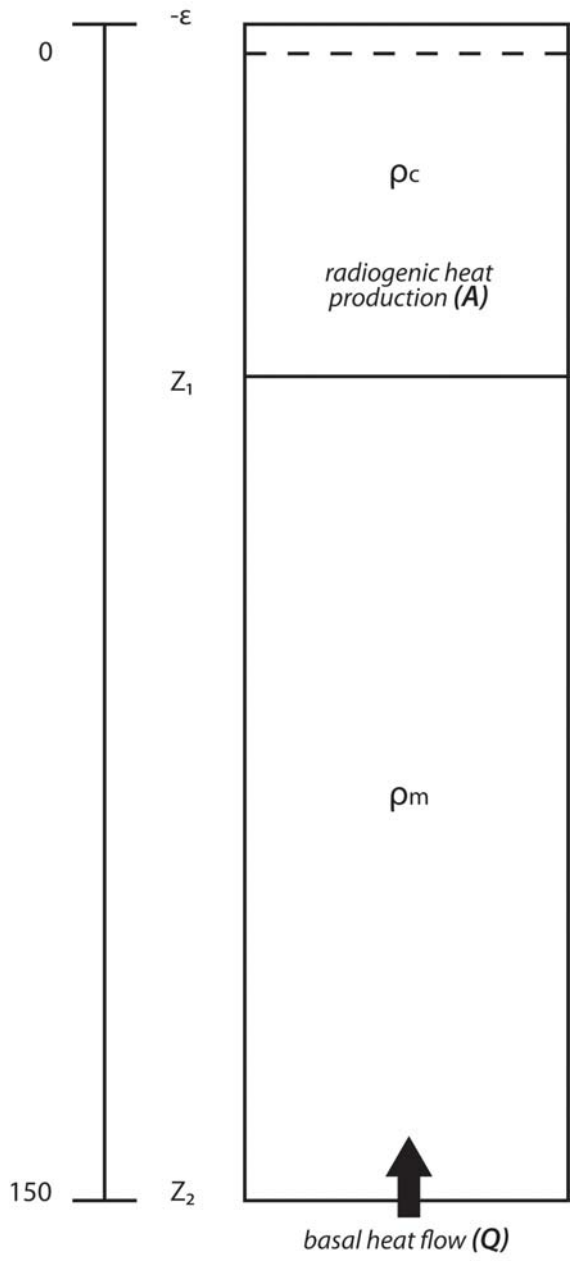

Figure 1. Two-layer lithosphere model incorporating surface elevation (ε) and a geotherm with two inputs—radiogenic heat production (A) and base of lithosphere heat flow (Q). Z1 is the base of the crust and Z2 is the isostatic compensation depth.

sufficient magnitude to overcome the inherent strength of the lithosphere as well as any external resisting forces; for example, plate tectonic boundary forces. These predications can be tested against the geologic record if proxy data for crustal thickness (restored balanced cross sections, subsurface seismic data) and paleoelevation (plant fossil and stable isotope estimates) are available. Three end member models were used in order to investigate the effect of lithosphere properties on tectonic regime: Model A is a thin and hot lithosphere (150 km thick and .035 W/m^2 heat flow (Q) into base of lithosphere), model B is thin and cool (150 km and .025 W/m2) and model C is thick and cool (180 km and .025 W/m^2). Isostatic compensation depth varies, but along the geologically active western margin of North America, a value in the range of 150 to 180 km is a reasonable estimate (Zoback and Mooney, 2003; Zurek and Dueker, 2005). The results of ΔPE analysis are shown in figures 2, 3 and 4.

Examination of the plots for models A–C indicates that differences in lithospheric properties can lead to differences in the predicted tectonic behavior. A thick and cool lithosphere (model C) is capable of supporting a thicker crust and higher paleoelevations than either of the two thin lithosphere models. Similarly, decreasing the heat flux (Q) at the base of the 150-km-thick lithosphere by .01 W/m^2 (model B) permits a thicker, higher elevation crust compared to model A. Applying these theoretical results to the question of a stable Renova depocenter shows that if the Wyoming craton underlying Paleogene southwestern Montana was thicker and colder than the neighboring lithosphere underlying the Sevier fold and thrust belt, then differences in tectonic behavior would be expected.

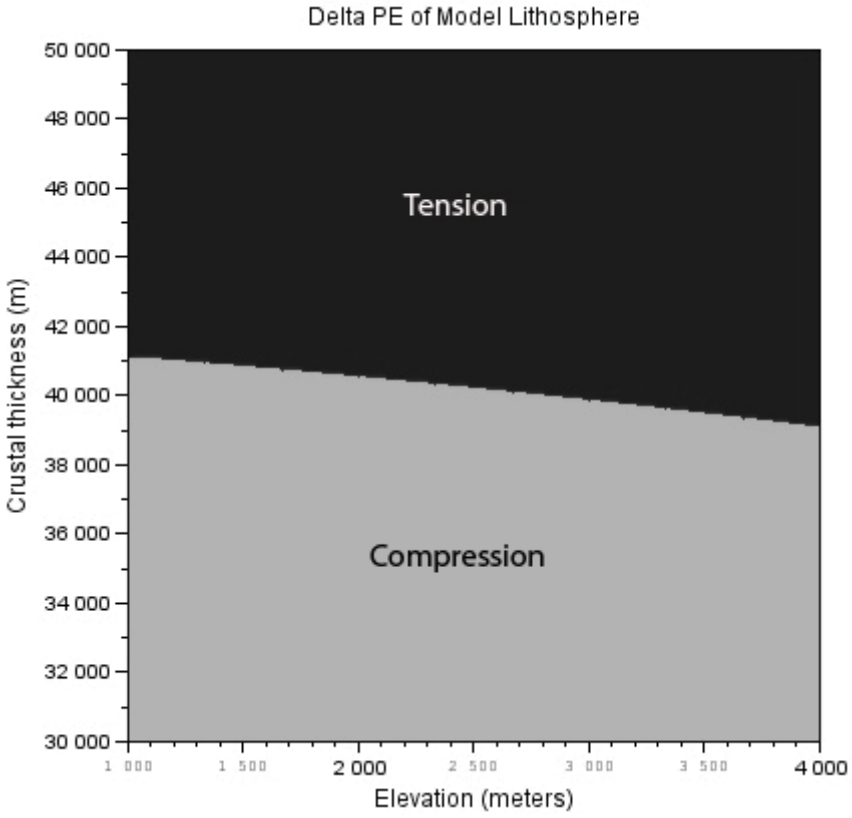

Figure 2. Plot of ΔPE for model A—a thin and hot (150 km thick and Q =.035 W/m^2) lithosphere—showing fields of tension and compression as a function of crustal thickness and paleoelevation.

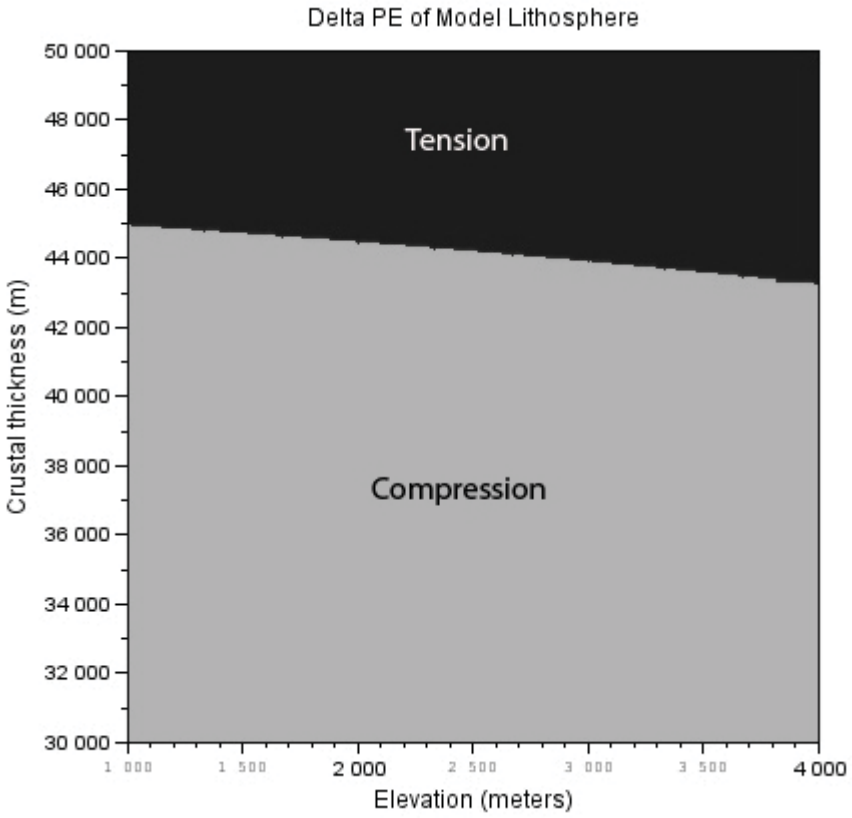

Figure 3. Plot of ΔPE for model B—a thin and cool (150 km thick and Q =.025 W/m^2) lithosphere—showing fields of tension and compression as a function of crustal thickness and paleoelevation.

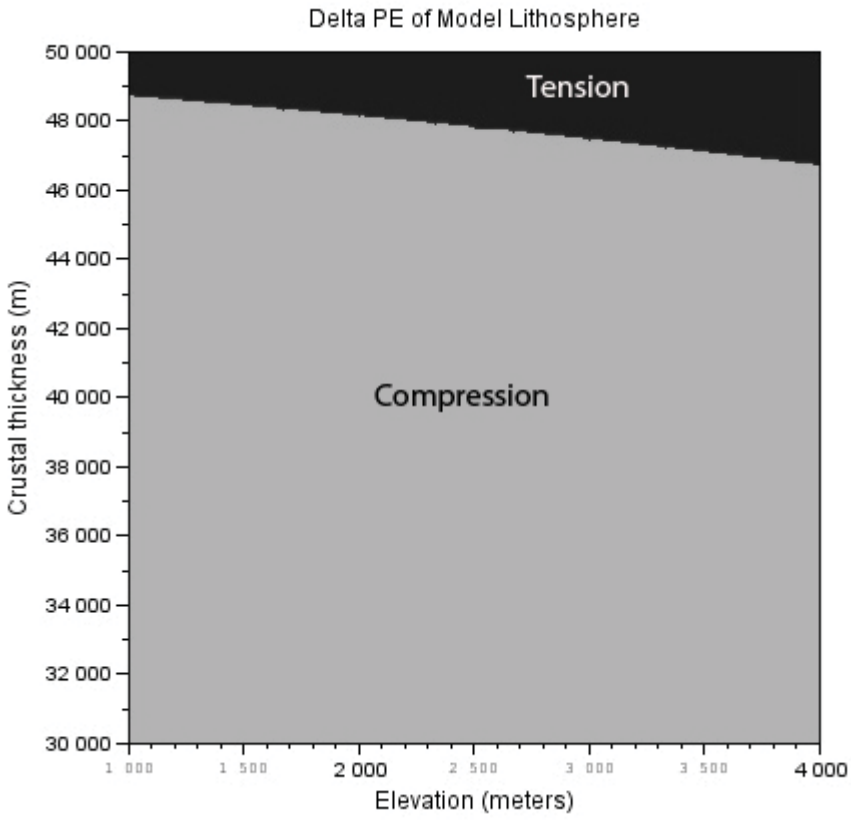

Figure 4. Plot of ΔPE for model C—a thick and cool (170 km thick and Q =.025 W/m^2) lithosphere—showing fields of tension and compression as a function of crustal thickness and paleoelevation.

Although accurate pre-extension estimates of crustal properties are difficult to obtain, some data are available for comparison purposes. Paleoelevation estimates from late Eocene to early Oligocene paleofloras indicate the presence of topography 1.5–2.5 km in elevation centered over the northwestern corner of the Wyoming province (Lielke and others, 2012), implying the existence of an intact high-elevation Paleogene plateau. Moreover, Cretaceous orogeny in this area occurred primarily by high-angle, Laramide-style reverse faulting rather than imbricate stacking of thrust sheets, which minimized crustal thickening (Schmidt and others, 1988). On the other hand, estimates of crustal thickness for the Sevier fold and thrust belt indicate a pre-extension crustal welt in the 45–60 km range (Constenius, 1996; Feinstein and others, 2007). Extensional collapse in the Sevier thrust belt preferentially reactivated preexisting thrust surfaces and was superposed on large-relief structural features such as thrust ramps, duplex zones, and culminations (Constenius, 1996). Collapse of elevated and thickened crust is a natural consequence of the reduction in lateral differences in gravitational potential energy due to juxtaposition of lithosphere of differing density and thickness (Flesch and Kreemer, 2010). Therefore, extension is predicted for the area of maximum crustal thickness and high elevation within the fold and thrust belt—provided that gravitational forces promoting extension exceed both the strength of the lithosphere and any external resisting forces. Thus, differences in lithospheric structure between the Sevier hinterland and the area of southwestern Montana south and east of its leading edge can account for the contemporaneous existence of a stable Paleogene Renova plateau delineated by zones of active extension.

During middle Miocene time, the stability of the craton underlying southwestern Montana was upset by a major thermal anomaly associated with the initiation of the Yellowstone hot spot. To test the effect of this event on the stability of the lithosphere,

a ΔPE comparison was made of two models—one representing undeformed Paleogene lithosphere and the other post-middle Miocene lithosphere. The 150 km modern value of Wyoming province lithosphere thickness (Dave and Li, 2016) was used as a baseline for the middle Miocene, while a conservative value of 160 km was assigned to Paleogene lithosphere. This assumes that the isostatic compensation depth became 10 km shallower due to the effects of thermo-mechanical erosion and alteration of the lithosphere induced by the outbreak of the Yellowstone hotspot. The base of lithosphere heat flow (Q) was also increased by .01 W/m^2. As figure 5 indicates, even using these conservative estimates for the alteration of lithospheric properties, significant changes in tectonic response can occur. The checkered area in figure 5 indicates values of crustal thickness and paleoelevation whose tectonic polarity would shift from compressional to tensional due to this change in physical properties. If the original lithosphere was colder and thicker than assumed or the increase in heat flow was greater, this shift would be more dramatic. As a further test of the viability of this model, the deviatoric stress ($\Delta\sigma_{xx}$) exerted by the reference column on the model lithosphere was calculated in order to determine the magnitude of tectonic stress potentially available to drive deformation. Figure 6 shows the deviatoric stresses calculated for the two models above plotted against crustal thickness. Values for undeformed ancient craton (200 km thick and .02 W/m^2) are included for comparison purposes. Following established convention, positive values of $\Delta\sigma_{xx}$ are compressional and negative values are tensional. A similar shift in tectonic polarity is observed on this plot; moreover, $\Delta\sigma_{xx}$ values of 10–30 MPa, derived solely from body forces inherent to the lithosphere, are available to drive extension. These values are comparable to deviatoric stresses calculated for high-angle normal faults from the Anderson theory of faulting (Turcotte and Schubert, 2002) and are similar to modern average deviatoric stress magnitudes in the western United States, which range from 30 to 40 MPa

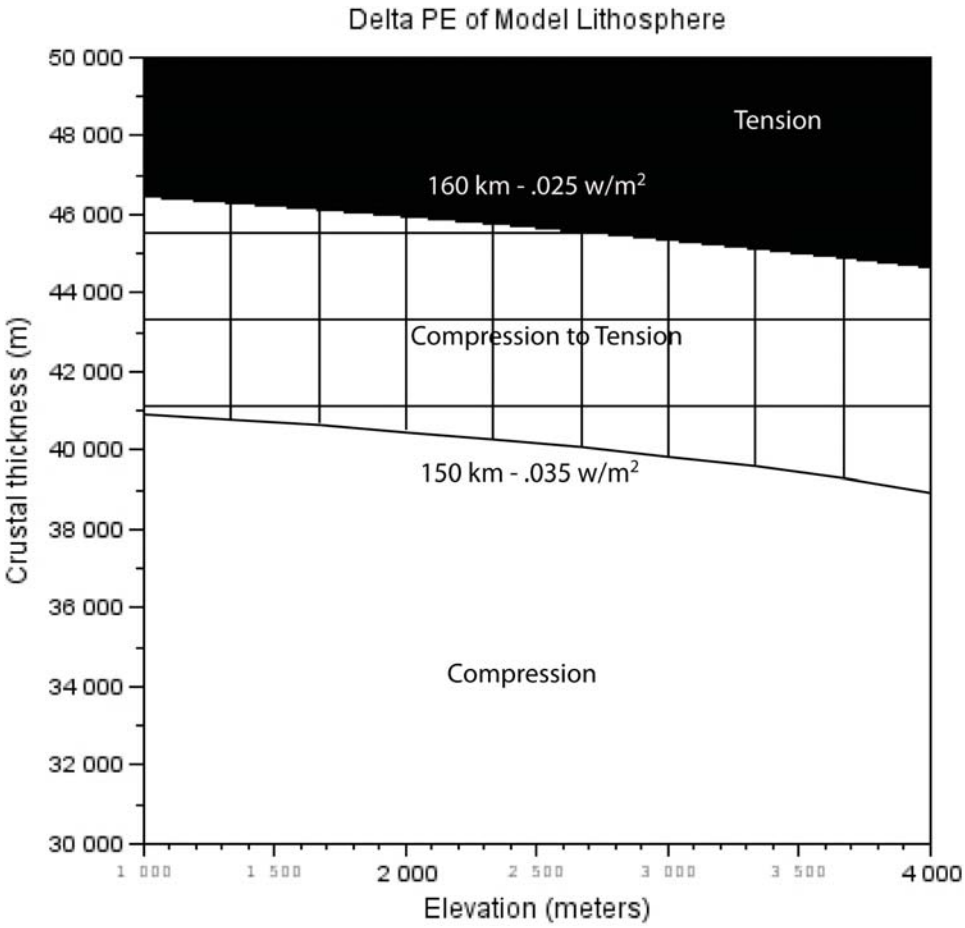

Figure 5. Plot of ΔPE comparing tectonic response before (160 km thick and Q =.025 W/m^2) and after (150 km thick and Q =.035 W/m^2) heating and mantle erosion caused by outbreak of the Yellowstone hotspot. The checkered area indicates values of crustal thickness and paleoelevation whose tectonic polarity would shift from compressional to tensional.

(Ghosh and others, 2013). Therefore, a relatively small change to the properties of the lithosphere—decreasing the isostatic compensation depth by 10 km and increasing the basal heat flow by .01 W/m^2—is sufficient to switch the tectonic polarity of a previously stable Paleogene plateau and generate deviatoric stresses sufficiently large to drive deformation. This theory accounts for the correspondence between the outbreak of the Yellowstone hotspot and the widespread middle Miocene angular unconformity, and dramatic change in sedimentary depositional environments, observed in southwestern Montana (Sears and Thomas, 2007; Sears and others, 2009).

DISCUSSION

One major conceptual problem with the idea of a stable, possibly high-elevation, Renova basin in southwestern Montana involves the question of how this area avoided deformation within a regional Paleogene tectonic framework that included Eocene core complex formation and extensive volcanism in the Low-

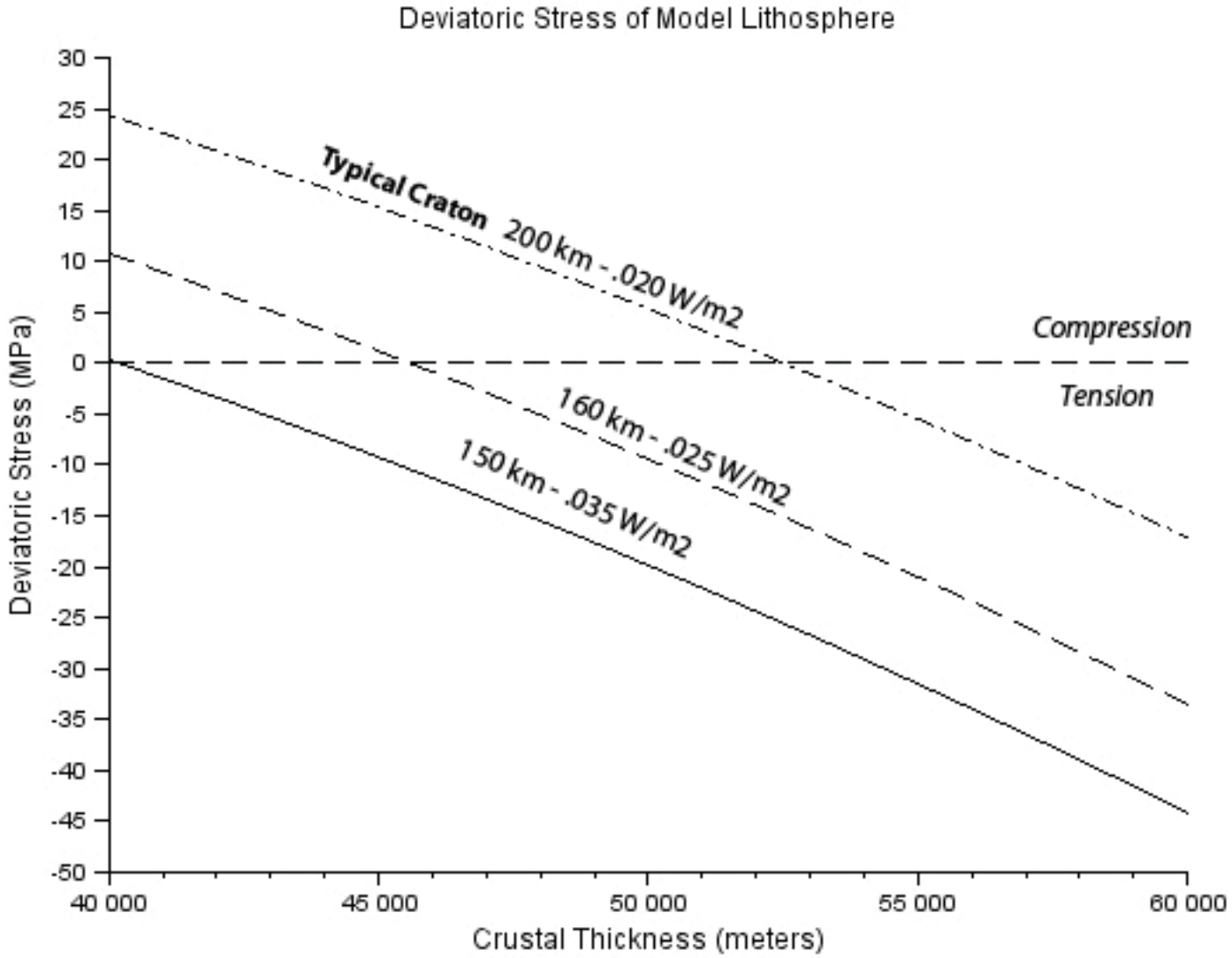

Figure 6. Plot of deviatoric (tectonic) stress for three different lithosphere models representing typical undeformed craton and Wyoming province craton before and after outbreak of the Yellowstone hotspot.

land Creek, Absaroka, and Challis volcanic fields. One possible explanation is the presence of Archean basement underlying the proposed Renova depocenter and its differing response to tectonic stress and changes to its thermal structure. Geodynamic modeling results show that, assuming a realistic set of initial parameters for Cenozoic lithosphere, varying the depth of isostatic compensation and the geotherm leads to differing tectonic responses that closely correspond to the observed spatial and temporal pattern of extension in southwestern Montana. The area underlain by the northwestern corner of the Wyoming province, south and east of the Sevier fold and thrust belt, was mechanically strong enough to resist gravitational collapse following the end of Cretaceous compression. Thermomechanical erosion and heating of the lithosphere caused by mantle convection associated with the outbreak of the Yellowstone hotspot led to the destabilization of the formerly atectonic Renova plateau, initiating extension and forming the angular unconformity underlying the Sixmile Creek Formation. It is important to note that gravitational potential energy, already present in the form of thickened crust and high topography, was sufficient to drive middle Miocene extension once freed by the mechanical weakening of the underlying cratonic lithosphere.

REFERENCES CITED

Chapin, C., and Cather, S., 1994, Tectonic setting of the axial basins of the northern and central Rio Grande rift, *in* Keller, G. and Cather, S., eds., Basins of the Rio Grande Rift: Structure, stratigraphy, and tectonic setting: Geological Society of America Special Paper 291, p. 5–25.

Condie, K.C., 2001, Mantle plumes and their record in Earth history: Cambridge, UK, Cambridge University Press, 306 p.

Constenius, K., 1996, Late Paleogene extensional collapse of the Cordilleran foreland fold and thrust belt: Geological Society of America Bulletin, v. 108, no. 1, p. 20–39.

Dave, R., and Li, A., 2016, Destruction of the Wyoming craton: Seismic evidence and geodynamic processes: Geology, v. 44, no. 11, p. 883–886.

Davies, G., 1994, Thermomechanical erosion of the lithosphere by mantle plumes: Journal of Geophysical Research, v. 99, no. 15, p. 709–722.

Feinstein, S., Kohn, B., Osadetz, K., and Price, R., 2007, Thermochronometric reconstruction of the prethrust paleogeothermal gradient and initial thickness of the Lewis thrust sheet, southeastern Canadian Cordillera foreland belt, *in* Sears, J., Harms, T., and Evenchick, C., (eds).: Whence the mountains? Inquires into the evolution of orogenic systems: Geological Society of America Special Paper 433, p. 167–182.

Fields, R., Rasmussen, D., Tabrum, A, and Nichols, R., 1985, Cenozoic rocks of the intermontane basins of western Montana and eastern Idaho: A summary, *in* Flores, R., and Kaplan, S., Cenozoic paleogeography of west-central United States: SEPM-RMS, p. 9–36.

Flesch, L.M., and Kreemer, C., 2010, Gravitational potential energy and regional stress and strain rate fields for continental plateaus: Examples from the central Andes and Colorado Plateau: Tectonophysics, v. 482, p. 182–192.

Foster, D.A., Grice, W.C., and Kalakay, T.J., 2010, Extension of the Anaconda metamorphic core complex: $^{40}Ar/^{39}Ar$ thermochronology and implications for Eocene tectonics of the northern Rocky Mountains and the Boulder Batholith: Lithosphere, v. 2, no. 4, p. 232–246.

Fowler, C.M.R., 1994, The solid Earth—An introduction to global geophysics: Cambridge, U.K., Cambridge University Press, 472 p.

Ghosh, A., Holt, W., and Flesch, L.M., 2009, Contributions of gravitational potential energy differences to global stress field: Geophysical Journal International, v. 179, p. 787–812.

Ghosh, A., Becker, T., and Humphreys, E., 2013, Dynamics of the North American continent: Geophysical Journal International, v. 194, p. 651–669.

Griffiths, R., and Campbell, I., 1991, Interaction of mantle plume heads with the Earth's surface and onset of small-scale convection: Journal of Geophysical Research, v. 96, no. 18, p. 295–310.

Hanneman, D., 1989, Cenozoic basin evolution in a part of southwestern Montana: Missoula, University of Montana, Ph.D. dissertation, 347 p.

Hanneman, D., and Wideman, C., 1991, Sequence stratigraphy of Cenozoic continental rocks, southwestern Montana: Geological Society of America Bulletin., v. 103, no. 10, p. 1335–1345.

Jones, C., Sonder, L., and Unruh, J., 1998, Lithospheric gravitational potential energy and past orogenesis: Implications for conditions of initial Basin and Range and Laramide deformation: Geology, v. 26, no. 7, p. 639–642.

Jones, C., Mahan, K., Butcher, L., Levandowski, W., and Farmer, G., 2015, Continental uplift through crustal hydration: Geology, v. 43, no. 4, p. 355–358.

Lielke, K., 2008, Paleogeographic reconstruction of the Renova Formation in southwestern Montana: American Association of Petroleum Geologists Bulletin, v. 92, no. 11, p. 1605.

Lielke, K., 2010, Paleogene topography, drainage patterns, and climate change in southwestern Montana: American Association of Petroleum Geologists abstracts, 2010 annual convention and exhibition, v. 19, p. 149.

Lielke, K., Manchester, S., and Meyer, H., 2012, Reconstructing the environment of the northern Rocky Mountains during the Eocene/Oligocene transition: Constraints from the palaeobotany and geology of south-western Montana, USA: Acta Palaeobotanica, v. 52, no. 2, p. 339–380.

Liu, M., and Shen, Y., 1998, Crustal collapse, mantle upwelling, and Cenozoic extension in the North American Cordillera: Tectonics, v. 17, no. 2, p. 311–321.

Luedke, R., 1994, Maps showing distribution, composition and age of early and middle Cenozoic volcanic centers in Idaho, Montana, west-central South Dakota and Wyoming: U.S. Geologic Survey Misc. Investigations Series Map I-2291-C.

Moore, W., Schubert, G., and Tackley, P., 1999, The role of rheology in lithospheric thinning by mantle plumes: Geophysical Research Letters, v. 26, p. 1073–1076.

Pardee, J.T., 1950, Late Cenozoic block faulting in western Montana: Geological Society of America Bulletin, v. 61, no. 4, p. 359–406.

Rothfuss, J.L., Lielke, K., and Weislogel, A.L., 2012, Application of detrital zircon provenance in paleogeographic reconstruction of an intermontane basin system, Paleogene Renova Formation, southwest Montana, *in* Rasbury, E.T., Hemming, S.R., and Riggs, N.R., (eds.): Mineralogical and Geochemical Approaches to Provenance: Geological Society of America Special Paper 487, p. 63–95.

Schmidt, C., O'Neill, J., and Brandon, W., 1988, Influence of Rocky Mountain foreland uplifts on the development of the frontal fold and thrust belt, southwestern Montana, *in* Schmidt, C., and Perry, W., eds., Interaction of the Rocky Mountain foreland and the Cordilleran thrust belt: Geological Society of America Memoir 171, p. 171–201.

Sears, J., Hurlow, H., Fritz, W., and Thomas, R., 1995, Late Cenozoic disruption of Miocene grabens on the shoulder of the Yellowstone hotspot track in southwest Montana: Field guide from Lima to Alder, Montana: Northwest Geology, v. 24, p. 201–219.

Sears, J., and Fritz, W., 1998, Cenozoic tilt domains in southwestern Montana: Interference among three generations of extensional fault systems: Geological Society of America Special Paper 323, p. 241–247.

Sears, J., and Thomas, R., 2007, Extraordinary middle Miocene crustal disturbance in southwest Montana: Birth record of the Yellowstone hot spot?: Northwest Geology, v. 36, p. 133–142.

Sears, J., Hendrix, M., Thomas, R., and Fritz, W., 2009, Stratigraphic record of the Yellowstone hotspot track, Neogene Sixmile Creek Formation grabens, southwest Montana: Journal of Volcanology and Geothermal Research, v. 188, p. 250–259.

Sonder, L., and Jones, C., 1999, Western United States extension: How the west was widened: Annual Review of Earth and Planetary Sciences, v. 27, p. 417–462.

Turcotte, D.L., Haxby, W., and Ockendon, J., 1977, Lithospheric instabilities, *in* Talwani, M., and Pitman W., (eds.), Island arcs, deep sea trenches and back-arc basins: American Geophysical Union, p. 63–69.

Turcotte, D.L., and Schubert, G., 2002, Geodynamics, second edition: Cambridge, U.K., Cambridge University Press, 456 p.

Wannamaker, P., Bartley, J., Sheehan, A., Jones, C., Lowry, A., Dumitru, T., Ehlers, T., Holbrook, W., Farmer, G., Unsworth, M., Hall. D., Chapman, D., Okaya, D., John, B., and Wolfe, J., 2001, Great Basin—Colorado Plateau transition in central Utah: An interface between active extension and stable interior, *in* Erskine, M., and others, eds., The Geological Transition, High Plateaus to Great Basin—A symposium and field guide: Utah Geological Association, 30, p. 1–38.

Zoback, M., and Mooney, W., 2003, Lithospheric buoyancy and continental intraplate stresses, *in* Klemperer, S., and Ernst, W., eds., The lithosphere of western North America and its geophysical characterization: George A. Thompson International Book Series, v. 7, p. 367–390.

Zurek, B., and Dueker, K., 2005, Lithospheric stratigraphy beneath the southern Rocky Mountains, USA, *in* Karlstrom, K., and Keller, G., eds., The Rocky Mountain region: An evolving lithosphere: Geophysical Monograph Series, v. 154, p. 317–328.

DIVIDING THE BEAVERHEAD GROUP AT THE CONTINENTAL DIVIDE

Stuart D. Parker

Missoula, MT 59812, stuart.parker@umconnect.um.edu

ABSTRACT

The Divide unit is an 800-m-thick quartzite conglomerate of contested age and origin that sits atop the Continental Divide near Monida Pass, Montana/Idaho. The Divide unit was originally assigned to the Late Cretaceous Beaverhead Group despite a lack of conclusive age dating. Interstratified Kilgore Tuff at 4.5 Ma contests this designation to the Beaverhead Group. This study reports new detrital zircon ages from the Divide unit. Prior results are replicated, showing that Cretaceous age grains ranging from ~85 to 115 Ma dominate the detrital zircon population. Anomalous grains of Late Jurassic (~155 Ma) age were once again observed. Neither of these two characteristic age populations is documented in the Beaverhead Group.

Catalogued detrital zircon ages from 20 samples from a wide range of possible lithosomes, including three stratigraphic levels of the local Beaverhead Group, were compared using metric, multidimensional scaling (MDS). The Eocene–Miocene Cypress Hills Formation of Alberta is a consistent nearest neighbor to the Divide samples. When all age grains are included, a strong dissimilarity to the Beaverhead Group is evident. Filtering age data to include only grains older than the youngest sampled grain at the Divide (~85 Ma) reveals distinct population clusters. The Beaverhead Group samples show similarity to the Renova and Sixmile Creek Formations, but not to the Divide unit. MDS of pre-Cretaceous age grains of the Beaverhead and Divide recreates the local stratigraphic sequence and puts the Divide as an outlier to provenance trends within the Beaverhead Group. The observed detrital zircon age distribution of the Divide can be approximated by combining zircon data of the Cretaceous Vaughn member of the Blackleaf Formation and the Beaverhead Group.

This study corroborates field evidence (Parker and Sears, 2016) in rejecting the designation of the Divide quartzite conglomerate unit as a facies of the Beaverhead Group. Erosion and recycling of the underlying Beaverhead and Vaughn equivalent strata remains a viable hypothesis regarding zircon populations and observed clast compositions. MDS of catalogued detrital zircon data supports a Cenozoic (Miocene–Pliocene) age for the Divide unit and cannot rule out the possibility of fluvial linkage with the Colorado Plateau and the Cypress Hills Formation of Alberta as has been proposed (Sears, 2013). These results highlight a major fluvial system of contested origin that may require a new stratigraphic designation and place high priority on remapping this largely ignored deposit.

INTRODUCTION

The Divide unit (or Divide) has long been assigned to the Late Cretaceous Beaverhead Group despite several major discrepancies (Ryder and Scholten, 1973). One of two quartzite conglomerate facies of the Beaverhead Group, the Divide unit straddles the Continental Divide near the southern Montana/Idaho border (Ryder, 1967; Ryder and Scholten, 1973). The 160 km^3 deposit consists of predominantly (~70%) quartzite cobbles to boulders recording fluvial deposition in a major north-flowing river system (Ryder and Scholten, 1973; Parker and Sears, 2016). Northerly flow in the Beaverhead Group is unique to the Divide, and is not dominant in any of the 11 other facies of the Beaverhead Group, which are primarily thick packages of alluvial material shed off Laramide thrust sheets in the Late Cretaceous (Ryder and Scholten, 1973). Roughly 1/3 of all clasts in the Divide unit are red/purple quartzites resembling lithologies of the Belt Supergroup, although it's important to note that argillites are rare in the Divide but characterize much of the Belt (Parker and Sears, 2016; Lowell and Klepper, 1953; Ryder and Scholten, 1973). Contradictorily, the Belt Supergroup does not occur to the south (Ryder and Scholten, 1973; Winston and Link, 1993). This discrepancy between paleocurrent and inferred Belt Supergroup source poses an unresolved problem for our accepted interpretation of the Divide. Despite this unresolved and major flaw and observations that suggest otherwise, the Divide unit remains assigned to the Beaverhead Group.

Continuing the field study of Parker and Sears (2016), this study compares two detrital zircon samples from differing stratigraphic levels within the lower Divide unit to several possible analogues throughout the region in an attempt to correlate the deposit to a formal mappable unit (fig. 1; table 1). Three representative Beaverhead Group samples were compared to test the current stratigraphic designation. While the detrital zircon signature of the Divide unit is not required to be identical to other Beaverhead samples in order to satisfy stratigraphic correlation, it is required to contain local sources from Laramide thrust sheets to the south to southwest. The continuous habit of stratigraphic sequences in the Cordilleran Fold and Thrust

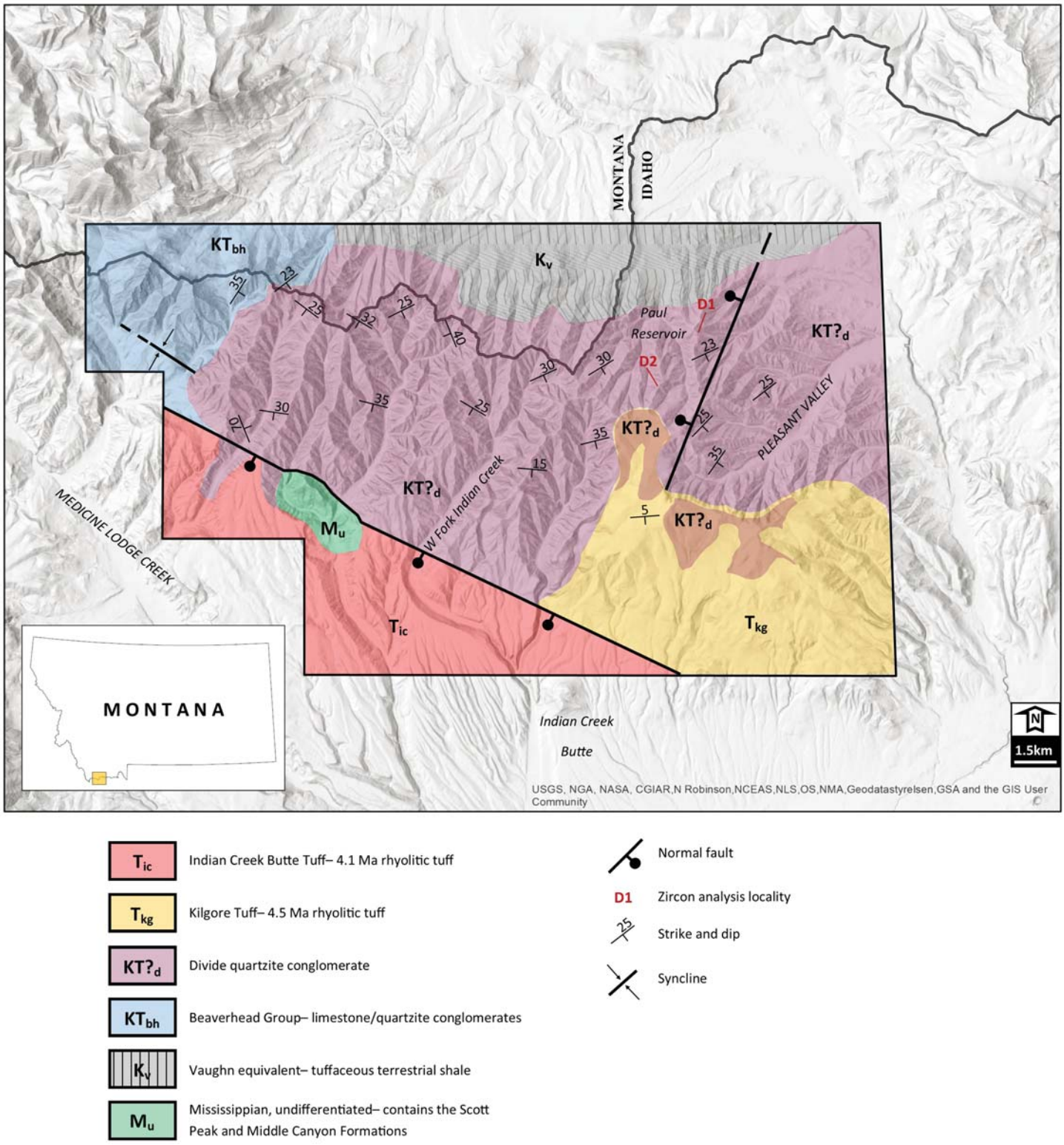

Figure 1. Simplified bedrock geologic map of the study area. Adapted from Parker and Sears (2016). Contentious conglomerates underlying the Divide quartzite are not visible at this scale.

Table 1. Sample attribute table. Sample CR is a composite of samples CR1–CR7. Sample GC is a composite of samples GC1—GC3 combined. Sample names for CR and GC modified from Kimbrough and others (2011). N = number of zircons per sample.

Sample ID	Sample Name	Relation to Divide Unit	Formation	Age	N	Reference	Latitude/ Longitude
CR	Colorado River	Modern analogue to possible headwaters, proto-Colorado river model	Alluvium	Modern	522	Kimbrough and others, 2011	(see CR1–CR -6)
CR1	Colorado River 1	"	"	"	56	Kimbrough and others, 2011	39.14695° -108.74417°
CR2	Colorado River 2	"	"	"	53	Kimbrough and others, 2011	38.60354° -109.57597°
CR3	Colorado River 3	"	"	"	115	Kimbrough and others, 2011	39.11521° -110.10978°
CR4	Colorado River 4	"	"	"	55	Kimbrough and others, 2011	37.25959° -109.61782°
CR5	Colorado River 5	"	"	"	120	Kimbrough and others, 2011	37.15011° -109.86591°
CR6	Colorado River 6	"	"	"	59	Kimbrough and others, 2011	35.00699° -110.65320°
CR7	Colorado River 7	"	"	"	64	Kimbrough and others, 2011	35.87567° -111.40573°
CY	Cypress Hills	Possible lithosome, proto-Colorado River model	Cypress Hills	Miocene	493	Leckie and Leier, 2016	NA
D1	Divide 1	Basal Divide unit	Basal Divide	?	84	Parker and Sears, 2016	44.46549° -112.32979°
GC	Grand Canyon	Modern analogue to possible headwaters, proto-Colorado river model	Alluvium	Modern	189	Kimbrough and others, 2011	(see GC1–GC3)
GC1	Grand Canyon 1	"	"	"	59	Kimbrough and others, 2011	36.26125° -111.82689°
GC2	Grand Canyon 2	"	"	"	65	Kimbrough and others, 2011	36.04435° -111.91874°
GC3	Grand Canyon 3	"	"	"	65	Kimbrough and others, 2011	36.22953° -112.33879°
MLCO	Medicine Lodge Creek at 0 Ma	Modern erosion of the Divide unit, proxy for DZs of the Divide unit	Alluvium	Modern	40	Link and others, 2005	44.12448° -112.39921°
MLC3	Medicine Lodge Creek at 3 Ma	Paleo-drainage postdating deposition of the Divide unit	Alluvium	Pliocene ~3 Ma	69	Link and others, 2005	43.76419° -112.74664°
R1	Renova 1	Possible lithosome, proto-Colorado River model	Renova	Oligocene	37	Rothfuss and others, 2012	44.73593° -112.56558°
R2	Renova 2	Possible lithosome, proto-Colorado River model	Renova	Oligocene	37	Rothfuss and others, 2012	44.71512° -112.54667°
BLR	Big Lost River	Modern proxy to western source terrane	Alluvium	Modern	130	Link and others, 2005	43.54672° -113.00613°
PO	Portneuf River	Modern analogue to possible headwaters	Alluvium	Modern	46	Link and others, 2005	42.91389° -112.49935°

Table 1. Sample attribute table. Sample CR is a composite of samples CR1–CR7. Sample GC is a composite of samples GC1—GC3 combined. Sample names for CR and GC modified from Kimbrough and others (2011). N = number of zircons per sample.

Sample ID	Sample Name	Relation to Divide Unit	Formation	Age	N	Reference	Latitude/ Longitude
RR	Raft River	Modern analogue to possible headwaters, constrained by Late Jurassic point source	Alluvium	Modern	66	Link and others, 2005	42.06734° -113.44453°
D2	Divide 2	Lower to middle Divide unit	Lower-Mid Divide?	?	91	This study	44.44489° -112.34206°
SC1	Sixmile Creek 1	Possible lithosome, proto-Colorado River model	Sixmile Creek, Anderson Creek member	Miocene - 6 Ma	64	Stroup and others, 2008	44.72774° -112.25985°
SC2	Sixmile Creek 2	Possible lithosome, proto-Colorado River model	Sixmile Creek, Anderson Creek member	Miocene - 6 Ma	64	Stroup and others, 2008	45.04609° -112.25985°
BH1	Beaverhead 1	Mapped lithosome	Red Butte Conglomerate, Upper Beaverhead Group	Cretaceous Danian	89	Laskowski and others, 2013	44.76333° -112.63363°
BH2	Beaverhead 2	Mapped lithosome	Upper Beaverhead Group	Cretaceous Maastricht-ian	92	Laskowski and others, 2013	45.11174° -112.87203°
BH3	Beaverhead 3	Mapped lithosome	McKnight member, Upper Beaverhead Group	Cretaceous Campanian	90	Laskowski and others, 2014	44.77060° -112.81545°
V	Vaughn	Proxy to zircon signature recycled from the base of the Divide unit	Blackleaf, Vaughn member	Cretaceous 100 Ma	92	Fuentes and others, 2011	47.62111° -112.67139°
KA	Kootenai	Proxy to zircon signature recycled from the base of the Divide unit	Kootenai, basal conglomerate	Cretaceous 110 Ma	84	Fuentes and others, 2011	47.61167° -112.73611°

Belt create a characteristic and consistent provenance in associated foreland sediments (Laskowski and others, 2013). Samples of the Beaverhead Group included in this study have an internal consistency of 100%, indicating they are all statistically indistinguishable within 95% certainty (Laskowski and others, 2013). Divergence of the Divide detrital zircon signatures from the Beaverhead is most likely to be explained from either exhumation of deeper and older sources or recycling of previous Laramide sediments. Anomalous age populations present in the Divide but absent in the rest of the Beaverhead are not expected if the two are time-equivalents.

The method of multi-dimensional scaling (MDS) was chosen for this assessment. This method effectively and quantitatively characterizes subtle shifts in provenance, such as highlighting data series with similar populations as well as evolving chains of related data series (Vermeesch, 2013). It also has the capability of comparing large series of varying sizes. We use this method to test hypotheses based on field observations from a previous field study (Parker and Sears, 2016). The primary goal is to test for shared provenance between the Divide unit and the Beaverhead Group, with a secondary goal of testing the proto-Colorado River hypothesis of Sears (2013). This hypothesis, which is partially supported by the analysis of Parker and Sears (2016), speculates a Miocene–Pliocene age for the deposit and places the early (Oligocene–Miocene) headwaters of the system in the Grand Canyon, with progressive truncation occurring in the Basin and Range of Nevada (Sears, 2013). The primary prediction of this hypothesis is a linkage to strata far to the south, including the Colorado Plateau (Sears, 2013). The Cypress Hills Formation of Alberta, as well as the Renova and Sixmile Creek Formations of Montana, may also be integrated in this drainage (Sears, 2013; Leckie and Leier, 2016; Leier and others, 2016). Modern sand samples from river systems of the region were also compared. The primary goal of this study is to quantify the relation between detrital zircons in the Divide unit and the Beaverhead Group, thereby investigating whether the current stratigraphic designation is warranted.

STRATIGRAPHIC BACKGROUND

Original Stratigraphic Designation

The Beaverhead Formation was first designated by Lowell and Klepper (1953), although much of what we know about the Divide unit of the Beaverhead Formation stems from later field investigations, most notably Ryder and Scholten (1973). The Beaverhead Formation was later raised to Group status by Nichols and others (1985). The Divide unit was largely overlooked, remaining a formal unit but not a formal formation. Various dating methods have revealed a Late Cretaceous age for other facies of the Beaverhead, while limited fossil abundance prevented accurate dating of the Divide unit (Ryder and Scholten, 1973; Nichols and others, 1985).

In both quartzite conglomerate facies of the Beaverhead (Kidd and Divide), red to purple quartzites and white orthoquartzite clasts dominate (Ryder and Scholten, 1973; Parker and Sears, 2016). Argillite clasts are abundant in the Kidd, but nearly absent in the Divide (Ryder and Scholten, 1973). Several clast lithologies are unique to the Divide, including; white quartzite with red specks, blue-black quartzite, cherty lithic arenite, and dacite porphyry containing bi-pyramidal smoky quartz crystals (Ryder and Scholten, 1973). Another quartzite conglomerate ascribed to the Divide unit contains gneiss and granite–syenite clasts (Ryder and Scholten, 1973). Gneiss and granite–syenite clasts are not present in the Divide deposit proper, which is the focus of this study. Transport direction in the Kidd is predominantly SE, while in the Divide it is consistently NNE (Ryder and Scholten, 1973; Parker and Sears, 2016). Transport directions are typically E to SE in the Beaverhead Group, with the exception of local transport to the W/SW off the active western limb of the Blacktail–Snowcrest Arch (Ryder and Scholten, 1973; Nichols and others, 1985). NNE flow in the Divide unit is attributed to flow off the ESE-striking Medicine Lodge Thrust to the immediate south (Ryder and Scholten, 1973).

Divide quartzite conglomerate is typified by channels and over-bank deposits of coarse sandstone with crude bedding at meter scale plus well-sorted, well-rounded clasts. These features suggest an anastomosing river environment of a relatively low slope/energy environment achieved near a local base level (Makaske, 2001). The neighboring Divide limestone conglomerate contains larger and poorly sorted subangular to rounded clasts, indicating higher slope/energy environments (Haley and Perry, 1991; Ryder and Scholten, 1973; Nichols and others, 1985). The Divide limestone conglomerate is heavily oxidized and bright red in outcrop, containing numerous paleosols (Haley and Perry, 1991; Ryder and Scholten, 1973). It is important to note that thrust faults and folds are observable in nearly all facies of the Beaverhead, the exception being the Divide quartzite conglomerate (Ryder and Scholten, 1973; Nichols and others, 1985; Parker and Sears, 2016) (fig. 2).

Red/purple quartzites were attributed as first-cycle Belt Supergroup sediments. Absence of the Belt Supergroup in the Medicine Lodge Thrust was resolved with a hypothetical Late Cretaceous–Paleocene uplift by Ryder and Scholten (1973) (Targhee uplift of Love, 1956, 1973). In the paleotopographic interpretation of Ryder and Scholten (1973), this sealed the southern end of the drainage with high topography without acknowledging the low-slope, fluvial depositional environment of the Divide quartzite conglomerate (Ryder and Scholten, 1973). It was later proposed that Late Cretaceous–Eocene quartzite conglomerates of Wyoming, such as the Harebell, Pinyon, and Pass Peak Formations, were eastern continuations of quartzite conglomerates sourced from Laramide thrust sheets such as the Kidd and Divide units (ex. Schmitt and Steidtmann, 1990). The Targhee uplift hypothesis, which was solely constrained by sediments in the undated Divide unit, was rejected on structural, geophysical, and stratigraphic bounds (Love, 1973; Schmitt and Steidtmann, 1990). The Divide quartzite conglomerate remained assigned to the Beaverhead Group despite these advancements in thought and lack of a subsequent test of hypotheses.

Conflicting Field Observations and Revised Interpretation

The discrepancies discussed above and incomplete interpretations for the Divide unit have led to conjectures of a post-Cretaceous age. An interbedded layer of 4.5 Ma Kilgore Tuff occurs high in the section (Sears, 2014; Parker and Sears, 2016). Sears (2013) infers a Miocene–Pliocene age and correlates the system to the proto-Colorado River and Sixmile Creek Formation. While the proto-Colorado River hypothesis uses independent lines of evidence to restore the early drainage from the Grand Canyon to the Labrador

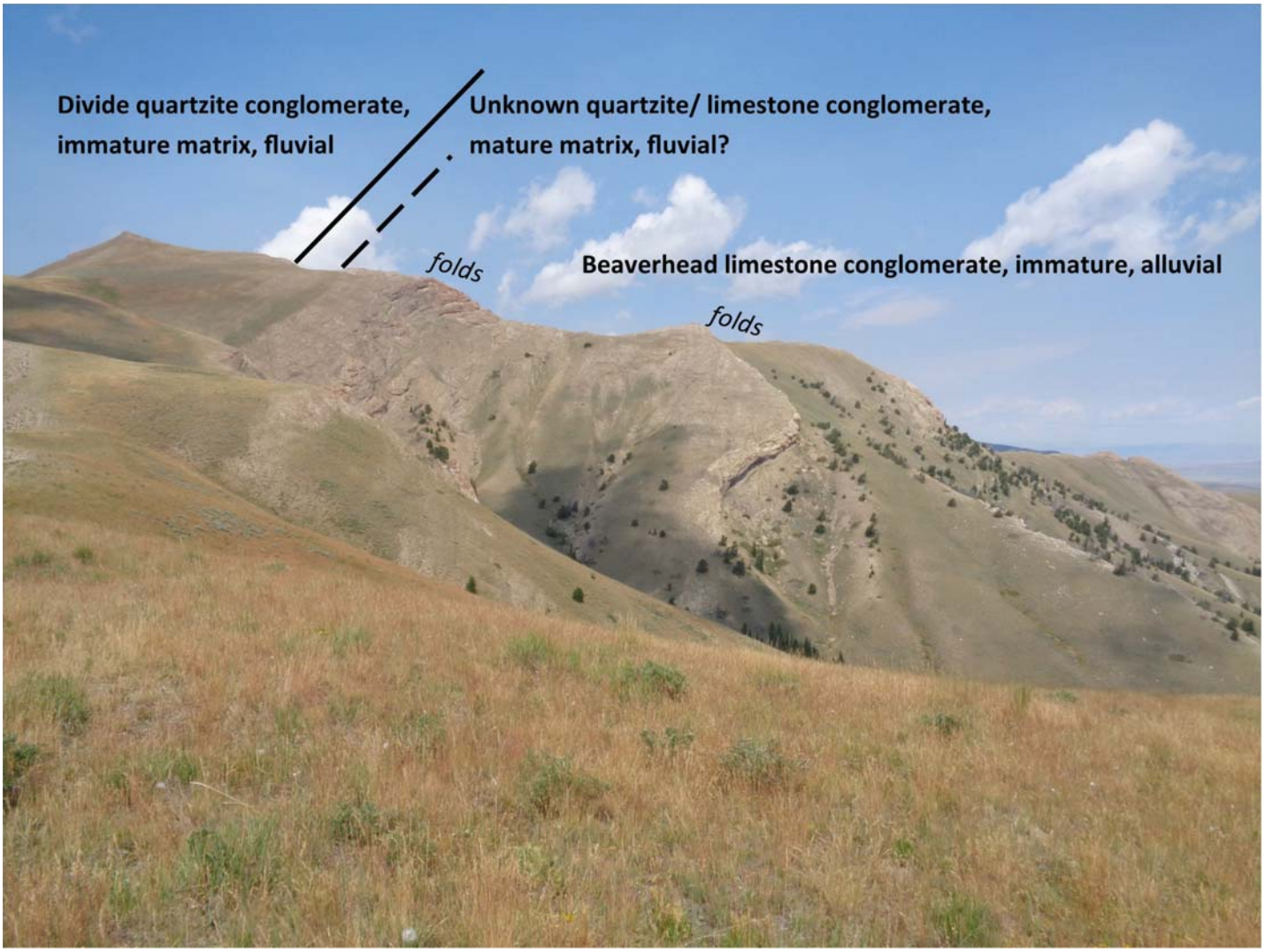

Figure 2. Field photo of basal contact relationships of the Divide quartzite conglomerate. The basal contact is visible as the change in slope and vegetation, projected as solid line. Contact between unknown conglomerate and the Beaverhead Group is visible as sudden change in vegetation (lush grass to sparse cover) and outcrop prominence, projected as a dashed line. Descriptions of corresponding units are in bold. Gently folded strata are labeled.

Sea, it constrains the river through the Divide deposit by correlating the widespread lithic chert arenite and quartz-veined chert clasts in the Divide to bedrock sources in Nevada and Utah (Sears, 2013). These clasts are common in the Mississippian Diamond Peak and Devonian Milligen Formations (Brew and Gordon, 1971; Sandberg and others, 1975). The Devonian Milligen Formation and the Mississippian Copper Basin Group (correlative to the Diamond Peak) also occur in uplifts of central Idaho, hundreds of kilometers to the west of the Divide (Sandberg and others, 1975; Paull and Gruber, 1977; Wust and Link, 1988). Either interpretation requires long-distance transport either by thrust sheets and subsequent fluvial transport, or fluvial transport alone, both of which seem unlikely given the large size of the clasts, which approach 10 cm in diameter.

A subsequent field study by Parker and Sears (2016) found a local outcrop of quartz-veined chert. Recent field observations have found lithic chert arenite clasts in the basal conglomeratic unit of the early Cretaceous Kootenai Formation near Dillon, MT, considerably north. The Kootenai lies beneath the Aspen/ Blackleaf shale at the Divide locality that underlies the Divide quartzite conglomerate as well as the neighboring limestone conglomerate (Ruppel, 1978; Parker and Sears, 2016; Ryder and Scholten, 1973). Therefore, lithic chert arenite clasts may be recycled out of the Kootenai Formation, which occurs as far south as the Continental Divide (DeCelles, 1986).

A quartzite clast within the Divide, containing detrital zircons, which do not match typical Belt Supergroup signatures, was tentatively attributed to the Brigham Group (Parker and Sears, 2016). This re-

quires ~200 km of transportation of cobbles. This idea remains highly speculative, although recent research in Jackson Hole and the Big Horn Basin suggests the quartzite clasts, which dominate the region, were sourced from the Brigham Group after the Laramide (Malone and others, 2017a). The study in part revives the long-dead Targhee uplift hypothesis, claiming that Brigham and non-Belt quartzites occurred in the vicinity of the Snake River Plain, thus considerably shortening the required transport distance to the Divide (Malone and others, 2017a). This hypothesis differs from the classic Targhee uplift hypothesis in that evidence of the source is preserved in the Paris Thrust sheet, which lies far south of the local Medicine Lodge Thrust sheet and exposes a different assemblage of strata (Malone and others, 2017a; Ruppel, 1978; Ruppel and Lopez, 1984). The Medicine Lodge Thrust lacks any evidence of Belt or Brigham quartzites (Ruppel, 1978). These recent results demonstrate that coarse sediment sources can be explained entirely with semi-local sources but require recycling of Beaverhead Group conglomerates because sources are absent within thrust sheets to the immediate south (Parker and Sears, 2016; Ruppel, 1978).

The most recent field study of the Divide quartzite conglomerate and precursor to this study constrains the Divide quartzite conglomerate to the Neogene, proposing a middle Miocene–Pliocene age and correlation to the Sixmile Creek Formation of Montana (Parker and Sears, 2016). Parker and Sears (2016) found extensive evidence of west-to-east mass wasting events that entered the channel at a high-angle during all stratigraphic levels through the middle of the deposit (Parker and Sears, 2016). Two distinct clast assemblages are identified; one dominated by mass wasting events in the west (containing local Paleozoic sedimentary rocks), the other from downstream transport containing quartzite, and some intermediate-to-felsic volcanic clasts (Parker and Sears, 2016). Several clast lithologies were shown to decrease in abundance through time, suggesting recycling and winnowing (Parker and Sears, 2016). Early Cretaceous (~100 Ma) felsic to intermediate volcanoclastic sediment dominates the Divide and is not contemporaneous with deposition (Parker and Sears, 2016).

Tectonic deformation within the Divide unit is entirely extensional to transtensional in nature with no evidence for shortening (Parker, in review; Parker and Sears, 2016). Deposition ceased between 4.5 and 4.1 Ma, with long-lived recycling of Beaverhead strata occurring within a major fault-bounded north-flowing river system (Parker and Sears, 2016). While these interpretations are supported by extensive field measurements and observations, they are limited by a lack of post-Cretaceous age detrital zircons. Without conclusive, post-Cretaceous age dates, the question remains —does the Divide quartzite conglomerate belong to the Beaverhead Group?

METHODOLOGY

A sample (D2) of 91 detrital zircons separated out from a sandstone lens within the lower to middle Divide unit (fig. 1) was analyzed. Laser ablation-inductively coupled plasma-mass spectrometry (LA-ICP-MS) was used along with standard procedures of separation, preparation, and U-Pb dating of detrital zircons. These procedures were carried out by technicians at the Boise State University Isotope Geology Laboratory.

Sixteen additional detrital zircon samples were catalogued from selected modern drainages, Late Cretaceous and Neogene strata. Sample descriptions, locations, and justification for collecting the samples are given in table 1. Selected samples were chosen based on possible correlations of Parker and Sears (2016) and Parker (2016). A Kolmogorov–Smirnov (KS) test was used to compare each sample. Dissimilarity values (D) were used to quantitatively assess the degree of fit between samples. We do not report proximity (P) values as they display a strong negative correlation with sample size, making them an ineffective method for comparison (Vermeesch, 2013). We do use P values of a KS test consisting of the two Divide unit samples. This is appropriate because the two samples are of comparable size. A P value of >0.05 signifies the two samples are statistically indistinguishable within 95% certainty. We arbitrarily define D values of <0.3 as representing a "good fit," thereby reflecting a correlation between the datasets. This value of D <0.3 is a reasonable approximation to P >0.05 (Satkoski and others, 2013). Empirical data of Satkoski and others (2013) suggests that D = 0.25 is a closer approximation of P = 0.05. The D value definition of a "good fit" when D <0.3 is less stringent than that set by the P statistic. For this reason, it should be noted that the "good fit" parameter used here is close to, but not equal to, statistically indistinguishable as defined by P values. While D <0.3 is only an approximation of P >0.05, the

D parameter is more reliable in assessing likeness as it is not skewed by sample size. Internal consistency is defined by the percentage of comparisons that satisfy a "good fit" (D <0.3).

All reported ages were compared before filtering the data by removing any grains younger than the minimum observed age in the Divide unit of ~85 Ma. Because the age of the Divide is unknown, we chose to compare both unfiltered and filtered age data in order to avoid false assumptions of age. We also filtered data from all three Beaverhead Group samples as well as the two samples from the Divide, removing all grains <115 Ma. This removed the major Cretaceous peak that is dominant in the Divide signature. This filter was chosen in order to test the hypothesis that the Divide contains a detrital zircon signature of the Beaverhead Group, but with an additional population of Cretaceous-age grains. Using an identity matrix, D values of the 17 samples and 136 KS comparisons were catalogued.

Metric multidimensional scaling (MDS) was performed on identity matrices of D values following methodology of Vermeesch (2013). Three iterations of MDS were performed on (1) unfiltered age data of all samples, (2) all sample data with <85 Ma ages removed, and (3) Beaverhead and Divide samples with <115 Ma ages removed. Goodness of fit was assessed using Kruskal stress values (K) and standard conventions for goodness of fit (Kruskal, 1964). All MDS was carried out in Xlstat, an add-on for Microsoft Excel (www.xlstat.com). A nearest neighbor test was performed on the MDS plot. Nearest neighbors (calculated from D values, not the graphical model) were connected with solid lines and second nearest neighbors were connected with dashed lines to visually aid in interpretation of MDS plots.

RESULTS

New DZ Data

Sample D2 reveals a major unimodal peak at ~90 Ma with a youngest grain of 87 ± 9 Ma (fig. 3). Early–Mid Cretaceous ages dominate, with 36% of all ages falling between 87 and 115 Ma. A secondary unimodal peak occurs at ~155 Ma with 8% of all grains occurring within the Late Jurassic. Six grains (7%) have overlapping ages with a mean of 155 Ma ranging from 152 ± 8 Ma to 158 ± 9 Ma. Another Jurassic age grain of 171 ± 8 also occurs. A broad, dispersed, and symmetrical peak centered at ~1,750 Ma encapsulates 36% of all grains ranging from 1,643 ± 70 Ma to 1,952 ± 39 Ma. Additional peaks in order of magnitude occur at 440 Ma (2 grains), 2,600 Ma (5 grains), and 1,395 Ma (4 grains). A KS test between this sample and the basal sample (D1) from Paul Reservoir (Sample PRMX1 of Parker and Sears, 2016) reveals a D value of 0.13 and a P value of 0.43. We therefore classify this comparison as a "good fit" and deem the two samples statistically indistinguishable within 95% certainty. All major peaks of sample D1 were reproduced in sample D2, with the exception of a Grenville-age peak at ~1,075 Ma in sample D1.

Unfiltered Age Data MDS

KS results are shown in table 2. Sample MLC0, of the modern Medicine Lodge Creek drainage, had the highest number of "good fit" comparisons of any sample. Samples MLC3 (Pliocene Medicine Lodge Creek drainage), BLR (modern Big Lost River), and SC2 (Sixmile Creek Formation) revealed no positive correlations. The basal sample (D1) shows a good fit with 56% of the investigated samples with the lowest D value when compared to D2. A strong correlation to MLC0 and R2 (Renova Formation) was also observed. The average D value comparing the Divide to the Beaverhead Group is 0.32 and does not qualify as a good fit. Sample D2 of the Divide unit shows a good fit with 44% of all samples. The three strongest correlations in order of ascending D value are D1, CY (Cypress Hills Formation), and MLC0. Comparisons with Beaverhead Group samples have a mean D value of 0.43. There is 100% internal consistency within the two Divide samples as well as within the three Beaverhead samples. No comparison of Divide to Beaverhead revealed a good fit with the mean D value of 0.38.

Multidimensional scaling reveals a dispersed, irregular polygon containing Divide samples and a sublinear polygon containing Beaverhead samples (fig. 4). These polygons are each interconnected with 2nd nearest neighbor lines (fig. 4). Samples D1 and D2 form a line with CY and R2 at opposite ends. The two Colorado Plateau samples (CR, GC) are far away, but in line with this polygon, on the R2 end. MLC0 plots in close proximity to Divide samples. Beaverhead and Divide samples do not plot in close proximity and contain no connections. BLR, MLC3, and SC2 are distant outliers. A stress value of K = 0.146 indicates the two-dimensional model is a fair fit for the data.

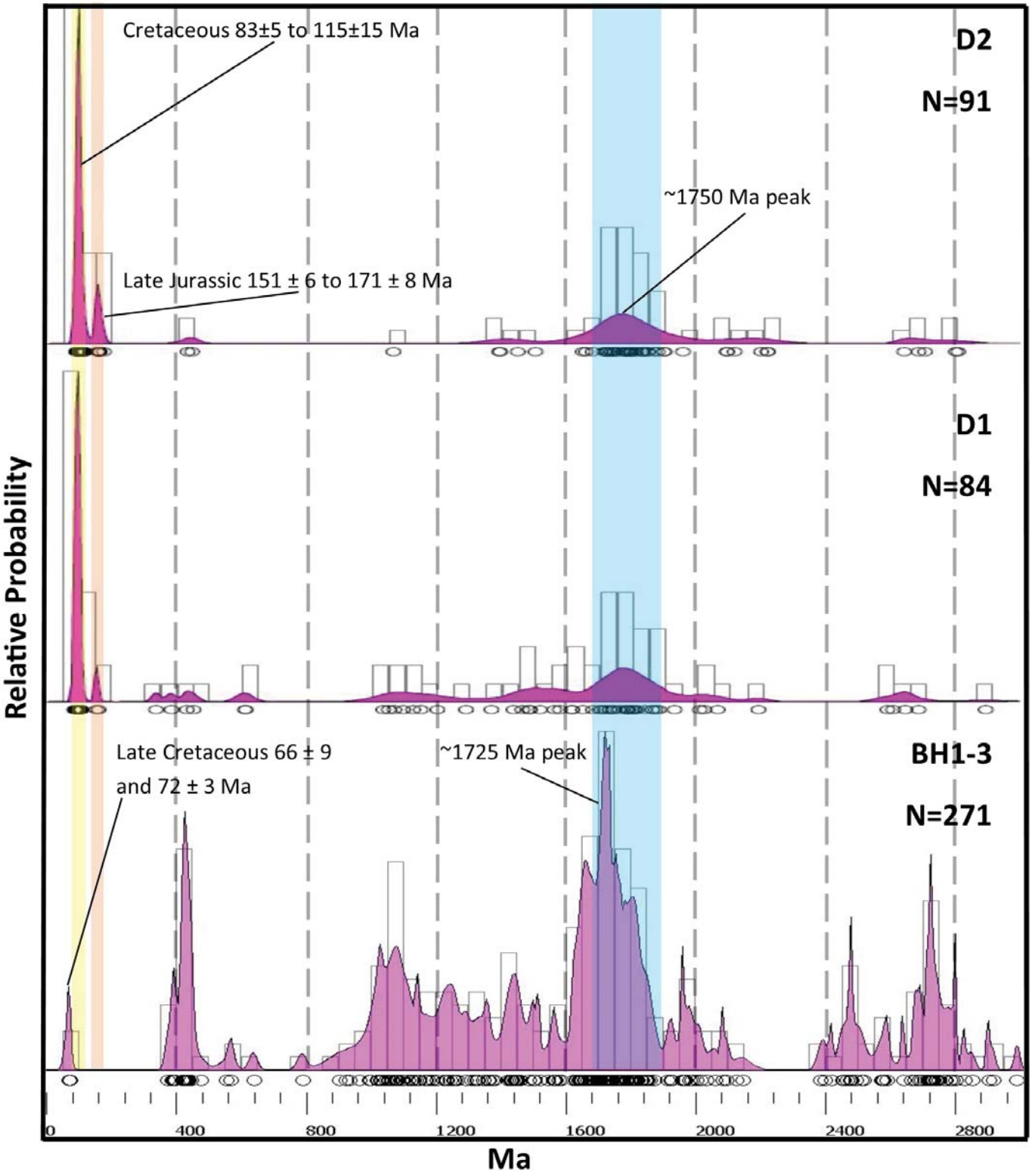

Figure 3. Stacked Kernal density estimator (KDE) plots for Divide samples (D2 and D1) and Beaverhead Group samples (BH1-3). All ages from samples BH1, BH2, and BH3 are included. Characteristic age populations of the Divide samples are highlighted. Minimum, maximum, and peak ages for corresponding age populations are noted. Dashed lines denote 400 m.y. intervals.

Table 2. Symmetrical matrix of dissimilarity (D) values of sample comparisons containing all age data. D values multiplied by 100. Values deemed as a "good fit" are highlighted in orange. Divide samples are highlighted in red.

	CR	CY	D1	GC	MLC0	MLC3	R1	R2	BLR	PO	RR	D2	SC1	SC2	BH1	BH2	BH3
CR	0	43	23	8	27	73	29	20	74	19	24	35	31	80	33	35	23
CY	43	0	27	47	31	42	29	37	74	53	36	16	33	80	59	55	58
D1	23	27	0	27	15	51	30	19	76	29	20	13	25	81	35	30	32
GC	8	47	27	0	25	78	31	24	75	18	19	39	25	81	33	39	22
MLC0	27	31	15	25	0	54	29	16	63	23	18	16	24	69	30	26	28
MLC3	73	42	51	78	54	0	49	60	32	75	60	46	56	57	81	78	81
R1	29	29	30	31	29	49	0	32	55	29	23	30	29	77	43	47	32
R2	20	37	19	24	16	60	32	0	63	23	23	23	28	80	32	23	23
BLR	74	74	76	75	63	32	55	63	0	72	57	76	53	78	85	78	78
PO	19	53	29	18	23	75	29	23	72	0	26	40	26	77	36	37	19
RR	24	36	20	19	18	60	23	23	57	26	0	24	16	67	46	39	33
D2	35	16	13	39	16	46	30	23	76	40	24	0	25	81	44	41	44
SC1	31	33	25	25	24	56	29	28	53	26	16	25	0	58	35	29	31
SC2	80	80	81	81	69	57	77	80	78	77	67	81	58	0	81	81	81
BH1	33	59	35	33	30	81	43	32	85	36	46	44	35	81	0	15	19
BH2	35	55	30	39	26	78	47	23	78	37	39	41	29	81	15	0	24
BH3	23	58	32	22	28	81	32	23	78	19	33	44	31	81	19	24	0

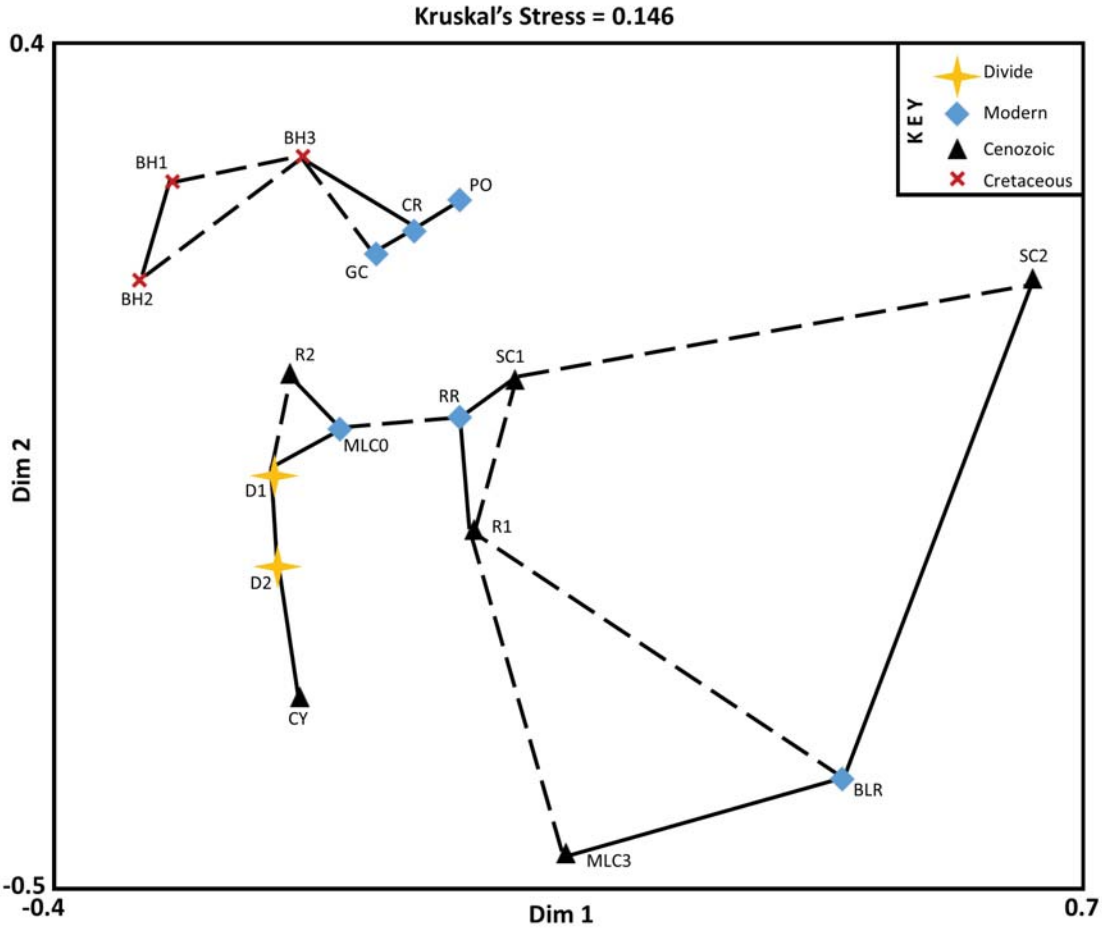

Figure 4. Two-dimensional, multidimensional scaling plot of detrital zircon samples. All age data are included. Nearest neighbors are connected with solid lines. 2nd nearest neighbors are connected with dashed lines. Axes are unitless.

>85 Ma Age Data MDS

KS results are shown in table 3. D1 is most similar to D2 but also shows a good fit with MLC0, CY, and four other samples, none of which are Beaverhead. D2 is most similar to D1 and also shows a strong fit to CY as well as MLC0 and MLC3. Divide samples show 100% internal consistency, as do Beaverhead samples. Sixmile Creek and Beaverhead samples show 90% internal consistency. No comparison between Divide and Beaverhead shows a good fit with a mean D value of 0.38.

All data points are connected with 2nd or less nearest neighbor lines in a 4-armed complex polygon (fig. 5). Divide samples are nearest neighbors also connected to CY. MLC0 and MLC3 are slightly more distant connections. Connection to Beaverhead samples requires a pathway of at least three connections occurring at large angles. Sixmile Creek samples cluster near Beaverhead samples. The model is a poor-to-fair fit to the data, K = 0.165.

>115 Ma Beaverhead and Divide Data MDS

KS results show 90% internal consistency between the Beaverhead and Divide when ages <115 Ma are removed (table 4). Comparison of BH3 and D2 does not qualify as a good fit. MDS reveals a linked polygon with two axes (fig. 6). One axis links BH3, BH1, and BH2. The other axis links BH1, D1, and D2. The model is a good-to-fair fit to the data as demonstrated by a K value of 0.078.

DISCUSSION

Divide and Beaverhead Comparisons

A systematic separation between Beaverhead and Divide samples persists in this data, consistent with the extensive body of field evidence that does not support a correlation (Parker and Sears, 2016). It has been argued that the youngest grain within Divide samples (83 ± 5 Ma) supports a Cretaceous age for the deposit in that no post-Cretaceous grains are present. This argument is faulty because sources are not evenly distributed in time and space, and source terranes especially in SW Montana and Idaho area are typified by large gaps in detrital zircon ages. For instance, the 272 grains within the three samples of the Beaverhead Group contain only two Cretaceous age grains, both of which occur in BH2 (Laskowski and others, 2013). A major gap exists until the Devonian (Laskowski and others, 2013). This is likely explained by the lack of allocthonous Mesozoic strata in the Medicine Lodge Thrust (Ruppel, 1978).

Age gaps spanning considerable chunks of geologic time are ubiquitous in detrital zircon signatures. Another prominent local example is in the Cambrian Flathead Formation, which is typified by a peak at ~1.8 Ga with no younger grains (ex. Mueller and others,

Table 3. Symmetrical matrix of dissimilarity (D) values of sample comparisons containing ages >85 Ma. D values multiplied by 100. Values deemed as a "good fit" are highlighted in orange. Divide samples are highlighted in red.

	CR	CY	D1	GC	MLC0	MLC3	R1	R2	BLR	PO	RR	D2	SC1	SC2	BH1	BH2	BH3
CR	0	40	26	9	34	60	23	30	28	22	32	39	44	43	32	35	23
CY	40	0	22	41	38	27	50	50	47	53	49	17	52	55	52	53	52
D1	26	22	0	27	21	35	30	30	28	35	30	14	30	37	34	33	31
GC	9	41	27	0	34	61	26	38	25	24	27	37	42	48	32	41	22
MLC0	34	38	21	34	0	50	29	19	37	26	17	29	32	22	22	17	26
MLC3	60	27	35	61	50	0	61	62	59	65	62	26	65	65	65	65	65
R1	23	50	30	26	29	61	0	34	50	20	30	42	37	41	28	37	21
R2	30	50	30	38	19	62	34	0	48	35	28	42	39	23	30	20	24
BLR	28	47	28	25	37	59	50	48	0	34	28	41	44	58	52	49	40
PO	22	53	35	24	26	65	20	35	34	0	19	46	38	41	32	37	16
RR	32	49	30	27	17	62	30	28	28	19	0	44	24	38	33	30	21
D2	39	17	14	37	29	26	42	42	41	46	44	0	44	46	44	44	44
SC1	44	52	30	42	32	65	37	39	44	38	24	44	0	21	17	23	25
SC2	43	55	37	48	22	65	41	23	58	41	38	46	21	0	19	10	31
BH1	32	52	34	32	22	65	28	30	52	32	33	44	17	19	0	14	19
BH2	35	53	33	41	17	65	37	20	49	37	30	44	23	10	14	0	27
BH3	23	52	31	22	26	65	21	24	40	16	21	44	25	31	19	27	0

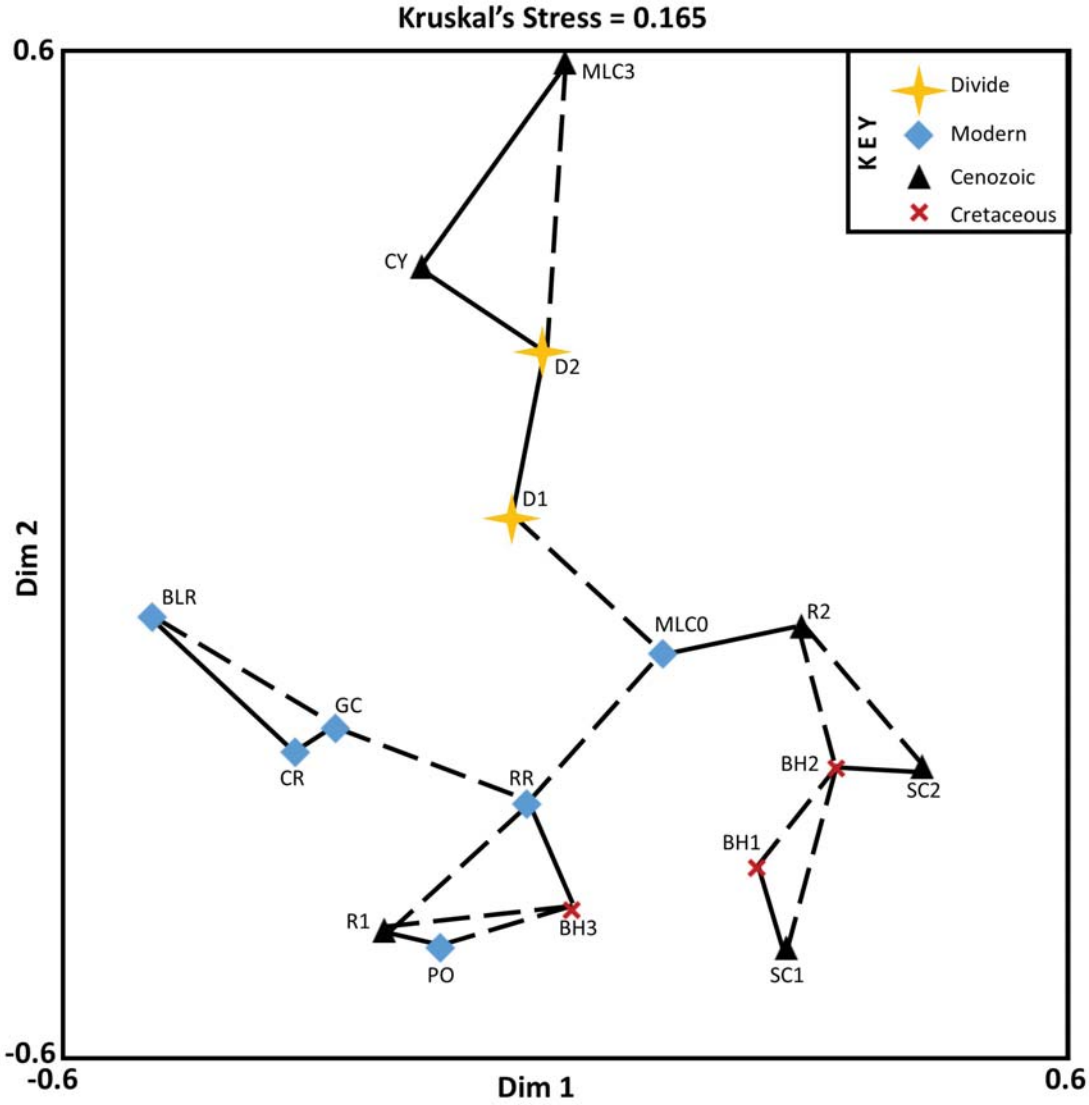

Figure 5. Two-dimensional, multidimensional scaling plot of detrital zircon samples, standardized for youngest observed grain in the Divide. Age data include only values > 85 Ma. Nearest neighbors are connected with solid lines. 2nd nearest neighbors are connected with dashed lines. Axes are unitless.

Table 4. Symmetrical matrix of dissimilarity (D) values of Divide and Beaverhead sample comparisons containing ages >115 Ma. D values multiplied by 100. Values deemed as a "good fit" are highlighted in orange. Divide samples are highlighted in red.

	D1	D2	BH1	BH2	BH3
D1	0	21	11	10	20
D2	21	0	24	24	33
BH1	11	24	0	14	19
BH2	10	24	14	0	27
BH3	20	33	19	27	0

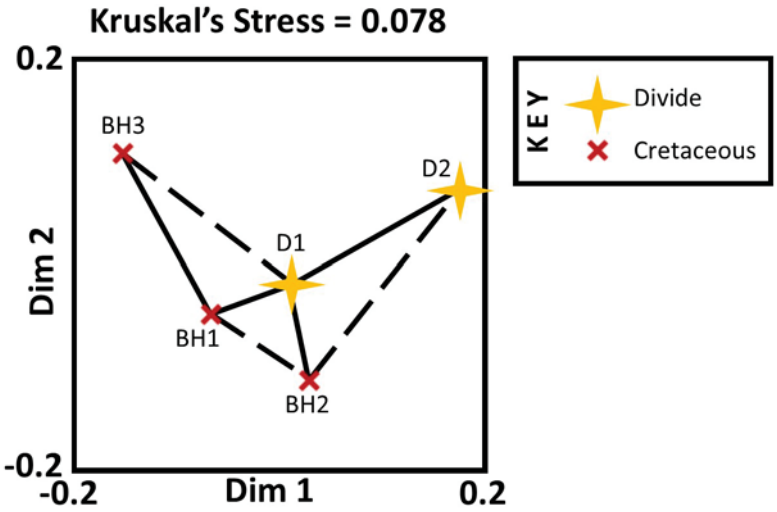

Figure 6. Two-dimensional, multidimensional scaling plot of Divide and Beaverhead detrital zircon samples, filtered to remove Cretaceous age populations. Age data include only values >115 Ma. Nearest neighbors are connected with solid lines. 2nd nearest neighbors are connected with dashed lines. Axes are unitless.

2008). The Ordovician Bighorn Dolomite has a similar signature, with all grains >1.1 Ga in age (Malone and others, 2017b). Catalogued youngest grain populations in the Belt Supergroup exhibit a negative age slope, where youngest age of zircons increases by ~45 m.y. while the depositional age of the strata decreases by ~15 m.y. (Parker and Winston, 2017). Countless examples like this exist, demonstrating the low reliability of youngest detrital zircon ages in constraining depositional age. Age gaps of hundreds and even thousands of m.y. are not uncommon in detrital zircon populations, making the absence of post-Cretaceous ages in the Divide a very poor argument for a Cretaceous age.

MDS is a particularly useful tool for assessing similarities in detrital zircon curves that may not be apparent through visual inspection alone. D indices from KS statistics, which are the basis of MDS, measure the maximum distance between cumulative probability curves of two series. This makes D values sensitive to not only the range of ages in a population (peak position), but also the number of occurrences (peak magnitude) as well. This makes the abundance of ages in a population the primary variable, not just the range of the age population.

While many of the age populations of the samples are similar, the prominent peaks in the Divide (Early Cretaceous and Late Jurassic) are not found in the Beaverhead and the prominent peaks in the Beaverhead (Ordovician–Devonian, Grenville age, and Archean) are only minor in the Divide to varying degrees (fig. 3). This results in notable separation on the MDS plots. Notably, the ~400 Ma spike, which is dominant in the Beaverhead, is minor in both Divide samples. The same is true for Archean and Grenville (~1.0–1.2 Ga) age populations. Sample BH2, a quartzite conglomerate identified as Upper Beaverhead from the Bannack, MT area, contains a comparably small Grenville and Archean peak. On the MDS plot containing only >115 Ma ages, this BH2 sample is a nearest neighbor with the basal Divide sample (D1). This BH2 sample also contains the only 2 Cretaceous age grains (65.7 ± 9 Ma and 71.6 ± 3.4 Ma) which postdate the characteristic age population of the Divide (~84–115 Ma). These discrepancies between the Divide and Beaverhead are not likely to be explained from poor sampling in the Beaverhead, as foreland sediments in the Cordilleran Fold-and-Thrust belt have high internal consistencies (Laskowski and others, 2013).

MDS of all ages fails to reveal a linkage between Divide and Beaverhead samples. Older grains (>85 Ma) of the Sixmile Creek and Renova samples show similarity to the Beaverhead. This is intuitive, as the Sixmile Creek and Renova eroded comparable strata and recycled Laramide sediments such as the Beaverhead (Sears and Ryan, 2003; Rothfuss and others, 2012). No relation between the Beaverhead and Divide persists, even when >85 Ma grains are excluded. When the characteristic Cretaceous population is removed from the Divide samples, the basal D1 sample plots closely to the BH1 sample of the Red Butte Conglomerate. The Red Butte Conglomerate is an Upper Beaverhead deposit containing quartzite, carbonates, and recycled Lower Beaverhead (Haley and Perry, 1991). This lithology seems to correlate with conglomerates that underlie the Divide (Divide limestone conglomerate) to the immediate west, although changes to nomenclature make this claim tenuous (Ryder and Scholten, 1973; Haley and Perry, 1991).

Sample D2, further up-section in the Divide, is an outlier. BH1, D1, and D2 fall in a line according to stratigraphic position. Sample BH3, the oldest (Campanian) of the Beaverhead samples, is not in close proximity to the Divide samples. The perpendicular nature of both axes suggests that each is moving towards a different end-member population. The BH axis is arranged in an unroofing sequence, with BH3 being the oldest, B1 being younger and exposing older strata, and B2 exposing the oldest strata in that it con-

tains Precambrian quartzites. The Divide samples are not a continuation of this progression, highlighting a break in the unroofing sequence. These results are interpreted as indicative of recycling of the Beaverhead in post-Cretaceous time, consistent with field observations of a perceived unconformity below the Divide and the presence of recycled coarse sandstone clasts resembling the matrix of the neighboring Beaverhead.

Detrital zircon age distributions of the Divide are much longer wavelength than those of the Beaverhead. Long-wavelength signatures are a demonstrated habit of heavily reworked sediment systems (Satkoski and others, 2013). It is important to note that the detrital zircon population of the Divide is not only consistently different from the Beaverhead, but also from the Sixmile and Renova. This demonstrates that the characteristic age population of the Divide, with extensive early Cretaceous and Late Jurassic age grains, is very uncommon regionally, at least in these proportions, suggesting that the neighboring Medicine Lodge Thrust is not the sole sediment provider.

Exotic Sources and the Proto-Colorado River

The Divide was integrated into the proto-Colorado River hypothesis of Sears (2013), based on evidence regarding coarse clasts (cherty lithic arenite and quartz-veined black chert) found locally and in the Sixmile Creek Formation, which are absent in the local stratigraphy but have lithosomes (Diamond Peak and Milligen Formation) in the Great Basin. This line of evidence has since been removed in that local sources of these lithologies have been identified (Parker and Sears, 2016). Cherty lithic arenite clasts occur in the Cretaceous Kootenai Formation. Its presence in the Divide requires recycling of this lower Cretaceous strata. Deposition of the Kootenai occurred in an active foreland basin during the Sevier orogeny in the early Cretaceous (DeCelles, 1986). The Kootenai was one of the first units to be eroded and deposited during Laramide deposition of the Beaverhead Group (Haley and Perry, 1991; Laskowski and others, 2013). Thus, this lithology is both local and found in the Beaverhead (Lower and Upper). The cherty lithic arenite is likely sourced from the Mississippian Copper Basin Group in central Idaho, which is correlative to the Diamond Peak in the Great Basin, but occurs in much greater thicknesses in central Idaho (Paull and Gruber, 1977; Brew and Gordon, 1971; Ruppel, 1978; Ruppel and Lopez, 1984). Eastward transport off highlands of the Sevier orogeny during deposition of the Kootenai and reworking of the Kootenai is the simplest explanation of source. Coarse sediment within the Divide can therefore be satisfied with local sources, but requires recycling of Cretaceous strata.

Investigation of coarse sediment may not be the appropriate method for testing a far southern source, as coarse clasts may only record reworking from local strata. This removes a line of evidence that correlates the Divide to the proto-Colorado River, although it does little to detract from the proto-Colorado River hypothesis as a whole. While the MDS results suggest that local thrust sheets are not the only sediment sources, decoupling what is exotic and what is recycled locally is a remaining challenge in provenance studies of the Divide unit.

The anomalous populations of Cretaceous and Late Jurassic ages in the Divide highlights this issue of local versus exotic sources. Jurassic ages are completely absent in all Beaverhead samples, as are early Cretaceous ages (~85–115 Ma). These populations are unique to the Divide samples, likely being sourced from the extensive volcanoclastic sediment that constitutes much of the coarse, sand size fraction and a considerable (7%) amount of the cobble size fraction. We can confidently assign the ~100 Ma populations to recycling of local felsic to intermediate volcanic sediment extruded from the Idaho Batholith prior to deposition (Parker and Sears, 2016). Correlative volcanics are absent in local thrust sheets such as the Medicine Lodge Thrust, providing further evidence for a post-Laramide age.

Jurassic-age grains are tightly clustered with a mean of 156.0 ± 5.5 Ma. A total of nine grains (5%) are Jurassic, with all but one falling in the range of 151–158 Ma. This tight clustering of ages implies a single point source, most likely to the south, which provided minor amounts of sediment. This was the original interpretation of Parker and Sears (2016), who speculated point sources in northern Nevada. Field evidence, however, speaks to the dominance of recycled local sources. Jurassic age populations within the modern Salmon Falls Creek of southern Idaho and northern Nevada, which samples local Jurassic intrusions, have a mean age of 163.3 ± 8.2 Ma (Beranek and others, 2006). Ages of the Salmon Falls Creek overlap with ages within the Divide, although they span a much wider and older range (Beranek and

others, 2006). Jurassic plutons of northern Nevada, such as those within the modern Salmon Falls Creek, reasonably satisfy a possible first-cycle point source. It is important to note that Miocene-age grains are also abundant in northern Nevada but have not been identified in the Divide.

MDS results highlight the uniqueness of the Divide signature, and similarities with distant sediment packages. In the unfiltered MDS plot, Renova, Sixmile Creek, Raft, Portneuf, and Colorado River (Grand Canyon and Upper) samples all lie in closer proximity to the Divide than the Beaverhead. Jurassic-age grains in the Raft River and Colorado River samples give constraint. The Cypress Hills Formation of Alberta is also a close neighbor. These correlations to southern sediment as well as local and northern Neogene strata satisfy predictions of the proto-Colorado River hypothesis. It must be acknowledged that this solution supported by MDS is non-unique and merely highlights correlations in age populations. That being said, the predicted evolution from Colorado Plateau to the Divide to the Cypress Hill can be argued in the MDS data; it has been demonstrated that detrital zircon signatures in continental scale drainages are comparable over great distances (Satkoski and others, 2013).

The detrital zircon distribution of Divide samples are statistically indistinguishable from the modern Medicine Lodge Creek (D = 0.15 and 0.16), suggesting that rapid erosion of the Divide deposit dominates sediment in the modern Medicine Lodge Creek. All major peaks of the Divide are reproduced in the Medicine Lodge Creek signature. An anomalous grain of middle Miocene age is present in this sample. Grains in this age range (15–20 Ma) are restricted in the Yellowstone area to four drainages that are integrated with the Divide deposit (Link and others, 2005). These grains are not interpreted as related to early Yellowstone volcanism as they are not widespread in distribution. Rather, they seem to suggest a unique population within the Divide.

Extensive ignimbrites of this age occurred in the Great Basin area (Axen and others, 1993; Best and others, 2013). Parker and Sears (2016) and Parker (2016) suggest linkage between the Divide deposit and ignimbrites to the south during deposition in the middle Miocene. The initial detrital zircon sample D1 taken near the base of the deposit did not capture such a peak. To further test this hypothesis, an additional sample higher in the section, D2, was analyzed. Sample D2 is likely in the middle to lower portion of the deposit, although distributed deformation makes it difficult to identify stratigraphic position. Several hundred meters of strata overlie the sample location below the interbedded Kilgore Tuff. Identification of mid-Miocene age grains higher in the section would conclusively identify a far southern source and provide a robust age constraint. Until the mid- and upper-strata are probed, the interpretation of a far southern source is merely speculation. That being said, the anomalous nature of the Divide deposit is evident and the possibility of a distal southern source is difficult to discount.

Recreating the DZ Signature Using Local Sources

With these speculations on southern source in mind, the Divide signature using only local sources can now be tested. Jurassic grains are sparse in the region, making this limited age population a natural place to start. Reworking of the Jurassic Morrison Formation is not likely given its minimal volume (Ruppel, 1978). Recycling of the Cretaceous Kootenai may satisfy this unique age population as 25% of detrital zircons in the Kootenai contain a notable Jurassic age population (Fuentes and others, 2011). Average ages (161.9 ± 10.4 Ma, ranging from ~140 to 175 Ma) overlap with those of the Divide. Nearly 10% of ages in the Kootenai sample fall within the range observed at the Divide, although the Jurassic population of the Kootenai has a much wider range. Tuff layers in the Kootenai have been dated at ~110 Ma, loosely satisfying the major age population of the Divide (Fuentes and others, 2011). While the Kootenai signature satisfies these characteristic peaks, it does not correlate well with the Divide, with D values of 0.31 and 0.36.

The Cretaceous Blackleaf Formation (Aspen Formation equivalent) also contains Jurassic-age grains, with an average age of 162.1 ± 14.2 Ma (Fuentes and others, 2011). This average also overlaps that of the Divide (156.0 ± 5.5 Ma). Ages in the Vaughn member of the Blackleaf range from 150 to 176 Ma, although most are mid- to early-Jurassic (Fuentes and others, 2011). Cretaceous-age grains are also dominant, accounting for 51% of the population. They range from ~95 to 115 Ma and average 102 ± 2 Ma, coincident with the average of 97 ± 5 Ma within the Divide. Distal tuffs and ash layers occur within the Vaughn equivalent which underlies the Divide deposit, coincident

in lithology to dated layers within the Vaughn member that constrain depositional age to ~98 Ma (Fuentes and others, 2011). This makes the Vaughn contemporaneous with volcanic activity in the Atlanta Lobe of the Idaho Batholith, considerably west of the extent of the Vaughn (Kiilsgaard and Lewis, 1985; Parker and Sears, 2016).

Significant eastward transport is required to place the coarse volcanic clasts of the Atlanta Lobe atop their distal fine grain counterparts. Obviously, the thick diverse coarse sediment package and relatively high-energy environment of the Divide deposit works against correlation with the Vaughn. Stripping of this volcanic cover likely occurred in early Beaverhead Group time. It is important to note that extensive dacite cobbles can also be found just west of the Divide unit, in an extensive and gently folded conglomerate that grades from quartzite rich at the base to limestone rich at the top, a reverse unroofing sequence. This conglomerate likely records eastward transportation of the volcanic material, after deposition of the Vaughn and possibly the mid Beaverhead Group. Immature feldspar and bipyramidal quartz crystals are widespread in sand of the Divide, and volcanic cobbles are often highly degraded in outcrop, suggesting that volcanic material was then reworked from underlying or neighboring strata (Parker and Sears, 2016). Both characteristic peaks of the Divide can be satisfied by the Vaughn, although direct comparison is weak, with an associated D value of 0.39 and 0.27 (table 5).

A reasonable explanation of the uniqueness of the Divide signature may lie in mixing of local Cretaceous strata. This is supported by local stratigraphy and mapping that place the Divide curiously atop the uppermost Beaverhead Group in the west and the Vaughn equivalent in the east (Skipp and Janecke, 2004; Parker and Sears, 2016). To test this hypothesis, an additional MDS plot was constructed. This plot includes the previously mentioned three Beaverhead and two Divide samples as well as the Vaughn (V) and Kootenai (KA). These age data are unfiltered. Additionally, a mixture of all Beaverhead and the Vaughn as well all Beaverhead, Vaughn, and Kootenai ages were included as two synthetic signatures. These data were included as an additional MDS rather than integrating them into the previous plots, because it includes synthetic datasets that should not be confused with direct observations.

The MDS plot qualifies as a good fit to the data (K = 0.095), resulting in a sub-linear big dipper type polygon (fig. 7). Beaverhead and Vaughn samples form end members, with the Kootenai and Divide samples occupying the middle perimeters. Mixed data lie among the Divide, Beaverhead, and Kootenai. The Divide samples fall midway and in line with the Beaverhead and Vaughn. This shows that while neither the Beaverhead nor Vaughn alone can satisfy the age distributions observed in the Divide, a mixture of the two produces a reasonable fit. The addition of the Kootenai shifts the data point no closer towards the Divide, suggesting that while recycled Kootenai may be present, it is not dominant.

The mixture samples are closer to the Beaverhead population because they are weighted so. The dominance of the Cretaceous and Late Jurassic populations in the Divide suggests that the Vaughn is a major contributor of sediment to the Divide. Interestingly, the basal sample is more similar to the Beaverhead and the sample upsection becomes more similar to the Vaughn. This may represent decreased sediment input

Table 5. Symmetrical matrix of dissimilarity (D) values of hypothetical mixture sample comparisons containing all age data. D values multiplied by 100. Values deemed as a "good fit" are highlighted in orange. Divide samples are highlighted in red.

	BH1	BH2	BH3	D1	D2	BH+V	BH+V+KA	V	KA
BH1	0	15	19	35	44	23	24	70	31
BH2	15	0	24	30	41	22	21	66	29
BH3	19	24	0	32	44	18	21	70	31
D1	35	30	32	0	13	19	20	39	31
D2	44	41	44	13	0	28	29	27	36
BH+V	23	22	18	19	28	0	5	51	28
BH+V+KA	24	21	21	20	29	5	0	49	23
V	70	66	70	39	27	51	49	0	53
KA	31	29	31	31	36	28	23	53	0

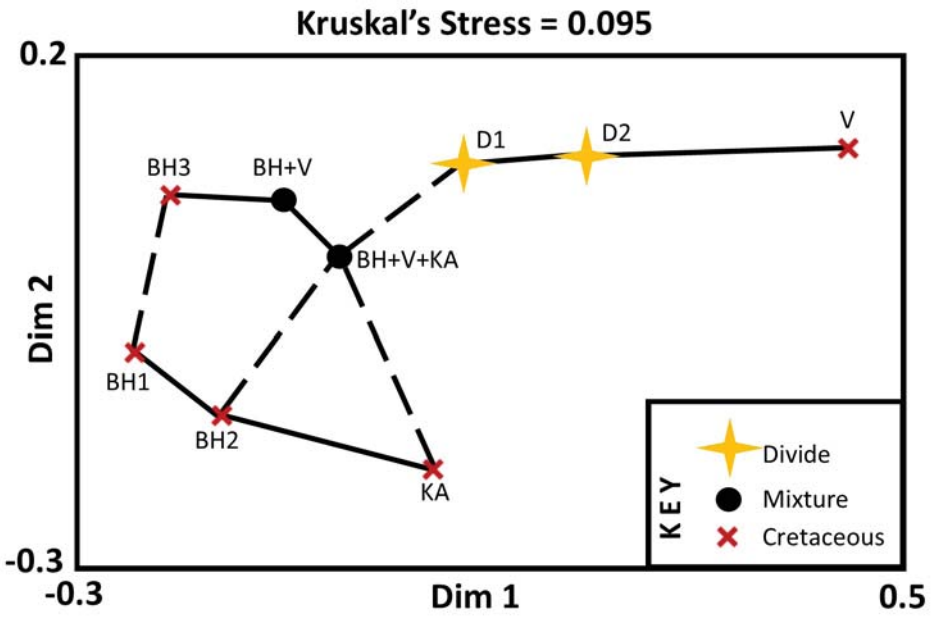

Figure 7. Two-dimensional, multidimensional scaling plot of detrital zircon samples, comparing Divide, Cretaceous, and hypothetical mixtures of Cretaceous strata. Age data are included. Nearest neighbors are connected with solid lines. 2nd nearest neighbors are connected with dashed lines. Axes are unitless.

from the Beaverhead through time, or it may support a southern point source.

The mixture of Beaverhead and Vaughn detrital zircons are a reasonable approximation of the distribution in the Divide unit (D = 0.19 and 0.28, table 5). It is crucial to note that the Vaughn and Kootenai Formation are absent in the Medicine Lodge Thrust plate but occur locally beyond the leading edge of the thrust (Ruppel, 1978). This explains the lack of Mesozoic ages in the Beaverhead and requires erosion of strata beneath the Medicine Lodge Thrust, thus providing a strong argument for post-Cretaceous deposition of the Divide unit.

Stratigraphic Designation

The results of this study, along with a recent field study, do not support correlation of the Divide unit to the Beaverhead Group (Parker and Sears, 2016). Strata of the Beaverhead Group record systematic unroofing of local strata, stripped from uplifting thrust sheets during the Laramide Orogeny (Ryder and Scholten, 1973; Haley and Perry, 1991). Younger and less diverse sediment in the lower Beaverhead gradually gives rise to older and increasingly diverse sediment (Ryder and Scholten, 1973; Haley and Perry, 1991; Laskowski and others, 2013). In the coarse size fraction, recycled Mesozoic sedimentary rocks give way to early Paleozoic quartzites and eventually become dominated by red, purple, and green quartzites and argillites of the Precambrian Belt Supergroup (Ryder and Scholten, 1973; Haley and Perry, 1991).

The Divide unit and all measured Beaverhead samples occur along the leading edge of the Medicine Lodge Thrust, which locally lacks Mesozoic strata (Ruppel, 1978). Mesozoic strata are common ahead of the thrust, including below the Divide, demonstrating that the characteristic Mesozoic age populations of the Divide cannot be attributed to erosion of the local Medicine Lodge Thrust plate.

In many locations, high-grade metamorphic basement rocks are present in the Beaverhead Group (Ryder and Scholten, 1973). The detrital zircon signature accordingly shifts from containing few pronounced unimodal young peaks to encompassing a complex and wide range of various peaks back to Archean (Laskowski and others, 2013). High in the Beaverhead, recycling of Lower Beaverhead occurs as the overriding thrust sheets and compressional stress field of the Laramide migrates eastward, overprinting prior foreland sediments (Haley and Perry, 1991).

The great complexity and diversity in the Divide requires the deposit to be at least upper Beaverhead. Detailed mapping is needed to investigate the basal contact of the Divide, which appears to overlay uppermost Beaverhead in the west and Vaughn equivalent in the east, creating an unconformity. The Vaughn equivalent appears to underlay the Beaverhead Group section to the west, and several mysterious conglomerates occur in the west between the limestone conglomerate of the Beaverhead and the Divide. At present, no break in deposition has been observed between the base of the Divide and the Pliocene Kilgore Tuff.

The abundance of red/purple quartzites belonging to the Belt Supergroup is only possible with reworking of previous Beaverhead, such as the Kidd, that itself is high in the Beaverhead Group. First-cycle sedimentation of red/purple quartzites may be possible in the Cretaceous or later if a Brigham Group source exists

and the Neoproterozic basin extended through the Snake River Plain as has been proposed (Malone and others, 2017a; Parker and Sears, 2016).

Results of this study dispel the argument that the Divide is the uppermost Beaverhead Group in the area in that the major peaks of the Divide are not found in Beaverhead samples and the major peaks of the Beaverhead are sparse in the Divide. Mesozoic strata are absent from the local Medicine Lodge Thrust, arguing against the presence of corresponding zircon ages in local Laramide sediments. This leaves the recycling after the Cretaceous as the most viable hypothesis as supported by extensive field observations.

Recycling of local Cretaceous strata satisfies all observations regarding the coarse and fine sediment load and is thus the preferred model for the Divide. Field relationships near the base of the Divide paint an interesting picture. The great thickness of gravel and influence from mass wasting events implies deposition in an active down-dropping graben (Parker and Sears, 2016). However, a significant amount of erosion appears to have taken place, removing the entirety of the Beaverhead package in the eastern area and creating an unconformity on the Vaughn equivalent. This boundary is poorly exposed and requires further investigation. This conflicting evidence for extensive deposition and erosion must be resolved in the future. This question will likely provide valuable tectonic information regarding regional Neogene tectonics.

While these results offer robust support for a post-Cretaceous age for the Divide unit and differentiation from the Beaverhead Group, countless questions remain. This study must draw the somewhat unsatisfying conclusion that local recycling prevailed, although the influence and extent of southerly derived sediment is unclear. The timing of early deposition remains poorly constrained. The Sixmile Creek Formation seems a natural correlative for the Divide deposit in that it represents a broad regional trend of recycling of Beaverhead strata in active normal fault-bounded drainages in the Miocene–Pliocene (Sears and Ryan, 2003). While MDS plots show some similarity between the Sixmile and Divide, they do not offer strong support for this correlation. The older age fraction (>85 Ma) of the Sixmile Creek Formation appears consistent and tightly related to Beaverhead strata, but dissimilar from the Divide. This likely records the influence from upstream, possibly Neoproterozoic and younger sources. The younger age fraction (<85 Ma) records high variability between the Sixmile Creek and the Divide. Therefore, the Sixmile seems to recycle relatively homogeneous Laramide sediment in a complex drainage network, which results in widely different young age populations. The Cypress Hill Formation retains its relationship to the Divide in both MDS plots, showing a similarity in both young and old age populations. Southern sources including the Raft, Portneuf, and Colorado River samples are also similar in both young and old age populations, showing slight similarity to the Divide. Further work is needed to assess the spatial variability in the Sixmile Creek in order to determine whether this is a suitable correlation for the Divide, or whether a new stratigraphic distinction is required.

While the Sixmile Creek–Divide relation is variable, the southern source–Divide–Cypress Hills relation is consistent. This distinction may speak to a distinct and long-lived drainage similar to that proposed by Sears (2013). Alternatively, it may speak to a drainage with more tectonically stable head and tail waters and significant fragmentation in SW Montana. The Bitterroot and Clark Fork Rivers of Montana are modern analogues of such a system, as they have well-established headwaters, but are altered by active normal faulting in the area of the Nine Mile fault before reestablishing a consistent drainage downstream. The model of Sears (2013) also solicits a stable head and tail water segment, with tectonic alteration in the middle. It is important to note that river courses affected by tectonic alteration often become dissected in their middle reaches. The case of the Divide is likely a matter of scale. Just how far the drainage extended to the south, just which gravels were hydraulically linked, and for how long remains uncertain.

CONCLUSION

This detrital zircon study of the Divide quartzite conglomerate unit in the southern Beaverhead Mountains of Montana/Idaho finds no correlation to the Beaverhead Group. The Divide unit is a distinct mappable unit characterized by extensive recycling of coarse quartzite clasts of the Beaverhead Group, northerly flow, eastward transport of large blocks of local Paleozoic strata in large mass wasting events, extensive intermediate to felsic volcanic sediment, and characteristic zircon populations of ~100 Ma and ~155 Ma. These results necessitate continued investigation, field mapping, and ultimately a new stratigraphic

designation.

The detrital zircon signature of the Divide unit can be approximated with recycling of the basal Cretaceous shale of Vaughn equivalence and various stratigraphic levels of the Beaverhead Group. Local stratigraphy reasonably satisfies all age populations, but requires post-Cretaceous recycling, consistent with field observations. The influence of additional sources to the south remains uncertain. A point source of Late Jurassic (~155 Ma) age in northern Nevada is possible. The possibility of a major Miocene–Pliocene drainage extending as far south as the Grand Canyon and north to the Cypress Hills Formation of Alberta cannot be ruled out and requires further investigation. The presence of Miocene-age grains higher in the section, derived from ignimbrites of the Great Basin, would support this model but at present have yet to be identified.

ACKNOWLEDGMENTS

Foremost, I would like to thank Jim Sears, the driving force of the initial field study, for his ongoing encouragement and support. This study comes as a response to suggestions of my thesis committee at the University of Montana who I thank deeply for pushing me towards quantitative methodology. Key field observations from Kyle Hays and other students and staff of the 2016 South Dakota School of Mines summer field camp were pivotal in steering this project towards the Kootenai. I thank Jim Crowley and the staff at the Boise State Isotope Geology Lab for ongoing analytical support. Finally, I extend deep gratitude to Katie McDonald, Jesse Mosolf, Dick Gibson, Paul Link, Don Winston, and all members of the Tobacco Root Geological Society for their ongoing encouragement, support, and collaboration.

REFERENCES CITED

Axen, G.J., Taylor, W.J., and Bartley, J.M., 1993, Space-time patterns and tectonic controls of Tertiary extension and magmatism in the Great Basin of the western United States: Geological Society of America Bulletin, v. 105, no. 1, p. 56–76.

Beranek, L.P., Link, P.K., and Fanning, C.M., 2006, Miocene to Holocene landscape evolution of the western Snake River Plain region, Idaho—Using the SHRIMP detrital zircon provenance record to track eastward migration of the Yellowstone hotspot: Geological Society of America Bulletin, v. 118, no. 9–10, p. 1027–1050.

Best, M.G., Christiansen, E.H., Deino, A.L., Gromme, S., Hart, G.L., and Tingey, D.G., 2013, The 36–18 Ma Indian Peak–Caliente ignimbrite field and calderas, southeastern Great Basin, USA: Multicyclic super-eruptions: Geosphere, v. 9, no. 4, p. 864–950.

Brew, D.A., and Gordon Jr., M., 1971, Mississippian stratigraphy of the Diamond Peak area, Eureka County, Nevada, with a section on the biostratigraphy and age of the Carboniferous formations: Geological Survey Professional Paper 661, 84 p.

DeCelles, P.G., 1986, Sedimentation in a tectonically partitioned, nonmarine foreland basin: the Lower Cretaceous Kootenai Formation, southwestern Montana: Geological Society of America Bulletin, v. 97, p. 911–931.

Fuentes, F., DeCelles, P.G., Constenius, K.N., and Gehrels, G.E., 2011, Evolution of the Cordilleran foreland basin system in northwestern Montana, USA: Geological Society of America Bulletin, v. 123, no. 3-4, p. 507–533.

Haley, J.C., and Perry, W.J., Jr., 1991, The Red Butte Conglomerate, a thrust-belt-derived conglomerate of the Beaverhead Group, southwestern Montana: U.S. Geological Survey Bulletin 1945, 19 p.

Kiilsgaard, T.H., and Lewis, R.S., 1985, Plutonic rocks of Cretaceous age and faults in the Atlanta Lobe of the Idaho Batholith, Challis quadrangle, *in* McIntyre D.H., ed, Symposium on the geology and mineral deposits of the Challis 1° x 2° quadrangle, Idaho: U.S. Geological Survey Bulletin 1658, p. 29–42.

Kimbrough, D.L., Grove, M., Gehrels, G.E., Mahoney, J.B., Dorsey, R.J., Howard, K.A., House, P.K., Pearthree, P.A., and Flessa, K., 2011, Detrital zircon record of Colorado River integration into the Salton Trough, *in* CREvolution 2—Origin and Evolution of the Colorado River System, Workshop Abstracts: U.S. Geological Survey Open-File Report 2011-1210.

Kruskal, J., 1964, Multidimensional scaling by optimizing goodness of fit to a nonmetric hypothesis: Psychometrika, v. 29, no. 1, p. 1–27.

Laskowski, A.K., DeCelles, P.G., and Gehrels, G.E., 2013, Detrital zircon geochronology of Cordil-

leran retroarc foreland basin strata, western North America: Tectonics, v. 32, no. 5, p. 1027–1048.

Leckie, D.A., and Leier, Andrew, 2016, The geologic setting for new detrital zircon data of Paleogene-Neogene conglomerates of the Canadian plains: Geological Society of America Abstracts with Programs, Rocky Mountain Section, v. 48, no. 6.

Leier, Andrew, Leckie, D.A., Ames, C., and Chesley, J., 2016, Detrital zircon data from Paleogene-Neogene fluvial conglomerates of the Canadian plains: Geological Society of America Abstracts with Programs, Rocky Mountain Section, v. 48, no. 6.

Link, P.K., Fanning, C.M. and Beranek, L.P., 2005, Reliability and longitudinal change of detrital-zircon age spectra in the Snake River system, Idaho and Wyoming: an example of reproducing the bumpy barcode: Sedimentary Geology, v. 182, no. 1, p. 101–142.

Love, J.D., 1956, New geologic formation names in Jackson Hole, Teton County, northwestern Wyoming: American Association of Petroleum Geologists Bulletin, v. 40, p. 1899–1914.

Love, J.D., 1973, Harebell Formation (Upper Cretaceous) and Pinyon Conglomerate (uppermost Cretaceous and Paleocene), northwestern Wyoming: U.S. Geological Survey Professional Paper 734-A, 54 p.

Lowell, W.R., and Klepper, M.R., 1953, Beaverhead formation, a Laramide deposit in Beaverhead County, Montana: Geological Society of America Bulletin, v. 64, no. 2, p. 235–244.

Makaske, B., 2001, Anastomosing rivers: A review of their classification, origin and sedimentary products: Earth-Science Reviews, v. 53, no. 3, p. 149–196.

Malone, D.H., Craddock, J.P., Link, P.K., Foreman, B.Z., Scroggins, M.A., and Rappe, J., 2017a, Detrital zircon geochronology of quartzite clasts, northwest Wyoming: Implications for Cordilleran Neoproterozoic stratigraphy and depositional patterns: Precambrian Research, v. 289, p. 116–128.

Malone, D.H., Craddock, J.P., Konstantinou, A., McLaughlin, P.I., and McGillivray, K.M., 2017b, Detrital zircon geochronology of the Bighorn Dolomite, Wyoming, USA: Evidence for Trans-Hudson dust deposition on the western Laurentian Carbonate Platform: The Journal of Geology, v. 125, no. 2, p. 261–269.

Mueller, P.A., Foster, D.A., Gifford, J., Wooden, J.L., and Mogk, D.W., 2008, Tectonic and stratigraphic implications of detrital zircon suites in Cambrian and Precambrian sandstones from the eastern margin of the Belt Basin: Northwest Geology, v. 37, p. 61–68.

Nichols, D.J., Perry, W.J., and Johns, J.H., 1985, Reinterpretation of the palynology and age of Laramide syntectonic deposits, southwestern Montana, and revision of the Beaverhead Group: Geology, v. 13, no. 2, p. 149–153.

Parker, S.D., in review, More than one way to shear: Rethinking the kinematics of the eastern Snake River Plain and Yellowstone: Lithosphere.

Parker, S.D., 2016, Tectonic alteration of a major Neogene river drainage of the Basin and Range: Missoula, University of Montana Graduate Student Theses, Dissertations, and Professional Papers, v. 10637.

Parker, S.D., and Sears, J.W., 2016, Neotectonics and polycyclic quartzite-clast conglomerates of the northern Basin and Range Province: Northwest Geology, v. 45, p. 47-68.

Parker, S.D., and Winston, Don, 2017, Revised interpretations of detrital zircon populations in the Mesoproterozoic Belt and Purcell Supergroups of Montana, Idaho and British Columbia: Geological Society of America Abstracts with Programs. v. 49, no. 5.

Paull, R.A., and Gruber, D.P., 1977, Little Copper Formation; new name for lowest formation of Mississippian Copper Basin Group, Pioneer Mountains, south-central Idaho: Geologic Notes, AAPG Bulletin, v. 61, no. 2, p. 256–262.

Rothfuss, J.L., Lielke, K., and Weislogel, A.L., 2012, Application of detrital zircon provenance in paleogeographic reconstruction of an intermontane basin system, Paleogene Renova Formation, southwest Montana: Geological Society of America Special Papers, v. 487, p. 63–95.

Ruppel, E.T., 1978, Medicine Lodge thrust system, east-central Idaho and southwest Montana: U.S. Geological Survey Professional Paper 1031, 32 p.

Ruppel, E.T., and Lopez, D.A., 1984, The thrust belt in southwest Montana and east-central Idaho: U.S.

Geological Survey Professional Paper 1278, 41 p.

Ryder, R.T., 1967, Lithosomes in the Beaverhead Formation, Montana and Idaho: Montana Geologic Society Guidebook, 18th Field Conference, p. 63–70.

Ryder, R.T., and Scholten, R., 1973, Syntectonic conglomerates in southwestern Montana: Their nature, origin, and tectonic significance: Geological Society of America Bulletin, v. 84, no. 3, p. 773–796.

Sandberg, C.A., Hall, W.E., Batchelder, J.N., and Axelsen, C., 1975, Stratigraphy, conodont dating, and paleotectonic interpretation of the type Milligen Formation (Devonian), Wood River area, Idaho: U.S. Geological Survey Journal of Research, v. 3, no. 6, p. 707–720.

Satkoski, A.M., Wilkinson, B.H., Hietpas, J., and Samson, S.D., 2013, Likeness among detrital zircon populations—An approach to the comparison of age frequency data in time and space: Geological Society of America Bulletin, v. 125, no. 11–12, p. 1783–1799.

Schmitt, J.G., and Steidtmann, J.R., 1990, Interior ramp-supported uplifts: Implications for sediment provenance in foreland basins: Geological Society of America Bulletin, v. 102, no. 4, p. 494–501.

Sears, J.W., 2013, Late Oligocene–early Miocene Grand Canyon: A Canadian connection: GSA Today, v. 23, no. 11, p. 4–10.

Sears, J.W., 2014, Tracking a big Miocene river across the Continental Divide at Monida Pass, Montana/Idaho: Exploring the Northern Rocky Mountains, v. 37, p. 89.

Sears, J.W., and Ryan, P.C., 2003, Cenozoic evolution of the Montana Cordillera: Evidence from paleovalleys, *in* Raynolds, R.G., and Flores, R.M., eds., Cenozoic systems of the Rocky Mountain region: Denver, CO, Rocky Mountain Society of Economic Paleontologists and Mineralogists, p. 289–301.

Skipp, Betty, and Janecke, S.U., 2004, Geologic map of the Montana part of the Dubois 30’ × 60’ quadrangle, southwest Montana: Montana Bureau of Mines and Geology Open-File Report 90, 12 p., scale 1:100,000.

Stroup, C.N., Link, P.K., and Fanning, C.M., 2008, Provenance of late Miocene fluvial strata of the Sixmile Creek Formation, southwest Montana: Evidence from detrital zircon: Northwest Geology, 37, p.69-84.

Vermeesch, P., 2013, Multi-sample comparison of detrital age distributions: Chemical Geology, v. 341, p. 140–146.

Winston, Don, and Link, P.K., 1993, Middle Proterozoic rocks of Montana, Idaho and eastern Washington: The Belt Supergroup, *in* Reed, J.C., Bickford Jr., M.E., Houston, R.S., Link, P.K., Rankin, R.W., Sims, P.K., Van Schmus, W.R. (eds.), Precambrian: Conterminous U.S., C-2. Geological Society of America, p. 487–517.

Wust, S.L., and Link, P.K., 1988, Field guide to the Pioneer Mountains core complex, south-central Idaho: Guidebook to the geology of central and southern Idaho: Idaho Geological Survey Bulletin, v. 27, p. 43–54.

THE MOUNT EVANS GOSSAN: A SOURCE OF NATURAL ACID ROCK DRAINAGE AND POSSIBLE SOURCE OF METALS AND SULFUR FOR THE BUTTE PORPHYRY-LODE OREBODIES

K.A. Eastman,[1] M.F. Doolittle,[1] C.H. Gammons,[1] and S.R. Poulson[2]

[1]Geological Engineering Department, Montana Tech of The University of Montana, Butte, Montana
[2]Department of Geological Sciences and Engineering, University of Nevada-Reno, Reno, Nevada

ABSTRACT

The bedrock source of naturally occurring acid rock drainage is investigated at Mount Evans in the Anaconda Range of southwestern Montana. Pyrrhotite-bearing pelitic paragneiss of the Mesoproterozoic Belt Supergroup is identified as the primary acid and sulfur source. A combination of post-glacial colluvial features, including slumps, talus, and rock glaciers, have increased the surface area available to weathering. These processes, in addition to the rapid oxidation of pyrrhotite, are creating acidic runoff, with pH values as low as 4.3 measured by Doolittle (2017). Red-brown Fe-bearing in-stream precipitates (ISPs), and white Al-bearing ISPs, were observed in and around the streams that drain the Mount Evans gossan. X-ray fluorescence and scanning electron microscopy are used to determine sulfide and gangue mineralogy, and to quantify concentrations of metals adsorbed onto secondary iron oxides in the gossan. Secondary iron oxides contain As to 1,800 ppm, REEs (La+Ce) to 3,000 ppm, and base metals (Cu, Zn, Pb, Ni) individually to 100s of ppms. A Tertiary biotite–muscovite granite in contact with the Belt metasediments hosts molybdenite-bearing pegmatites, as well as minor quartz veins containing molybdenite, pyrite, sphalerite, and chalcopyrite. Sulfur isotope analyses yield $\delta^{34}S$ values of +7.9‰ for pyrrhotite, +1.4‰ for molybdenite, and +6.9‰ for pyrite. A comparison to the S-isotope composition of dissolved sulfate in acidic headwater streams indicates that the Precambrian sedimentary pyrrhotite is the most likely source of the acid drainage to the watersheds, not the younger magmatic system. Tectonic reconstructions by previous workers (Kalakay and others, 2014), combined with the S-isotope study of Field and others (2005), suggest that the Mount Evans area could represent a metasedimentary source of metals and hydrothermal sulfur for the giant porphyry-lode deposit at Butte, Montana.

Keywords: acid rock drainage, gossans, glacial geomorphology, sulfur isotopes, Belt Supergroup, Butte.

INTRODUCTION

Mount Evans is located along the Continental Divide at an elevation of 3,243 m and is the second highest peak in the Anaconda-Pintler mountains (fig. 1). Satellite imagery of the area reveals a distinct iron-oxide color anomaly at Mount Evans (fig. 2), and the presence of orange-red and white, in-stream precipitates (ISPs) in the creeks that drain the mountain's north and south flanks.

The geology of the Mount Evans area consists primarily of metamorphosed Belt Supergroup sediments and late Cretaceous-to-Tertiary intrusions. The Belt Supergroup sediments at Mount Evans were mapped by Elliott and others (1985) and Lonn and others (2009) as the mid-Proterozoic Greyson Formation (Ygg). Kalakay and others (2014) mapped the Belt units in the Mount Evans area as pelitic paragneiss, and did not assign a formation name. These sediments reached amphibolite grade metamorphism (to 700°C), with peak metamorphism coinciding with the intrusion of the late Cretaceous Storm Lake granodiorite and quartz diorite (Kalakay and others, 2014). Tertiary intrusions in contact with metasediments at Mount Evans have been mapped as biotite–muscovite granite (Tbmg). Porphyritic dikes are common and crosscut all other units at Mount Evans.

Under the provisions of the 1964 Wilderness Act, the USGS conducted a Mineral Resource Potential assessment of the Anaconda-Pintler Wilderness, which included the Mount Evans area as part of the contiguous roadless area (Elliott and others, 1985). That assessment noted elevated Mo, Sn, Ag, Cu, As, Zn, W, and Bi concentrations, coincident with a positive magnetic anomaly. They reported the presence of late dikes with trace molybdenite and ferrimolybdite, as well as disseminated sulfides in quartzite and schist along the contact metamorphosed zone. Elliott and others (1985) hypothesized that this area has moderate potential for Mo and Cu resources in a porphyry-style

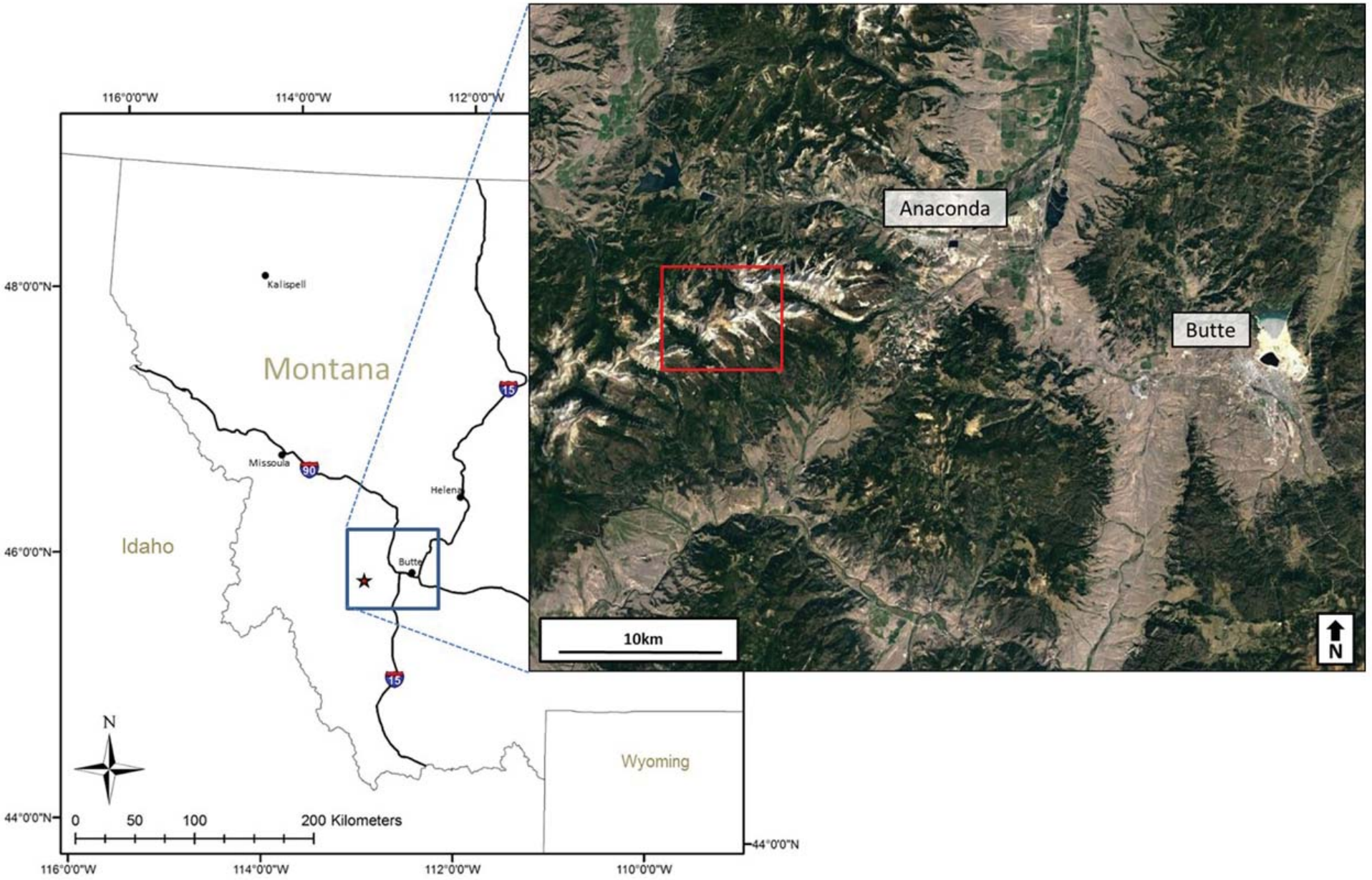

Figure 1. Location of Mt. Evans in southwestern Montana. Red box shows area with gossan development and naturally acidic streams. Satellite imagery from Google Earth (2014).

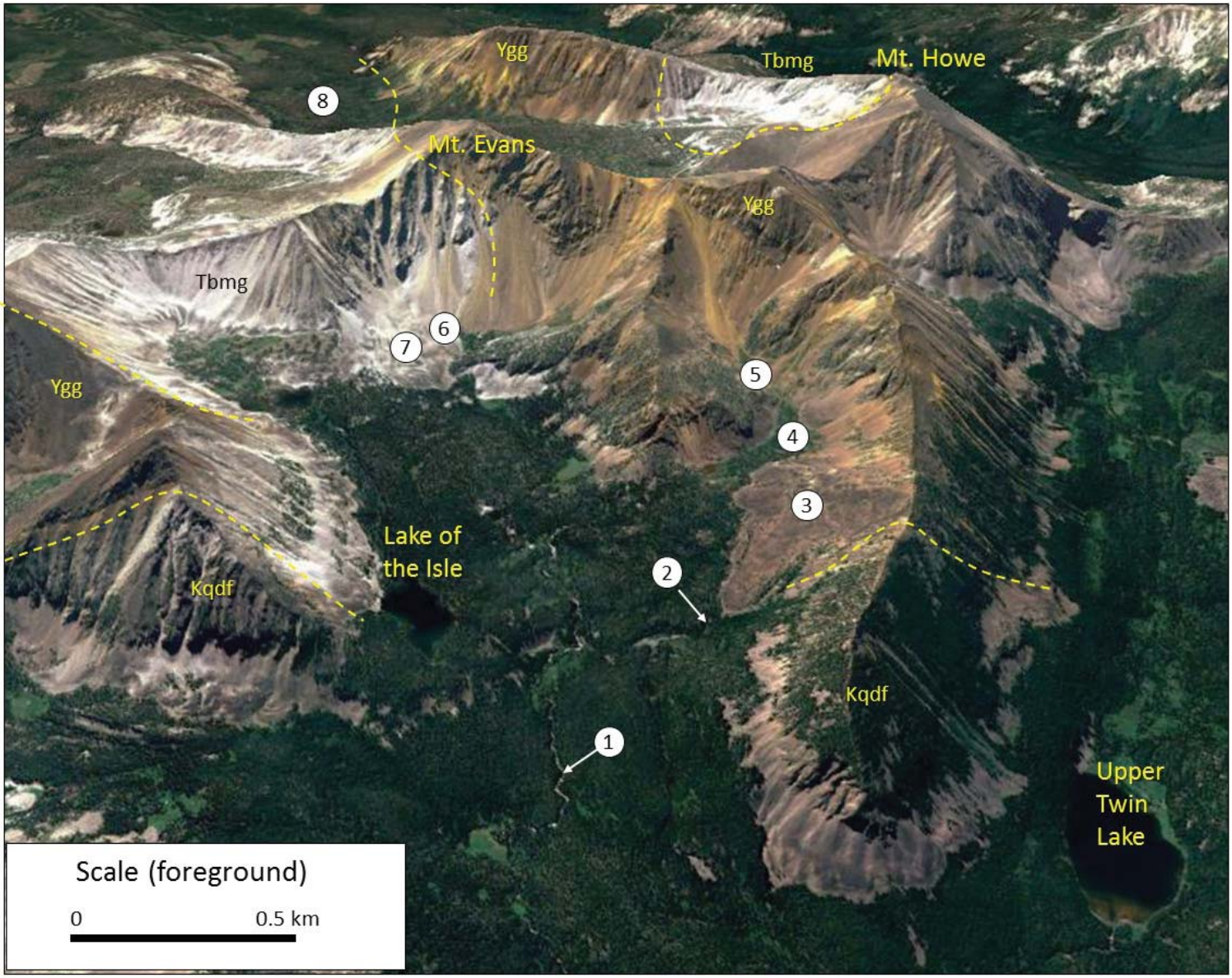

Figure 2. Perspective aerial photo of Mt. Evans (looking south). Points of interest: (1) East Fork Twin Lakes Creek (EFTLC) with white hydrous aluminum oxide staining; (2) source of the "White Fork" of EFTLC; (3) Rock glacier/slump; (4) Head of the "Red Fork" of EFTLC; (5) Pyrrhotite sample for S-isotope analysis; (6) Molybdenite sample for S-isotope analysis; (7) Pyrite vein for S-isotope analysis and location of rock glacier; (8) Sullivan Creek (drains south to Big Hole River). Bedrock units: Ygg = paragneiss of the mid-Proterozoic Greyson Fm. (?); Kqdf = late Cretaceous quartz diorite; Tbmg = biotite-muscovite granite of Eocene (?) age. Source: Google Earth, circa 2005.

and/or mesothermal stockwork system. Felling (1985) identified disseminated sulfides in metasediments at Mount Evans, and suggested that the bulk of the sulfide mineralization could have been syn-sedimentary (Precambrian) in origin. A recent tectonic reconstruction of extensional faulting in southwestern Montana suggests that the porphyry Cu-Mo system at Butte could be allochthonous, with an original location somewhere near the northern part of the Anaconda Range (Kalakay and others, 2014). This raises the interesting possibility that the Mount Evans area could represent the deep roots of the Butte magmatic/hydrothermal deposit.

The main purpose of the present study was to better characterize the bedrock source of acid rock drainage in streams draining Mount Evans as a complement to the water-quality study of Doolittle (2017). A second objective was to test the idea that Mount Evans could have been a source region for assimilation of metals and sulfur into late Cretaceous magmas such as those that formed the Butte deposit.

METHODS

A Thermo Scientific Niton XL3t GOLDD+ portable X-ray fluorescence (pXRF) spectrometer was used to obtain a semi-quantitative determination of elemental abundances of rock samples and ISPs in the field. Level of detection (LOD) for each element reported

Table 1. Selected water-quality data from Doolittle (2017): locations are shown in Figure 2. Samples were filtered to 0.2 µm.

Sample site	pH	Temp ˚C	Al mg/L	SO_4 mg/L	Cd µg/L	Ce µg/L	Cu µg/L	Fe µg/L	Mn µg/L	Ni µg/L	Zn µg/L
White Fork source[1]	4.34	0.9	16.4	417	0.7	145	131	<5	1100	217	291
Red Fork source[2]	4.32	2.0	5.2	85	1.9	11	52	<5	1800	203	944
EFTLC[1]	4.63	6.4	2.6	87	0.4	16	16	17	210	40	112
Upper Sullivan Crk.[1]	4.53	5.9	3.7	64	0.8	4.5	10	85	244	58	245

[1] sampled in Sept., 2014; [2] sampled 8/8/2015

by the Niton pXRF varies between samples, and the instrument only reports concentrations if they are three times the standard deviation of the measurement. Mineral assemblages and textures in polished sections were investigated with reflected light microscopy, then confirmed and imaged with the LEO 1430VP Scanning Electron Microscope located in the Center for Advanced Mineral and Metallurgical Processing (CAMP) at Montana Tech. Sulfur isotopic analyses were performed at the University of Nevada–Reno. All S-isotope data in this study are reported in per mil (‰) relative to Vienna Canyon Diablo Troilite (VCDT). Estimated analytical uncertainty based on replicate measurements is ±0.1‰. Refer to Doolittle (2017) for water chemistry analytical techniques.

RESULTS

Geochemistry

Doolittle (2017) recently conducted synoptic sampling of the streams that drain to the north (East Fork of Twin Lakes Creek, or EFTLC) and to the south (Sullivan Creek) of Mount Evans. Low-pH (~3.8–4.5) springs were found in the source areas of these streams; pH increases to ~5.5 in the lower stretches as dilution with non-acidic tributaries occurs. Fe-oxides are abundant in the acidic (pH <4.5), boggy headwaters of the drainages, and the streambeds are coated with white hydrobasaluminite ($Al_4(SO_4)(OH)_{10}\cdot 15H_2O$) farther downstream as pH rises above 5. Aquatic life standards for Zn, Cu, Cd, and Ni are exceeded in the upper reaches of both creeks, and ISPs contain high concentrations of As, Co, Cu, Mn, Pb, Zn, and REEs. Table 1 shows selected data from Doolittle's study for the upper EFTLC and Sullivan Creek drainages.

Field examination of mineralization in the area concentrated on the glacial valley and cirques immediately north of Mount Evans; talus and outcrops were visited throughout the headwaters of the East Fork of Twin Lakes Creek. Investigation of secondary iron oxides in talus with the pXRF revealed As contents to 1,800 ppm, REE (La+Ce) to 3,000 ppm, and base metals (Cu, Zn, Pb, Ni) to 100s of ppm. Table 2 summarizes pXRF data for the iron-stained surfaces on these rocks.

Table 2. Selected pXRF data of secondary iron oxides on pelitic paragneiss of the Greyson Fm, within the EFTLC drainage area (all concentrations in mg/kg). A total of 33 scans were performed, the number of scans with concentrations greater than the level of detection (LOD) are shown, and statistics for each element are calculated for that subset.

n=33	Mo	Pb	As	Zn	Cu	Ni	Co	Fe	Mn	Cr
n > LOD	17	30	20	30	28	22	2	33	24	31
Min	3	6	9	13	29	71	1340	24720	109	136
Max	157	663	1820	274	482	447	1520	591000	1270	523
Mean	18	96	281	89	151	165	1430	272000	333	321
STD	37	132	399	66	129	86	90	142000	280	86

	V	Ti	S	Ba	Ce	La	Bi	P	Al	Si
n > LOD	33	33	33	33	33	33	8	28	32	33
Min	56	114	2240	254	176	195	12	826	4543	10200
Max	327	6500	103000	1540	1610	1580	493	20300	68600	384000
Mean	177	1040	25000	859	631	613	108	6520	26200	85300
STD	57	1250	25600	351	277	279	163	4870	15400	74800

Mineralogy

Finding fresh sulfide minerals in the metasediments on Mount Evans proved to be difficult due to the advanced level of weathering. Eventually, pyrrhotite ($Fe_{(1-x)}S$) was found in the more quartz-rich layers. SEM-EDS confirmed the presence of pyrrhotite, as well as quartz, K-feldspar, anorthite, pyroxene, titanite, apatite, zircon, monazite, and allanite-Ce (figs. 3A, B). A small amount of pale brown-to-green translucent tourmaline, with pencil-like subhedral crystals to 3 cm length, was found with muscovite in Fe-stained metasediment, and a few zones of iron-cemented, vuggy breccia were found within the most heavily altered gossan boulders. Molybdenite was found at several locations in pegmatites and quartz veins within talus boulders composed of Tertiary biotite–muscovite granite (Tbmg). Bladed ilmenite up to 2 cm long was identified intergrown with quartz and feldspars in a pegmatite within Tbmg talus. A 10-cm-wide, pyrite-rich vein was observed in talus of Tbmg, east of the contact with metasediments. SEM-EDS analysis of this vein (figs. 3C, D) identified pyrite, chalcopyrite, sphalerite, and acanthite, as well as gypsum, carbonates, Fe and Mn oxides, and muscovite (sericite). Molybdenite was not found within this late vein, and molybdenite was never observed to be associated with pyrite or pyrrhotite.

Sulfur Isotopes

The S-isotope composition of sulfide minerals from Mount Evans is given in table 3 along with the $\delta^{34}S$ of dissolved sulfate in streams draining both sides

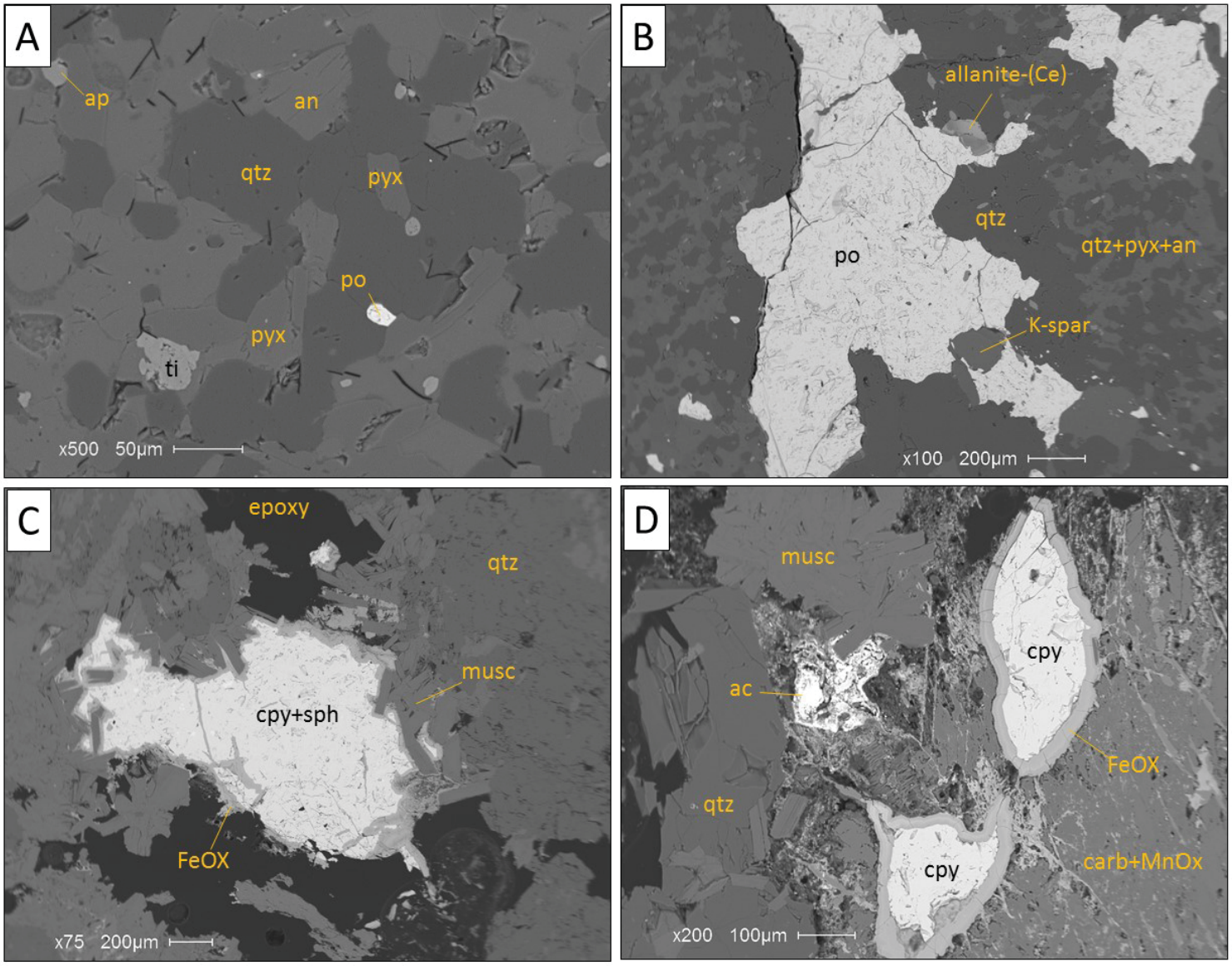

Figure 3. SEM imagery of metasediments (A and B), and a vein hosted in Tbmg (C and D). Mineral abbreviations are: ap=apatite, an=anorthite, qtz=quartz, pyx=pyroxene, po=pyrrhotite, K-spar=K-feldspar, musc=muscovite, cpy=chalcopyrite, sph=sphalerite, FeOX=iron oxides, MnOX=manganese oxides, carb=Mn and Ca carbonates, ac=acanthite.

Table 3. S-isotope data for sulfide minerals and dissolved sulfate in streams in the Mt. Evans area.

	Sulfide minerals on Mt. Evans[a]			Dissolved sulfate in streams[b]				
	pyrite	pyrrhotite	MoS_2	Red Fork	White Fork	SC-lower	SC-mid	SC-upper
$\delta^{34}S$, ‰	+6.9	+7.9	+1.4	+8.2	+10.0	+9.5	+10.1	+10.3
Fig. 2 location	(7)	(5)	(6)	(4)	(2)		(8)	

[a]This study; [b]Doolittle, 2017; SC = Sullivan Creek

of Mount Evans (the Red and White Forks are tributaries to EFTLC; SC = Sullivan Creek). The $\delta^{34}S$ of pyrrhotite from the metasedimentary rocks (+7.9‰) is slightly lighter than the $\delta^{34}S$ of dissolved sulfate in the acidic streams (+8.2 to +10.3‰). The molybdenite sample from the granite–pegmatite had much lighter S (+1.4‰), whereas the pyrite vein cutting the Tertiary granite had a $\delta^{34}S$ value of +6.9‰. It is possible that the vein pyrite inherited some of its S from the surrounding metasediments. The isotope data also suggest that the molybdenite and pyrite veins in the granite formed from different hydrothermal fluids.

Because S isotopes are not fractionated when sulfide minerals are oxidized (Seal, 2003), it is likely that oxidation of pyrrhotite is the main source of sulfate and acidity to EFTLC and Sullivan Creek. This interpretation is consistent with the observations that the extensive gossan is developed in the metasediments, and that pyrrhotite is the main sulfide mineral found in this unit. The slightly heavier stream $\delta^{34}S$-sulfate values could be explained by mixing of pyrrhotite-S with an isotopically heavier S source, possibly derived from either: (1) sedimentary sulfate minerals (barite, anhydrite) in the metamorphosed Greyson Fm., or (2) hydrothermal sulfate minerals in the intrusions. It is also possible that the average $\delta^{34}S$ of sedimentary sulfide in the metamorphosed Greyson Fm. is closer to +10‰, and that the one sample of pyrrhotite collected in this study was slightly lighter than this average. The value of +1.4‰ for the molybdenite sample is much lighter than the bedded pyrrhotite or the dissolved sulfate in the streams, but is a typical value for sulfide minerals that have a magmatic origin (Ohmoto and Rye, 1979).

ROCK GLACIERS

The effect of glacial geomorphology on the generation of acidic surface flow was considered in this study. A post-glacial slump and rock glacier (fig. 2, location 3) was identified as the source area for the spring that creates the White Fork of EFTLC (fig. 2, location 2), which was also the most acidic spring found by Doolittle (2017). The talus upstream of the spring is mainly sulfide-bearing metasediment with strong iron-oxide staining. The White Fork spring has a year-round temperature near 1ºC, suggesting the presence of permanent ice under the talus. Melting of concealed ice also helps to explain the robust discharge of this spring, even in late summer. A second rock glacier was identified within unit Tbmg (fig. 2, location 7). Most of the float in this deposit is unmineralized with a lack of iron-staining, although sparse molybdenite and pyrite veins were found. The aqueous chemistry of springs emerging at the base of this feature is currently unknown. A comparison of modern satellite imagery with stereo aerial imagery from 1970 shows no changes at the toe of the rock glaciers, suggesting that they are both presently inactive.

DISCUSSION

Post-glacial mass wasting processes have had a significant effect on the aqueous chemistry of streams that drain the Mount Evans area. Slump features and rock glaciers increase the effective surface area available for weathering to occur, and freeze–thaw processes work to further comminute the foliated metasediments. Krainer and Mostler (2002) and Williams and others (2006) investigated the hydrology of rock glaciers in the Austrian Alps and the Colorado Front Range, respectively. Both studies attributed elevated total dissolved solids in the rock glacier outflows to an accelerated rate of chemical weathering of the crushed rock in the interior of the periglacial deposits. At Mount Evans, the presence of actively weathering sulfide minerals within and below the rock glacier serves to further increase the SC, lower the pH, and mobilize metal ions. Pyrrhotite, shown here to be a disseminated component of the pelitic paragneiss, is unstable under oxidizing surface conditions, and breaks down to form ferric hydroxide ($Fe(OH)_3$) and protons as shown below (Belzile and others, 2004).

$$FeS + 9/4\ O_2 + 5/2\ H_2O \rightarrow Fe(OH)_{3(s)} + SO_4^{2-} + 2H^+.$$

Ferric hydroxide stabilizes over time to produce hematite and/or goethite. Acid produced from the above reactions breaks down feldspars to release Al^{3+}, and REE-bearing minerals (e.g., monazite and allanite) to release Ce^{3+} and other lanthanide elements to solution. Trace metals and REEs released by weathering processes then strongly adsorb to secondary iron and aluminum oxides that form on the streambed (Dzombak and Morel, 1990). For example, Doolittle (2017) measured REEs (La+Ce) as high as 1,000 ppm in ferricretes and ISPs in the Mount Evans area. An analogous situation exists at Red Mountain, an unmined, volcanogenic, massive sulfide orebody in east-central Alaska where dissolved REE concentrations in naturally acidic springs are as high as 59 mg/L but are rapidly attenuated by adsorption onto ISPs (Eppinger and others, 2007).

Sedimentary sulfides are abundant in the Newland and Greyson formations of the Belt Supergroup (Strauss and Schieber, 1990; Spry and others, 1996), and these units host at least two sedimentary exhalative (SEDEX) orebodies: the Black Butte Cu (Co-Ag) deposit near White Sulphur Springs (Graham and others, 2012; White and others, 2014), and the Soap Gulch Pb-Zn deposit, near Butte. Field and others (2005) investigated sulfur isotopes of sulfide and sulfate minerals at Butte, and proposed that most of the hydrothermal sulfur in the orebody was assimilated from the Belt Supergroup. The presence of inherited zircons dated at 1.5–2.5 Ga within quartz porphyry dikes at Butte supports this idea (Field and others, 2005).

As shown by Kalakay and others (2014), the Boulder Batholith and Butte orebody may once have been located above the Anaconda Range during the Late Cretaceous, prior to Tertiary extension and crustal detachment. If so, it is possible that the disseminated pyrrhotite on Mount Evans represents the remains of a much bigger, pyrite-rich, SEDEX-style deposit that lost most of its sulfur and metals during Cretaceous magmatism. Sulfur released during the desulfidation conversion of pyrite to pyrrhotite at elevated metamorphic temperatures (Poulson and Ohmoto, 1989) in the metasediments could have been recycled in a series of telescoping magmatic-hydrothermal events, eventually forming the Butte ores. If so, the isotopic composition of S in the Butte ore body should be similar to that of the sedimentary sulfides in the Belt metasediments. Field and others (2005) estimated that the isotopic composition of total S in the Butte porphyry system was near +10‰. Coincidently, this estimate is close to the value for $\delta^{34}S$ of dissolved sulfate in the streams draining the Mount Evans area (+8.2 to +10.3‰). Although the pyrrhotite sample analyzed in this study had a slightly lighter $\delta^{34}S$ value (+7.9‰), this represents a single hand sample, as opposed to an entire watershed: many more analyses would be needed to compute the average $\delta^{34}S$ of the sedimentary sulfides on Mount Evans.

CONCLUSIONS

The conspicuous Fe-oxide color anomaly on Mount Evans is due to weathering of disseminated pyrrhotite in the metamorphosed Belt sediments. This weathering, accelerated by rapid physical erosion in an alpine, periglacial landscape, is generating acidic and metal-rich runoff in streams that drain both sides of the Continental Divide. High concentrations of REE in the headwaters of one of these streams are explained by the presence of REE minerals, including allanite and monazite, in the metasediments. Dissolved sulfate in the acidic streams has a S-isotope composition that is similar to that of the sedimentary sulfides, but is dissimilar to molybdenite in Tertiary granitoids and late hydrothermal veins. The isotopic composition of sulfur in the Mount Evans watershed is also similar to the estimated bulk composition of sulfur in the Butte ore body (Field and others, 2005).

Recent workers have suggested that Butte may have been located above the present-day Anaconda Range prior to Tertiary extension and crustal detachment. Following this idea, the mineralization at Mount Evans, now uplifted and exposed in the footwall of the detachment, could have been directly below the Butte ore body when it formed. If not the actual source of the sulfur and metals that now reside in Butte, the Mount Evans area may at least have experienced similar metamorphic conditions as the roots of the Butte system. More research is needed to test this idea.

ACKNOWLEDGMENTS

The Tobacco Root Geological Society provided funding for Kyle Eastman to do fieldwork at Mount Evans. The authors thank Gary Wyss, Alero Gure, Sara Edinberg, Ryan Winters, Zane de la Cruz, and Katharine Kangas for help in the lab and in the field.

REFERENCES CITED

Belzile, N., Chen, Y., Cai, M., and Li, Y., 2004, A review on pyrrhotite oxidation: Journal of Geochemical Exploration, v. 84.2, p. 65–76.

Doolittle, M.F., 2017, Naturally occurring acid rock drainage in the Anaconda-Pintler mountain range, Montana: A case study of geochemistry in two streams flowing from Mount Evans: Butte, Montana Tech of The University of Montana, unpublished M.S. research paper.

Dzombak, D.A., and Morel, F.M.M., 1990, Surface complexation modeling: Hydrous ferric oxide: New York, Wiley, 416 p.

Elliott, J.E., Wallace, C.A., O'Neill, J.M., Hanna, W.F., Rowan, L.C., Segal, D.B., Zimbelman, D.R., and Pearson, R.C., 1985, Mineral potential of the Anaconda-Pintlar Wilderness and contiguous roadless area, Granite, Deer Lodge, Beaverhead, and Ravalli Counties, Montana: U.S. Geological Survey Miscellaneous Field Studies Map MF-1633-A Pamphlet, 35 p.

Eppinger, R.G., Briggs, P.H., Dusel-Bacon, C., Giles, S.A., Gough, L.P., Hammarstrom, J.M., and Hubbard, B.E., 2007, Environmental geochemistry at Red Mountain, an unmined volcanogenic massive sulphide deposit in the Bonnifield district, Alaska Range, east-central Alaska: Geochemistry: Exploration, Environment, Analysis, v. 7, p. 207–223.

Felling, R.A., 1985, Geology and mineralization of the Mount Evans area, Deer Lodge County, Montana: M.S. thesis, University of Colorado, 159 p.

Field, C.W., Zhang, L., Dilles, J.H., Rye, R.O, and Reed, M.H., 2005, Sulfur and oxygen isotopic record in sulfate and sulfide minerals of early, deep, pre-Main Stage porphyry Cu-Mo and late Main Stage base-metal mineral deposits, Butte district, Montana: Chemical Geology v. 215, p. 61–93.

Graham, G., Hitzman, M.W., and Zieg, J., 2012, Geologic setting, sedimentary architecture, and paragenesis of the mesoproterozoic sediment-hosted sheep creek Cu-Co-Ag deposit, Helena embayment, Montana: Economic Geology, v. 107.6, p. 1115–1141.

Kalakay, T.J., Foster, D.A., and Lonn, J.D., 2014, Polyphase collapse of the Cordilleran hinterland: The Anaconda metamorphic core complex of western Montana—The Snoke symposium field trip: Geological Society of America Field Guides, v. 37, p. 145–159.

Krainer, K., and Mostler, W., 2002, Hydrology of active rock glaciers: Examples from the Austrian Alps: Arctic, Antarctic, and Alpine Research, v. 34.2, p. 142–149.

Lonn, J.D., McDonald, C., Lewis, R.S., Kalakay, T.J., O'Neill, J.M., Berg, R.B., and Hargrave, P., 2009, Geologic map of the Philipsburg 30' x 60' quadrangle, western Montana: Montana Bureau of Mines and Geology Open-File Report 483, scale 1:100,000.

Ohmoto, H., and Rye, R.O., 1979, Isotopes of sulfur and carbon, *in* Barnes, H.L. ed., Geochemistry of Hydrothermal Ore Deposits: New York, John Wiley & Sons, p. 509–567.

Poulson, S.R., and Ohmoto, H., 1989, Devolatilization equilibria in graphite-pyrite-pyrrhotite bearing pelites: Contributions to Mineralogy and Petrology, v. 101, p. 418–425.

Seal, R.R., 2003, Stable-isotope geochemistry of mine waters and related solids: Mineralogical Association of Canada Short Courses, v. 31, p. 303–334.

Spry, P.G., Paredes, M.M., Foster, F., Truckle, J.S., and Chadwick, T.H., 1996, Evidence for a genetic link between gold-silver telluride and porphyry molybdenum mineralization at the Golden Sunlight deposit, Whitehall, Montana; fluid inclusion and stable isotope studies: Economic Geology, v. 91, p. 507–526.

Strauss, H., and Schieber, J., 1990, A sulfur isotope study of pyrite genesis: The mid-Proterozoic Newland Formation, Belt Supergroup, Montana: Geochimica et Cosmochimica Acta, v. 54.1, p. 197–204.

White, J., Gammons, C.H., and Zieg, G.A., 2014, Paragenesis of cobalt and nickel in the Black Butte shale-hosted copper deposit, Belt Basin, Montana, USA: Mineralium Deposita, v. 49, p. 335–351.

Williams, M.W., Knauf, M., Caine, N., Liu, F., and Verplanck, P.L., 2006, Geochemistry and source waters of rock glacier outflow, Colorado Front Range: Permafrost and Periglacial Processes, v. 17, p. 13–33.

RARE EARTH ELEMENTS IN A PLACER IN HALFWAY PARK, JEFFERSON COUNTY, MONTANA

D.H. Vice[1,*] and Charles M. Hauptman[2]

[1]Penn State Hazleton, 76 University Dr., Hazleton, Pennyslvania 18202
[2]Park Lane, Billings, Montana 59102
*Corresponding author

INTRODUCTION

Rare earth elements have become critical for many aspects of modern life and for the operation of many of our modern conveniences (Van Gosen, 2014). For example, cell phones or color TVs would not work without trace amounts of rare earths. Europium is the red phosphor in the liquid crystal displays of computer monitors and televisions (Haxel and others, 2002); there is no known substitute. A more mundane example of rare earth use is that nearly all glass products, including eyeglasses, car mirrors, precision lenses, etc. are best polished with cerium oxide (Haxel and others, 2002). Other materials can be used to polish these glass products but will not do as well. Abraham (2015) gives a third example of the importance of the use of rare earth elements. Air conditioners built without the use of a rare earth magnet motor are significantly less efficient, which could mean a large increase in energy consumption—air conditioning takes about 5 percent of the electricity produced in the U.S.

The 2010 decision by China to restrict exports of rare earths led to a shortage of rare earth metals and caused a temporary, but significant, spike in prices that affected many industries because of the widespread use of many of these metals (Van Gosen and others, 2014). This spike has led to concern about resource availability for the future and has resulted in an inventory of domestic deposits of rare earths metals (Long and others, 2010). The purpose of this paper is to briefly describe a placer deposit in Montana that is similar to rare-earth-containing placers in Idaho (Hammond, 1967), so that it can be added to this inventory of deposits.

HALFWAY PARK PLACER

The Halfway Park placer occurs on the Boulder Batholith (Smedes and others, 1962; Vuke and others, 2009) approximately 30 miles northeast of Butte, Montana, in Jefferson County (secs. 11 and 12, T. 3 N., R. 6 W., fig. 1). The area is a large meadow traversed by a stream in a Lodgepole pine forest.

A glacial deposit overlies Butte quartz monzonite (Smedes and others, 1962). Drilling data from 12 holes on the Halfway Park placer suggest that the glacial deposits are just over 10 ft thick (Hammond, 1967). The younger of two vein systems extends approximately west–northwest just north of Halfway Park. The vein is approximately ½ mile north of and upstream from Halfway Park and consists of brecciated quartz latite cemented with minor amounts of quartz, calcite, pyrite, adularia, iron-bearing carbonates, argentite, silver, and gold (Smedes and others, 1962).

The placer contains primarily gold as a commodity but also contains titanium, zirconium, and niobium in the black sands. The gold concentrations were approximately 8.81 cents per cubic yard based on 1967 prices (Hammond, 1967). At more current prices, (9/14/16 USA Today, p. 5B), the value would be over $2.30 per cubic yard. The titanium, zircon, and niobium are about 1 percent (20 pounds per ton) of the concentrate recovered using a magnetic separator (Hammond, 1967).

The Halfway Park deposit appears to be similar to a number of rare earth element occurrences described by the USGS on the Idaho Batholith (Long and others, 2010) in that the rare earths occur in other heavy minerals in alluvial material that weathered from the Idaho Batholith.

The Idaho placer deposits occur in alluvial deposits in Bear and Long Valley on the western flank of the Idaho Batholith (Long and others, 2010). These deposits were mined by dredges for monazite in the 1950s. The primary heavy minerals are ilmenite, magnetite, sphene, garnet, monazite, euxenite, zircon, and uranothorite (a uranium-rich thorite) (Long and others, 2010). The euxenite contains tantalum as well as niobium.

Figure 1. General location map of the area surrounding the Halfway Park placer. Base map from Google Maps.

One important reason to have a variety of different types of rare earth deposits in an inventory for the United States is that some deposits will take longer to develop than others. Supply lines can take between 10 and 15 years or longer to go from the initial discovery to production because of challenging mining regulations, the high costs of opening a new mine, and environmental concerns (Abraham, 2015).

CONCLUSIONS

The Halfway Park placer is significant because deposits similar to those described by Long and others (2010) in Idaho are more widespread than have been reported. These deposits are shallow, near-surface occurrences could easily be mined and the valuable minerals separated, and so deserve more detailed study.

REFERENCES

Abraham, D.S., 2015, The next resource shortage?: The New York Times, November 20, p. A27.

Hammond, R.M., 1967, A report and analysis of the testing program on the Halfway Park placer, Jefferson County, Montana: Unpublished report to C.M. Hauptman, 4 p.

Haxel, G.B., Hendrick, J.B., and Orris G.J., 2002, Rare earth elements—Critical resources for high technology: United States Geological Survey Fact Sheet 087-02, 12 p.

Long, K.R., Van Gosen, B.S., Foley, N.K., and Cordier, Daniel, 2010, The principal rare earth elements deposits of the United States—A summary of domestic deposits and a global perspective: United States Geological Survey Scientific Investigations Reports 2010-5220, 96 p.

Smedes, H.W., Klepper, M.R., Pinckney, D.M., Becraft, G.E., and Ruppel, E.T., 1962, Preliminary geologic map of the Elk Park quadrangle, Jefferson and Silver Bow Counties, Montana: United States Geological Survey Mineral Investigations Field Studies Map MF-246, scale 1:48,000.

Van Gosen, B.S., Verplanck, P.L., Long, K.R., Gambogi, Joseph, and Seal II, R.R., 2014, The rare-earth elements—Vital to modern technologies and lifestyles: United States Geological Survey Fact Sheet 2014-3078, 4 p.

Vuke, S.M., Porter, K.W., Lonn, J.D., and Lopez, D.A., 2009, Geologic map of Montana: Field notebook: Montana Bureau of Mines and Geology Geologic Map 62-E, 59 p., scale 1:500,000.

POSTER ABSTRACTS

EXPLORING THE LITHOLOGIC INFLUENCE ON BEDROCK RIVER MORPHOLOGY THROUGH THE SALMON RIVER WATERSHED OF CENTRAL IDAHO

Nate Mitchell

Department of Earth and Atmospheric Sciences, Indiana University, Bloomington, Indiana 47405

ABSTRACT

Bedrock river morphologies reflect both a range of drivers (e.g., climate, tectonics, and their interaction with lithology) and the erosion processes allowed by these drivers (e.g., abrasion and plucking), yet quantitative relationships between morphology and drivers remain elusive. The Salmon River watershed of central Idaho presents an excellent natural experiment through which to quantify the lithologic influence on bedrock river morphology. This suitability is due to: (1) an ongoing transient adjustment of the landscape leading to a morphological contrast between the relict upper reaches and adjusted lower reaches; (2) the wide range of lithologies within the watershed (e.g., basalt, schist, granodiorite, quartzite, and gneiss); (3) the incision of certain tributary streams into only one rock type throughout transient adjustment; and (4) the relatively uniform climate shared by all tributaries due to their proximity.

The poster presents results comparing the morphologies of steady-state and transient streams underlain by different lithologies. The steady-state streams include both relict and adjusted channels eroding at low and high rates, respectively. Channel steepness and concavity from slope-area and the slope-integral methods are considered. Results derived from either of these two methods generally agree. Although steady-state channels with different lithologies do exhibit some statistically significant morphological differences, these differences are only apparent when considering the entire distribution of morphological metrics; individual metrics of fluvial morphology are not always representative of substrate properties. The wide range of transient streams do, however, exhibit a wide range of morphologies that reflect bedrock properties. The poster addresses the implications of these morphological differences in the context of different erosion processes. Preliminary results for analyses that utilize transient stream morphologies to constrain the timing of incision across the Salmon watershed are also presented. Quantifying relationships between the channel morphologies and drivers of bedrock rivers remains an important challenge in the geomorphological community, and the Salmon River watershed highlights the role of lithology in these systems.

AN INTERPRETATION OF SELECTED INFORMATION CONCERNING THE BOULDER BATHOLITH, THE SAPPHIRE BLOCK, AND THE IDAHO BATHOLITH

Michael R. Garverich

P.E., Butte, Montana 59701

ABSTRACT

The premise of this poster is that the Boulder Batholith and Elkhorn Mountains Volcanics were a carapace over the Sapphire Block, which in turn was a carapace over the Idaho Batholith during Sevier thrusting. During extension, the Sapphire Block, the Idaho Batholith, and the metamorphic terranes west of the Salmon River suture "floated" out from under the overlying block(s). In addition, the metamorphic terranes west of the Salmon River suture are obducted island arcs that have been exhumed by extension and the Salmon River suture represents the subduction shear zone that has been exhumed by the same extension.

Felsic magma was introduced into the Sevier Orogeny thrust sheet pile from the subduction zone and flowed up dip along thrust faults. Mineralizing fluids were concentrated in the upper parts of the system (Boulder Batholith), thus providing the Boulder Batholith with its abundance of metals deposits and resulting in the relative lack of metals in the Idaho Batholith. The Challis Volcanics magmas were generated during extension by decompression of residual magmas previously held deep in the system.

This interpretation also includes the hypothesis that extension was triggered by tensional failure of the subducting oceanic slab due to buoyancy loads created by the obducting island arc terranes. This interpretation suggests an extension of about 180 miles. This interpretation also implies that the Montana Lineament should be considered the northern boundary of the Basin and Range province.

THE GRAVELLY RANGE CRATER/ASTROBLEME: A RECENTLY RECOGNIZED PROBABLE IMPACT SITE

Michael R. Garverich

P.E., Butte, Montana 59701

ABSTRACT

In about 2012, the author observed a potential impact crater while examining satellite imagery for the Gravelly Range, Madison County, Montana. A site visit with Ted Antonioli of Missoula revealed a flooded, circular crater with a diameter of about 90 ft at the water surface. Two other circular depressions are located nearby.

The crater is located on the east side of the Gravelly Range crest in the SE¼ SW¼ NE¼ sec. 33, T. 8 S., R. 2 W., about ¼ mi east of the Gravelly Range road on U.S. Forest Service, Beaverhead–Deerlodge National Forest administered land. The most convenient access is from the Ruby River road (Highway 100) by way of the Warm Springs Creek road (FS 163), and then north along the Gravelly Range road (FS 290) for about 2 mi, then take the unimproved two-track eastward to a fence about 200 yd from the crater.

The circular depression is centered on an east-facing, gentle slope with thin soil cover and underlain by thin-to-medium bedded limestone bedrock; limestone outcrops are common. Bedrock is likely Mississippian Mission Canyon limestone that dips gently to the west. The area is contained within the Ennis 1:100,000 scale geologic map (Kellogg and Williams, 2006). The target rock is a light gray weathering limestone that has been pervasively shattered on centimeter scale, but the fragments remain locked together. The margins of debris fragments have been etched by weathering but retain an angular shape. Fractures are generally etched to about 1 mm below the weathered surface.

The crater is asymmetric in plan view due to its location on a slope. The eastern side is the low point of the rim and serves as the spillway for runoff that enters the crater. The western side is a steep slope that extends upward about 15 ft to the local surface. The sides of the crater are covered by blocks and rubble of shattered limestone. At the time of our visit, the water surface of the pond was near the elevation of the outflow. A cursory examination of the area with metal detectors failed to find any metal fragments.

At sometime in the past, a local drainage was diverted into the crater to form a pond for livestock water. The diverted drainage and trampling by livestock are degrading the crater. Tiger salamander larvae (or axolotls) were noted swimming in the pond.

REFERENCE

Kellogg, K.S., and Williams, V.S., 2006, Geologic map of the Ennis 30’ x 60’ quadrangle, Madison and Gallatin counties, Montana, and Park County, Wyoming: Montana Bureau of Mines and Geology Open-File Report 529, 27 p., 1 sheet, scale 1:100,000.

GEOLOGICAL CHARACTERIZATION OF PRECAMBRIAN NONCONFORMITIES: IMPLICATIONS FOR INDUCED SEISMICITY VIA DEEP WASTEWATER INJECTION IN THE MID-CONTINENT UNITED STATES

Laura Cuccio

Utah State University

ABSTRACT

Injection of wastewater into the deep subsurface, near the Precambrian nonconformity, has been linked to an increase in seismic activity over the past 20 years in the mid-continent United States (Walsh and Zoback, 2015; Weingarten and others, 2015; Keranen and others, 2014; Ellsworth, 2013). Deep wastewater injection results in an increase in pore fluid pressure at depth, which propagates along flow conduits, eventually reaching deep basement faults. This changes the stress state of the fault, inducing slip, and ultimately producing seismic activity (Sumy and others, 2014). The Precambrian nonconformity is a viable hydrologic connection between the injection point and the deep basement faults along which earthquakes are occurring (Zhang and others, 2016).

We investigate the geology of Precambrian nonconformities in map, in outcrop, and in core, to examine how this contact may behave as a conduit for fluid flow. Field sites include contact exposures in Cody, WY and Marquette, MI, and basement surface exposures in the northeastern Wind River Range, WY. Core study includes one core from northwestern Illinois, and one core from southeastern Michigan. We employ a multi-scale approach to document the geology of the contact zone. Detailed meter-scale mapping of lithologic variations and brittle features captures the geometry of the contact and related features. Petrographic analysis lets us document micro-scale textural and mineralogical variations throughout the contact zone. Geochemical analyses, including X-ray diffraction, whole-rock geochemistry, and carbon and oxygen stable isotope analysis, let us document specific mineralogical variations in relation to the contact, and allow us to investigate the type, mode, and degree of alteration throughout the contact zone.

We focus on the Wyoming sites for this meeting. The outcrop in Cody, WY exposes the contact between the Cambrian Flathead Sandstone and Precambrian granite and granitic gneiss in the shallow east-dipping limb of Rattlesnake Mountain. Here the contact is undulating and alteration is present solely in the basement rocks. The uppermost basement consists of grus horizons (>1.5 m thick) of varying compositions and textures for the majority of the exposure. Sub-vertical fractures both truncate at and cut through the contact (fig. 1). Small faults that bisect the contact exhibit clay, iron, and chloritic alteration on slip surfaces, whereas low-permeability deformation-band faults formed in the Flathead Sandstone.

Map-scale study of the Archean basement exposures adjacent to the nonconformity, in the northeastern Wind River Mountains, reveals a high-relief, brittlely deformed basement surface. Epidote ± chloritic oblique-slip shear zones strike east and dip steeply. Fracture transects reveal a primary E–W-oriented fracture set and a secondary NW–SE fracture set. Fracture intensity ranges between 0.2 and 0.9 fractures/m. Alteration horizons that may have once been present have likely been glacially removed.

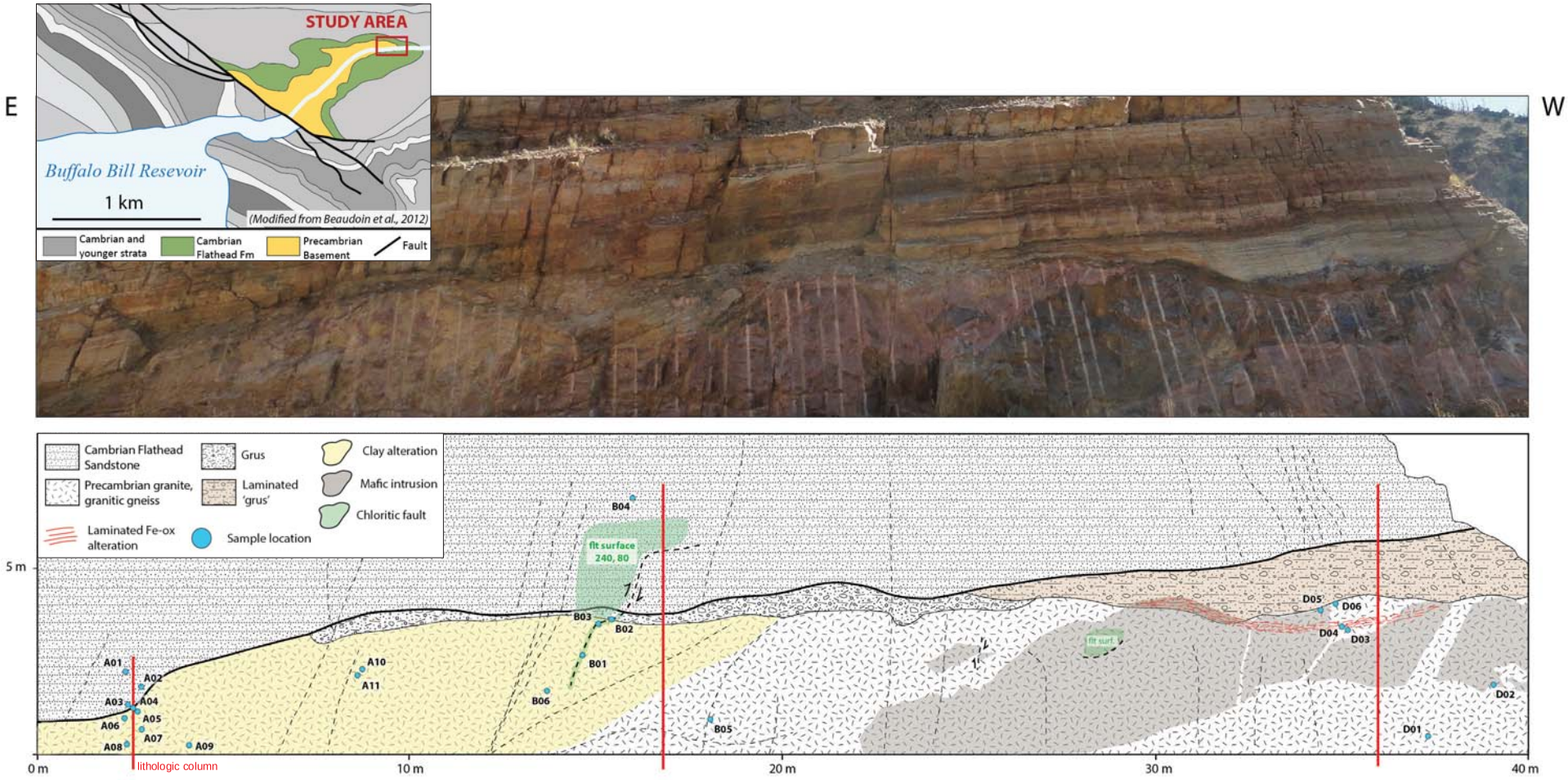

Figure 1. The contact between the Cambrian Flathead Sandstone and Precambrian granite and granitic gneiss is exposed in a roadcut approximately 9 km west of the town of Cody, Wyoming, in the shallow east-dipping limb of Rattlesnake Mountain. The overlying Flathead Sandstone exhibits little to no alteration. Alteration is concentrated along the contact in the basement rocks, varying laterally in degree, type, and thickness. A clay alteration horizon (yellow) in the granitic basement rocks extends up to 2 m or more below the contact in the eastern portion of the exposure. In the western half of the exposure, clay alteration is sparse to non-existent. A cohesive, finely laminated 'grus' horizon (tan) consisting of sub-rounded feldspar clasts in a clay-rich matrix lies directly below the contact. A sub-horizontal, Fe-rich, laminated alteration horizon (red streaks) cuts through both the laminated 'grus' and uppermost portion of the basement. Fault surfaces are commonly chloritic, iron- or clay-rich.

REFERENCES CITED

Ellsworth, W.L., 2013, Injection-induced earthquakes: Science, v. 341, p. 1225942, doi: 10.1126/science.1225942.

Keranen, K.M., Weingarten, M., Abers, G.A., Bekins, B.A., and Ge, S., 2014, Sharp increase in central Oklahoma seismicity since 2008 induced by massive wastewater injection: Science, v. 345, p. 448–451, doi: http://dx.doi.org.dist.lib.usu.edu/10.1126/science.1255802.

Sumy, D.F., Cochran, E.S., Keranen, K.M., Wei, M., and Abers, G.A., 2014, Observations of static Coulomb stress triggering of the November 2011 *M*5.7 Oklahoma earthquake sequence: Journal of Geophysical Research: Solid Earth, v. 119, p. 1904–1923, doi: 10.1002/2013JB010612.

Walsh, F.R., and Zoback, M.D., 2015, Oklahoma's recent earthquakes and saltwater disposal: Science Advances, v. 1, doi: 10.1126/sciadv.1500195.

Weingarten, M., Ge, S., Godt, J.W., Bekins, B.A., and Rubinstein, J.L., 2015, High-rate injection is associated with the increase in U.S. mid-continent seismicity: Science, v. 348, p. 1336–1340, doi: 10.1126/science.aab1345.

Zhang, Y., Edel, S.S., Pepin, J., Person, M., Broadhead, R., Ortiz, J.P., Bilek, S.L., Mozley, P., and Evans, J.P., 2016, Exploring the potential linkages between oil-field brine reinjection, crystalline basement permeability, and triggered seismicity for the Dagger Draw Oil field, southeastern New Mexico, USA, using hydrologic modeling: Geofluids, v. 16, p. 971–987, doi: 10.1111/gfl.12199.

FIELD TRIP GUIDES

GLACIATION OF THE CENTRAL LEMHI RANGE, IDAHO

Glenn D. Thackray and Harrison Colandrea

Idaho State University

BACKGROUND

The Lemhi Range preserves evidence of multiple Pleistocene glaciations, and of Holocene glacier and rock glacier activity. End moraines and outwash fans mark the mouths of several drainages in the central portion of the range near Gilmore, reflecting ice marginal fluctuations during at least two glaciations. In the upper valleys and cirques, active and fossil rock glaciers reflect local microclimatic and lithologic conditions.

Colandrea (2016) documented Lemhi Pleistocene glacial landforms and interpreted their paleoclimatic implications. He built upon earlier work by Wakefield Dort (e.g., Dort, 1962) and Knoll (1977), through: (a) surficial geologic mapping of the Gilmore 7.5-minute quadrangle, (b) glacier mass balance calculations from reconstructed glacier topography, and (c) cosmogenic radionuclide exposure dating of moraine boulders. The map (fig. 1) documents major end moraines of four distinct ages (Qm1–Qm4, oldest–youngest) and coeval alluvial fan surfaces (Qf1–Qf4). Qm1 through Qm3 are closely spaced on and adjacent to the range front in four major valleys, implying broadly similar glacial conditions during the associated phases, while Qm4 typically lies 3–6 km upvalley. Several smaller valleys contain landforms representing parts of that sequence, restricted to the middle to upper valleys. Younger moraines lying closer to the cirques are assumed to represent final, latest Pleistocene deglacial phases. Deglaciation was complete by 14 + 0.5 ka, as represented by radiocarbon dating in a Meadow Lake sediment core (B. Finney, personal commun.). Inferred equilibrium line altitudes associated with the three oldest moraines are ca. 2,700 m, representing an estimated 600 m equilibrium line depression caused by an unknown combination of summer cooling and enhanced snowfall.

A limited suite of cosmogenic radionuclide (CRN) exposure age samples on moraine boulders provides insight into moraine ages. Two samples reflect glaciation during the penultimate (Bull Lake) or earlier events. Six samples reflect phases of Pinedale glaciation, ranging from ca. 43 ka to 16 ka, and reveal likely influence of temperature and precipitation changes in driving regional glaciation.

The modern ice masses in the Lemhi Range take the form of rock glaciers. These are masses of mobile mixes of ice and talus. Johnson (2006) and Johnson and others (2007) documented 48 rock glaciers in 171 alpine valleys in the range. The rock glaciers were categorized within three morphological classes inferred to represent three states of activity. Multivariate statistical analysis demonstrated that the dominant factors in the distribution of rock glaciers of all three types are annual insolation and lithology. Annual sun-hour duration, which is strongly influenced by slope aspect topography, is naturally inferred to act through reduction of snow and ice melting, while lithology likely influences rock glaciers by controlling the dominant size of talus and the valley groundwater hydrology.

FIELD TRIP

The field trip will visit three main sites in the Lemhi Range. The mouths of Deer Creek (ca. 3 km north of Gilmore) and Meadow Lake Creek (northern edge of Gilmore) illustrate the spatial relationships and variable characteristics of the Qm1–Qm3 moraine-fan sequences and provide the context for CRN dating. The Meadow Lake rock glacier, occupying a well-shaded portion of the cirque, reveals the dominant characteristics of Lemhi Range rock glaciers and the factors that influence their distribution. The field trip will involve vehicle travel on gravel roads and dirt tracks, as well as moderate hikes of up to 2 mi.

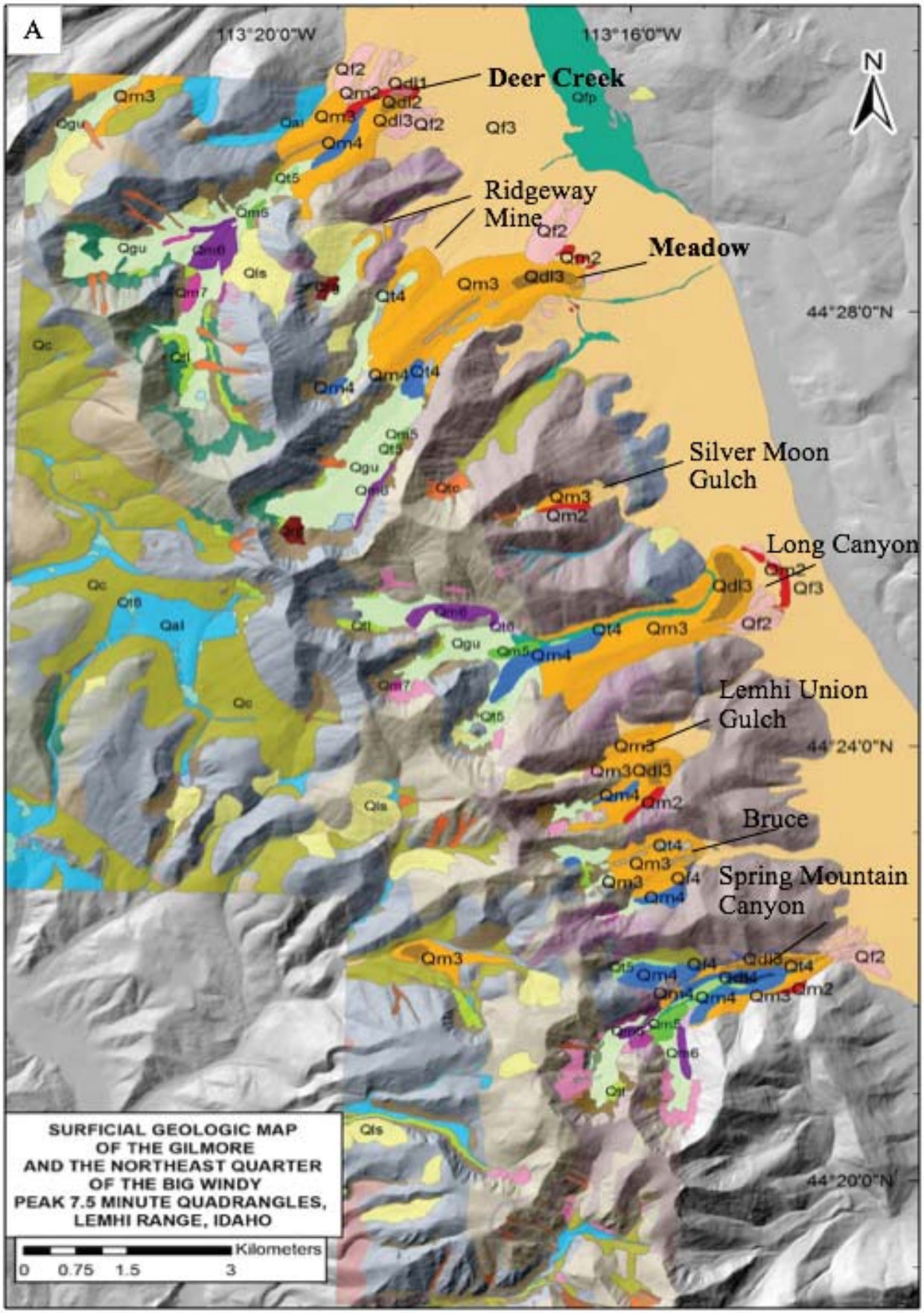

Figure 1A. Surficial geologic map of the Gilmore and northeast quadrant of the Big Windy Peak 7.5-minute quadrangles, superimposed on a 10 m DEM hillshade with major valley names denoted. Portions of the figure that lack content are located off of the quadrangle boundaries. Bedrock units (Ruppel and Lopez, 1981) are in muted colors. (Colandrea, 2016).

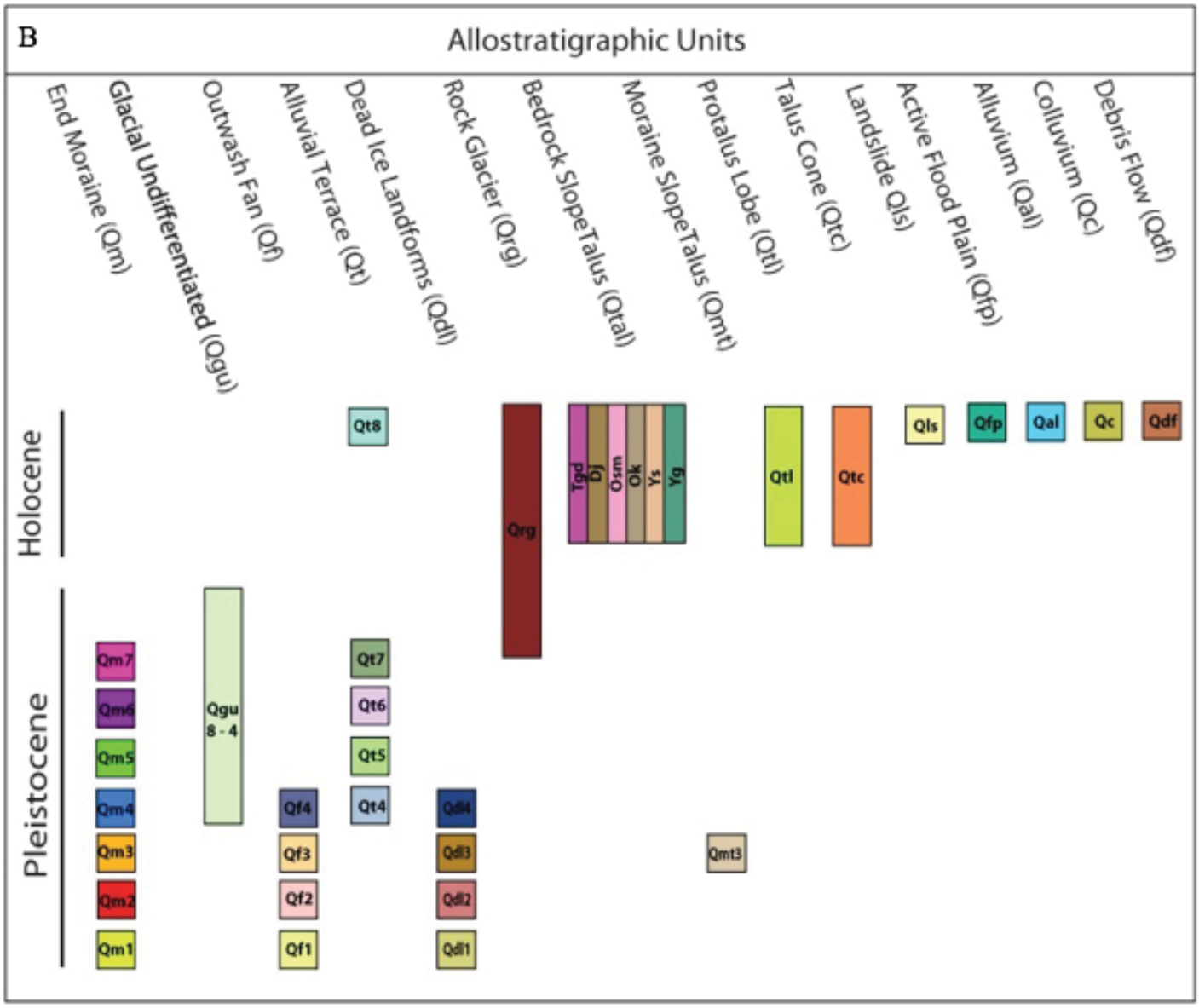

Figure 1B. Correlation of surficial map units, depicted in figure 1A, shows the relationship between the mapped surficial features type and relative ages (Colandrea, 2016).

REFERENCES CITED

Colandrea, H.A., 2016, Spatial and temporal patterns of Late Pleistocene glaciation in the Lemhi Range, east-central Idaho: Pocatello, Idaho State University, M.S. thesis.

Dort, Wakefield, 1962, Multiple glaciation of southern Lemhi Mountains, Idaho: Preliminary reconnaissance report, Tebiwa, 5.2, p. 2–17.

Johnson, B.G., 2006, The effect of topography, latitude, and lithology on the distribution of rock glaciers in the Lemhi Range, central Idaho: Pocatello, Idaho State University, M.S. thesis.

Johnson, B.G., Thackray, G.D., and Van Kirk, R., 2007, The effect of topography, latitude, and lithology on rock glacier distribution in the Lemhi Range, central Idaho, USA: Geomorphology, v. 91.1, p. 38–50.

Knoll, K.M., 1977, Chronology of alpine glacier stillstands, east-central Lemhi Range, Idaho, Idaho State University Museum.

Ruppel, E.T., and Lopez, D.A., 1981, Geologic map of the Gilmore quadrangle, Lemhi County, Idaho: U.S. Geological Survey Geologic Quadrangle Map GQ-1543, scale 1:62,500.

ORE CONTROLS OF THE LEADVILLE (JUNCTION) AND GILMORE MINING DISTRICTS, LEMHI COUNTY, IDAHO: A FIELD TRIP GUIDE

Bruce Cox and Ted Antonioli

Geologists, Missoula, Montana

INTRODUCTION

The casual observer driving Idaho Highway 28 in southern Lemhi County and northern Clark County would be struck by the grandeur of the Lemhi and Beaverhead peaks but might not appreciate the area's rich mining history—until they stop at the roadside historical marker near Gilmore. With few exceptions, mining and mineral exploration have been dormant in southern Lemhi County for several decades. However, the volume of historic and geologic literature on the subject is considerable. Several previous authors supplemented their field investigation reports with data supplied by the mine operators; most notably, Umpleby (1913), Ruppel and Lopez (1988), and Mitchell (2004). There is probably an equal or greater volume of unpublished mining and mineral exploration data for the Lemhi County districts. In aggregate, these data can help build a 4-dimensional picture of ore controls for the deposits that have been historically exploited and help construct models for deposits yet to be discovered.

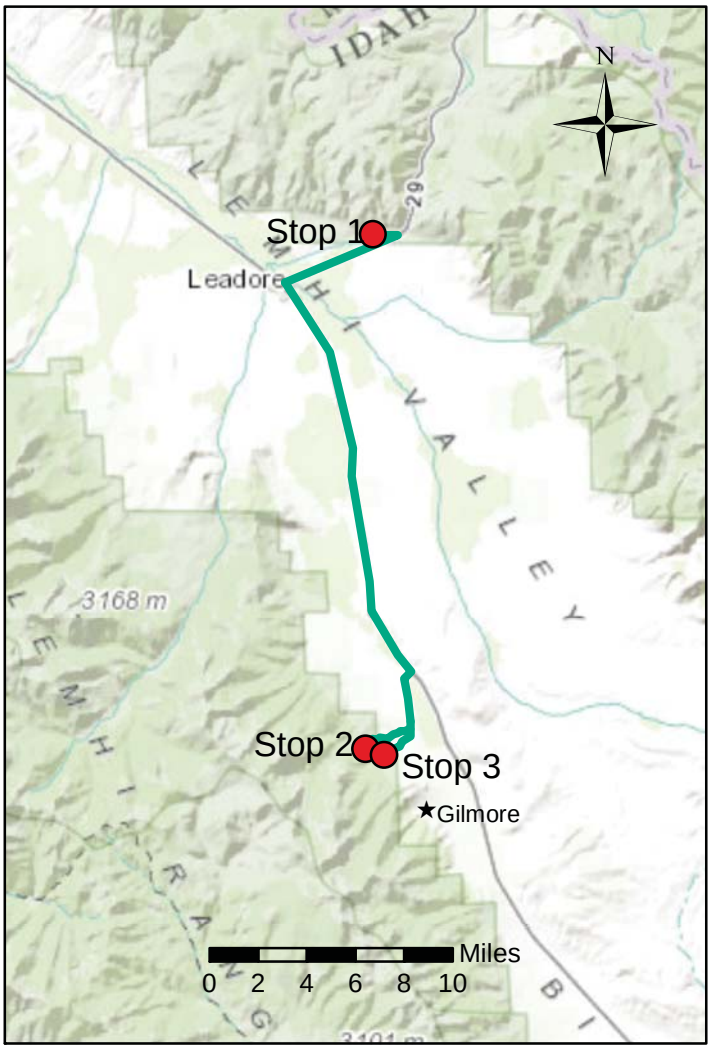

Figure 1. Field trip route and stops.

ACKNOWLEDGMENTS

We express our thanks to Eric Sims and Barry Marcus for permission to visit the Democrat mine, and to Pete Ellsworth for review of the text and assistance with the field guide figures.

FIELD GUIDE

Miles traveled:

0.0 Leadore. Junction Idaho Highways 28 and 29 (44.680686°N / 113.358147°W) (fig. 2).

3.68 Turn left (W) onto dirt road toward Smokey Cub Campground.

3.79 Cross cattle guard.

3.81 Keep straight. Smokey Cub Campground on left.

3.84 Cross Canyon Creek.

3.87 T intersection. Turn right (E) and follow main road which gradually curves uphill to NW.

4.19 Italian Gulch road enters from right; stay straight.

4.67 Road enters from right; stay straight.

3.57 **STOP 1**

Leadhill mine open cut. (44.706028°N / 113.30755°W). Examine exposures in the mine pit walls. Use caution: loose rock and snakes (?).

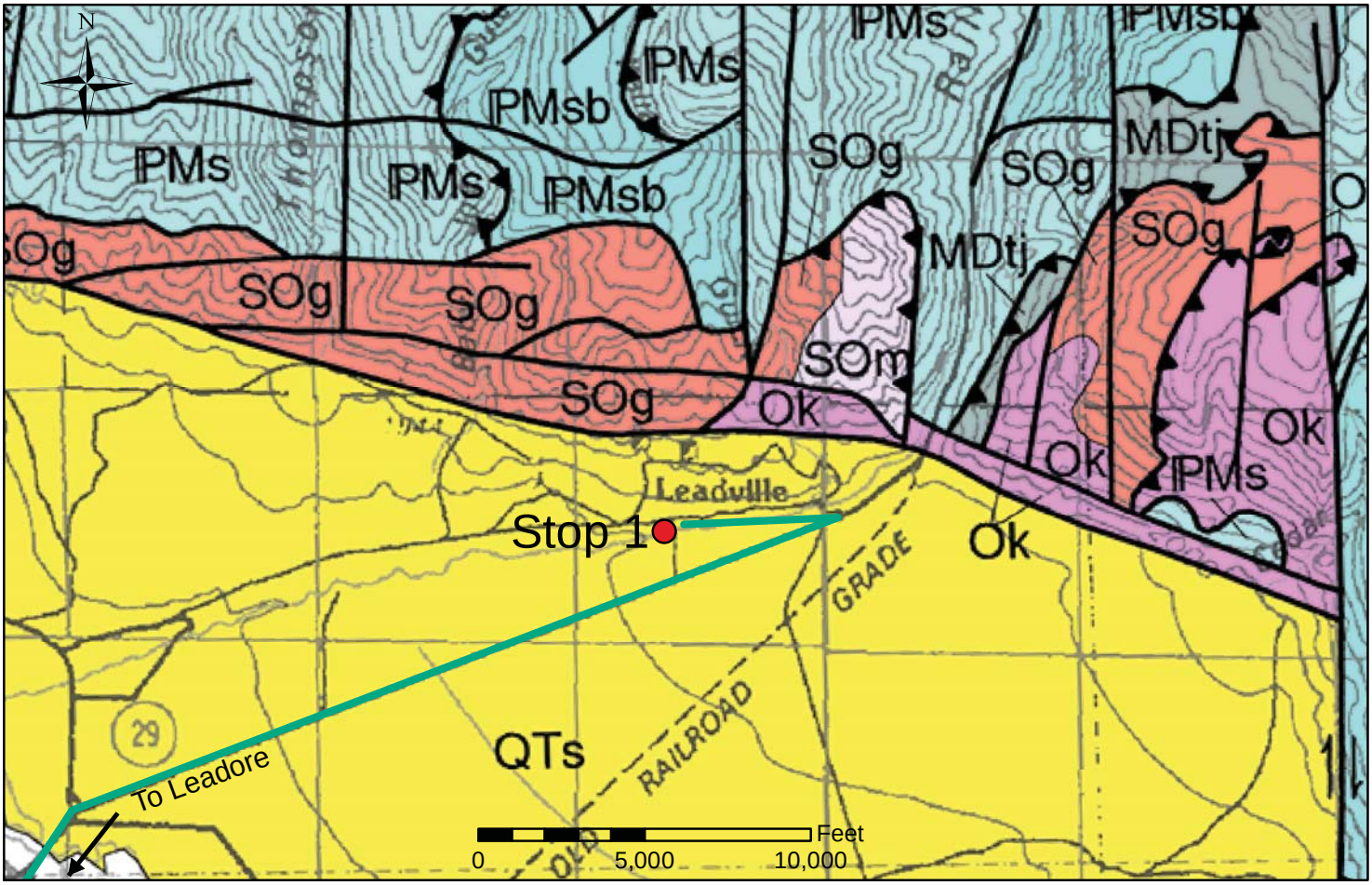

Figure 2. Geology of the Leadville mining district (see Ruppel, 1968 for legend).

Leadville (Junction) Mining District

The following description of Leadville district geology and mineralization is condensed from reports by Hershey (1920), Ruppel (1968), and Umpleby (1913).

The Beaverhead range front northeast from Leadore is underlain by limestone, quartzite, and granite within a WNW-trending fault zone that dips 35-40° SW; this fault places Quaternary fan gravels against older rocks. Mineralization post-dates the Ordovician (?) granite and pre-dates the latest movement on the range front fault, which movement is marked by a thin but impermeable clay gouge that protects the underlying mineralized rock from oxidation. Range front faulting likely began during Cenozoic extension and is the probable conduit for the mineralizing hydrothermal fluids.

The Leadville mine workings (fig. 3) provide a typical profile of the range front geology and mineralization. The upper portion of fault zone mineralization has been stoped up-dip (continuously?) for nearly 600 ft from the Union tunnel level. Altered rock has been mined from the open cut at Stop 1 (figs. 4 and 5), but data on tonnage and grade of this material was not found.

Questions that deserve further investigation: (1) Does district mineralization extend below the Lemhi Valley floor elevation?, (2) What are the ages of the discordant dikes and larger masses of granite?, and (3) Does district mineralization represent the lead-dominant zone of a concealed Cu-Au-Mo porphyry system?

Return to Leadore via the same route and reset odometer to 0.0 at junction with Highway 28.

0.0 Junction Highways 28 and 29 (44.680686°N / 113.358147°W). Drive south toward Idaho Falls.

12.14 Turn right (SW) onto gravel road (Texas Creek Rd.) (44.518633°N / 113.283131°W).

12.39 Fork. Follow main track to left (S).

13.93 Main track turns right toward Lemhi Range. This is the base of the Democrat mine road (44.494131°N / 113.283758°W). Return to this junction after visiting STOP 2.

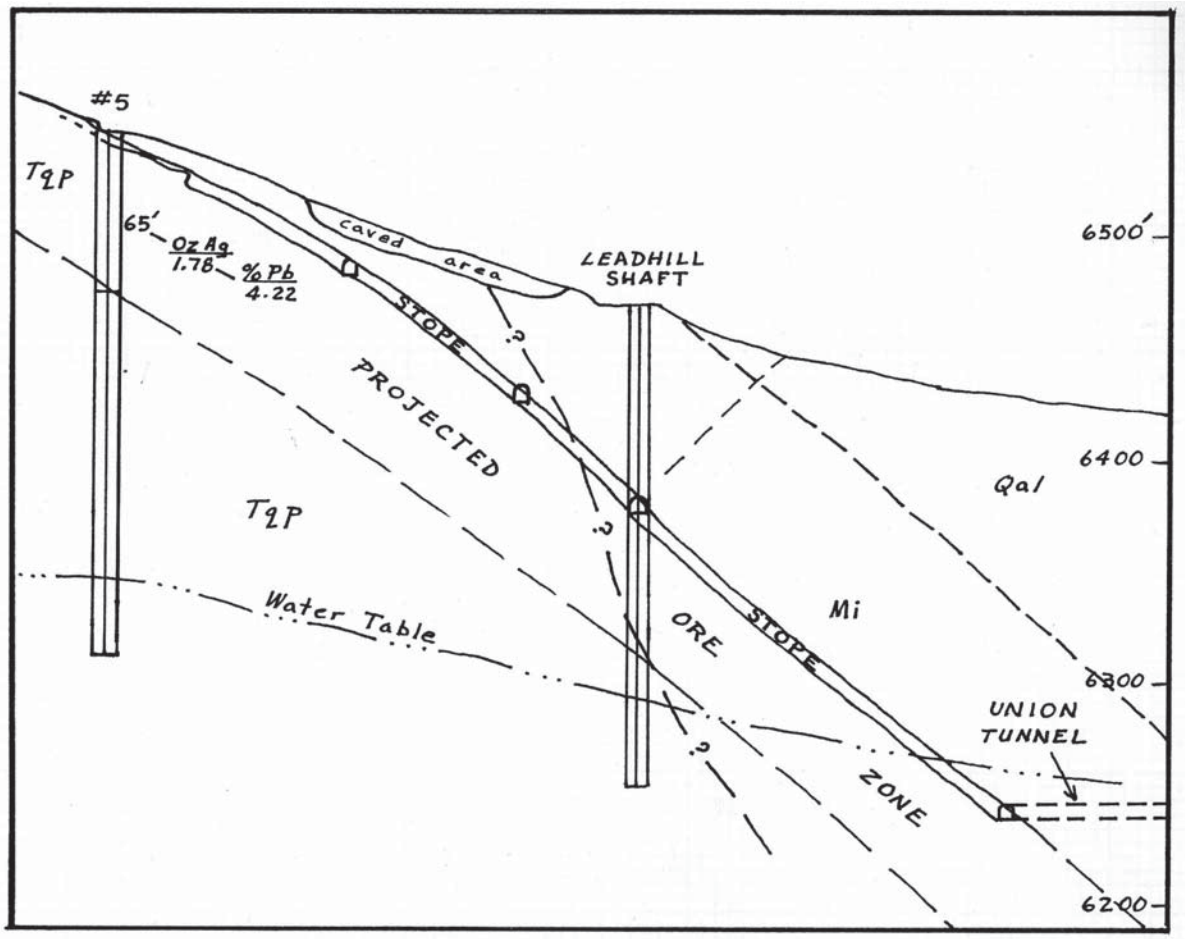

Figure 3. Cross-section of Leadville mining district range front deposits; redrawn from Melbye, 1965.

Figure 4. Mineralized shear fault exposed in east wall of the Leadville Mine open cut. Note hanging wall Quaternary fan gravels in the background.

Figure 5. Close-up from figure 4; sheared rock near the top of the range front fault zone.

15.01 Fork. Bear right here and around next curve. Cabin on left is on a millsite claim of Democrat Resources, LLC.

15.82 **STOP 2**

Democrat Mine: 800 Level main adit, shops and dumps (44.485047°N / 113.312058W).

Figure 6 is a geologic map for Stops 2 and 3. If an underground tour is available, visitors will be given site-specific mine safety training and will be required to use MSHA-certified personal safety equipment.

Recent Development

Under the guidance of Sandy Sims (fig. 7), Democrat Resources, LLC developed a decline below, and three new levels above the historic 800 mine level, respectively. This work confirmed the continuity of veining for a minimum 400 ft down-dip and reveals several aspects of vein geology that can guide continued development and production. The most recent mine plan (Lawrence, 1999) proposes narrow vein mining of 29,828 tons of proven and probable reserve containing 0.146 opt gold, 16.9 opt silver and 26% lead; zinc grade was not reported.

Hilltop Vein Geology

The Democrat (Hilltop) veins are hosted in tightly folded Jefferson Formation dolomite and are oriented sub-parallel to the Lemhi range front. The Hilltop veins occupy a shear fault system that generally strikes northwest and dips 60 degrees southwest. Vein thickness ranges from a few inches to several feet and averages approximately 1.5 ft (fig. 8). The principal displacement zone/fault structure ("PDZ ") that the vein occupies can be traced by the presence of brown-to-black clast-supported fault breccia even where veining pinches and ore minerals are absent. The rake of the ore shoots appears to be vertical or steeply inclined to the southeast. Veining locally cuts across the dolomite bedding at low angles. The previous two observations suggest that ore shoots occur as lenses that are more likely to pinch and swell along strike rather than up or down dip.

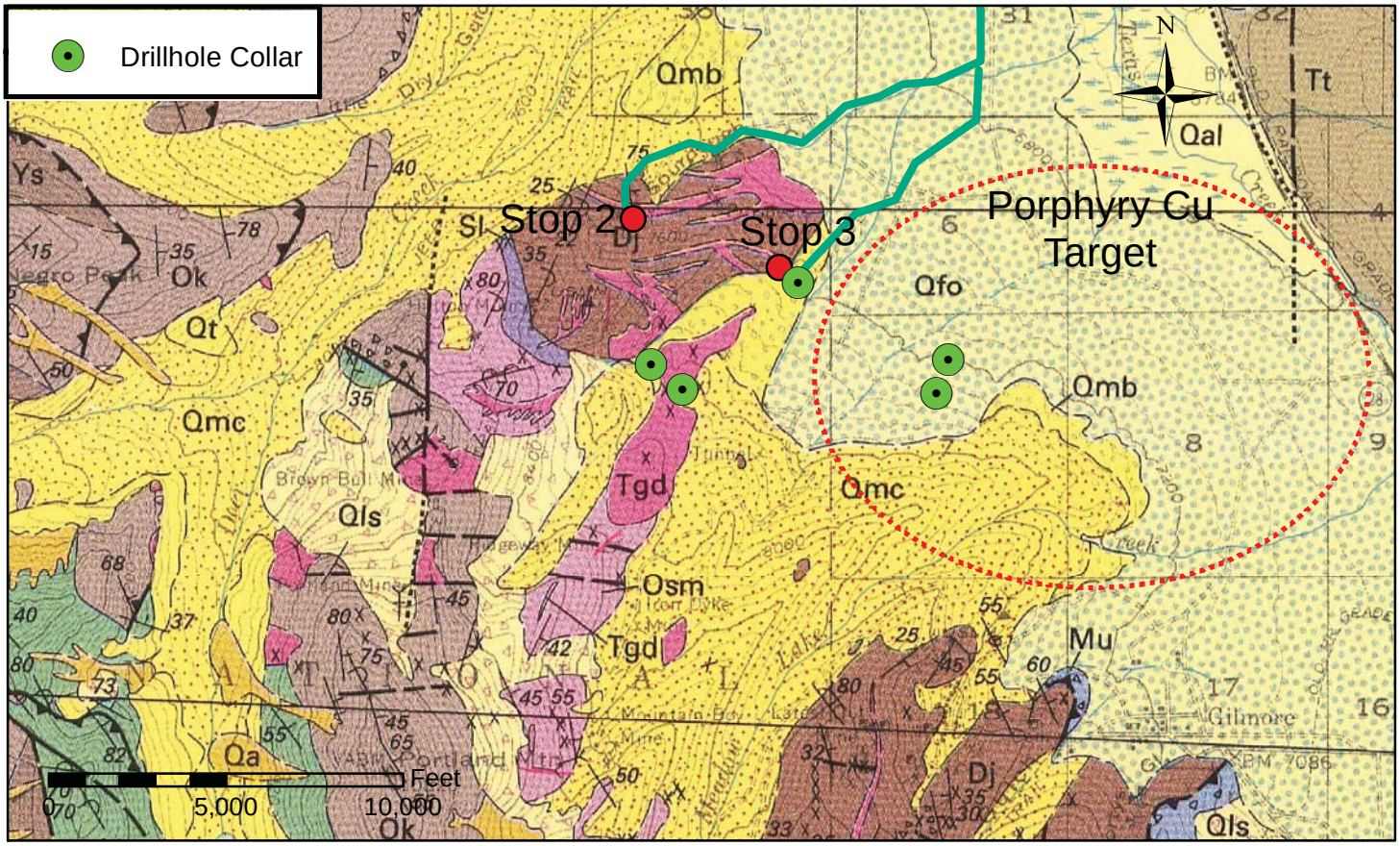

Figure 6. Surface geologic map of the Democrat (Hilltop) mine and Groom Creek porphyry target area, modified from mapping of Ruppel and others (1970).

Figure 7. Portal of the Democrat Mine—Sandy Sims (1941–2014), owner/miner.

Figure 8. Photo of Hilltop vein at west face of main stope above 800 level; clipboard for scale.

Probable ore-grade veining is exposed at the margins of stopes that have been mined upward from the 800 level and winze and in the floor of the 500 level. This observation indicates vein continuity in the reserve blocks described by previous investigators. In addition to the tabular veins, pipe-like masses of ore occur along and flanking the PDZ and may be controlled by synthetic (splay) faults that merge with the PDZ. Bleached, fine-grained concentric layering at the margins of several pipes suggests that ore minerals may have deposited in karst (cave) solution breccias that had opened along the rake of intersecting faults.

Return to valley floor (44.494131°N / 113.283758°W) and reset mileage to 0.00.

0.0 Travel south toward mouth of Groom Creek.

0.17 Turn right on road climbing along axis of the Groom Creek fan.

0.65 4-way intersection. Turn right (W).

1.19 **STOP 3**

Groom Creek intrusive porphyry target (44.483233°N / 113.298644°W) (fig. 6).

Park in unimproved campsite on the south side of Groom Creek. The campsite is atop a lateral (?) lobe of the Groom Creek till. Roadcuts in hillside to NW expose a diorite porphyry dike and carbonate exoskarn peripheral to the mineralized porphyry target (fig. 9).

Groom Creek Exploration

Historic development and production in the Gilmore or Texas mining district concentrated on the numerous lead–silver veins that outcrop in the central part of the district (Mitchell, 1997). Focus on "hidden targets" and "the big picture" received a major push during and after a USGS program of geochemical and geophysical investigations in the central Lemhi Range led by Ed Ruppel, who thought it probable that the quartz diorite stock exposed near Groom Creek was genetically related to the mineral deposits of the greater district (Ruppel and others, 1970).

At about the same time, Vanguard Exploration conducted regional aeromagnetic and other geological and geophysical work in a broad area generally east of Gilmore (The Greater Gilmore Project). As the project progressed, work focused in on the Groom Creek area (fig. 10). In 1970–1971, Vanguard drilled at least five holes totaling 7,780 ft through the glacial outwash and into altered and mineralized intrusive bedrock (Hinman, 1974).

The targets were principally areas showing a high chargeability response in induced polarization surveys. Exploration drilling indeed encountered extensive

Figure 9. Diorite porphyry dike (under hammer) flanked by carbonate exoskarn.

Figure 10. View southeast from northern margin of the Groom Creek porphyry target.

zones of sulfide mineralization but copper values were generally low. Follow-up work to refine targeting was not done, apparently because the copper price began a decade-long major downturn beginning in the early 1970s. As far as is known, the alteration found in the drilling was never placed into the context of a modern porphyry copper model.

End of field trip. If time allows, return to Highway 28, drive south, and visit the town and mines of the central Gilmore mining district.

REFERENCES CITED

Hershey, O.A., 1920, Report on Baby Joe, Kimmel, and Sunset Lead mines: unpublished report in Idaho Geological Survey's files, 8 p.

Hinman, R., 1974, Review and discussion of the geophysical data on the Groom Creek area, greater Gilmore project. Report to Teton Exploration Drilling Company, Casper, Wyoming, 40 p.

Lawrence, J.C., 1999, Feasibility study of the Democrat Mine, Lemhi County, Idaho: private intracompany report, 21 p.

Melbye, C.E., 1965, Progress report, April, 1965 drilling program and ore reserve evaluation, Leadville Property, Junction mining district, Lemhi County, Idaho: Unpublished report in Idaho Geological Survey's mineral property files, 5 p.

Mitchell, V.E., 1997, History of the mines in the Texas Mining District near Gilmore, Idaho: Moscow, Idaho, Idaho Geological Survey.

Mitchell, V.E., 2004, History of the Leadville, Kimmel, and Baby Joe mines, Lemhi County, Idaho: Idaho Geological Survey Staff Report 04-1, 35 p.

Ruppel, E.T., 1968, Geologic map of the Leadore quadrangle, Lemhi County, Idaho: U.S. Geological Survey Geologic Quadrangle Map GQ-733, scale 1:62,500.

Ruppel, E.T., and Lopez, D.A., 1988, Regional geology and mineral deposits in and near the central part of the Lemhi Range, Lemhi County, Idaho: U.S. Geological Survey Professional Paper 1480, 122 p.

Ruppel, E.T, Watts, K.C., and Peterson, D.L., 1970, Geologic, geochemical and geophysical investigations in the northern part of the Gilmore mining district, Lemhi County, Idaho: U.S. Geological Survey Open-File Report 70-282, 56 p.

Umpleby, J.B., 1913, Geology and ore deposits of Lemhi County, Idaho: U.S. Geological Survey Bulletin 528, 182 p.

FIELD GUIDE TO THE LEMHI ARCH AND MESOZOIC-EARLY CENOZOIC FAULTS AND FOLDS IN EAST-CENTRAL IDAHO: BEAVERHEAD MOUNTAINS

David M. Pearson and Paul K. Link

Idaho State University, Pocatello, Idaho

INTRODUCTION

This field trip will focus on a portion of the Rodinian rift margin on the western edge of Laurentia where Neoproterozoic to Lower Ordovician syn- and early post-rift clastic sedimentary rocks are absent. This region of missing stratigraphy, called the Lemhi arch, is in east-central Idaho, is roughly northwest-trending, and contains a belt of Cryogenian and Late Cambrian alkalic plutons (e.g., Lund and others, 2010). This region of thin or absent Neoproterozoic and lower Paleozoic strata correlates spatially with the boundary between the northern Wyoming salient and southwest Montana reentrant of the Mesozoic to early Cenozoic Sevier–Laramide fold-thrust belt (Armstrong, 1975) and likely influenced the transition from thin- to thick-skinned thrusting.

This field trip will contain two themes: (1) the Lemhi arch and its stratigraphic and magmatic expression in east-central Idaho; and (2) the structural style of the Mesozoic to early Cenozoic Sevier–Laramide fold-thrust belt within the Lemhi arch. The trip will begin with a visit to Skull Canyon in the southern Beaverhead Mountains, where we will examine the basal angular unconformity of the Lemhi arch between tilted Proterozoic sandstones of the upper Belt Supergroup and overlying Ordovician sandstones. We will then stop in lower Skull Canyon to see prominent folds in middle and upper Paleozoic carbonates; this style of folding seen here is characteristic of the structurally shallow levels of deformation within the Sevier fold-thrust belt in the region. This will be followed by a visit to Hawley Creek, east of Leadore, where an alkalic late Cambrian pluton intruded just prior to or during active exhumation of the Lemhi arch. This pluton was thrusted upon middle Paleozoic carbonates in Late Cretaceous time along the Hawley Creek thrust. The style of "basement involved" thrusting here is in contrast to the thin-skinned, detachment folding and thrusting in middle Paleozoic carbonate rocks observed in lower Skull Canyon.

GEOLOGIC SETTING

Neoproterozoic to early Paleozoic Stratigraphic Framework

Neoproterozoic to early Paleozoic rifting of the Rodinian supercontinent was fundamental in shaping what is now the western margin of North America. In addition to establishing the first-order geography, the rift geometry imposed the syn- and post-rift stratigraphic framework of western North America, which had a major influence on the subsequent geological evolution of the North American Cordillera. For much of the western margin of North America, the record of Neoproterozoic and early Cambrian rifting and the transition to passive margin sedimentation are well established (Stewart, 1972; Christie-Blick, 1982; Link and others, 1993; Yonkee and others, 2014). Early regional-scale studies proposed that syn-rift fill and westward thickening passive margin sedimentary rocks continued northward from southeastern Idaho into southeastern British Columbia (e.g., Stewart, 1972). However, the intervening region between the eastern Snake River Plain and southeastern British Columbia along the Idaho–Montana border seemed to not fit into that framework. There, workers documented Middle Ordovician rocks that unconformably overlie Mesoproterozoic Belt Supergroup rocks, and a completely missing Neoproterozoic to Lower Ordovician stratigraphic record (Ross, 1934, 1947; Sloss, 1954; Scholten, 1957). Neoproterozoic and lower Cambrian rocks are largely missing in southwestern Montana too, where middle Cambrian rocks of the Flathead Formation overlie Archean basement or rocks of the Belt–Purcell Supergroup (Deiss, 1941; Sloss, 1950; Bush and others, 2012), with likely Neoproterozoic to early Cambrian erosion prior to middle Cambrian deposition (Norris and Price, 1966).

A recent regional compilation of the tectonostratigraphic framework of early Laurentian rifting focused in Utah, southeastern Idaho, and Nevada recognized the major northward change in the character of the rift margin sedimentation pattern by demonstrating a

consistent 6- to 7-km-thick clastic section of Neoproterozoic and Cambrian rocks from SE Idaho south to central Utah (Yonkee and others, 2014). In addition, rocks in northern Utah and SE Idaho established a final transition to drift from 580 to 540 Ma (Yonkee and others, 2014). This is in stark contrast to the margin in east-central Idaho and southwestern Montana, where alkalic magmatism (Evans and Zartman, 1988; Lund and others, 2010; Todt and Link, 2013) and regional tectonism (Link and others, in review) persisted into late Cambrian and Early Ordovician time (500 to 485 Ma), nearly 50 m.y. later than the transition to drift and passive margin sedimentation documented to the south.

The absence of Neoproterozoic and Cambrian rocks in east-central Idaho and missing Neoproterozoic to lower Cambrian rocks in western Montana likely reflects the presence of a regional paleotopographic high at the rift margin. Because of several different names that have been used to describe this feature, for simplicity, we refer to the region of very thin or missing Neoproterozoic and Cambrian rocks in east-central Idaho (variably called the Lemhi arch, Salmon River arch, or Skull Canyon disturbance) as the Lemhi arch (see McCandless, 1982 for a discussion). For additional discussion of Montana, which we consider a separate feature, see Bush and others (2012). This trip will examine the basal unconformity of the Lemhi arch and the Late Cambrian Beaverhead pluton intruded just prior to or during its exhumation.

Mesozoic to Early Cenozoic Retroarc Shortening

Southeast of the Montana/Idaho border, thrust traces in the Sevier fold-thrust belt transition northward from north–south trending within the Wyoming salient to northwest–southeast trending, defining the southwestern Montana reentrant (fig. 1). Many workers have concluded that similar salients and reentrants in thrust belts are controlled by the pre-deformational geology (e.g., Crosby, 1969; Allmendinger and Gubbels, 1996). Hypotheses for the dominant controls for the abrupt transition from thin- to thick-skinned shortening in the Sevier fold-thrust belt vary widely, including impingement of the thrust system against early basement-involved structures to the east (e.g., Perry and others, 1988) or Proterozoic basement (Armstrong, 1975) and thickness variations in the pre-deformational stratal thicknesses (Crosby, 1969).

This field trip will visit two localities that support a correlation between thrust belt geometry and stratigraphic architecture. At shallow stratigraphic levels from central Idaho out to southwestern Montana, thin-skinned décollement horizons occur in thick Devonian and Lower Mississippian flysch (Skipp and Hait, 1977; Perry and others, 1989). However, thrusts at deeper structural levels in this part of the fold-thrust belt are rare and appear to have accommodated shortening in a markedly different structural style. In contrast to much of the Wyoming salient to the south, where décollements exploit weak shales of the Cambrian Gros Ventre Formation (Royse and oth-

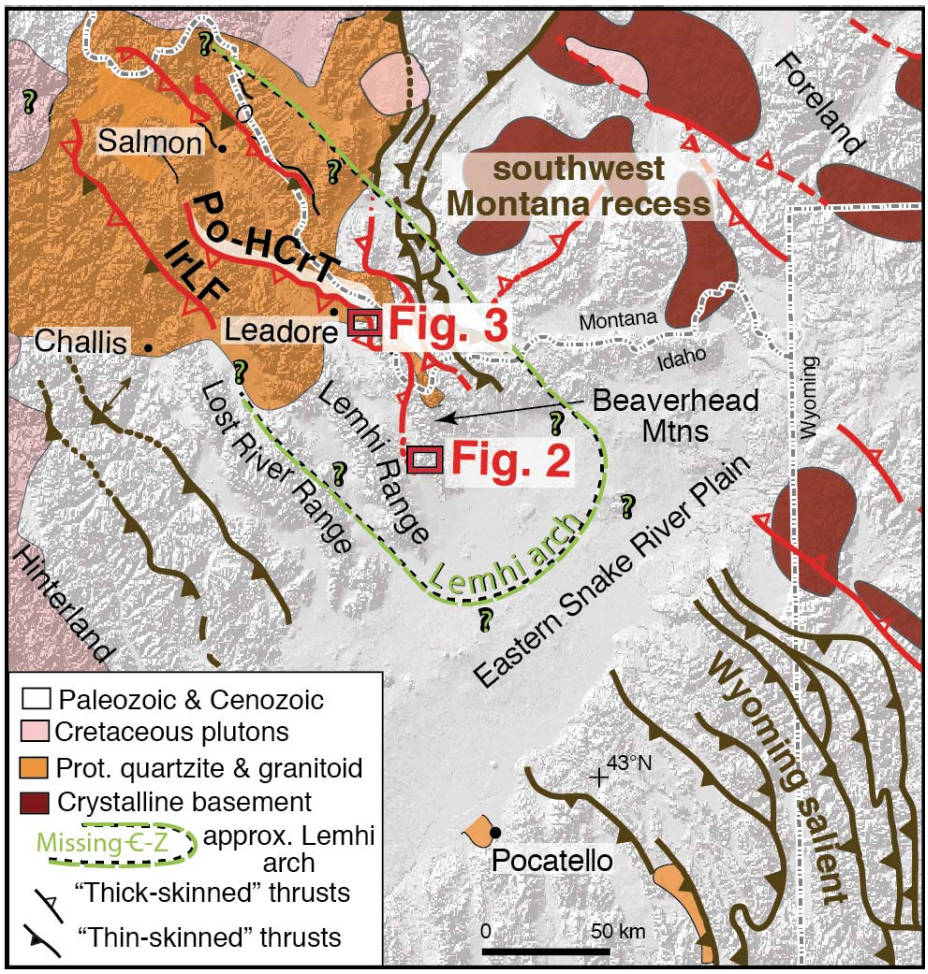

Figure 1. Index map of the geologic setting of the field trip localities (modified from Janecke and others, 2000). Po-HCrT: Poison-Hawley Creek thrust; IrLF: Iron Lake fault.

ers, 1975), in the absence of these rocks in east-central Idaho due to the Lemhi arch, thrusts display a structural style reminiscent of thick-skinned, basement-involved fold-thrust belt deformation. This structural style is characterized by inversion of older normal faults (Hansen and Pearson, 2016), large-wavelength folding (Lucchitta, 1966; Tysdal, 2002; Lonn and others, 2016), and involvement of crystalline basement rock and Proterozoic Belt Supergroup in thrust sheets (Skipp, 1988). This trip will examine the thin-skinned structural style exhibited by middle and upper Paleozoic carbonates as well as the more deeply rooted Hawley Creek thrust, which carries Late Cambrian hypabyssal plutons and may correlate alongstrike to the northwest with the inverted Poison Creek thrust.

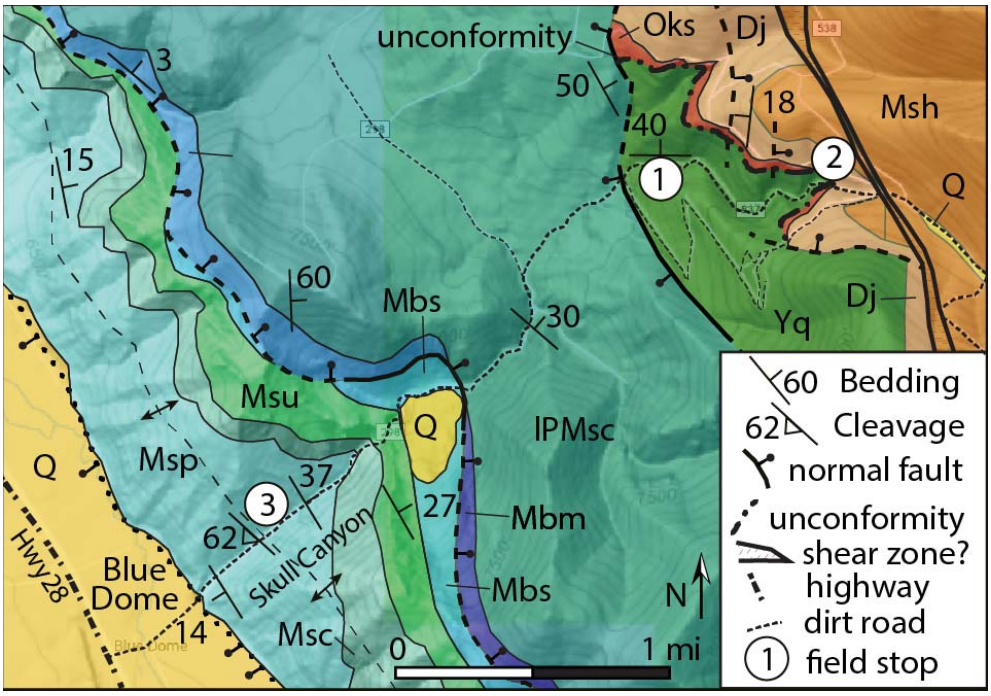

Figure 2. Simplified geologic map of the Skull Canyon area showing field trip Stops 1, 2, and 3 (modified from Scholten and Garmezy, 1980; Embree and others, 1983). Unit abbreviations: Yq-quartzite of likely Mesoproterozoic age; Oks-Ordovician sandstone of the Kinnikinic Formation and possible Summerhouse Formation; Dj-Devonian Jefferson Formation; Msh-undivided lower Scott Peak, Middle Canyon, and McGowan Creek formations; Msp-Mississippian Scott Peak Formation; Msc-Mississippian South Creek Formation; Msu-Mississippian Surrett Formation; Mbs-Mississippian Big Snowy Formation; Mbm-Mississippian Bluebird Mountain Formation; IPMsc-Pennsylvanian/Mississippian Snaky Canyon Formation; Q-undifferentiated Quaternary sediments.

ROAD LOG

The road log begins in Blue Dome, Idaho, which is located along Highway 28 approximately 45 mi southeast of Leadore and 32 mi northwest of Mud Lake. Reset your odometer at the intersection of Skull Canyon Road and Highway 28 (44.159779°N, 112.914156°W) and proceed northeast into Skull Canyon. Near the mouth of Skull Canyon, the road becomes USFS Road 298. Continue on the main road and stay right at the fork at 1.5 mi (44.179871°N, 112.883627°W), proceeding on USFS Road 837. Continue on this road until mile 2.2 at a sign for USFS Road 837 (44.185018°N, 112.876481°W), where a smaller jeep road branches to the right. Park on the northwestern side of the road intersection adjacent to the sign for USFS Road 837.

Skull Canyon Overview

Stops 1 and 2 involve a ~0.9 mi walk up USFS Road 837 to view likely Proterozoic sandstone (Belt Supergroup) and Ordovician sandstone that lies in angular unconformity above it. Rocks near this locality have been described by Scholten (1957), Beutner and Scholten (1967), McCandless (1982), and Skipp and Link (1992). Intrepid drivers with high-clearance vehicles who prefer not to walk can drive this portion of the trip. Stops 1 and 2 will be followed by a drive back down Skull Canyon toward Highway 28 to Stop 3. Stop 3 within lower Skull Canyon will focus on the style of deformation in structurally shallow, middle Paleozoic carbonates, which involves major detachment folding and fault-propagation folding. This is a regional décollement horizon that continues from central Idaho out to southwestern Montana (Skipp and Hait, 1977). In contrast to the thin-skinned style of deformation within the Paleozoic carbonates, structurally deeper rocks appear to have accommodated low-magnitude shortening in a basement-involved structural style. Preliminary geologic mapping of the area was conducted by Embree and others (1983) and Scholten and Garmezy (1980) (fig. 2).

STOP 1 (44.185995°N, 112.873151°W)

Stop 1 consists of a visit to the first prominent outcrops of Precambrian sandstone exposed in upper Skull Canyon (fig. 2). The outcrop we will visit is on the northwestern side of the drainage off USFS Road 837, ~0.2 mi from the parking locality described above. The descriptions provided here are partly

from Skipp and Link (1992). Outcrop here consists of dominantly thin-bedded, red, fine- to medium-grained arkosic to subarkosic sandstone that dips northward at ~40°. Parallel laminae and small-scale cross-laminations of iron oxide are common and there are local intercalated grayish-green mudstone or siltstone beds. Bedding plane concentrations of mudstone rip-up clasts locally are common. Most workers consider these rocks to be equivalent to Mesoproterozoic Belt Supergroup (Beutner and Scholten, 1967; McCandless, 1982), possibly the Gunsight Formation (Skipp and Link, 1992).

In the middle fork of Skull Canyon in the next drainage to the north of Stop 1, Beutner and Scholten (1967) described ~9 m of thicker-bedded, red, texturally immature, very fine-grained to very coarse-grained and locally conglomeratic sandstone that may overlie Belt Supergroup-equivalent rocks. Though these rocks match the general description of Neoproterozoic to Cambrian rocks of the Wilbert Formation (Ruppel, 1975), their similarities with underlying sandstones and their stratigraphic position below a distinctive angular unconformity suggest that they are probably also correlative with the Belt Supergroup (McCandless, 1982). Detrital zircon age-populations from Wilbert Formation exposed at several localities in the southern Beaverhead Mountains have a strong 1,720 to 1,740 Ma age-peak (Link, unpublished) and are statistically indistinguishable (may be reworked) from upper Belt Supergroup quartzites exposed throughout much of east-central Idaho and southwest Montana (Link and others, 2016).

STOP 2 (44.184839°N, 112.862333°W)

Walk back to USFS Road 837 and proceed an additional ~0.7 mi up the road to Stop 2 (total ~0.9 mi from the parking area). Intermittent outcrops and float of the Proterozoic sandstone can be found in and adjacent to the road. At Stop 2, on the northern and southern sides of the road are excellent exposures of the angular unconformity between Mesoproterozoic rocks of the Belt Supergroup and overlying Ordovician sandstones. The best outcrops are in cliffy exposures on the northern side of the drainage 10–20 m from the road. Underlying sandstones dip 20–40° to the north and northeast and are overlain by medium-bedded, white, coarse and pebbly quartz sandstone that grades upward into vitreous white, well-sorted, medium-grained sandstone of the Middle Ordovician Kinnikinic Quartzite (Beutner and Scholten, 1967; McCandless, 1982). McCandless (1982) considers the basal, coarse sandstone to be correlative to the Ordovician Summerhouse Formation exposed beneath the Middle Ordovician Kinnikinic Formation in the southern Lemhi Range.

The complete absence of Neoproterozoic and Cambrian syn- and early post-rift clastic sedimentary rocks in east-central Idaho is in stark contrast to in southeast Idaho and northern Utah, south of the Snake River Plain (Sloss, 1954; Scholten, 1957; Ruppel, 1986; Link and others, in review). In the central Lemhi Range and southern Beaverhead Mountains, the unconformity consists of Mesoproterozoic Belt Supergroup-equivalent sandstone and quartzite, with a very thin (<300 m) overlying section of Middle Ordovician Kinnikinic Formation. In southwestern Montana, Ruppel (1998) mapped Ordovician Summerhouse Formation (and overlying Kinnikinic) unconformably above Archean and Paleoproterozoic gneisses of Maiden Peak (Anderson, 2017). Overall, the thin region of Neoproterozoic and early Paleozoic strata within the Lemhi arch is northwest-trending and separates a thicker section of equivalent rocks on the southwestern side of the Lemhi arch in central Idaho from a thicker section of lower Paleozoic rocks in southwestern Montana (Sloss, 1950, 1954). In east-central Idaho, the Lemhi arch may represent the exhumed footwall of a Rodinian rift fault (Hansen and Pearson, 2016), with Cambrian and Ordovician carbonate and siliciclastic rocks of the Bayhorse assemblage (Hobbs and Hays, 1990; Krohe, 2016) deposited in the hanging wall of the west-dipping normal fault.

In addition to the thin Neoproterozoic and Paleozoic strata, the Lemhi arch contains Neoproterozoic to early Paleozoic alkalic magmatic rocks (Lund, 2008; Lund and others, 2010). The alkalic belt of plutons defining this magmatism is called the Big Creek–Beaverhead belt. In the central and southern Beaverhead Mountains these consist of a northwest-trending, Late Cambrian to Early Ordovician alignment of hypabyssal plutons that parallels the Lemhi arch (Lund and others, 2010). The overlying Middle Ordovician Kinnikinic and correlative sandstones that overlie the unconformity within the Lemhi arch contain far-traveled detritus, likely from the Peace River arch of western Canada, as shown by detrital zircon data (all grains >1,800 Ma) from across Idaho and south to Nevada (Baar, 2009; Linde and others, 2014, 2016; Hansen,

2015; Krohe, 2016; Beranek and others, 2016).

The spatial coincidence of the Lemhi arch and the geometry of the Mesozoic and early Cenozoic Sevier–Laramide fold-thrust belt suggests that they are related. Armstrong (1975) hypothesized that the presence of crystalline basement (called the "Salmon River arch" by him) acted as a buttress and hindered propagation of the fold-thrust belt to the east–northeast. Alternatively, an absence of fine-grained, Neoproterozoic and Cambrian shales that were exploited as the basal décollement within much of the Wyoming salient (e.g., Royse and others, 1975), may have inhibited propagation of the fold-thrust belt within the region of the southwest Montana reentrant and promoted a thick-skinned style of deformation in east-central Idaho and southwestern Montana (Pearson and Becker, 2015).

After viewing the Skull Canyon unconformity, return to the cars. Quick hikers can continue hiking up Skull Canyon to a prominent shear zone within shales of the McGowan Creek Formation mapped by Embree and others (1983) (fig. 2), which may represent the tilted basal décollement of detachment folds that we will see at Stop 3. We will revisit the topics of alkalic Cambrian plutonism and the structural style of the Mesozoic and early Cenozoic fold-thrust belt in later stops.

STOP 3 (44.166538°N, 112.902861°W)

Stop 3 can be reached by driving 1.9 mi southwestward from the parking area at Stop 1 to where a small side road parallels USFS Road 298 on its northwestern side. This locality was passed on the way into upper Skull Canyon for Stops 1 and 2. From the parking area for Stop 3, walk northward to outcrops of thick-bedded Mississippian Scott Peak Formation. On the northern and southern walls of the canyon, one can view a large (~1 km wavelength), northeast-verging, concentric fold. In addition to the regional-scale fold visible in the bottom of Skull Canyon, smaller wavelength (10–100 m), parasitic folds occur on both fold limbs and verge toward the crest of the major fold (Scholten and Garmezy, 1980). At the outcrop scale, thick-bedded Scott Peak Formation exhibits steeply southwest-dipping, axial planar, pressure solution cleavage. The orientations of fold axes and pressure solution cleavage in the southern Beaverhead Mountains suggest a bulk southwest–northeast shortening direction.

Northwest–southeast-trending parallel or kink folds, and upright to moderately overturned folds that are akin to this fold, are common in middle and upper Paleozoic carbonates in the southern Beaverhead Mountains, and Lemhi and Lost River Ranges (Ross, 1947; Skipp and Hait, 1977; Skipp, 1988; Anastasio and others, 1997). In the central Lost River Range, folds in upper Paleozoic carbonate rocks are demonstrably decoupled from underlying stratigraphy along a bedding plane-parallel décollement in thin-bedded siltstones and argillites of the Lower Mississippian McGowan Creek Formation (Anastasio and others, 1997). This style of folding is called detachment folding (Jamison, 1987). Some tight folds in the Lost River Range and southern Beaverheads also have apparent fault-propagation folds in their hinge zones (Fisher and Anastasio, 1994). In the Lost River Range, detachment and fault-propagation folding accommodated ~22% shortening (Anastasio and others, 1997). Detachment and fault-propagation folding above Devonian and Mississippian décollements is present northeastward into southwestern Montana (Perry and others, 1988; Skipp, 1988; Tysdal, 1988). In contrast to substantial shortening accommodated by folding and bedding-parallel slip that is typical of a thin-skinned structural style, structurally deeper rocks (i.e., Proterozoic to Devonian strata) within these same ranges do not exhibit the same magnitude of folding and instead accommodated shortening along discrete thrusts associated with large-wavelength folding; the latter structural style is similar to basement-involved, thick-skinned thrusting and will be discussed during later stops.

Hawley Creek Overview

Following the visit to Skull Canyon (Stops 1, 2, and 3), the trip will then travel northwestward along Highway 28 to Hawley Creek, Idaho. There, we will view the Late Cambrian Beaverhead pluton of the Big Creek–Beaverhead belt of plutons intruded within the Lemhi arch. We will also view the basement-involved Hawley Creek thrust and folded carbonates in its footwall. These rocks were mapped: as part of a Ph.D. dissertation by Lucchitta (1966); with a focus on phosphate resources by Oberlindacher and Hovland (1979); and at 100,000-scale by Ruppel (1998) and Evans and Green (2003).

STOP 4 (44.660465°N, 113.204454°W)

From the intersection of Skull Canyon Road and Highway 28, it is 46.2 mi to Stop 4. Reset the trip odometer and proceed northwestward on Highway 28 for 36.4 mi and turn right on Eighteenmile Road (44.573207°N, 113.310398°W). At 38.4 mi, stay left on the main road, and at 39.8 mi, stay right on the main road and proceed through Oxbow Ranch. At 40.4 mi at the "T," turn left. At 42.4 mi, stay right at the "Y," and continue straight to Hawley Creek. The road eventually becomes USFS road 275. Stop 3 is 10–20 m up canyon of the Hawley Creek bridge. Park along the pull-out to the right (44.660465°N, 113.204454°W). The most accessible place to view the Beaverhead pluton and the Hawley Creek thrust is on the northwestern side of the road, north of the Hawley Creek bridge, adjacent to a small, mineral exploration pit.

The Beaverhead pluton crops out on the southwestern portion of the prominent ridge on the north side of Hawley Creek (fig. 3). It consists of pink, medium- to coarse-grained, equigranular to subporphyritic biotite alkali-feldspar granite, with lesser alkali-feldspar syenite to alkali-feldspar quartz syenite (Scholten and Ramspott, 1968; Evans and Zartman, 1988; Lund and others, 2010). The granitoid commonly contains miarolitic cavities, which are suggestive of a shallow level of emplacement. Near Eighteenmile Creek, enclaves of quartzite in the Beaverhead pluton were interpreted as Kinnikinic Quartzite, and thus the Beaverhead pluton was considered to be post-Middle Ordovician in age (Scholten and Ramspott, 1968; Skipp, 1984). However, a discordant U-Pb age of ~483 Ma was obtained using isotope-dilution thermal ionization mass spectrometry and questioned the relative timing of the Kinnikinic Quartzite and Beaverhead pluton (Evans and Zartman, 1988). More recent U-Pb zircon geochronometry applied to the Beaverhead pluton conducted by sensitive high-resolution ion microprobe yielded one age of 488 ± 5 Ma (Lund and others, 2010); laser ablation–multicollector–inductively coupled plasma–mass spectrometry ages for two samples from the Beaverhead pluton are 496 ± 2 Ma and 500 ± 3 Ma (Todt and Link, 2013). In addition, initial εHf of zircons from the Beaverhead pluton range from -6.3 ± 1.1 to 2.7 ± 1.4 (Todt and Link, 2013). Reexamination of the contact between the Beaverhead Pluton and the Kinnikinic Quartzite near Eighteenmile Creek demonstrates that the contact is planar with no contact metamorphism, which is consistent with the Middle Ordovician Kinnikinic Quartzite nonconformably overlying the Late Cambrian Beaverhead pluton (Link and others, in review).

Together with the Cryogenian Big Creek belt of plutons, alkalic plutons of the Beaverhead belt define two temporally distinct northwest-trending pulses of magmatism within and adjacent to the Lemhi arch at ca. 665–650 Ma and 500–485 Ma (Lund and others, 2010). These plutons are thought to be extension-

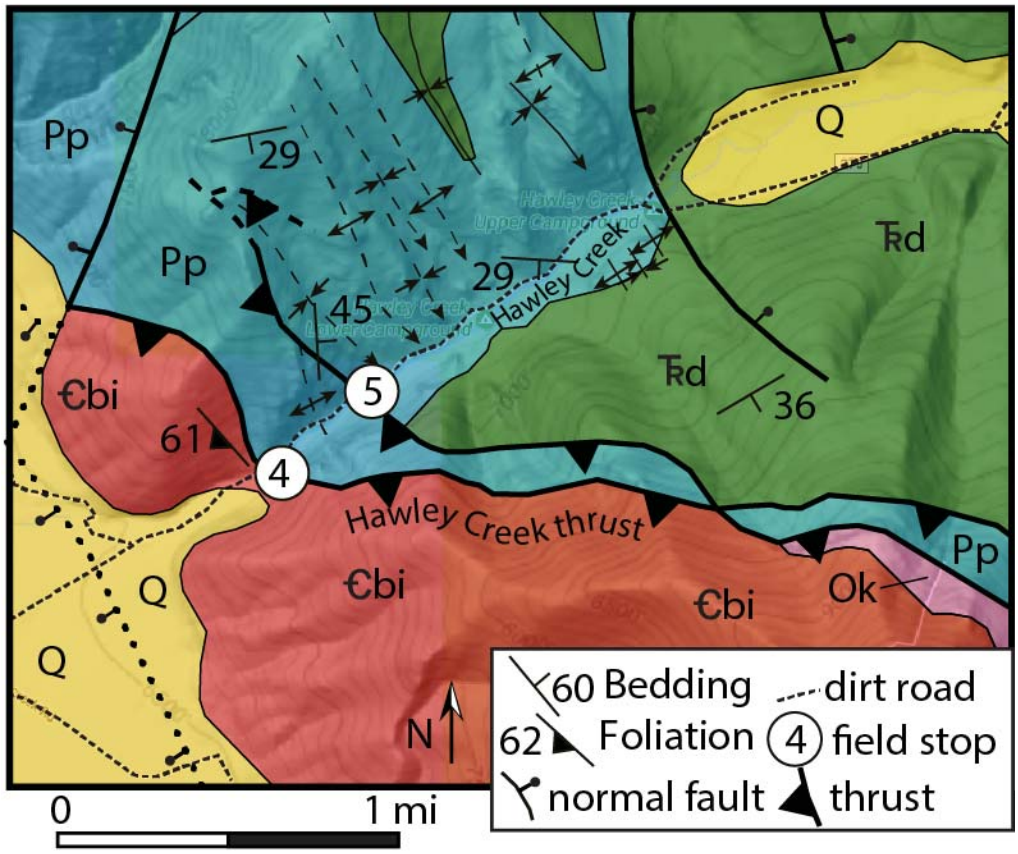

Figure 3. Simplified geologic map of the Hawley Creek area showing field trip localities Stops 4 and 5 (modified from Lucchitta, 1966; Hovland and Oberlindacher, 1979; Ruppel, 1998; and Evans and Green, 2003). Unit abbreviations: Ꞓbi-Cambrian Beaverhead pluton; Ok-Ordovician Kinnikinic Formation; Pp-Permian Phosphoria Formation; Ŧrd-Triassic Dinwoody Formation; Q-undifferentiated Quaternary sediments.

related; together with the thinned Neoproterozoic and early Paleozoic stratigraphy within this portion of the Laurentian rift margin, the results have been used to advocate for a detachment fault model in which along-strike changes in the character of the rift were proposed to result from a changing dip direction of a major, lithospheric detachment fault (Lister and others, 1986) across a transfer structure in the modern location of the eastern Snake River Plain (Lund, 2008; Lund and others, 2010). Considered in this context, the Lemhi arch and Big Creek–Beaverhead plutonic belt would have intruded into a largely intact hanging wall of a major detachment fault that accommodated rifting of the western Laurentian rift margin (Lund and others, 2010).

Though no volcanic equivalents of the Beaverhead plutons have been recognized, during Late Cambrian time, up to 300 m of feldspathic sandstone was deposited into a thick section of carbonate rocks in southeastern Idaho (Todt and Link, 2013; Link and others, in review). Utilizing U-Pb and Lu-Hf isotopic fingerprinting of zircons from these sandstones as well as those of the Beaverhead belt of plutons, Todt and Link (2013) showed that following shallow emplacement within and adjacent to the Lemhi arch, Late Cambrian plutons were rapidly exhumed along with their Belt Supergroup-equivalent country rocks and were the source of the anomalous feldspathic sand.

Hansen and Pearson (2016) mapped a likely Neoproterozoic or early Paleozoic normal fault that was inverted during Mesozoic shortening. This fault may locally bound the southwestern margin of the Lemhi arch and thus may have accommodated a portion of its exhumation (Hansen, 2016). Ongoing magmatism, faulting, and uplift and exhumation within the Lemhi arch attests to active tectonism in Late Cambrian time, ~40 m.y. after the transition to drift and slow, thermally driven subsidence in southeastern Idaho and northern Utah (Yonkee and others, 2014).

In its current configuration, the Beaverhead pluton exposed at Hawley Creek is in the hanging wall of a major Mesozoic thrust fault, the Hawley Creek thrust (Lucchitta, 1966; Skipp, 1988). Here, the thrust fault displaced the late Cambrian pluton against folded Permian and Triassic rocks of the Phosphoria and Dinwoody formations and thus has at least 3 km of stratigraphic separation (Lucchitta, 1966; Oberlindacher and Hovland, 1979). The thrust contact between the Beaverhead pluton and structurally lower Phosphoria Formation in its footwall is not directly exposed here, but a three-point problem yields a fault dip of ~40° to the southwest. Rare quartz stretching lineations in the pluton suggest transitional brittle-ductile deformation. Occasional slivers or phacoids of quartzite are also exposed within the fault zone. At Stop 4, a dioritic dike that crops out adjacent to the small mineral exploration pit apparently intruded the Hawley Creek fault zone here; it is presumably Eocene, associated with the Challis magmatic pulse. The Hawley Creek thrust exhibits some characteristics of a thick-skinned structural style. In addition to its involvement of crystalline basement of the Beaverhead pluton, the fault appears to have developed concurrently with several-kilometer-scale, northeast-vergent fault propagation folds, preserving its final configuration with an overturned hanging wall anticlinorium and footwall synclinorium (Lucchitta, 1966). This structural style differs markedly from the detachment folding at shallow structural levels that was seen at Stop 3.

The Hawley Creek thrust has been considered by some to be the along-strike equivalent of the Poison Creek thrust exposed in the northern Lemhi Range south of Salmon (Skipp, 1987, 1988; Janecke and others, 2000). There, despite the clear observation that the fault is a thrust by the juxtaposition of Mesoproterozoic Belt quartzites upon Ordovician Kinnikinic Quartzite (Tysdal, 2002), younger Mesoproterozoic Belt Supergroup occurs in the hanging wall relative to older Belt Supergroup rocks in the footwall; this is suggestive of a normal fault relationship prior to thrusting and suggests that the fault is a reactivated normal fault formed during Rodinian rifting (Hansen and Pearson, 2016). Two samples collected from the hanging wall of the Poison Creek thrust yielded zircon (U-Th)/He cooling ages (closure temperature ~180°C) of 68–57 Ma, which is interpreted as the timing of exhumation during thrusting along the fault (Hansen and Pearson, 2016). The structural style exhibited by the Poison Creek thrust southeast of Poison Peak includes truncation of an anticline-syncline pair of large-wavelength (>10 km), northeast-vergent, overturned folds (Tysdal, 2002) that are reminiscent of fault-propagation folds, and thick-skinned reactivation of an earlier normal fault (Hansen and Pearson, 2016). Thus, the structural style at deeper structural levels within the Lemhi arch is more characteristic of a thick-skinned deformation style rather than shallower Devonian and Lower Mis-

sissippian detachment folding, which is similar to the thin-skinned structural style exhibited by much of the Sevier fold-thrust belt. The spatial coincidence of the thick-skinned structural style and the Lemhi arch suggests that the arch may have controlled the northern end of the Wyoming salient and southwest Montana reentrant.

STOP 5 (44.662357°N, 113.201839°W)

If there is remaining time, we will walk northeastward up Hawley Creek road to view a southeast-plunging, northeast-verging fold train and several small, west-dipping imbricate thrusts within footwall rocks of the Phosphoria and Dinwoody formations (Lucchitta, 1966; Oberlindacher and Hovland, 1979). These folds likely developed synchronously with faulting along the structurally overlying Hawley Creek thrust (Lucchitta, 1966).

REFERENCES CITED

Allmendinger, R.W., and Gubbels, T., 1996, Pure and simple shear plateau uplift, Altiplano-Puna, Argentina and Bolivia: Tectonophysics, v. 259, p. 1–13.

Anastasio, D.J., Fisher, D.M., Messina, T.A., and Holl, J.E., 1997, Kinematics of décollement folding in the Lost River Range, Idaho: Journal of Structural Geology, v. 19, p. 355–368.

Anderson, N.D., 2017, The Bloody Dick and Maiden Peak gneisses, southwest Montana: Implications for Archean and Paleoproterozoic basement framework: Pocatello, Idaho State University M.S. thesis, 129 p., 1 plate.

Armstrong, R.L., 1975, Precambrian (1500 my old) rocks of central Idaho—The Salmon River Arch and its role in Cordilleran sedimentation and tectonics: American Journal of Science, v. 275-A, p. 437–467.

Baar, E.E., 2009, Determining the regional-scale detrital zircon provenance of the Middle-late Ordovician Kinnikinic (Eureka) quartzite, east-central Idaho, US: Washington State University M.S. thesis, 134 p.

Beranek, L.P., Link, P.K., and Fanning, C.M., 2016, Detrital zircon record of mid-Paleozoic convergent margin activity in the northern U.S. Rocky Mountains: Implications for the Antler orogeny and early evolution of the North American Cordillera: Lithosphere.

Beutner, E.C., and Scholten, R., 1967, Probable Cambrian strata in east-central Idaho and their paleotectonic significance: AAPG Bulletin, v. 51, p. 2305–2311.

Bush, J.H., Thomas, R.C., and Pope, M.C., 2012, Sauk megasequence deposition in northeastern Washington, northern Idaho, and western Montana, *in* J.R. Derby, R.D. Fritz, S.A. Longacre, W.A. Morgan, and C.A. Sternbach, eds., The great American carbonate bank: The geology and economic resources of the Cambrian–Ordovician Sauk megasequence of Laurentia: AAPG Memoir, v. 98, p. 751–768.

Christie-Blick, N., 1982, Upper Proterozoic and Lower Cambrian rocks of the Sheeprock Mountains, Utah: Regional correlation and significance: Geological Society of America Bulletin, v. 93, p. 735–750.

Crosby, G., 1969, Radial movements in the western Wyoming salient of the Cordilleran Overthrust Belt: Geological Society of America Bulletin, v. 80, p. 1061–1078.

Deiss, C., 1941, Cambrian geography and sedimentation in the central Cordilleran region: Geological Society of America Bulletin, v. 52, p. 1085–1115.

Embree, G. F., Hoggan, R.D., and William, E.J., 1983, Preliminary reconnaissance geologic map of the Copper Mountain quadrangle, Lemhi County, Idaho, U.S. Geological Survey Open-File Report No. 83-599.

Evans, K.V., Evans, K.V., Zartman, R.E., and Zartman, R.E., 1988, Early Paleozoic alkalic plutonism in east-central Idaho: Geological Society of America Bulletin, v. 100, p. 1981–1987.

Evans, K.V., and Green, G.N., 2003, Geologic map of the Salmon National Forest and vicinity, east-central Idaho: U.S. Geological Survey Geologic Investigations Series, I-2765, scale 1:100,000.

Fisher, D.M., and Anastasio, D.J., 1994, Kinematic analysis of a large-scale leading edge fold, Lost River Range, Idaho: Journal of Structural Geology, v. 16, p. 337–354.

Hansen, C., 2015, An investigation into the Poison Creek thrust: A Sevier thrust with Proterozoic implications: Idaho State University, M.S. thesis, 79 p., 1 plate.

Hansen, C.M., and Pearson, D.M., 2016, Geologic map of the Poison Creek thrust fault and vicinity near Poison Peak and Twin Peaks, Lemhi County, Idaho: Idaho Geological Survey Technical Report, #T-16-1, scale 1:24,000.

Hobbs, S.W., Hays, W.H., and McIntyre, D.H., 1991, Geologic map of the Bayhorse area, central Custer County, Idaho: U.S. Geological Survey Miscellaneous Investigations Series Map I-1882, scale 1:62,500.

Jamison, W.R., 1987, Geometric analysis of fold development in overthrust terranes: Journal of Structural Geology, v. 9, p. 207–219.

Janecke, S.U., Vandenburg, C.J., Blankenau, J.J., and M'gonigle, J.W., 2000, Long-distance longitudinal transport of gravel across the Cordilleran thrust belt of Montana and Idaho: Geology, v. 28, p. 439–442.

Krohe, N., 2016, Structural framework and detrital zircon provenance of the southern portion of the Clayton quadrangle, Custer County, Idaho: Idaho State University, M.S. thesis, 107 p., 1 plate.

Kulik, D.M., and Schmidt, C.J., 1988, Region of overlap and styles of interaction of Cordilleran thrust belt and Rocky Mountain Foreland: Geological Society of America Memoir 171, p. 75–98.

Linde, G.M., Cashman, P.H., Trexler, J.H., and Dickinson, W.R., 2014, Stratigraphic trends in detrital zircon geochronology of upper Neoproterozoic and Cambrian strata, Osgood Mountains, Nevada, and elsewhere in the Cordilleran miogeocline: Evidence for early Cambrian uplift of the Transcontinental Arch: Geosphere, v. 10, p. 1402–1410.

Linde, G.M., Trexler, J.H., Jr., Cashman, P.H., Gehrels, G., and Dickinson, W.R., 2016, Detrital zircon U-Pb geochronology and Hf isotope geochemistry of the Roberts Mountains allochthon: New insights into the early Paleozoic tectonics of western North America: Geosphere, v. 12, p. 1016–1031.

Link, P.K., Christie-Blick, N., Devlin, W.J., Elston, D.P., Horodyski, R.J., Levy, M., Miller, J.M.G., Pearson, R.C., Prave, A., Stewart, J.H., Winston, D., Wright, L.A., and Wrucke, C.T., 1993, Middle and Late Proterozoic stratified rocks of the western U.S. Cordillera, Colorado Plateau, and Basin and Range province, *in* Reed, J.C.J., Bickford, M.E., Houston, R.S., Link, P.K., Rankin, D.W., Sims, P.K., and Van Schmus, W.R., eds., The Geology of North America, Precambrian: Conterminous U.S, Boulder, CO, Geological Society of America, v. C-2, p. 1–131.

Link, P.K., Stewart, E.D., Steel, T., Sherwin, J.-A., Hess, L., and McDonald, C., 2016, Detrital zircons in the Mesoproterozoic upper Belt Supergroup in the Pioneer, Beaverhead, and Lemhi Ranges, Montana and Idaho: The Big White arc, *in* MacLean, J.S., and Sears, J.W., eds., Belt Basin: Window to Mesoproterozoic Earth: Geological Society of America Special Paper, v. 522, p. 163–183.

Link, P.K., Todt, M.K., Pearson, D.M., and Thomas, R.C, in review, 500 Ma detrital zircons in Upper Cambrian Worm Creek and correlative sandstones, ID, MT, and WY: Magmatism and tectonism within the passive margin, Lithosphere.

Lister, G.S., Etheridge, M.A., and Symonds, P.A., 1986, Detachment faulting and the evolution of passive continental margins: Geology, v. 14, p. 246–250.

Lonn, J.D., Burmester, R.F., Lewis, R.S., and McFaddan, M.D., 2016, Giant folds and complex faults in Mesoproterozoic Lemhi strata of the Belt Supergroup, northern Beaverhead Mountains, Montana and Idaho, *in* MacLean, J.S., and Sears, J.W., eds., Belt Basin: Window to Mesoproterozoic Earth: Geological Society of America Special Paper, v. 522, p. 139–162.

Lucchitta, B.K., 1966, Structure of the Hawley Creek area, Idaho-Montana: University Park, Pennsylvania State University, Ph.D. dissertation, 235 p.

Lund, K., 2008, Geometry of the Neoproterozoic and Paleozoic rift margin of western Laurentia: Implications for mineral deposit settings: Geosphere, v. 4, p. 429.

Lund, K., Aleinikoff, J.N., Evans, K.V., duBray, E.A., Dewitt, E.H., and Unruh, D.M., 2010, SHRIMP U-Pb dating of recurrent Cryogenian and Late Cambrian-Early Ordovician alkalic magmatism in central Idaho: Implications for Rodinian rift tectonics: Geological Society of America Bulletin, v. 122, p. 430–453.

McCandless, D.O., 1982, A reevaluation of Cambrian through Middle Ordovician stratigraphy of the

southern Lemhi Range: University Park, Pennsylvania State University M.S. thesis, 159 p.

Norris, D.K., and Price, R.A., 1966, Middle Cambrian lithostratigraphy of southeastern Canadian Cordillera: Bulletin of Canadian Petroleum Geology, v. 14, p. 384–404.

Oberlindacher, P., and Hovland, R.D., 1979, Geology and phosphate resources of the Hawley Creek area, Lemhi County, Idaho, U.S. Geological Survey Open-File Report 79-1283, 20 p.

Pearson, D.M., and Becker, T.P., 2015, Proterozoic rift systems and their influence on the formation of the Late Cretaceous-early Cenozoic Wyoming salient, GSA Rocky Mountain Regional Meeting, Abstracts with Programs.

Perry, W.J., Haley, J.C., Nichols, D.J., Hammons, P.M., and Ponton, J.D., 1988, Interactions of Rocky Mountain foreland and Cordilleran thrust belt in Lima region, southwest Montana, *in* Schmidt, C.J. and Perry, W.J., eds., Interaction of the Rocky Mountain Foreland and the Cordilleran Thrust Belt: Geological Society of America Memoirs, v. 171, p. 267–290.

Perry, W.J., Jr., Dyman, T.S., and Sando, W.J., 1989, Southwestern Montana recess of Cordilleran thrust belt, *in* French, D.E., and Grabb, R.F., eds., Montana Geological Society field conference guidebook, Montana centennial edition, Geologic resources of Montana: v. 1, p. 261–270.

Ross, C.P., 1934, Correlation and interpretation of Paleozoic stratigraphy in south-central Idaho: Geological Society of America Bulletin, v. 45, p. 937–1000.

Ross, C.P., 1947, Geology of the Borah Peak quadrangle, Idaho: Geological Society of America Bulletin, v. 58, p. 1085–1160.

Royse, F., Jr., Warner, M.A., and Reese, D.L., 1975, Thrust belt structural geometry and related stratigraphic problems Wyoming–Idaho–northern Utah, *in* Rocky Mountain Association of Geologists—1975 Symposium, Rocky Mountain Association of Geologists, p. 41–54.

Ruppel, E.T., 1975, Precambrian Y sedimentary rocks in east-central Idaho: U.S. Geological Survey Professional Paper 889-A, p. 1–42.

Ruppel, E.T., 1986, The Lemhi Arch: A late Proterozoic and early Paleozoic landmass in central Idaho: AAPG Memoir 41, p. 119–130.

Ruppel, E.T., 1998, Geologic map of the eastern part of the Leadore 30’ x 60’ quadrangle, Montana and Idaho: Montana Bureau of Mines and Geology Open-File Report 372, 9 p., scale 1:100,000.

Scholten, Robert, 1957, Paleozoic evolution of the geosynclinal margin north of the Snake River Plain, Idaho–Montana: Geological Society of America Bulletin, v. 68, p. 151–170.

Scholten, Robert, and Garmezy, L., 1980, Unpublished reconnaissance mapping of the Blue Dome quadrangle, Clark County, Idaho.

Scholten, Robert, and Ramspott, L.D., 1968, Tectonic mechanisms indicated by structural framework of central Beaverhead Range, Idaho–Montana: Geological Society of America Special Paper, v. 104, p. 1–60.

Skipp, B., 1987, Basement thrust sheets in the Clearwater orogenic zone, central Idaho and western Montana: Geology, v. 15, p. 220–224.

Skipp, B., 1988, Cordilleran thrust belt and faulted foreland in the Beaverhead Mountains, Idaho and Montana, *in* Schmidt, C.J., and Perry, W.J., Jr., eds., Interaction of the Rocky Mountain foreland and the Cordilleran thrust belt: Geological Society of America Memoir, v. 171, p. 237–266.

Skipp, B., 1984, Geologic map and cross sections of the Italian Peak and Italian Peak middle roadless areas, Beaverhead County, Montana, and Clark and Lemhi Counties, Idaho: U.S. Geological Survey Miscellaneous Field Studies Map 1601-B, scale 1:62,500.

Skipp, B., and Hait, M.H., Jr., 1977, Allochthons along the northeast margin of the Snake River Plain, Idaho: Wyoming Geological Association Guidebook, v. 29, p. 499–515.

Skipp, B., and Link, P.K., 1992, Middle and late Proterozoic rocks and late Proterozoic tectonics in the southern Beaverhead Mountains, Idaho and Montana: A preliminary report, *in* Link, P.K., Kuntz, M.A., and Platt, L.B., eds., Regional Geology of Eastern Idaho and Western Wyoming: Geological Society of America Memoir 179, p. 141–154.

Sloss, L.L., 1954, Lemhi arch, a mid-Paleozoic positive element in south-central Idaho: Geological Society of America Bulletin, v. 65, p. 365–368.

Sloss, L.L., 1950, Paleozoic sedimentation in Montana area: AAPG Bulletin, v. 34, p. 423–451.

Stewart, J.H., 1972, Initial deposits in the Cordilleran Geosyncline: Evidence of a Late Precambrian (<850 m.y.) Continental Separation: Geological Society of America Bulletin, v. 83, p. 1345–1360.

Todt, M.K., 2013, Sedimentary provenance of the upper Cambrian Worm Creek Quartzite, Idaho using U-Pb and Lu-Hf isotopic analysis of zircon grains: Northwest Geology, v. 42, p. 293–298.

Tysdal, R.G., 1988, Deformation along the northeast side of Blacktail Mountains salient, southwestern Montana: Geological Society of America Memoir 171, p. 203–216.

Tysdal, R.G., 2002, Structural geology of western part of Lemhi Range, east-central Idaho: U.S. Geological Survey Professional Paper 1659.

Yonkee, W.A., Dehler, C.D., Link, P.K., Balgord, E.A., Keeley, J.A., Hayes, D.S., Wells, M.L., Fanning, C.M., and Johnston, S.M., 2014, Tectono-stratigraphic framework of Neoproterozoic to Cambrian strata, west-central U.S.: Protracted rifting, glaciation, and evolution of the North American Cordilleran margin: Earth-Science Reviews, v. 136, p. 59–95.

WALKING TOUR OF THE MONUMENT FAULT NEAR THE CONFLUENCE OF BLOODY DICK CREEK AND HORSE PRAIRIE CREEK, SOUTHWESTERN MONTANA

Colleen Elliott and Jeff Lonn

Montana Bureau of Mines and Geology, 1300 W. Park Street, Butte, Montana 59701

INTRODUCTION

The Monument Fault juxtaposes Paleoproterozoic gneiss against Mesoproterozoic quartzite in the lower reaches of Bloody Dick Creek in southwestern Montana (fig. 1). There are currently at least five interpretations for the fault:

1. Reverse fault dipping south, placing older rocks over younger (Coppinger, 1974; Sherwin and others, 2016),
2. Steeply dipping SW-side-up fault that is part of the complex Beaverhead Divide fault system (Lonn and others, 2016),
3. Vertical left-lateral Great Divide Megashear that juxtaposes the Belt and Lemhi basins (O'Neill and others, 2007),
4. North–northeast-dipping reverse fault that places younger rocks over older rocks (Ruppel and others, 1993), or
5. No fault at all, but an angular unconformity folded into an upright anticline (S. Janecke and C. Elliott, unpublished).

Each of these interpretations has significant implications for regional geologic history. Geologists with different opinions on the nature of the contact will lead this field trip. We will walk the length of the fault and participants will weigh the different interpretations. Maybe we will even reach a consensus.

FIELD GUIDE

Distance from Leadore: 33 mi, 26 mi paved

Driving time: 1 hour

Walking distance: 2.5 mi, 815 ft vertical gain over 1.5 mi. Will require a vehicle shuttle.

We will leave our cars where we cross the first ridge on the Bloody Dick Road (44.9968°, -113.3215°). Volunteers will shuttle vehicles to Big Hollow. From there we will walk up the ridge.

Stops are shown on figures 1 and 2.

STOP 1 (45.0004°, -113.3224°)

Shear zones vs gneissosity vs schistosity in the Gneiss of Bloody Dick Creek at the Monument Mine. Colleen thinks we will find that there are multiple foliations in the gneiss, some of which are shear fabrics. She thinks we will find at least one generation of axial plane schistosity.

The quartz + plagioclase + biotite + garnet + pyroxene Gneiss of Bloody Dick Creek is interlayered with biotite schist and medium-grained augen gneiss mylonite. Quartz veins occur throughout. Sherwin and others (2016) report that the gneiss contains metamorphic zircons of about 1,800 Ma, and the youngest non-metamorphic zircons are about 1,830 Ma (fig. 3).

At the old Monument (Au Ag Cu Pb) Mine, you will mostly see brecciated and sheared quartz that might be vein quartz, altered quartzite, or both. The dominant fabric trends east–southeast and dips steeply north and south. Above and below the mine, gneiss and schist contain isoclinal folds and mylonitic fabrics with no clear orientation.

STOP 2 (45.0030°, -113.3243°)

Metamorphic foliation vs bedding in Swauger Formation (Mesoproterozoic) quartzites (description after Sherwin and others, 2016). The Swauger Formation here is white to light brownish gray, thick-bedded, predominantly poorly sorted, medium- to coarse-grained, feldspathic quartzite. Beds are from 10 cm to 1 m thick, with planar and trough crossbedding. Ripple marks are present but rare. The unit contains scattered interbeds of very light gray to light greenish gray, fine-

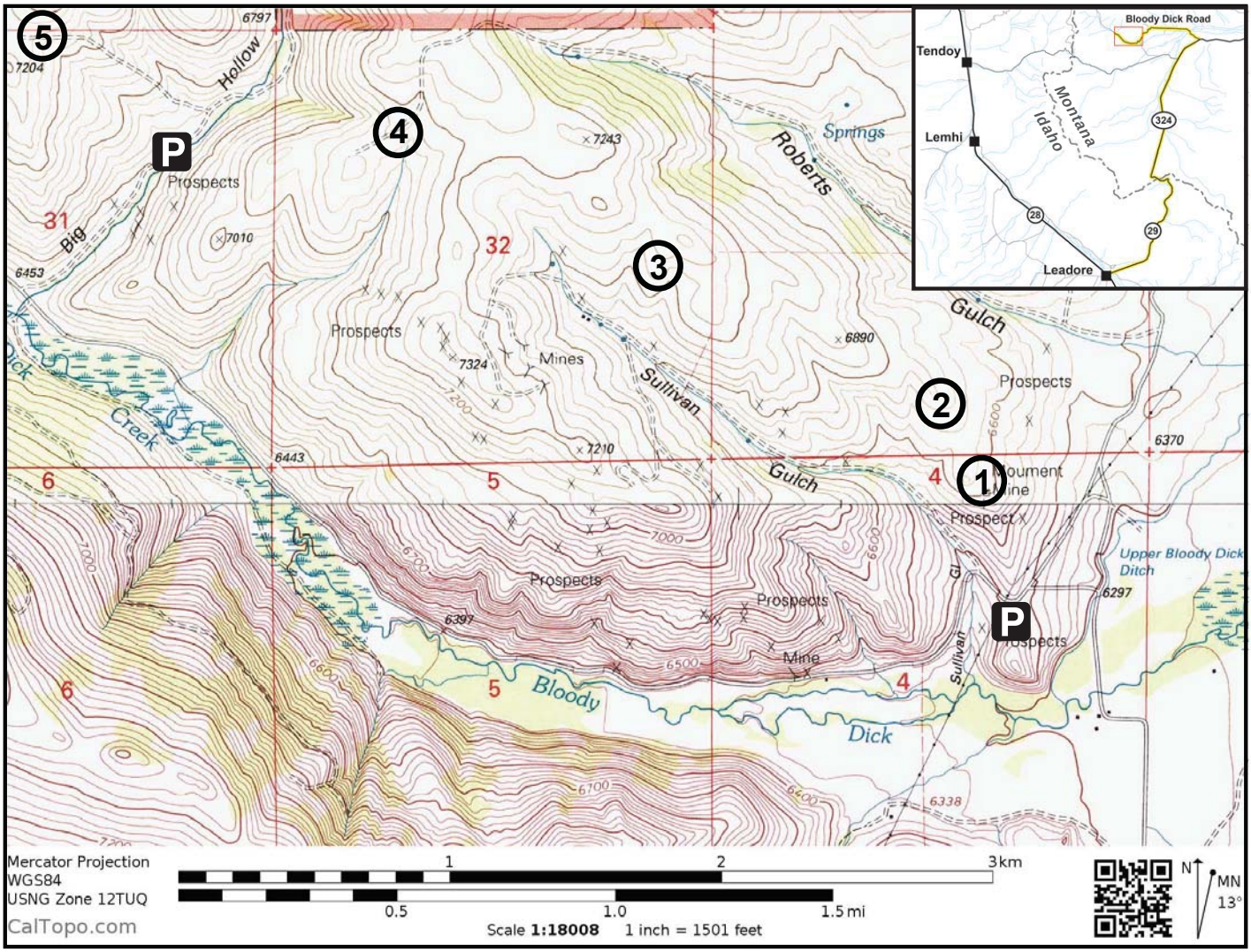

Figure 1. Location of stops described on field trip. Inset shows location of field trip in southwest Montana.

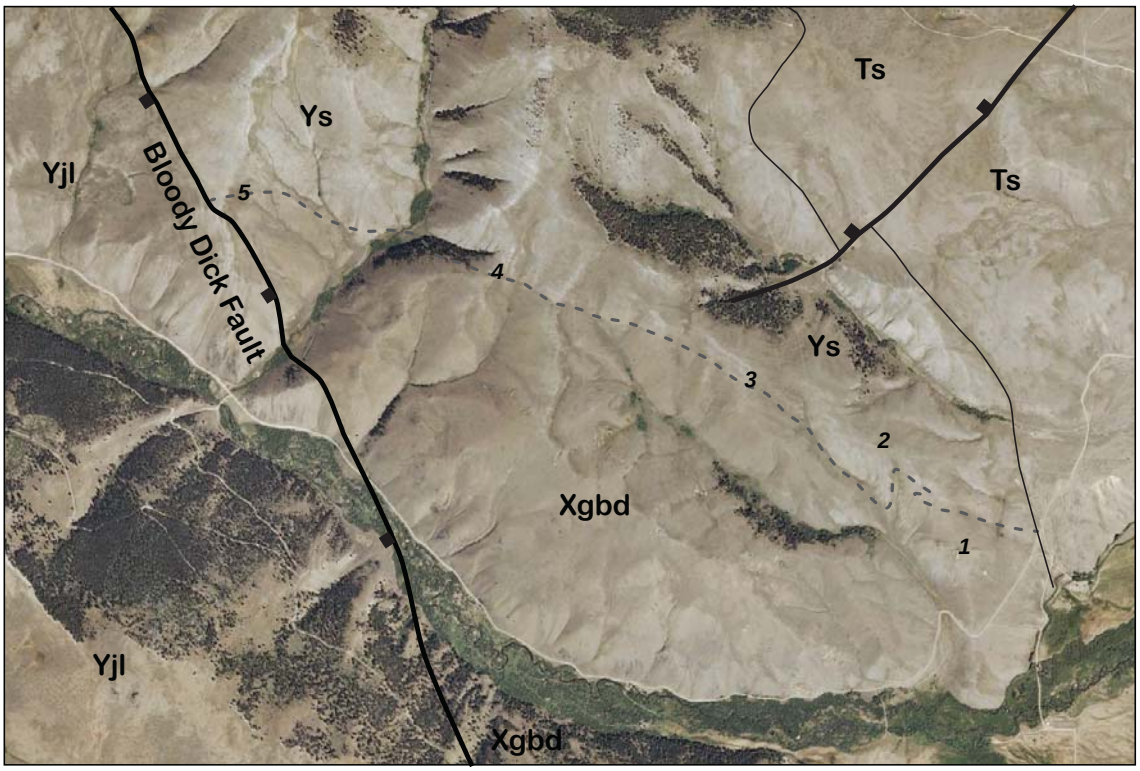

Figure 2. Geology of field trip area overlain on a Google Earth image. The dashed contact between the Swauger Formation (Ys) and the Gneiss of Bloody Dick Creek (Xgbd) is shown where Colleen Elliott and Petr Yakovlev (MBMG) walked it out in spring 2017. The Bloody Dick normal fault separates the Jahnke Lake Member of the Apple Creek Formation (Tjl) from the Swauger Formation, which is stratigraphically lower, and the Gneiss of Bloody Dick Creek (Xgbd). Tertiary sediments (Ts) overlie all other units.

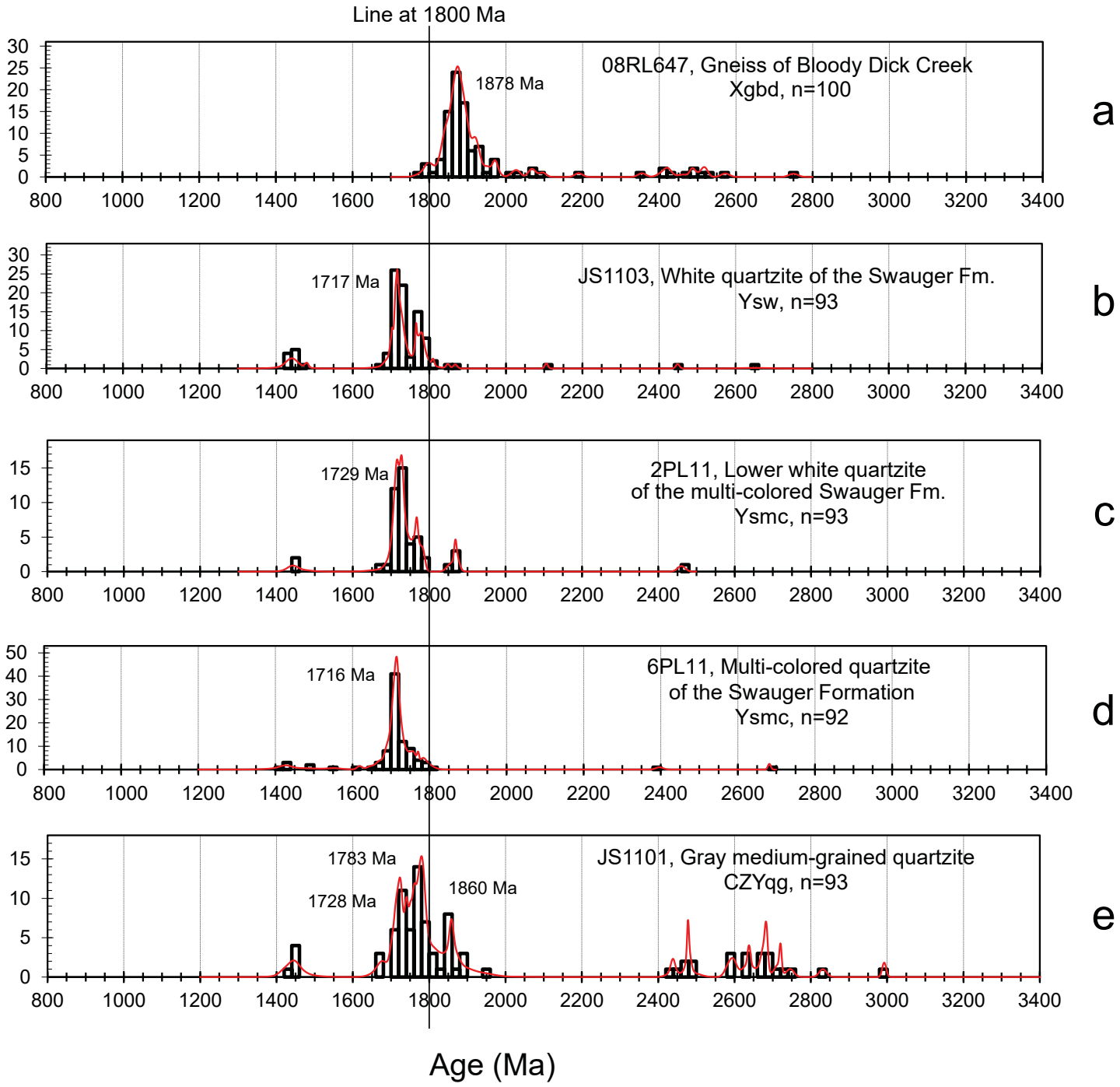

Figure 3. Detrital zircon ages from the Gneiss of Bloody Dick Creek (a), the Swauger Formation (b, c, d,), and quartzite west of Big Hollow (e) (Sherwin and others, 2016).

to medium-grained feldspathic quartzite and rare beds of grayish red-purple, coarse-grained, trough-cross-bedded quartzite. Near the contact with the Gneiss of Bloody Dick Creek, the quartzite contains 35–38 percent total feldspar (28–30 percent potassium feldspar and 7–8 percent plagioclase) (Sherwin and others, 2016). Sherwin and others (2016) U-Pb dated ninety-three detrital zircons and found a strong unimodal age peak at about 1,730 Ma, sparse grains as young as 1,400 Ma, and a few grains as old as 2,650 Ma (fig. 3).

The Swauger Formation is tentatively correlated with the Bonner Formation of the Missoula Group, Belt Supergroup, on the basis of lithologic similarity and stratigraphic position (Burmester and others, 2016; Lonn and others, 2016).

At Stop 2, a vertical foliation is perpendicular to horizontal bedding, indicating the hinge of an anticline. The foliation is defined by flattened quartz grains and fine-grained white mica. The most prominent foliation in the gneiss is also steep, defined by

layering and platy minerals, and approximately parallel to the contact. The most prominent foliation away from the fault is more variable. Colleen would argue that the steep foliation is an axial plane foliation overprinting the gneissic layering, which is sub-horizontal near the fault. Jeff would argue that layering is parallel to the fault and related to it.

From Stop 2 we will walk the contact between gneiss and quartzite, looking for relationships between foliations, bedding, and contact. Jeff found that the contact between gneiss and quartzite is parallel to a steep shear foliation. Colleen found that the contact meanders from one limb of a large anticline to another, causing the contact to wander between north and south dips.

STOP 3 (45.0153°, -113.3676°)

This stop is a prospect pit that exposes the near-vertical contact. Tom Kalakay (Rocky Mountain College, Billings) and Jeff observed the following: steeply east-raking lineations and shear sense indicators of oblique displacement, with the southwest side up and northeast.

STOP 4 (45.0117°, -113.3518°)

Overview of contact. Both sides of the contact here exhibit near vertical foliation. Are they shear fabric or an axial plane foliation? Look back over the contact as it has been traced from Stop 2, and look west towards where it is exposed in the hillside west of Big Hollow.

Walk down the gulch into Big Hollow, and then up the south facing shoulder on the west side of Big Hollow north of the "H" in Hollow on figure 1. If the contact has a gentle north dip, then gneiss should form the lower half of this slope. Now, traverse west to the saddle near elevation 7,204 ft and walk south, crossing the Bloody Dick fault, interpreted as a down-to-the-southwest normal fault by all (Coppinger, 1974; Ruppel and others, 1993; Sherwin and others , 2016; Lonn and others, 2016).

STOP 5 (45.0153°, -113.3676°)

At "7204" on figure 1, the feldspathic quartzite is different from the Swauger Formation (Ys) we have been viewing. Lonn and others (in preparation) assign the quartzite there to the Jahnke Lake member (Yjl) of the Apple Creek Formation, while Sherwin and others (2016) call it Cambrian, Neoproterozoic, or Mesoproterozoic quartzite. It is finer grained and better sorted than the Swauger Formation. Figure 4 is a detrital zircon age plot that compares a sample near the mouth of Big Hollow to Swauger Formation quartzite on the north side of the Bloody Dick Fault. Although both units have peaks at about 1,725 Ma, the first has its maximum at 1,780 Ma, a lesser peak at 1,860 Ma, and a significant scattering of Archean grains. Lonn observes that the 1,780 Ma maximum and scattering of Archean grains are characteristic of Jahnke Lake quartzite in this area (see Lonn and others, in prep.).

Walk down to the vehicles from here.

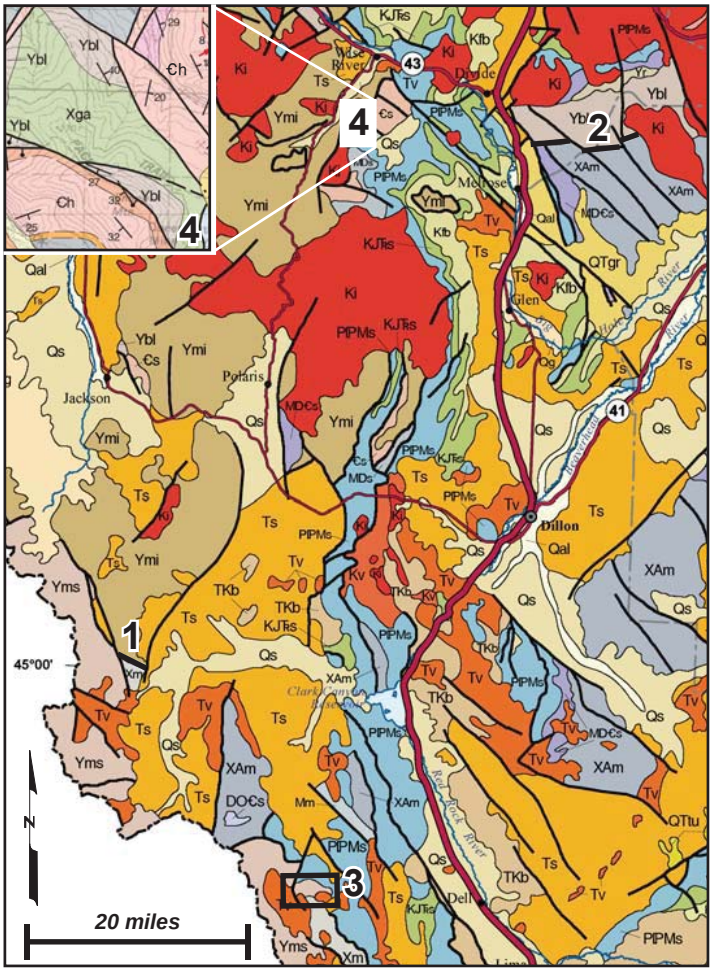

Main map from: Vuke, Susan M., 2015, Geologic Road Map of Montana: Montana Bureau of Mines and Geology Geologic Map 65

Inset from: McDonald, C., Elliott, C.G., Vuke, S.M., Lonn, J.D., and Berg, R.B., 2012, Geologic map of the Butte South 30' x 60' quadrangle, southwestern Montana: Montana Bureau of Mines and Geology Open-File Report 622

Figure 4. Locations in southwest Montana where Archean or Paleoproterozoic are in contact with Mesoproterozoic rocks: (1) Monument Fault, (2) Butte Highlands, (3) Ayers Canyon, and (4) Black Lion Mountain. (Main map from Vuke, 2015; inset from McDonald and others, 2012).

DISCUSSION

If the Monument Fault is a northeast-side-up reverse fault (Ruppel and others, 1993), it places younger over older rocks. While this is an uncommon relationship, 'younger over older' is found at the contact between Proterozoic and Archean rocks in the Butte Highlands (fig. 4) (O'Neill and others, 1996; McDonald and others, 2012). In the Butte Highlands, the north-dipping Camp Creek Fault with top-southwest motion placed Mesoproterozoic rocks of the Belt Group over crystalline Archean and/or Paleoproterozoic rocks. Whether this fault is an out-of-sequence thrust fault or a rotated extensional fault is not clear (McDonald and others, 2012).

If the Monument Fault is a southwest-side-up reverse fault (Coppinger, 1974; O'Neill and others, 2007; Sherwin and others, 2016; Jeff Lonn, this volume), then the Paleoproterozoic gneiss is a horst caught between this fault and the southwest-side-down Bloody Dick normal fault that we cross near Stop 5.

O'Neill and others (2007) include the fault in their Great Divide Megashear, the long-lived, left-lateral strike-slip fault that they propose juxtaposed the Mesoproterozoic Belt and Lemhi basins.

If the "fault" is an unconformity, it means that the Swauger Formation is the base of the Mesoproterozoic sequence in this location, and that it was a salient or erosional surface during deposition of the older Lemhi Group and Lower Belt Supergroup. Units older than the Swauger Formation are exposed within 3 mi of the Monument Fault where they have been thrust northward over rocks younger than Swauger. Two places in the region where Mesoproterozoic rocks are in depositional contact with the basement have unconformities that are more obvious. At Ayers Canyon (fig. 4), large angular clasts mark the base of the Mesoproterozoic strata (McDonald and Lonn, 2013). At Black Lion Mountain (fig. 4), pebbly grits overlie the unconformity (McDonald and Lonn, 2013). While the Swauger Formation along the field trip route is poorly sorted and contains some small angular and rounded pebbles, overall it does not look different from Swauger quartzite in other locations where it is underlain by more than 17,000 ft (5,200 m) of Mesoproterozoic sediments (Burmester and others, 2015; Lonn, this volume).

ACKNOWLEDGMENTS

Thanks to Petr Yakovlev for walking the contact and creating a story map for this guide. Thanks also to Susan Smith for drafting the figures and Katie McDonald for reviewing the manuscript.

REFERENCES CITED

Burmester, R.F., Lewis, R.S., Lonn, J.D., and McFaddan, M.D., 2015, The Hoodoo is the Swauger and other heresies: Lemhi subbasin correlations and structures, east-central Idaho: Northwest Geology, v. 44, p. 73–88.

Burmester, R.F., Lonn, J.D., Lewis, R.S., and McFaddan, M.D., 2016, Stratigraphy of the Lemhi subbasin of the Belt Supergroup, *in* MacLean, J.S., and Sears, J.W., eds., Belt Basin: Window to Mesoproterozoic Earth: Geological Society of America Special Paper 522, chapter 5, p. 121–138.

Coppinger, W., 1974, Stratigraphy and structural study of Belt Supergroup and associated rocks in a portion of the Beaverhead Mountains, southwestern Montana, and east-central Idaho: Oxford, Ohio, Miami University, Ph.D. dissertation, 224 p.

Lonn, J.D., 2017, The type Lemhi Group sections revisited and revised, east-central Idaho: Northwest Geology, v. 46, p. 15–28.

Lonn, J.D., Burmester, R.F., Lewis, R.S., and McFaddan, M.D., 2016, Giant folds and complex faults in Mesoproterozoic Lemhi strata of the Belt Supergroup, northern Beaverhead Mountains, Montana and Idaho, *in* MacLean, J.S., and Sears, J.W., eds., Belt Basin: Window to Mesoproterozoic Earth: Geological Society of America Special Paper 522, chapter 6, p. 139–162.

Lonn, J.D., Elliott, C.G., Lewis, R.S., Burmester, R.F., Janecke, S., and others, in preparation, Geologic map of the Montana portion of the Salmon 30' x 60' quadrangle, southwestern Montana: Montana Bureau of Mines and Geology Open-File Report, 1 sheet, scale 1:100,000.

McDonald, C., Elliott, C.G., Vuke, S.M., Lonn, J.D., and Berg, R.B., 2012, Geologic map of the Butte South 30' x 60' quadrangle, southwestern Montana: Montana Bureau of Mines and Geology Open-File Report 622, 1 sheet, scale 1:100,000.

McDonald, C., and Lonn, J.D, 2013, Revisions of Mesoproterozoic and Cambrian stratigraphy in the

Pioneer and Highland Mountains, southwestern Montana, and resulting implications for the paleogeography of the Belt Basin: Northwest Geology, v. 42, p. 93–102.

O'Neill, J.M., Klepper, M.R., Smedes, H.W., Hanneman, D.L., Fraser, G.D, and Mehnert, H.H., 1996, Geologic map and cross sections of the central and southern Highland Mountains, southwestern Montana: U.S. Geological Survey Miscellaneous Investigations Map I-2525, scale 1:50,000.

O'Neill, J.M., Ruppel, E.T., and Lopez, D.A., 2007, Great Divide megashear, Montana, Idaho, and Washington—An intraplate crustal-scale shear zone recurrently active since the Mesoproterozoic: U.S. Geological Survey Open-File Report 2007-1280-A, 10 p.

Ruppel, E.T., O'Neill, J.M., and Lopez, D.A., 1993, Geologic map of the Dillon 1° x 2° quadrangle, Idaho and Montana: U.S. Geological Survey Miscellaneous Investigations Series Map I-1803-H, scale 1:250,000.

Sherwin, J.A., Younggren, E.B, Link, P.K., and Gaschnig, R.M., 2016, Geologic map of the Coyote Creek 7.5' quadrangle, southwest Montana: Montana Bureau of Mines and Geology Geologic Map 67, 1 sheet, scale 1:24,000.

Vuke, S.M., 2015, Geologic Road Map of Montana: Montana Bureau of Mines and Geology Geologic Map 65, scale 1:1,000,000.

ROAD LOG TO THE GEOLOGY AND MINERALIZATION OF THE AGENCY CREEK AND LEMHI PASS AREAS, IDAHO AND MONTANA

Reed S. Lewis,[1] Virginia S. Gillerman,[2] Russell F. Burmester,[1,3] Jesse Mosolf,[4] and Jeffrey D. Lonn[4]

[1]Idaho Geological Survey, University of Idaho, Moscow, Idaho 83844-3014
[2]Idaho Geological Survey, Idaho Water Center, Boise, Idaho 83702-7359
[3]Geology, Western Washington University, Bellingham, Washington 98225-9080
[4]Montana Bureau of Mines and Geology, Montana Tech, Butte, Montana 59701

INTRODUCTION

This field guide explores the geology of Lemhi Pass along the Idaho–Montana border in the central Beaverhead Mountains. The oldest strata along the route are Mesoproterozoic-age metasedimentary rocks of the Lemhi subbasin of the Belt Basin (fig. 1). Related metasedimentary rocks in the Salmon River Mountains were intruded by ~1,380 Ma megacrystic A-type granite. We will see some boulders derived from those intrusions near Lemhi Pass and wonder how they got there. We will also see a Cambrian intrusion in place and speculate about its relationship with mineralization. Tertiary volcanic and sedimentary rocks of the Challis Volcanic Group, preserved in the hanging walls of younger normal or detachment faults, also warrant stops. Tertiary deposits, which vary from coarse conglomerate to shale, record a wide range of depositional environments in a basin formed during extensional faulting. Thin Quaternary deposits document erosion by glacial, alluvial, and mass-movement processes primarily during times of Pleistocene glacial climate.

Fieldwork by the Idaho Geological Survey (IGS) in the Lemhi Pass thorium district started in 2000 as part of a hazard inventory of inactive mine sites. The field crew spent 10 days in the area, surveying the Copper Queen mine and several of the larger thorium pits, including the Lucky Horseshoe Mine, Buffalo Mine, and Wonder Lode in Idaho (Gillerman and others, 2006). This led to the first TRGS trip to the area (Gillerman and others, 2003). This initial work was expanded to the entire district in 2006 with the assistance of a USGS mineral resources research grant to the Idaho Geological Survey. By 2008, a small exploration company, Thorium Energy, later re-named U.S. Rare Earths, was also conducting exploration work in the region and their assistance was invaluable.

According to Umpleby (1913), early prospectors discovered copper–gold mineralization of the Copper Queen Mine in 1883 along a tributary to Agency Creek 2 mi west of Lemhi Pass. Thorium was discovered there in 1951 and a prospecting boom followed, along with considerable geologic work (e.g., Anderson, 1958, 1961; Sharp and Cavender, 1962). Staatz (1972, 1979) produced geologic maps and the most comprehensive description of the numerous mineral deposits. However, his interpretation that the thorium was related to the Eocene-age Challis volcanics was inconsistent with a number of the IGS crew's field observations. Those suggested the Cu and Th mineralization was at least pre-Cretaceous, and most likely Proterozoic in age, and had a striking similarity to the Olympic Dam-type Cu-U-Fe oxide-REE class of mineral deposits (Gibson, 1998; Gillerman and others, 2000).

The IGS research project included mapping, sampling, and dating of newly rediscovered syenitic and mafic porphyry intrusives, which constitute a Cambrian bimodal magmatic assemblage (Gillerman and others, 2008). Ages of the Th-REE-Fe deposits were determined by U-Pb chemical dating of monazite in the Lucky Horseshoe prospect (Gillerman and others, 2010). Although initial attempts suggested mineralization events at about 1,000 Ma, final results show the Lucky Horseshoe monazite to be Paleozoic in age (Mississippian) with minor Cretaceous remobilization (Gillerman and others, 2010, 2013). Whether the age of the Lucky Horseshoe deposit is representative of the whole district is uncertain. The deposit is anomalous in that the Lucky Horseshoe host rocks are strongly mylonitized. However, the Lucky Horseshoe ores do show the very unusual (and unexplained) "hump" of middle rare earth enrichment that characterizes the entire district (Staatz and others, 1972).

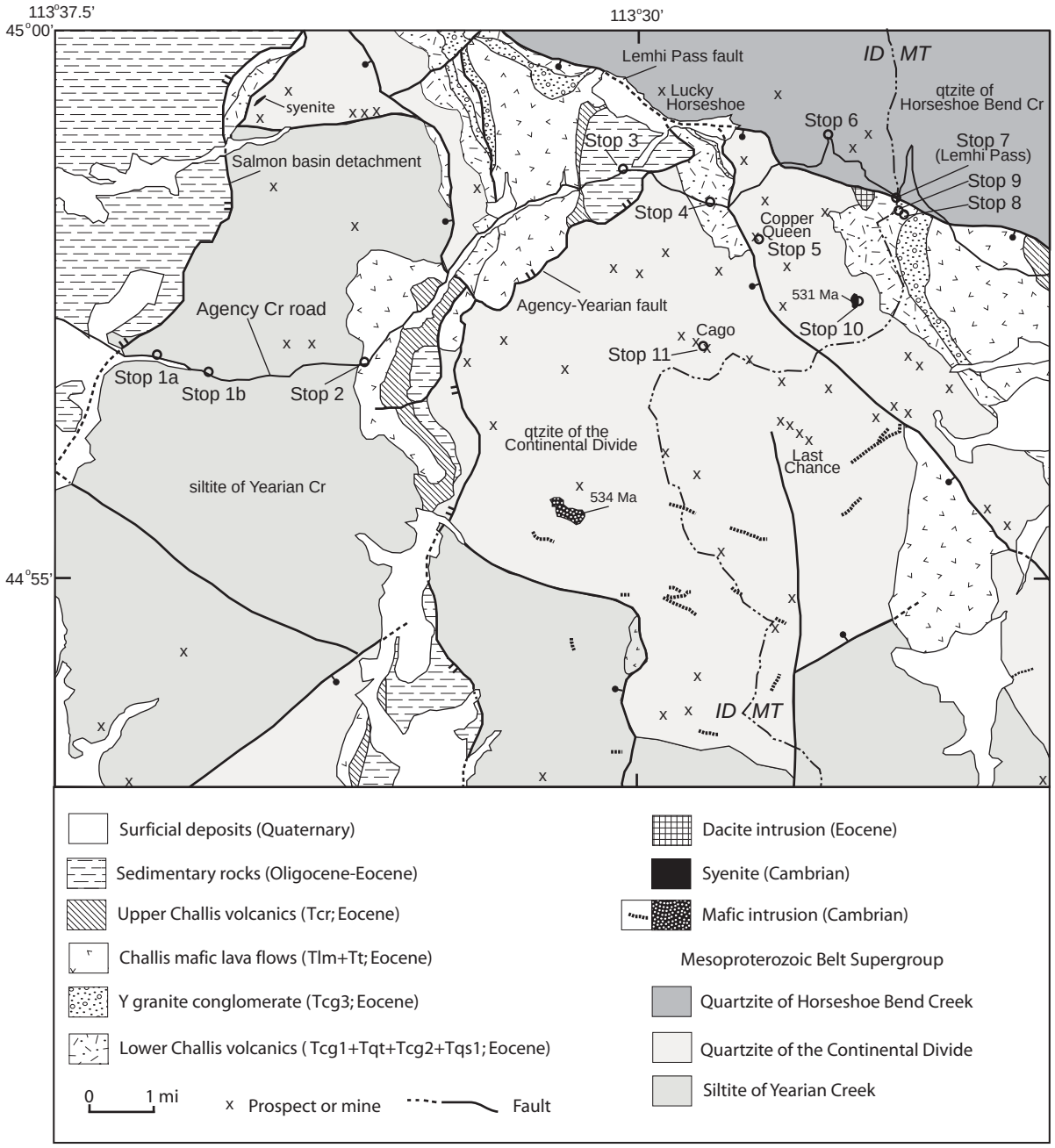

Figure 1. Simplified geologic map of the Agency Creek and Lemhi Pass area showing field trip stops.

Though the lack of known intrusives of Mississippian age is puzzling, the vein and replacement deposits were classified as "metamorphic" by earlier workers, an acknowledgement of the lack of obvious connection to any intrusives. The late Paleozoic hydrothermal activity does match the approximate timing of the Antler orogeny in Nevada and probably similar, if less known, far-field structural movements in southern Idaho. The syenites are highly enriched in incompatible elements and rare earths, and an alternate hypothesis is that the undated Th-REE quartz veins may be older than Mississippian and related to the Cambrian bimodal magmatism. $^{40}Ar/^{39}Ar$ age dating of feldspars in three Th-REE vein envelopes returned oldest ages stepping up to about 200 Ma, proving a pre-Cretaceous age, and closer to Mississippian than Cambrian, but not definitive of a mineralization age. Their alteration mineral assemblage is similar to that at the Lucky Horseshoe. Lead isotopes show that vein feldspars are more radiogenic than the Cambrian intrusives, suggestive of a crustal source for the veins. Additional information, geological and geochemical data, and speculations on the origin of the mineral deposits and the geologic setting can be found in the 2008 USGS contract report (Gillerman, 2008) and in the several abstracts and papers listed in the references.

Work in the area resumed in 2016 and 2017 as part

of a cooperative project between the Idaho Geological Survey and Montana Bureau of Mines and Geology as part of the USGS STATEMAP Program. Geologic mapping of both the Agency Creek and Lemhi Pass quadrangles will eventually be posted to the respective state websites. Regional geology immediately north of the area is now available at 1:75,000 scale (Burmester and others, 2016a) and a discussion of the regional Precambrian stratigraphy is given in Burmester and others (2016b).

ROAD LOG

Travel north from Leadore, Idaho, 25.5 mi to Tendoy. Road log begins in Tendoy. Travel east, following signs to Agency Creek. Latitudes and longitudes listed below use the WGS84 datum.

1.9 Deformed rocks on the left are Mesoproterozoic strata in the footwall of the Salmon basin detachment. We will be in the same but less mangled unit until stop 3.

2.2 STOP 1a

Siltite of Yearian Creek (possible Lawson Creek Formation) (44.950°N, 113.605°W).

Or, if parking is insufficient, continue up road 0.6 mi farther to wide pullout on left at

2.4 STOP 1b

Siltite of Yearian Creek (44.948°N, 113.594°W).

Because of correlation uncertainties, the 2016–2017 name for this Mesoproterozoic unit is siltite of Yearian Creek. It consists of graded siltite and argillite couplets with scattered beds and cosets of quartzite. The unit is characterized by undulating, graded, uncracked couplets and rarer couples of medium green siltite and light green to gray argillite (fig. 2). Cracked couplets are rarer, but look for mud cracks and angular light-colored mud chips. Mud chips are in bases of some beds along with well-rounded fine to spherical medium quartz grains in dark-green scour channels a few cm wide and as thick as 1 cm. Some chips and thin layers are chert. Look for those because they provide a good tie with the Lawson Creek Formation, a likely correlative to this unit. The Lawson Creek is correlative to the McNamara Formation of the main Belt basin. Common to this unit along Agency Creek are 1 to 3 dm beds of green to white, very fine- to fine-grained feldspathic quartzite, some with ripple tops and ripple cross lamination. Also common in some intervals are centimeter-scale, intricately interbedded, white and green quartzite with wide variation of grain sizes and feldspar content. Near the Divide to the south, the upper contact appears gradational into quartzite of the unit that hosts the syenite of stop 10 and the Cago mine at stop 11. Lower contact is faulted but apparently against an anomalously thin section of Swauger Formation. See Burmester and others (this volume) for more discussion on the stratigraphic conundrum.

4.2 Cow Creek is to the right. For most of its lower reach, it follows closely the basal contact of the Challis section on the Mesoproterozoic rocks of stop 2. As we approach stop 2, observe the flatirons of mafic lavas east of Cow Creek. A simple explanation for their tilt to the east is listric rotation on the Agency-Yearian detachment of its hanging wall, which they occupy.

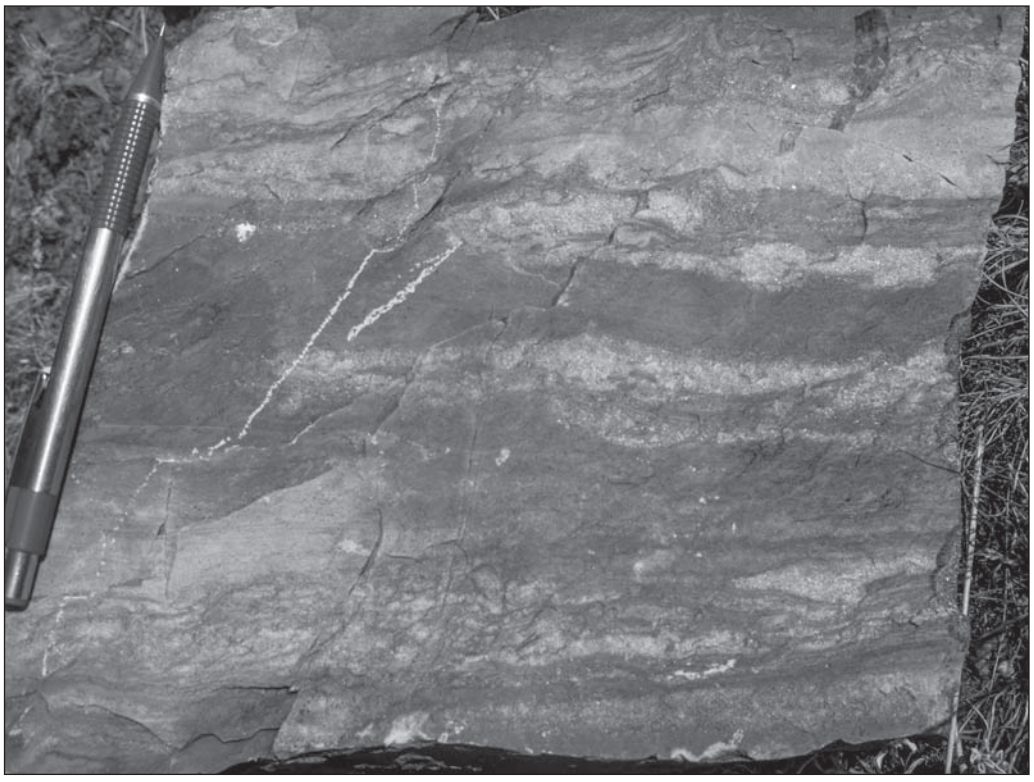

Figure 2. Loose block at Stop 1a of siltite of Yearian Creek. Note uneven dark siltite to light argillite couplets with lenses of spherical medium quartz grains and mud chips.

4.6 STOP 2

Mafic to intermediate flows of the Challis Volcanic Group (44.949°N, 113.559°W).

These mafic to intermediate flows are a widespread and important stratigraphic marker in the region (fig. 3). They locally contain round to irregular vesicles or amygdules and flow breccias, and are intercalated with thin, discontinuous rhyolitic tuffs. Secondary chalcedony and calcite are common, and xenocrystic quartz and plagioclase are found locally. Compositions include basalt, basaltic trachyandesite, trachyandesite, and andesite. Phenocrysts are primarily pyroxene and olivine, although Staatz (1972) also reported minor amounts of biotite and plagioclase in some of the flows. Equivalent to Tl unit of Blankenau (1999) and Tcl unit of VanDenburg (1997), and correlative with Tl unit of potassium-rich andesite, latite, and basalt lava in the Challis 1° x 2° quadrangle to the southwest (Fisher and others, 1992). We obtained LA-ICPMS U-Pb zircon age of 46.99 ± 0.24 Ma for an intercalated rhyolitic tuff sampled on the east (Montana) side of the pass. Staatz (1972) reported a thickness of about 1,000 m (3,300 ft).

4.7 Entrance to small BLM campground (44.950°N, 113.558°W).

6.0 Narrow watergap through Challis mafic flows (44.955°N, 113.552°W).

7.4 Contact of Mesoproterozoic metasedimentary rocks with tuff (44.969°N 113.535W°).

9.0 Wide spot on left (44.978°N, 113.506°W), or proceed to

9.2 Flume Creek and walk back west to outcrop. The Lucky Horseshoe mine is about 1 mi NE up Flume Creek.

STOP 3

Uppermost conglomerate (44.978°N, 113.505°W).

Clast-supported pebble to boulder conglomerate (fig. 4). Rounded to subrounded pebbles, cobbles, and some small boulders of Mesoproterozoic quartzite and siltite predominate, but clasts of Challis volcanics also are present. A single small boulder of coarse-grained Mesoproterozoic biotite granite, similar to boulders in Tcg3, is present northeast of the mouth of Flume

Composite stratigraphy for the Challis Volcanic Group near Lemhi Pass

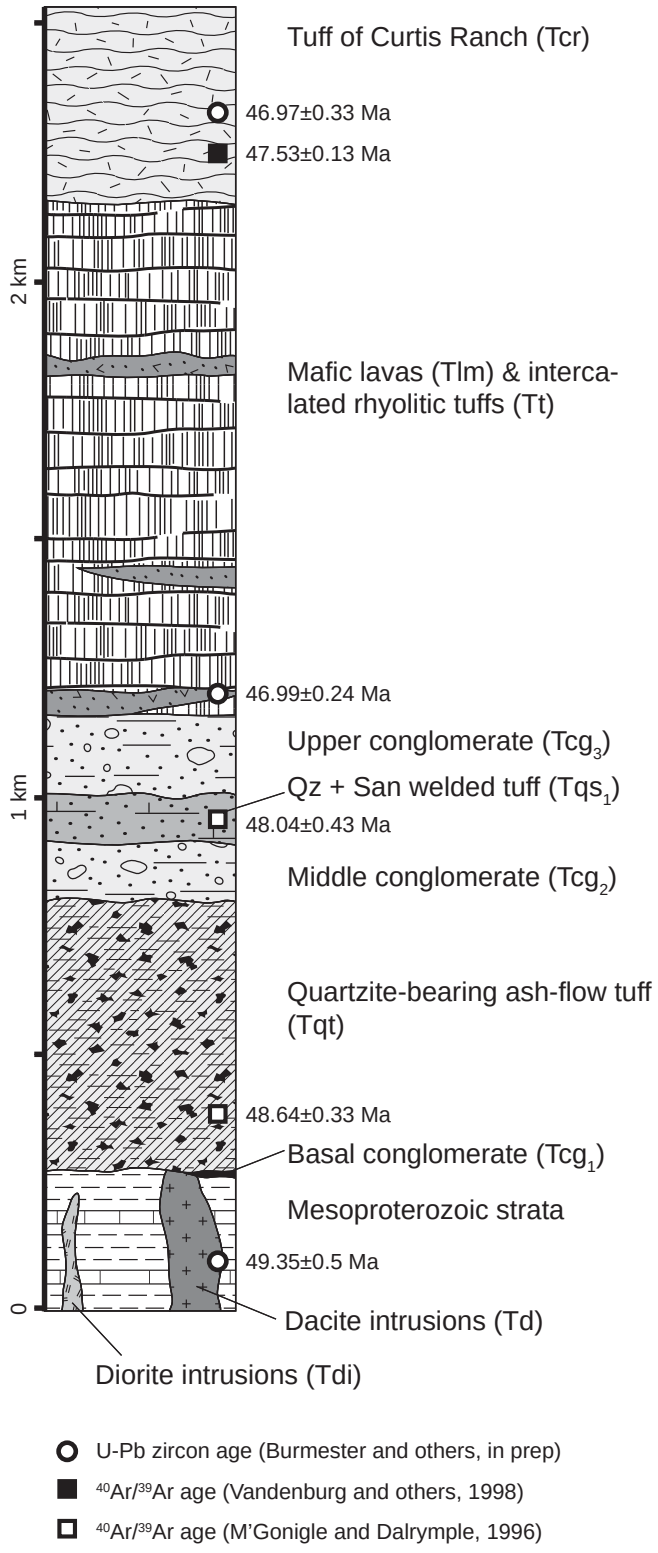

Figure 3. Stratigraphic column showing the Challis Volcanic Group and overlying sedimentary rocks in the Lemhi Pass area.

Figure 4. Uppermost conglomerate near the mouth of Flume Creek.

Creek. Unit is equivalent to Blankenau's (1999) middle conglomerate of the sedimentary rocks of Tendoy (Flume Creek facies of Tcg3 unit) and portions of the conglomerate of Flume Creek of Staatz (1972; 1979).

10.1 STOP 4

Quartzite-bearing ash-flow tuff (44.973°N, 113.485°W).

Outcrop is on corner and some parking is available beyond the corner (wide spot at cattle guard = 9.0 mi). Parking also available on shoulders between here and next stop.

Exposure here is a distinctive Challis tuff that contains abundant angular dark gray to black quartzite lithic fragments, less abundant quartz and plagioclase, and minor sanidine. Equivalent to Tcq unit of VanDenburg (1997) and Tqt unit of Blankenau (1999). The latter obtained a $^{40}Ar/^{39}Ar$ age on single sanidine crystals of 49.51 ± 0.14 Ma on a sample collected along Withington Creek about 30 km (18 mi) to the west–northwest in the Sal Mountain quadrangle. M'Gonigle and Dalrymple (1996) reported a $^{40}Ar/^{39}Ar$ weighted mean age of 48.64 ± 0.12 Ma from a sample collected near Lemhi Pass. Estimated to be as thick as 520 m (1,700 ft) in the area south of Lemhi Pass (Staatz, 1972), but thins to the south and is absent in the southeast part of map.

10.4 STOP 5

Copper Queen Mine fork—Road and creek crossing is rough and steep, so walking is probably better. Walk southeast about 2/3 of a mile to Copper Queen Mine (44.969°N, 113.477°W)

The Copper Queen Mine was the largest of several small copper mines and prospects in the Lemhi Pass region. Located on a small tributary of Agency Creek, the prospect was discovered and staked in 1883 by Mr. F.B. Sharkey and Mr. G. Chamberlain (Schipper, 1955). Mining commenced in 1906 with sinking of an inclined shaft, tunnel development, and erection of a small mill. The property was worked for several years, with a small tonnage of high-grade copper–gold ore extracted (over 25% Cu and over 1 oz/ton Au, with significant silver credit). Schipper (1955) detailed the mine's history and noted that in 1954 the property was leased and the workings dewatered to the 250 level, allowing access for geological study.

Several open stopes and caved-in shafts were observed by IGS geologists in 2000. Rocks on the waste dumps provided excellent samples of the mineralization and host rocks. Subsequent safety closures have obscured some of the stopes and outcropping geology, but much should still be available for examination.

The Mesoproterozoic host rock here and at stop 11

is currently mapped as "quartzite of the Continental Divide." Like many Belt Supergroup units, it consists of feldspathic quartzite and siltite with minor argillite. Quartzite beds are as thick as 1 m but more commonly thinner. These are repeated in cosets, or interbedded with thinner beds of siltite. Contacts with siltite are more commonly sharp than graded. Sedimentary structures include trough cross bedding, climbing ripple or ripple drift cross laminations, large loads, convolute bedding, and soft-sediment deformation. Internal lamination of quartzite is commonly even, centimeter-thick dark green to light coloration with little macroscopic grain size change, but platy partings have fine muscovite on surfaces. Finer grained material is locally phyllite. Three quartzite samples south of here ranged from 32 to 80 percent quartz with the rest plagioclase. Youngest U-Pb ages of two detrital zircons isolated from samples collected near the Copper Queen Mine are 1,371 and 1,375 Ma (Gillerman, 2008), consistent with the unit being above the Swauger Formation. Correlation with the Jahnke Lake member of the Apple Creek Formation currently is favored but not proven.

These metasedimentary rocks host mafic intrusive rocks including a greenstone dike (or flow?) and pyroxene porphyry lamprophyres (fig. 5). Lamprophyre intrusions occur elsewhere in the district, and are shown as Tertiary dikes on previous maps (e.g., Staatz, 1972, 1979). Phenocrysts include large pyroxenes, amphiboles, and pseudomorphs of olivine replaced by talc and tremolite assemblages. The dikes are similar to alkaline basalt in chemistry.

Due to the unreactive nature of the quartzite, alteration is hard to find, though some chloritic alteration, hornfels, and a weak iron stain are present. Potassium feldspar locally replaces the metamorphic muscovite in the metasedimentary rocks. The copper ores are contained in quartz veins with chalcopyrite, bornite, and sparse molybdenite (fig. 6). Green secondary copper minerals can be found, but unoxidized, primary sulfide minerals are also common on the dump. Schipper (1955) described copper mineralization in the greenstone dike, and a sample of a chalcopyrite–calcite vein cutting pyroxene porphyry was found on the dump, proving that the base metal deposition was later than the mafic intrusive event. Schipper also described a radioactive veinlet with copper and thorium that cuts the copper veins. Subhorizontal faults, which offset the quartz–copper veins, are exposed in the outcropping walls of the open stopes, which were partially filled by the closure work. These structures presumably formed during Cretaceous crustal shortening in the region (fig. 7).

One sample of molybdenite from the waste dump at the Copper Queen Mine contained sufficient Re to obtain a Re-Os date of 1,053 Ma, similar to ages obtained initially for the monazite cores (Gillerman and others, 2002). The Proterozoic age did correspond with literature reports of some type of "Grenville-age" thermal event in the region, but not with any known geologic events in the Salmon region (Anderson and Davis, 1995). Subsequent work in Idaho has yielded more evidence for Grenville-age events in central Idaho. However, dating of the mafic porphyries suggests that copper mineralization is more likely Cambrian in age. An $^{40}Ar/^{39}Ar$ age on hornblende in the pyroxene porphyry returned a messy "reset" age of about 400 Ma, with another hornblende sample preserved in a calcite matrix breccia dated at 558 Ma ± 1.6 Ma with a good plateau age (Gillerman, 2008). Zircon isolated from a similar

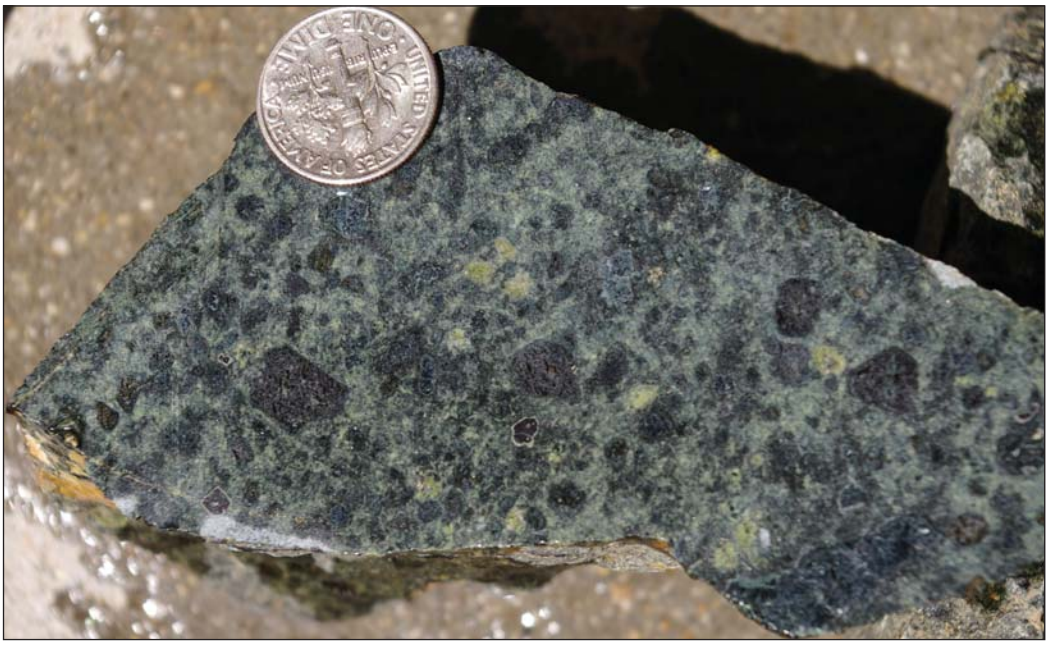

Figure 5. Pyroxene porphyry from Copper Queen Mine dump. Note large euhedral pyroxene phenocrysts.

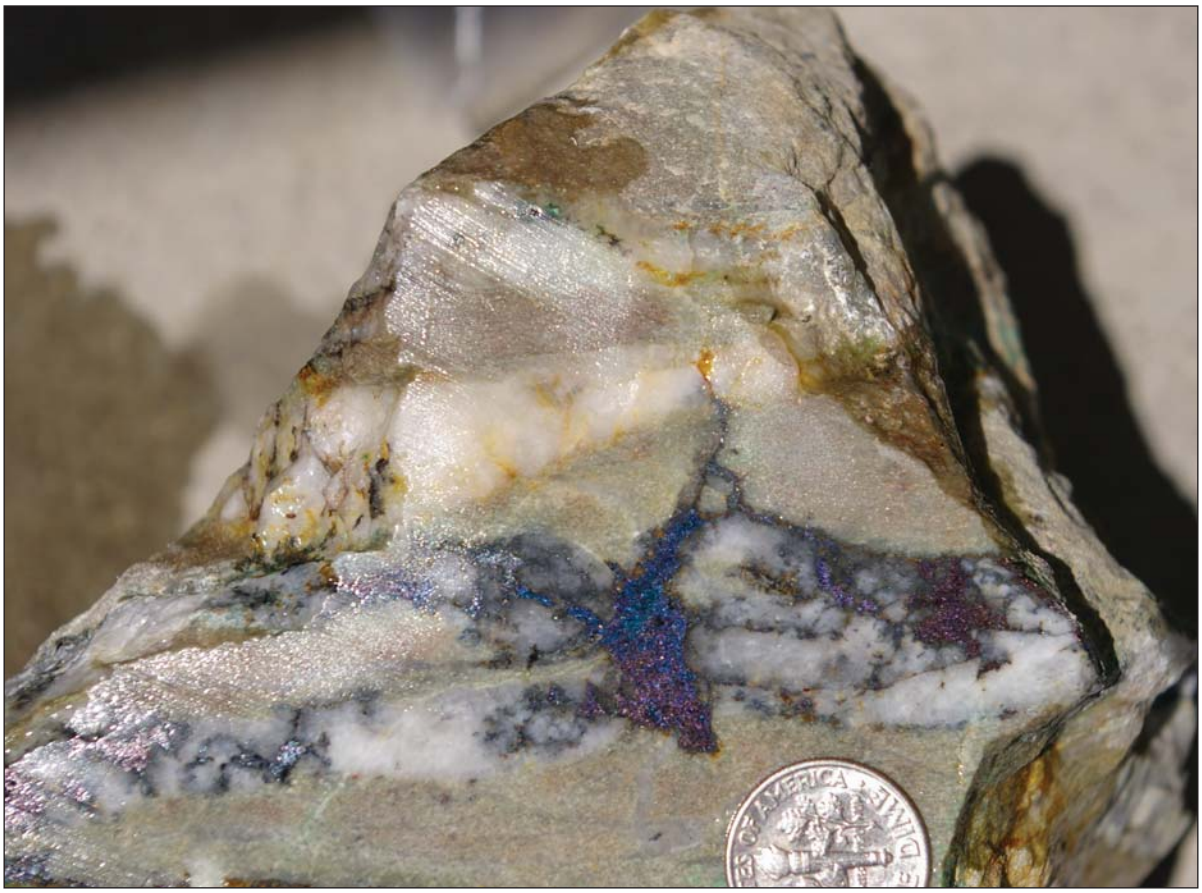

Figure 6. Bornite in possible pull-aparts of boudinaged quartz–copper vein, Copper Queen Mine. No clear alteration envelope present, but diffuse hornfels(?) developed in quartzite wall rock.

Figure 7. Gouge and low-angle faults cutting quartz–copper vein at Copper Queen Mine, adit 3, looking N12°E.

mafic plug sampled in Cow Creek on the south of the district yielded a U-Pb ID-TIMS age of 534.37 ± 0.22 Ma (Gillerman and others, 2010). It is likely that the copper–gold mineralization is Cambrian in age, possibly with some metals recycled from earlier times, but more work is needed to verify this age assignment. There are also many other small copper–gold mines in the Salmon region as well as several iron deposits.

12.9 STOP 6

Horseshoe bend. Parking best on NW outside bend (44.984°N 113.460°W)

We are now on the footwall of the Lemhi Pass fault. Because of correlation uncertainties, we have applied an informal name "quartzite of Horseshoe Bend Creek" to this Mesoproterozoic rock unit. It consists of feldspathic quartzite, siltite, and argillite. Surprised? Characteristically, quartzite beds as thick as 1 m are flat laminated and grade to siltite and argillite tops. Here the grading from light quartzite to dark siltite and argillite gives the rock a candy-striped appearance (fig. 8). Where these rocks are more deformed, this gradation is emphasized by cleavage curving to be more parallel to bedding in the finer grained tops. Less common but widespread in this unit are hummocky and trough cross stratification, climbing ripple or ripple drift cross laminations, loads into argillite tops of underlying beds, and soft-sediment deformation. Platy parting with muscovite surfaces are rare. Some intervals contain decimeter- to meter-thick beds of white, very fine- to fine-grained, feldspathic quartzite in sets of more than 10. Some of the thicker beds have bedding defined by dark millimeter-scale laminations. A stained quartzite sample contained 40 percent plagioclase and no potassium feldspar. Potassium feldspar is similarly lacking in about half of the samples from Kitty Creek quadrangle (Lewis and others, 2009) to the north, and constitutes less than a third of the feldspar in the other half. Two years ago, this quartzite was correlated with the Gunsight Formation (Burmester and others, 2016a), but a single detrital grain from the Lucky Horseshoe Mine west of here yielded a 1,373 Ma age (Gillerman, 2008), which supports current thought that this unit is instead a member of the Apple Creek Formation above the Swauger, perhaps a variation of the banded siltite member and (or) quartzite of Lake Mountain. Such a call is consistent with little stratigraphic throw on the Lemhi Pass fault.

Figure 8. Outcrop exposures of the quartzite of Horseshoe Bend Creek.

12.2 STOP 7

Lemhi Pass (44.975°N 113.445°W)

Beware, the last stretch of road is steep and rough. Proceed into Montana 0.1 mi and stop on left near facility.

On August 12, 1805, Meriwether Lewis and three other members of the Lewis and Clark Expedition crossed the Continental Divide at Lemhi Pass. Lewis found a "large and plain Indian road" over the pass. This was the first time that white men had seen present-day Idaho.

The Lemhi Pass fault strikes east–southeast to west–northwest across Lemhi Pass. It juxtaposes Mesoproterozoic rocks on the north against Tertiary rocks to the south. VanDenburg (1997), VanDenburg and others (1998), and Blankenau (1999) interpreted the structure as a 22° to 24° south-dipping detachment fault that likely formed at a higher angle before rotating to its present dip during the latest phase of extensional faulting. Eocene volcanic and volcaniclastic deposits are interpreted to have accumulated in a half-graben formed by the Lemhi Pass fault, and therefore the fault's minimum heave is roughly equivalent to the stratigraphic thickness of the Challis group in this area, estimated as 1 km (VanDenburg and others, 1998). Gillerman (2008) speculated that the fault might have a prolonged history, however, and that Tertiary extension reactivated older structures including Neoproterozoic faults that contributed to localization of REE mineralization in this district, and possibly Cretaceous thrust faults.

Walk or drive from Lemhi Pass SE along road toward Sacagawea picnic area. First exposures along the road are light-colored Challis tuff.

STOP 8

Quartz–sanidine tuff (44.973°N, 113.443°W)

Eocene quartz–sanidine welded tuff of the Challis Volcanic Group. Unit contains sparse, euhedral to subhedral crystals of sanidine and quartz. Our estimate of maximum thickness is 60–90 m (200–300 ft). Equivalent to Tqs1 of Blankenau (1999). Locally mapped as vitric tuff of Lemhi Pass by Staatz (1972, 1979). M'Gonigle and Dalrymple (1996) reported an $^{40}Ar/^{39}Ar$ weighted mean age of 47.95 ± 0.12 Ma for this unit near Lemhi Pass.

Hike up the hill from Stop 8, or south from Lemhi Pass to Stop 9.

STOP 9

Mesoproterozoic boulders (44.973°N, 113.445°W)

Lag deposits of cobbles and boulders from Eocene conglomerate. Most are quartzite, but the unit includes distinctive cobbles and boulders of coarse-grained Mesoproterozoic biotite granite (fig. 9) that are likely derived from exposures 40 km (25 mi) to the northwest (Burmester and others, 2016a). Rare garnet amphibolite cobbles have also been observed north of Agency Creek. Because of the general east dip of the Challis strata, these lag deposits have formed west of the actual surface exposures of the unit. Equivalent to

Figure 9. Small boulder of Mesoproterozoic granite south of Lemhi Pass that formed as a lag deposit. Weathered from Eocene conglomerate unit.

the granite clast conglomerate (Tcg2) of Blankenau (1999), but mapped higher in the stratigraphic section in the area north of Agency Creek. Blankenau (1999), Janecke and others (2000), and Chetel and others (2011) postulated that an Eocene paleoriver flowed through the Salmon basin and transported the granite clasts across the Beaverhead Range at Lemhi Pass. As thick as 150 m (500 ft), but thins southward and is absent in the southern part of the Lemhi Pass quadrangle.

Drive or walk south along the Continental Divide Trail about 1.4 mi from Lemhi Pass and stop before the trees. Follow the track to the WNW 0.3 to 0.4 mi through trees to exploration pits.

STOP 10

Fine-grained syenite plug 1.9 km (1.2 mi) south-southwest of Lemhi Pass (44.959°N, 113.453°W)

Field mapping in 2006 discovered a series of trenches that exposed an outcrop of syenite, a feldspar-rich, low-silica intrusive rock. Though not shown on Staatz's (1979) detailed map of the district, the syenite was shown on a thesis map by Hansen (1983). The syenite consists largely of inclusion-rich potassium feldspar with few mafic minerals and local specular hematite alteration. It crops out primarily in dozer cuts and does not exhibit any deformational fabric where seen, but it looks "old." Check out 44.9586°N, 113.4548°W for pit with non-veined rock, 44.9584°N, 113.4535°W for pit with veining. Prospecting the trench with a Geiger counter failed to find anomalous radioactivity.

The tan-colored syenite intrudes the Proterozoic quartzite and is locally cut by specular hematite veins (fig. 10). The syenite contains about 64 weight percent SiO_2 and 10 percent alkalis. The rock is largely composed of feldspar laths of orthoclase, mantled with albite rims. While a few grains of original biotite are present locally, most of the dark grains in the rock are now specular hematite probably replacing the biotite. A trace amount of interstitial quartz is also present. Zircons from the syenite were dated with U-Pb methods on the SHRIMP at Canberra, Australia, and returned an age of 529.1 ± 4.5 Ma, or earliest Cambrian (fig. 11; Gillerman and others, 2008, 2010).

The spatial and temporal coincidence of felsic and

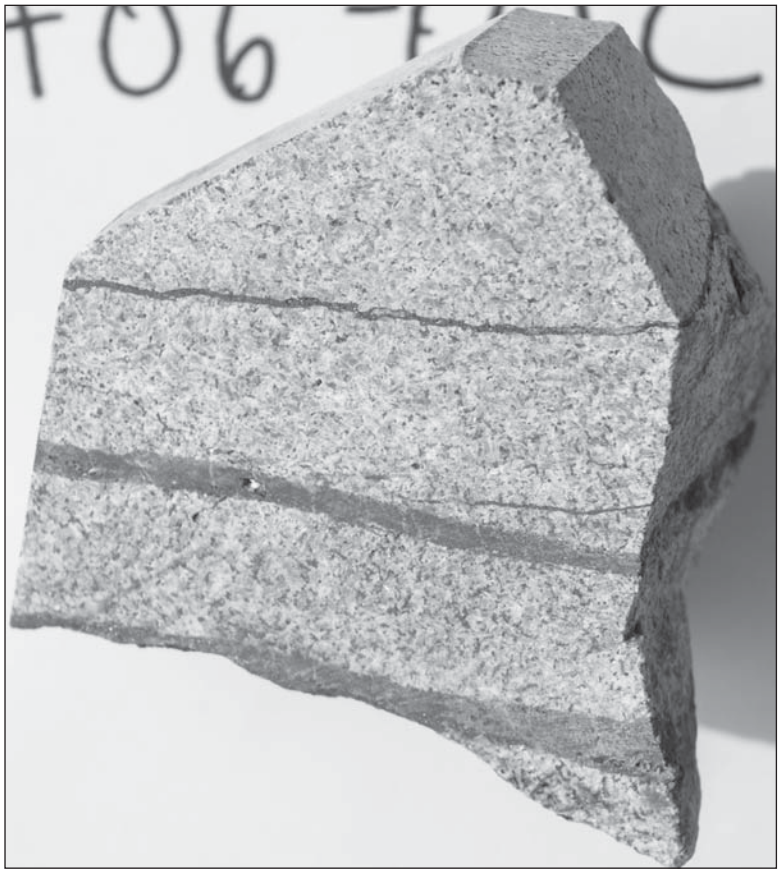

Figure 10. Hand specimen of syenite from prospect trench showing cross-cutting specular hematite alteration.

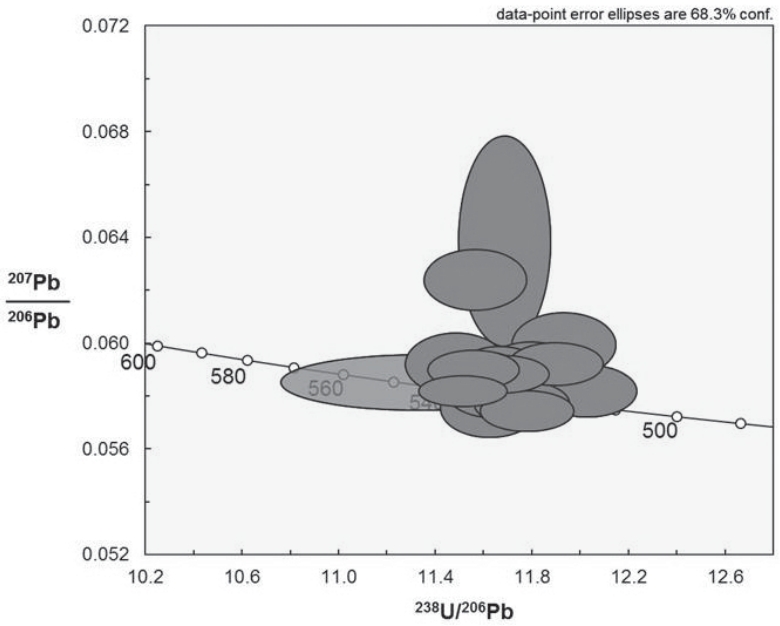

Figure 11. Isochron plot of geochronology results for Lemhi Pass syenite sample JA06-01A. Best age of crystallization is 529 Ma ± 4.5 Ma, or lower Cambrian (from Gillerman, 2008; Gillerman and others, 2008).

mafic alkaline igneous rocks at Lemhi Pass indicate a bimodal magmatic, possibly rift-related event in the region at about 530 Ma. The Lemhi Pass alkaline rocks are part of a northwest-trending belt of Neoproterozoic to early Paleozoic age alkaline intrusives that

extend from the Beaverhead Mountains into central Idaho. Unfortunately, no detailed geophysical surveys, which could potentially delineate buried intrusive complexes, are available for the region. The bimodal character of the Lemhi Pass Cambrian suite is evident in trace element geochemistry, as shown on a plot of Nb versus Th to demonstrate the highly evolved composition of the syenite (fig. 12; Gillerman, 2008).

Proceed about 2.3 mi along the divide trail, then turn off to the northwest for another quarter of a mile to 44.951°N, 113.486°W. No guarantee that the road is drivable. The last part drops about 400 ft.

STOP 11

Cago Th-REE Mine (optional) (44.951°N, 113.486°W)

The Cago Mine is located at the end of a mile-long narrow jeep trail that diverges off the Continental Divide road approximately 2 mi southwest of Lemhi Pass. Turn-around spots are few but the stop is easily accessible by foot and provides an excellent exposure of the thorium-REE-iron oxide veins. The Cago vein trends northwest and dips moderately southwest into the hillside. It is approximately 6 ft thick where exposed in the trench. The Cago vein is on trend with, and likely an extension of, the Last Chance vein, which is located on the Montana side of the district. The Last Chance vein was explored into the 1980s with underground adits, and a small resource of Th-REE ore developed. REE is the abbreviation for "rare earth elements" and defines the row of elements on the periodic table from lanthanum with atomic number 57 and the extra row from atomic number 58 (cerium) through atomic number 71 (lutetium). REEs share similar chemical properties and are referred to as the lanthanides. See Gillerman (2011) for a summary of the REE deposits in Idaho. A sample of the vein and adjacent wall rock is shown in figure 13.

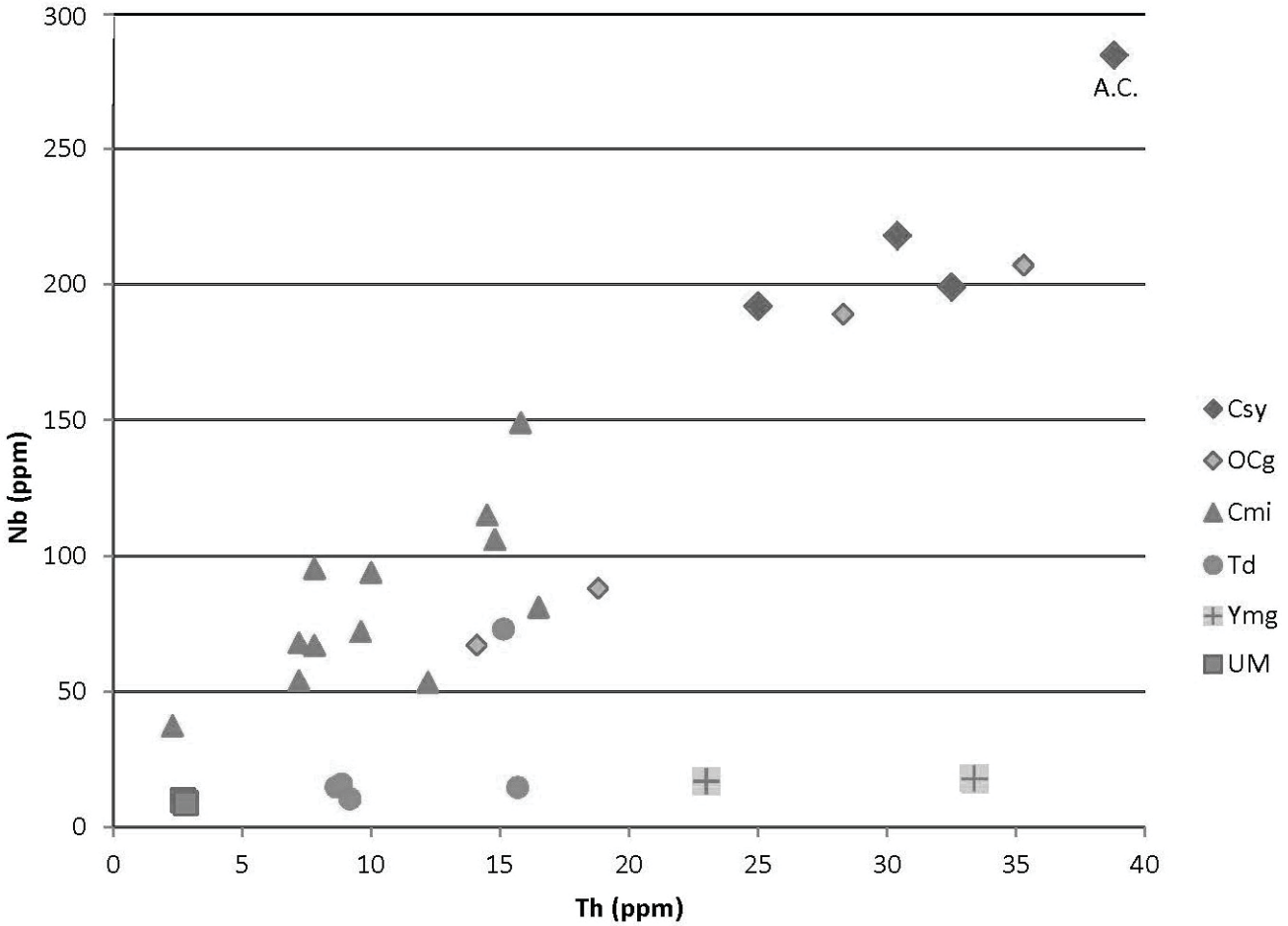

Figure 12. Plot of Nb versus Th for Lemhi Pass and regional intrusive samples. Circles = Eocene volcanics; dark diamonds = Cambrian syenites; lighter diamonds = Paleozoic granites near Leadore; triangles = Cambrian-age mafic dikes; solid square = Lucky Horseshoe ultramafic sill; crosses in squares = regional Precambrian megacrystic granite. The syenite is the most enriched in Th and Nb, as well as alkalis and REE. Syenite labeled A.C. is from north of Agency Creek in the western part of the area.

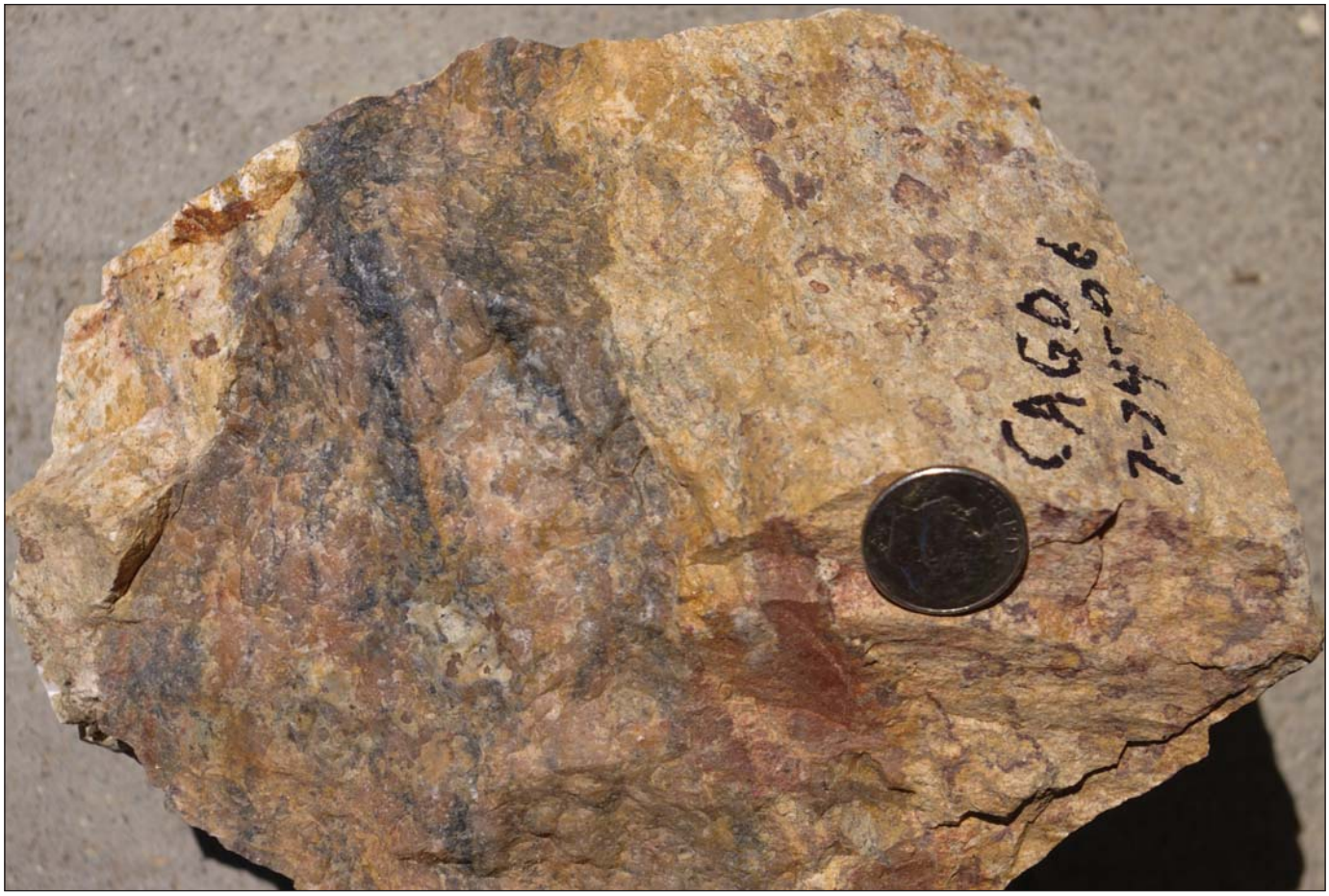

Figure 13. Pink quartz–potassium feldspar–specular hematite–thorite vein from the Cago prospect. The white outer envelope contains additional potassium feldspar plus albite and rutile.

Most of the thorium deposits in the district are quartz veins, and the quartz has a distinctive waxy to greasy luster. The quartz veins are typically fine grained and strongly colored in shades of pink to brown due to abundant hematite and thorite in them. The veins are steep to moderately dipping, of variable size, and share an assemblage of quartz–hematite–thorite with alkali feldspar and lesser but variable amounts of apatite, monazite, biotite, barite, carbonate, fluorite, and allanite. Thin sections from the Cago vein and others show that the muscovite in the host quartzite is converted to potassium feldspar adjacent to the vein though alteration extends only a few feet away from the vein (Gillerman, 2008). Locally, albite twins are visible, but most of the potassium feldspar is untwinned and occurs in patchy masses near the veins. Microprobe analyses also detected albite and rutile in altered zones. Brecciation and crackle veins are common to all the thorium deposits, and multi-generational strained quartz is typical.

The major rare-earth-bearing mineral in the district is monazite, a REE-bearing phosphate (Ce, La, Y, Th, U) PO_4 that is not visible in hand sample. The major thorium-bearing mineral is thorite, a silicate with the formula: (Th, U)SiO_4· Thorite is typically a reddish brown to brown with resinous luster; it looks very similar to hematite. The thorite is also microscopic in grain size and highly radioactive.

The primary gangue mineral, in addition to quartz, is specular hematite. It is intergrown with the thorite and abundant. Extensive weathering has produced a variety of reddish to brownish earthy hematite- and goethite-coated material in and near the veins. A few of the veins contain traces of copper minerals as well. In the Lemhi Pass area, there is very little uranium or thorium in the monazite. Instead, the deposits and monazites are unusually enriched in the rare earth element neodymium (Nd). Most monazites contain higher values of the lighter REEs, La and Ce. Monazites from the Lucky Horseshoe deposit contain 35 weight percent Nd oxide in their lattice, approximately double that of other monazites. Globally, Nd is particularly sought after for applications such as magnets.

A special *in situ* U-Pb electron microprobe chemical age-dating technique developed at the University

of Massachusetts was used to date the monazites from the Lucky Horseshoe replacement deposit. That material contains lenses with abundant monazite that is easily visible in thin section. Monazite crystals will typically take in uranium but not much lead due to crystallographic constraints; thus any lead present in the crystal has formed from radiogenic decay. Whole-rock geochemistry confirms that there was very little lead in the Lemhi Pass hydrothermal system, so if one can measure the trace amounts of uranium and lead in the monazites with electron probe microanalysis, an age can be determined. Chemical mapping of the monazites revealed domains of distinct composition, with cracks and rims that correspond to areas reset in the Cretaceous. Ages of the monazite cores and ages on the thorites overlap with a range from about 400 to 300 Ma. A best estimate of 355 Ma corresponds to late Devonian or earliest Mississippian in age. In addition, the ages on four zircon crystals derived from an ultramafic sill below the Lucky Horseshoe Mine were measured by U-Pb methods using ID-TIMS. The resulting U-Pb age of 315 Ma may represent an igneous crystallization age or a hydrothermal age, but it does provide an independent confirmation of a Mississippian event at Lemhi Pass (Gillerman and others, 2010). Whether some of the Th-REE mineralization elsewhere in the district is older remains an open question. Additional regional mapping and geochronologic study would better confirm the age and origin of Idaho's regional-scale REE-Th-Fe mineralization, as many questions remain for discussions and debate (Gillerman, 2011; Gillerman and others, 2013).

END OF TRIP

REFERENCES CITED

Anderson, A.L., 1958, Uranium, thorium, columbium, and rare earth deposits in the Salmon region, Lemhi County, Idaho: Idaho Bureau of Mines and Geology Pamphlet 115, 81 p.

Anderson, A.L., 1961, Thorium mineralization in the Lemhi Pass area, Lemhi County, Idaho: Economic Geology, v. 56, no. 1, p. 177–197.

Anderson, H.E., and Davis, D.W., 1995, U-Pb geochronology of the Moyie sills, Purcell Supergroup, southeastern British Columbia: Implications for the Mesoproterozoic geological history of the Purcell (Belt) basin: Canadian Journal of Earth Sciences, v. 32, p. 1180–1193.

Blankenau, J.J., 1999, Cenozoic structural and stratigraphic evolution of the southeastern Salmon Basin, east-central Idaho: Logan, Utah State University, M.S. thesis, 143 p., 3 plates.

Burmester, R.F., Lewis, R.S., Othberg, K.L., Stanford, L.R., Lonn, J.D., and McFaddan, M.D., 2016a, Geologic map of the western part of the Salmon 30' x 60' quadrangle, Idaho and Montana: Idaho Geological Survey Geologic Map 52, scale 1:75,000.

Burmester, R.F., Lonn, J.D., Lewis, R.S., and McFaddan, M.D., 2016b, Stratigraphy of the Lemhi subbasin of the Belt Supergroup, *in* MacLean, J.S., and Sears, J.W., eds., Belt Basin: Window to Mesoproterozoic Earth: Geological Society of America Special Paper 522, p. 121–137.

Chetel, L.M., Janecke, S.U., Carroll, A.R., Beard, B.L., Johnson, C.M., and Singer, B.S., 2011, Paleogeographic reconstruction of the Eocene Idaho River: Geological Society of America Bulletin, v. 123, no. 1/2, p. 71–88.

Fisher, F.S., McIntyre, D.H., and Johnson, K.M., 1992, Geologic map of the Challis quadrangle, Idaho: U.S. Geological Survey Miscellaneous Investigations Series Map I-1819, scale 1:250,000.

Gibson, P.E., 1998, Origin of the Lemhi Pass REE-Th deposits, Idaho/Montana: Petrology, mineralogy, paragenesis, whole-rock chemistry and isotope evidence: Moscow, University of Idaho, M.S. thesis, 320 p.

Gillerman, V.S., 2008, Geochronology of iron oxide-copper-thorium-REE mineralization in Proterozoic rocks at Lemhi Pass, Idaho, and a comparison to copper-cobalt ores, Blackbird mining district, Idaho: Final Technical Report to U.S. Geological Survey, December, 149 p. MRERP Award #06HQGR0170, https://minerals.usgs.gov/mrerp/reports.html#2006

Gillerman, V.S., 2011, Rare earth elements and other critical metals in Idaho: Idaho Geological Survey GeoNote 44, 4 p.

Gillerman, V.S., Fanning, C.M., Link, P.K., Layer, P., and Burmester, R.F., 2008, Newly discovered intrusives at the Lemhi Pass thorium-REE-iron oxide district, Idaho: Cambrian syenite and mystery ultramafics: Signatures of a buried alkaline complex or two systems?: Geological Society of

America Abstracts with Programs, v. 40, no. 1, p. 51.

Gillerman, V.S., Jercinovic, M.J., and Stein, H.J., 2002, U-Pb and Re-Os geochronology suggest a multistage Precambrian-Mesozoic history for thorium and copper mineralization, Lemhi Pass, Idaho: Geological Society of America Abstracts with Programs, v. 34, no. 6, p. 337.

Gillerman, V.S., Lund, K., and Evans, K.V., 2003, Stratigraphy, structure, and mineral deposits of the Lemhi Pass area, central Beaverhead Mountains, eastern Idaho: Northwest Geology, v. 32, p. 134–146.

Gillerman, V.S., Otto, B.R., and Griggs, F., 2000, Lemhi Pass Thorium District: A variant of Proterozoic iron oxide (Cu-U-Au-REE) deposits?: Geological Society of America Abstracts with Programs, v. 32, no. 7, p. 83.

Gillerman, V.S., Otto, B., and Griggs, F.S., 2006, Site inspection report for the abandoned and inactive mines in Idaho on U.S. Bureau of Land Management property in the Lemhi Pass area, Lemhi County, Idaho: Idaho Geological Staff Report S-06-4, 170 p.

Gillerman, V.S., Schmitz, M.D., Jercinovic, M.J., and Reed, R., 2010, Cambrian and Mississippian magmatism associated with neodymium-enriched, rare-earth and thorium mineralization, Lemhi Pass district, Idaho: Geological Society of America Abstracts with Programs, v. 42, no. 5, p. 334.

Gillerman,V.S., Schmitz, M.D., and Jercinovic, M.J., 2013, REE-Th deposits of the Lemhi Pass region, northern Rocky Mountains—Paleozoic magmas and hydrothermal activity along a continental margin: Geological Society of America Abstracts with Programs, v. 45, no. 5, p. 41.

Hansen, P.M., 1983, Structure and stratigraphy of the Lemhi Pass area, Beaverhead Range, southwest Montana and east-central Idaho: University Park, Pennsylvania State University, M.S. thesis, 112 p.

Janecke, S.U., VanDenburg, C.J., Blankenau, J.J., and M'Gonigle, J.W., 2000, Long-distance longitudinal transport of gravel across the Cordilleran thrust belt of Montana and Idaho: Geology, v. 28, no. 5, p. 439–442.

Lewis, R.S., Burmester, R.F., Stanford, L.R., Lonn, J.D., McFaddan, M.D., and Othberg, K.L., 2009, Geologic map of the Kitty Creek quadrangle, Lemhi County, Idaho and Beaverhead County, Montana: Idaho Geological Survey Digital Web Map 112 and Montana Bureau of Mines and Geology Open-File Report 582, scale 1:24,000.

M'Gonigle, J.W., and Dalrymple, G.B., 1996, $^{40}Ar/^{39}Ar$ ages of some Challis Volcanic Group rocks and the initiation of Tertiary sedimentary basins in southwestern Montana: U.S. Geological Survey Bulletin 2132, 17 p.

Schipper, W.B., 1955, The Tendoy Copper Queen Mine: Moscow, University of Idaho, M.S. thesis, 38 p.

Sharp, W.N., and Cavender, W.S., 1962, Geology and thorium-bearing deposits of the Lemhi Pass area, Lemhi County, Idaho, and Beaverhead County, Montana: U.S. Geological Survey Bulletin 1126, 76 p.

Staatz, M.H., 1972, Geology and description of the thorium-bearing veins, Lemhi Pass quadrangle, Idaho and Montana: U.S. Geological Survey Bulletin 1351, 94 p., 2 plates.

Staatz, M.H., 1979, Geology and mineral resources of the Lemhi Pass thorium district, Idaho and Montana: U.S. Geological Survey Professional Paper 1049-A, 90 p.

Staatz, M.H., Shaw, V.E., and Wahlberg, J.S., 1972, Occurrence and distribution of rare earths in the Lemhi Pass thorium veins, Idaho and Montana: Economic Geology, v. 67, p. 72–82.

Umpleby, J.B., 1913, Geology and ore deposits of Lemhi County, Idaho: U.S. Geological Survey Bulletin 528, 182 p.

VanDenburg, C.J., 1997, Cenozoic tectonic and paleogeographic evolution of the Horse Prairie half-graben, southwest Montana: Logan, Utah State University, M.S. thesis, 152 p., 2 plates.

VanDenburg, C.J., Janecke, S.U., and McIntosh, W.C., 1998, Three-dimensional strain produced by >50 My of episodic extension, Horse Prairie basin area, SW Montana, U.S.A.: Journal of Structural Geology, v. 20, issue 12, p. 1747–1767.

FIELD GUIDE TO COMPRESSIONAL STRUCTURES ALONG THE WESTERN MARGIN OF THE SOUTHERN BEAVERHEAD MOUNTAIN RANGE, SCOTT BUTTE 7.5' QUADRANGLE, EAST-CENTRAL IDAHO

William W. Little and Robert W. Clayton

Brigham Young University–Idaho, Rexburg, Idaho 83460

INTRODUCTION

The Brigham Young University–Idaho Advanced Field Methods course (field camp) has conducted bedrock geologic mapping in the southern Beaverhead Mountain Range of east-central Idaho for 13 yr (Clayton and Little, 2009, 2014; Roemer and others, 2007; Bagley and Little, 2009; Little and others, 2010). Additional mapping has been and continues to be done by other workers, with significant differences among interpretations (Skipp, 1985; Embree, in review; Abplanalp and others, 2008; Pearson, pers. commun., 2017). The primary contribution of our work is identification of previously undescribed compressional structures along the western flank of the range, including: (1) a north-trending thrust fault, referred to here as the Copper Mountain Thrust Fault, that consistently places the Mississippian Scott Peak through Surrett Canyon formations over the interbedded Mississippian Big Snowy/Arco Hills interval, (2) high-angle reverse faults at the core of fault propagation folds, and (3) large-scale overturned and recumbent folds. From outcrop to range scale, folds are asymmetrical, east to northeast vergent, and found in the hanging wall of the Copper Mountain thrust. Footwall strata are relatively undeformed, other than an initial relatively steep dip that flattens to the west away from the fault. These structural features represent deformation associated with east to northeast compression and displacement in development of the Medicine Lodge thrust sheet during the Cretaceous Sevier orogenic event. The compressional features have subsequently been dissected by north- to northwest-trending normal faults related to Late Miocene to Recent Basin-and-Range extension, as well as west-trending normal faults, possibly caused by extension during Late Miocene passage of the area over the Yellowstone Hot Spot.

Stratigraphically, the southern Beaverhead Range consists of a thick succession of Middle Proterozoic through Permian strata dominated by Mississippian and Pennsylvanian carbonates (Sandberg, 1975; Skipp and others, 1979; Wardlaw and Pecora, 1985; Batt and others, 2007; Billman & Little, 2007; Isaacson and others, 2007), many of which are highly similar in appearance, making some structural interpretations difficult as these units are juxtaposed by faulting or repeated in overturned folds. However, subordinate sandstone and mudstone intervals serve as stratigraphic markers that, in most cases, allow proper interpretation of stratigraphic position. The Paleozoic succession is underlain to great depth by Middle to Late Proterozoic sandstones (Skipp and Link, 1992; Little and Little, 2009).

The purpose of this half-day trip is to visit outcrops that show structural features, primarily the Copper Mountain Thrust Fault, and to follow these structures from south to north to observe changes in character and expression. This trip will focus on features found on the Scott Butte, Idaho 7.5-minute quadrangle, beginning at the intersection of Idaho State Highway 28 and a gravel road just south of the southern tip of the mountain range and progressing through Petersen, Deadman, Bloom, and Spring Canyons. Stops are shown on a highly preliminary geologic map (fig. 1) and stratigraphic units are listed and described in table 1.

FIELD TRIP

STOP 1

Highway 28 (Basin and Range overview)

The Beaverhead Mountain Range forms a Basin and Range horst, bordered both to the west and the east by deeply filled grabens (fig. 2). A down to the west bounding normal fault defines the western margin of the range at its southern end and steps eastward near Copper Mountain. A second down to the west normal fault, here called the Reno Gulch Fault, is present within the horst to the east of the range-front fault, where it displaces the base of the Snaky Canyon Formation by approximately 5,000 ft. Displacement on

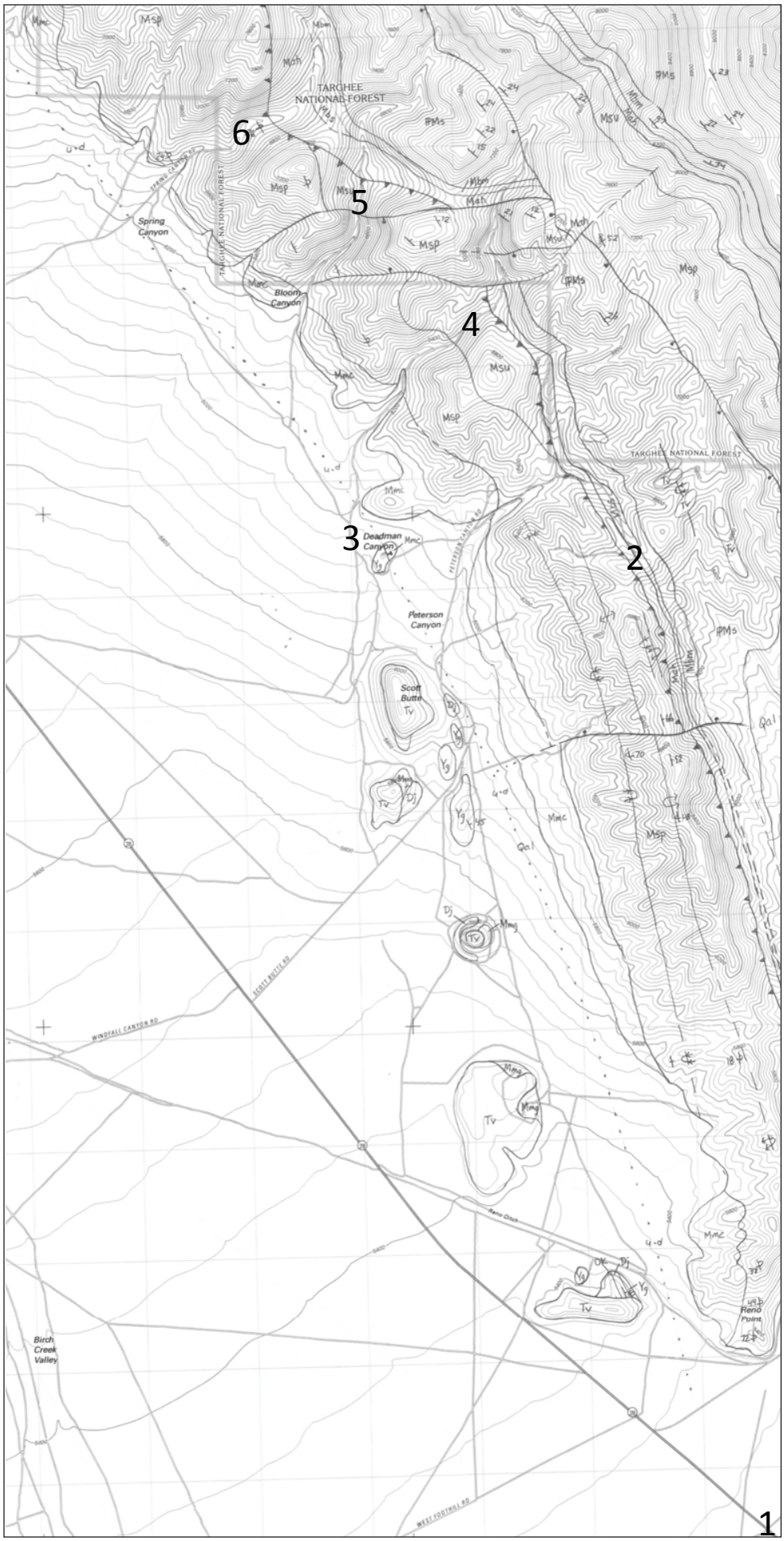

Figure 1. Preliminary geologic map of the Beaverhead Mountains portion of the Scott Butte, Idaho 7.5-minute quadrangle showing localities visited during the field trip.

Table 1. Description of stratigraphic units found in the southern Beaverhead Mountain Range, including ages and map symbols.

Description of Stratigraphic Units				
Age	**Symbol**	**Formation**	**Member**	**Description**
Permian	IPsj	Snaky Canyon Fm	Juniper Gulch Mbr	Crinoidal grainstones, packstones, and wackstones interbedded with calcareous siltstones and sandstones (quartz wackes) in the lower part, grading upward to thicker bedded wackstone and carbonate mudstone with scattered oolitic grainstones in the middle, then thinner-bedded cherty, nonfossiliferous dolostones in the upper part. Overall, chert content increases and fossil content decreases upward. Forms alternating ledges and slopes. Thickness is about 1600 feet.
Pennsylvanian	IPsg		Gallager Peak Mbr	Tan to light brown or light reddish-brown, thinly bedded calcareous siltstones and very fine- to medium-grained calcareous quartz wackes that can be ripple bedded or contain horizontal to trough cross-bedding. Sandstones and siltstones are interbedded with medium-bedded crinoidal packstones. Forms silty/sandy slopes with small limestone ledges. Approximately 150 feet in thickness.
	IPsb		Bloom Mbr	Light to dark gray, cherty, crinoidal grainstone, packstone, wackstone, and carbonate mudstone interbedded with calcareous siltstone and, near the base, tan silty sandstone (quartz arenite to wacke). Horn corals are common in the upper part of the member. One of the more diagnostic features is a concentrically-banded chert that can mimic the structure of stromatolites. Thickness is around 900 feet. Interbedded lower contact with the Bluebird Mountain Formation. Forms alternating limestone and sandstone ledges separated by silty slopes.
	IPMb	Bluebird Mountain Fm		Orangish-tan, fine-grained quartz arenite and interbedded carbonate mudstones. Medium-bedded with occasional low-angle trough cross-bedding. Sometimes partly altered to a light gray or tan quartzite. Thickness is approximately 30 feet. The lower contact appears to be interbedded with the Arco Hills Formation. Expressed primarily as a fragment-covered slope but can form discontinuous but prominent outcrops.
Mississippian	Mbs	Big Snowy Fm		The Big Snowy Formation is a black to dark-green, fissile, clay-rich, laminated shale to slate that occurs mostly in hill-top saddles and slopes. Brachiopods are found in some outcrops. It is often located along thrust faults and associated with large landslides. The Big Snowy Formation interfingers with the Arco Hills Formation and ranges from 0 to around 50 feet in thickness.
	Mah	Arco Hills Fm		The Arco Hills Formation is a gray-brown shaly carbonate mudstone with interbedded black chert. It appears to interfinger with the Big Snowy Formation. Thickness ranges from 0 to about 100 feet. The Arco Hills Formation weathers to a slope and can closely resemble the South Creek Formation.
	Msu	Surrett Canyon Fm		Medium-gray, fossiliferous carbonate mudstone to grainstone containing abundant horn corals and crinoid fragments. Dark gray chert occurs in nodules and partially replaces limestone beds. Thickness is approximately 300 feet. Nearly always forms a prominent cliff and has a gradational lower contact. The Surrett Canyon Formation can closely resemble the middle member of the Scott Peak Formation.
	Msc	South Creek Fm		Medium-gray, nonfossiliferous carbonate mudstone interbedded with thin beds of tan to orange chert. Chert is slightly calcareous in places, possibly due to incomplete replacement. Thickness is approximately 350 feet and it gradationally overlies the Scott Peak Formation. Weathers mostly to a slope but can form significant ledge outcrops. The South Creek Formation can closely resemble the Arco Hills Formation, particularly on weathered slopes.
	Msp	Scott Peak Fm	General	The Scott Peak Formation was defined in the southern Lemhi Mountain Range, where it was separated into three informal members on the basis of geomorphic expression. While that expression is evident in the southern Beaverhead Mountain Range, it is less distinct, and each of the three members can resemble one another due to lateral facies changes and relative abundances of limestone to siltstone. Total thickness of the three members is around 4,000 feet, with individual member thickness varying, depending on local expression. The contact with the underlying Middle Canyon Formation is interbedded and is typically placed at the first occurrence of a highly-fossiliferous limestone (grainstone or packstone).
	Mspu		Upper	Interbedded medium to dark gray bioclastic grainstone, packstone, wackstone, and mudstone and brownish to gray siltstone in medium to thick bed sets. Locally, limestones can be cherty. Distinguished from the lower member primarily by a smaller abundance of siltstone beds and greater number of beds rich in chert. In areas where siltstones are lacking, the upper member can resemble the middle member. Weathers mostly to thin, alternating slopes and ledges.
	Mspm		Middle	Mostly gray bioclastic grainstone with lesser boundstone and interbedded packstones, wackstones, and siltstones. Bioclasts consist primarily of crinoid columnals with some horizons rich in horn corals, bryozoa, brachiopods, and/or cephelopods. Weathers primarily to a thick cliff with small reentrants but can resemble the lower or upper members where shaly intervals are better developed.
	Mspl		Lower	Interbedded medium to dark gray bioclastic grainstone, packstone, wackstone, and mudstone and brownish to gray siltstone in medium to thick bed sets. Locally, limestones can be cherty. Distinguished from the upper member primarily by a greater abundance of siltstone beds and smaller number of beds rich in chert. In areas where siltstones are lacking, the lower member can resemble the middle member. Weathers mostly to thin, alternating slopes and ledges.
	Mmc	Middle Canyon Mbr		Medium to very dark gray carbonate mudstone containing chert interbeds and nodules. Thickness is approximately 500 feet, and the lower contact is gradational with the McGowan Creek Formation. Weathers to alternating slopes of brownish soil with black chert fragments and thin limestone
	Mmg	McGowan Creek Fm		Thinly-bedded, structureless, light to dark gray calcareous shale and silty limestone that weather to mostly slopes with a probable gradational lower contact. Thickness is around 300 feet.
	Mmn	Milligan Fm		Silvery-gray to black platy mudstone (now phyllite) highly altered by hydrothermal processes. Can show internal deformation in the form of chevron folds. Forms a slope that is often covered by small, angular phyllite fragments Appears to have a sharp lower contact. Approximately 400 feet thick.
	MDt	Three Forks Fm		Medium to dark gray bioclastic grainstone, packstone, and wackstone. Contains abundant crinoids and other fossil fragments. Has a sharp lower contact and weathers to a slope with a distinct ledge about 5 feet thick. Thickness is approximately 30 feet.
Devonian	Dj	Jefferson Fm		Medium to dark gray or yellowish-brown, medium-grained, thin-bedded dolostone. Unconformably overlies the Belt Supergroup or Kinnikinik Quartzite. Weathers primarily to a slope with occasional small ledges. Ranges from 0 to around 40 feet in thickness.
Ordovician	Ok	Kinnikinik Qt		White to tan, medium- to coarse-grained quartz arenite sandstone (now quartzite) with occasional indistinct horizontal laminations and trough cross-bedding. It is often hydrothermally altered and forms thin ledges that overly the Belt Supergroup by an angular unconformity. Ranges in thickness from 0 to around 30 feet.
Proterozoic	Y	???		Orangish-pink to purplish-brown, medium- to course-grained, trough cross-bedded sandstone (feldspathic arenite) in bed sets that fine upward with scattered white quartzite pebbles near the base. Sandstone beds are locally separated by up to a few inches of laterally discontinuous intervals of greenish-gray mudstone (now slate). Weathers to fractured ledges. As the lower contact is not exposed, thickness is unknown but is in excess of a thousand feet. May correlate to the Wilbert (Skip & Link, 1992), Swauger (Abplanalp et al. 2008), or Gunsight (Little & Little, 2009) Formation of the Lemhi Mountain Range.

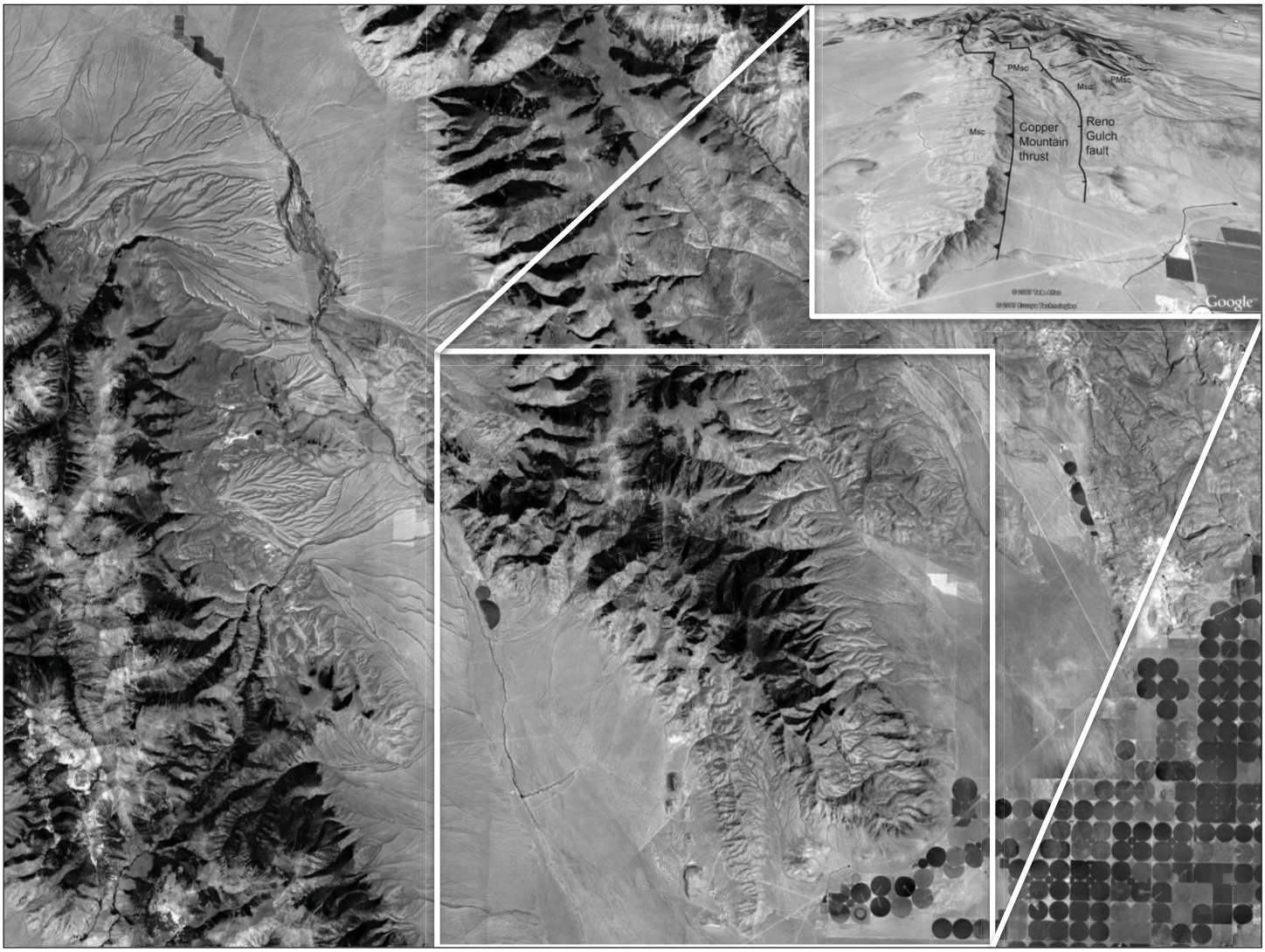

Figure 2. Google Earth images showing the horst nature of the Beaverhead Mountains block, with an inset showing location of the Copper Mountain Thrust and Reno Gulch faults discussed at localities 2 through 6.

the Reno Gulch Fault decreases over a relatively short distance northward to zero near Copper Mountain.

STOP 2

Petersen Canyon (stratigraphic and structural overviews)

Several brief stops will be made in Petersen Canyon to become familiar with stratigraphic units, including exposures of Proterozoic sandstone and the Milligen, McGowan Creek, Middle Canyon, Scott Peak, Arco Hills, Big Snowy, and Bluebird Mountain Formations. The Kinnikinik Quartzite, Jefferson Formation, and Three Forks Formation are not present in Petersen Canyon, presumably because of nondeposition over an early Paleozoic topographic high, as each of these units progressively overlies the Proterozoic sandstone and thickens to the north.

From the hilltop saddle, both the Copper Mountain and Reno Gulch faults are clearly visible (fig. 3). To the east, the Reno Gulch Fault is expressed as a steep cliff composed primarily of the Scott Peak Formation but capped by the Bloom Member of the Snaky Canyon Formation. At the base of the cliff, on the downthrown block, are nearly vertical beds of the Snaky Canyon Formation, most likely the Bloom Member. Immediately to the west, a less distinct ridge is composed of Scott Peak limestones, but the topographic expression is very different from that of the eastern cliff.

During the first year we had students mapping the area, our initial interpretation was that a second normal fault was present, in this case down to the east. This would provide a simple explanation to topographically low exposures of Pennsylvanian Snaky Canyon Formation between two topographically high

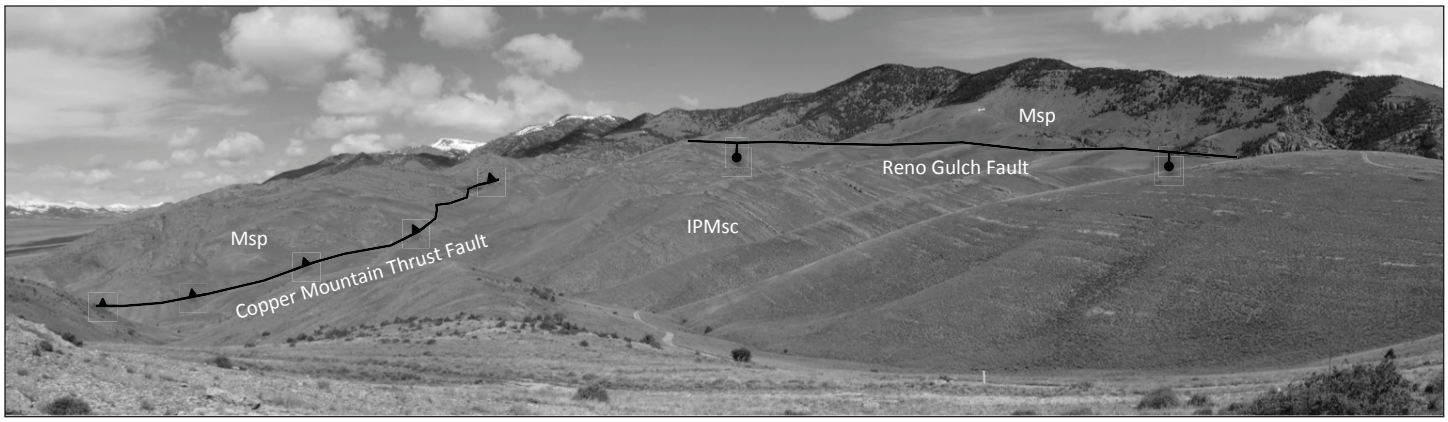

Figure 3. Structural relationships looking north from the saddle at the head of Petersen Canyon.

outcrops of Mississippian Scott Peak Formation, as a simple graben between two horsts. However, continued mapping the next season eliminated that hypothesis, as the structure could not be carried to the north. The reason now is quite clear. To the north, it is evident that the Scott Peak and underlying units are highly folded, whereas those of the Snaky Canyon Formation are nearly vertical but otherwise show little deformation. The contact between the Scott Peak and Snaky Canyon Formations makes a marked V pattern dipping to the west. Additionally, along the canyon floor, the Scott Peak Formation is in structural contact with the Arco Hills Formation, cutting out the South Creek and Surrett Canyon Formations. A similar relationship is present on this saddle, as we can walk across vertical beds of the Bluebird Mountain and Big Snowy formations into the Scott Peak Formation. Our revised interpretation is that this structure is a thrust fault (Copper Mountain Thrust) dipping to the west, in which the upper plate is highly deformed, and the lower plate is tilted but less deformed, a pattern that persists the entire length of the fault and that is also present in fault propagation folds.

STOP 3

Road between Petersen and Deadman Canyons (large-scale overturned fold)

A large-scale overturned fold that, within some canyons, appears to be nearly recumbent (fig. 4), is mapped from at least the mouth of Petersen Canyon to the mouth of Long Canyon. The general expression, scale, and extent of this fold can be observed as we drive along a mountain front dirt road. We will make one brief stop for discussion and photographs.

STOP 4

Deadman Canyon (drive through the fold)

Deadman Canyon provides an opportunity to drive along the axis of the overturned fold (fig. 5) and see difficulties associated with proper identification of stratigraphic units. On the geologic map (fig. 1), there is a distinctive west-trending horst bound by two normal faults that cut across the Copper Mountain Thrust Fault. This interpretation is based on the entire horst

Figure 4. Recumbent fold that forms the mountain front from Deadman Canyon at the south end (right side of photo) to Long Canyon in the north (left side of photo).

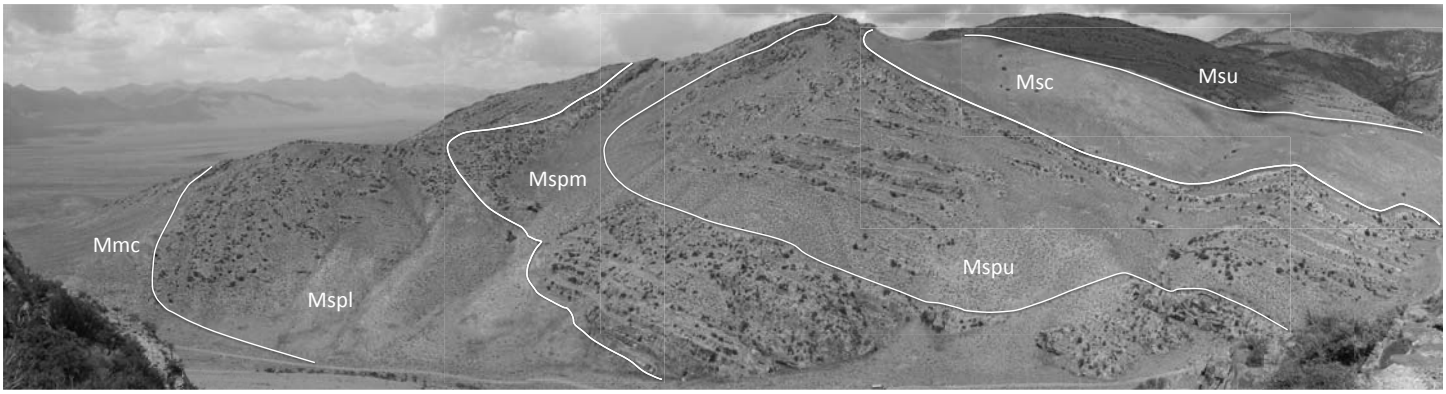

Figure 5. Recumbent fold as expressed along the north wall of Deadman Canyon.

being composed of Scott Peak Formation limestones at the surface. However, a recent visit to the canyon has suggested that limestones at the eastern end of the block might actually be the Surrett Canyon Formation, forming a normal stratigraphic succession that would either eliminate or move the fault boundaries. This relationship needs further analysis before making a final determination. In part, this conflict reflects a change in our understanding of area stratigraphy as our mapping has progressed from south to north and we have become better acquainted with stratigraphic units. We are now revisiting earlier mapped southern localities and making reassessments based on this improved stratigraphic understanding before producing a final geologic map. Other west-trending faults are present along the mountain front and are thought to be the result of passage of the region over the Yellowstone hotspot during latest Miocene.

STOP 5

Bloom Canyon

Bloom Canyon provides the next opportunity to visibly trace the Copper Mountain Thrust and Reno Gulch faults.

STOP 6

Spring Canyon (cross-sectional view of the Copper Mountain Thrust Fault)

The head of Spring Canyon is near the point at which the Reno Gulch Fault terminates to the north and provides the northernmost easily accessible view of the Copper Mountain Thrust Fault before the fault cuts through the range to the eastern side near the base of Copper Mountain. In the distance, a ridge-top saddle between Bare Canyon and Long Canyon exposes an excellent cross section of the Copper Mountain Thrust Fault (fig. 6A). As at previous localities, the upper plate consists of intensely deformed Upper Scott Peak and South Creek Formations (figs. 6B and C), which, once again, override the Arco Hills/Big Snowy interval. Stratigraphic units in the lower plate dip to the west, away from the fault, and flatten away from the fault to the east. This ridge represents the most clear and dramatic exposure of the Copper Mountain Thrust Fault. Figure 6D shows the same locality but viewed from the north.

Unvisited Localities (Fault Propagation Fold)

A well-developed fault propagation fold, and several smaller such folds, occur in the highly deformed upper plate of the Copper Mountain Thrust Fault to the west of and structurally above the persistent large-scale overturned fold. It first appears near the mouth of Spring Canyon (fig. 7A) and becomes well exposed between Long and Skull Canyons (figs. 7B and 7C) to the north of the field trip area on the Copper Mountain and Blue Dome, Idaho quadrangles. Because of constraints of time and outcrop accessibility, these features will not be visited as part of this trip; however, as they represent a significant part of the compressional-tectonic story, we feel it important to bring them to light and include a few pertinent photographs.

SUMMARY

Compressional and extensional tectonic features formed during the Sevier, and Basin and Range, tectonic events, respectively, are well exposed in a highly deformed Proterozoic through Paleozoic stratigraphic succession along the western margin of the southern Beaverhead Mountain Range. Dominant compressional structures include the Copper Mountain Thrust Fault, in which the upper plate is highly deformed resulting from overturned and fault-propagated

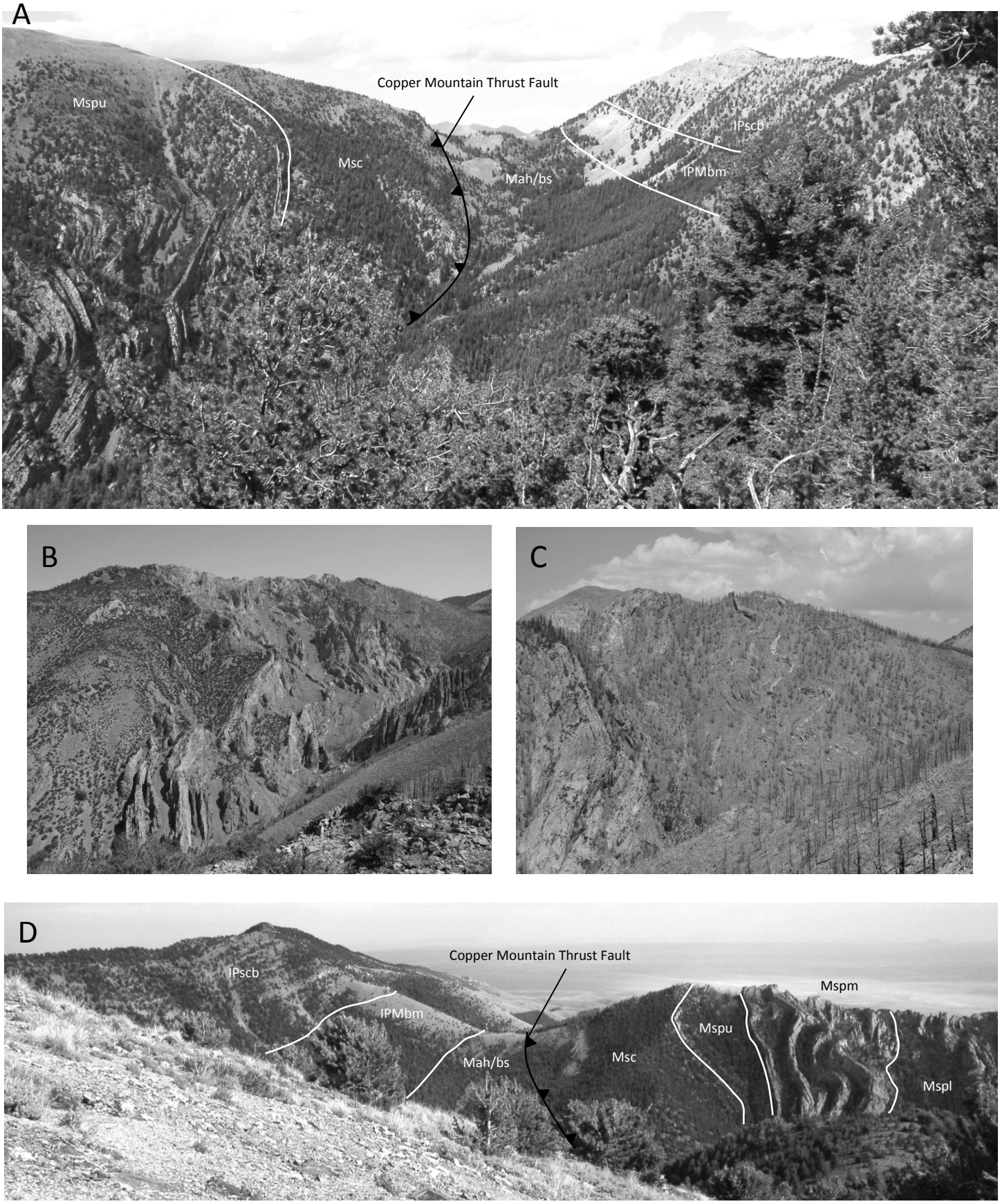

Figure 6. Copper Mountain Thrust Fault as seen from the south in the saddle between Bare and Long Canyons. Extensive upper plate deformation in the middle and upper Scott Peak Formation is shown in figures 6B and 6C, respectively, which were taken immediately to the west of 6A. Figure 6D shows the same relationship from the north.

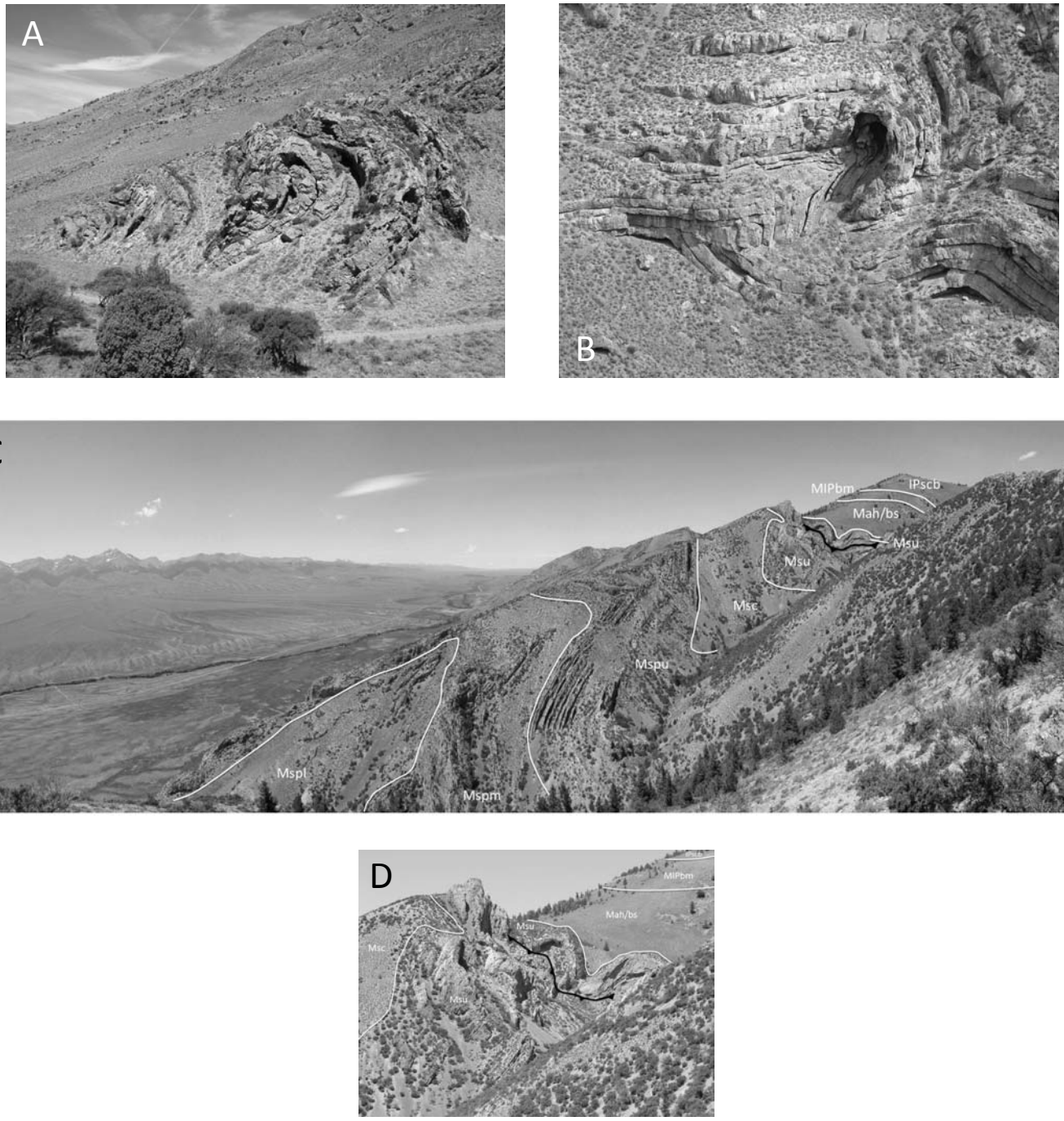

Figure 7. Fault propagation folds. Figure 7A was taken a short distance inside the mouth of Spring Canyon and is possibly the southernmost exposure of these features. Figure 7B shows a small fault propagation fold within Goddard Canyon, the next canyon north of Long Canyon, and is one of several such folds within that canyon. Figure 7C represents a completely exhumed, well-developed fault propagation fold in an unnamed small canyon just north of Goddard Canyon that continues northward to Skull Canyon, where it appears to pass away from the mountain front and into the valley, where it is cut off by the range-front fault. Displacement along the fault at the core of this fold is probably just a few feet, as intensely folded limestones of the Surrett Canyon Formation on the west (upper plate) are juxtaposed against nearly undeformed Surrett Canyon Formation limestones on the eastern side (lower plate), in similar fashion to the Copper Mountain Thrust Fault. Figure 7D is an enlargement of the upper part of the structure in 7C.

folding, and the lower plate is relatively undeformed, demonstrating only a simple flattening of dip away from the fault. The primary extensional structure is the Reno Gulch Fault, which shows a significant amount of displacement at the southern end of the range but terminates northward. These features are easily viewed and traced through several canyons that dissect the mountain range. Work remains to resolve discrepancies in the current map interpretation of this complex region.

ACKNOWLEDGMENTS

We are grateful to Glenn F. Embree for introducing us to the Beaverhead Mountain Range in the early 2000s and for sharing his prior mapping expertise in this area. Well over 100 undergraduate students and their TAs have participated in mapping exercises since 2005 as part of the BYU–Idaho Advanced Field Methods course, better known as "field camp," providing the basic data for the current map compilation. A few students, including Stefanie Roemer, M. Evan Bagley, and Daniel W. Little, performed early compilations of their respective field camp groups as senior research projects. These were subsequently presented at professional meetings and have been referenced in this report. Mark D. Lovell stepped in during years that one or the other of us could not participate, and Blake Rothlisberger assisted in preparation of figures. The work could not have been conducted without time and funding provided by Brigham Young University–Idaho.

REFERENCES CITED

Abplanalp, J.M., Pink, C., Pope, M.C., and Watkinson, J.A., 2008, Geologic map of the southern Beaverhead range (parts of Copper Mountain, Shamrock Gulch, Scott Butte, and Snaky Canyon quadrangles), Clark, Jefferson, and Lemhi Counties, east-central Idaho: Idaho Geological Survey Technical Report T-08-1.

Bagley, M.E., and Little, W.W., 2009, Preliminary bedrock geologic map of a portion of the Copper Mountain, ID 7.5- minute quadrangle, Beaverhead Mountains, Clark County, Idaho: Abstracts with Programs, Rocky Mountain Section Meeting of the Geological Society of America, Orem, UT, v. 41, no. 6, p. 50.

Batt, L.S., Pope, M.C., Isaacson, P.E., Montañez, I., and Abplanalp, J., 2007, Upper Mississippian Antler foreland basin carbonate and siliciclastic rocks, east-central Idaho and southwestern Montana, U.S.A.: Distinguishing tectonic and eustatic controls on deposition, *in* Lukasik, J., and Simo, J.A., eds., Controls on carbonate platform and reef development: SEPM Special Publication No. 89, p. 147–170.

Billman, G.S., and Little, W.W., 2007, Correlation of Mississippian and Pennsylvanian strata in the southern Beaverhead Mountain Range, Idaho: Rocky Mountain Section Meeting of the American Association of Petroleum Geologists, Snowbird, Utah.

Clayton, R.W., and Little, W.W., 2009, New interpretations of Sevier thrust belt structures, southern Beaverhead Mountains, Idaho: Abstracts with Programs, Annual Meeting of the Geological Society of America, Portland, Ore., v. 41, no. 7, p. 294.

Clayton, R.W., and Little, W.W., 2014, Geologic mapping in the southern Beaverhead Mountains, eastern Idaho (west side): New structural interpretations: Abstracts with Programs, Rocky Mountain and Cordilleran Sections Joint Meeting of the Geological Society of America, Bozeman, MT, v. 46, no. 5, p. 91.

Embree, G.F., in review, Bedrock geologic map of the Copper Mountain quadrangle: Idaho Geological Survey.

Isaacson, P.E., Grader, G.C., Pope, M.C., Montañez, I.P., Butts, S.H., Batt, L.S., and Abplanalp, J.M., 2007, Devonian-Mississippian Antler foreland basin carbonates in Idaho: Significant subsidence and eustasy events: The Mountain Geologist, v. 44, no. 3, p. 119–140.

Little, D.W., and Little, W.W., 2009, Identification and correlation of Precambrian fluvial units in the southern Beaverhead Mountain Range, Idaho: Abstracts with Programs—Geological Society of America, v. 41, issue 6, 49 p.

Little, D.W., Little, W.W., Lovell, M., and Clayton, R.W., 2010, Newly identified compressional structures along the western margin of the southern Beaverhead Mountain Range, Idaho: Abstracts with Programs, Annual Meeting of the Geological Society of America, Denver, CO, v. 22, no. 5, p. 266.

Roemer, S., Little, W.W., and Clayton, R.W., 2007, Complex deformation of Paleozoic strata due to folding and faulting in the southern Beaverhead Mountains, Clark County, Idaho: Rocky Mountain Section Meeting of the American Association of Petroleum Geologists, Snowbird, Utah.

Sandberg, C.A., 1975, McGowan Creek Formation, New name for Lower Mississippian flysch sequence in east-central Idaho: U.S. Geological Survey Bulletin 1405-E, 16 p.

Skipp, B., 1985, Contraction and extension faults in the southern Beaverhead Mountains, Idaho and Montana: U.S. Geological Survey Open File Report 85-545, 170 p.

Skipp, B., Hoggan, R.D., Schleicher, D.L., and Douglass, R.C., 1979, Upper Paleozoic carbonate bank in east-central Idaho—Snaky Canyon, Bluebird Mountain, and Arco Hills Formations, and their Paleotectonic Significance: U.S. Geological Survey Bulletin 1486, 82 p.

Skipp, B. and Link, P.K., 1992, Middle and Late Proterozoic rocks and Late Proterozoic tectonics in the southern Beaverhead Mountains, Idaho and Montana: A preliminary report, *in* Link, P.K., Kuntz, M.A., and Platt, L.B. (eds.): Regional Geology of Eastern Idaho and Western Wyoming, Geological Society of America Memoir 179, p. 141–154.

Wardlaw, B.R., and Pecora, W.C., 1985, New Mississippian-Pennsylvanian stratigraphic units in southwest Montana and adjacent Idaho, *in* Sando, W.J. (ed.), Mississippian and Pennsylvanian stratigraphy in southwest Montana and adjacent Idaho: U.S. Geological Survey Bulletin 1656, p. B1–B9.

LITHOLOGIC AND STRUCTURAL CONTROLS OF MINERAL DEPOSITS IN THE HORSE PRAIRIE BASIN, BEAVERHEAD COUNTY, MONTANA, WITH NOTES ON HORSE PRAIRIE HISTORY

Elizabeth Brenner-Younggren[1] and Bruce E. Cox[2]

[1]Geologist and Snowbird, Horse Prairie, Montana and Boulder City, Nevada
[2]Geologist and Snowbird, Missoula, Montana and Truth or Consequences, New Mexico

ABSTRACT

The oldest mining activity in Horse Prairie dates back 11,000 years when Native American people first developed stone tool quarries in silicified Tertiary sediments. The first prospecting and mining developments for gold and other metals were initiated by homesteaders in the 1860s. Modern gold exploration was most intense in the 1980s and 1990s, concurrent with renewed placer gold production. Geologic mapping since 1980 indicates that gold, base metals, +/- uranium mineralization in Horse Prairie are controlled by a Tertiary structural fabric.

ACKNOWLEDGMENTS

Stops 2 and 5 are on private land; the authors gratefully acknowledge permission granted by the Bar TT Ranch and the White and Kajin families to visit the mines on their properties. Future entry must first be secured from the landowners. Thanks also to Jo-Ann Sherwin for her contribution to mapping at the Monument Mine and to Tony Van der Poel and Bill Neal for contributing exploration data on Chinatown and Pete Ellsworth for help with the figures.

HORSE PRAIRIE HISTORY

Horse Prairie, until modern times, was a major east–west route for Native Americans, trappers, and prospectors. Native Americans living in Idaho traveled through Horse Prairie to hunt bison, which did not occur west of the Continental Divide. Sacajawea led Lewis and Clark through the valley in 1805. Their route was later followed by fur trappers. In the mid-1900s, George Shoup found an old aspen inscribed with the words "Josh Jones 1810." Shoup learned (from pictographs) that Josh Jones was a trapper for the Hudson Bay Company and was in Horse Prairie with a small party of Indians.

During the 1860s, Lemhi Pass was the main route between the gold fields around Salmon, Idaho, and Bannack and Virginia City, Montana. In 1884, the Red Rock Stage line was established. It ran from Salmon, Idaho, to Red Rock, Montana, where it connected with the Union Pacific Railroad. Heavier freight was routed over Bannock Pass; Lemhi Pass was too steep for freight wagons. Then, in 1906, the Gilmore and Pittsburg Railroad (aka the "Get Out and Push Railroad") was built between Armstead, Montana, and Salmon, Idaho. The builders kept the total rail bed length under 100 mi and its stations a mile or so outside of town, conforming to interstate commerce restrictions. The G & P Railroad was dismantled in 1939 and Montana Highway 324 was built on much of the old railroad bed.

The first European settlers in the valley came during the gold rush to Bannack. They settled and supplied meat and dairy products to the miners. In 1877, Chief Joseph and the Nez Perce came through Horse Prairie after the Battle of the Big Hole. The settlers had plenty of warning. Women and children were taken to Bannack. All might have been fine, but when the Indians stopped to get fresh horses and bandages, legend has it that the ranch cook panicked and started shooting. The battle was on. Four people were killed, including Montegue, one of the ranch owners. The Nez Perce moved on to cross Bannock Pass, but one miner was killed in Jeff Davis Gulch on their way. He was buried in his sluice box. No serious problems with Indians in the area happened after that. Ranches continued to raise dairy cattle, horses, and beef for miners, and still do to this day.

The oldest mining activity in Horse Prairie dates to 11,000 years BP when Native American people developed stone tool quarries in silicified Tertiary sediments along Everson Creek. Tools and weapons made of material from these sites have been found in Alberta, Canada (Bonnichsen, 1988). Prospecting and mining developments for gold and other metals started in the

1860s. Modern gold exploration was most intense in the 1980s and 1990s concurrent with renewed placer gold production. Geologic mapping since 1980 indicates that gold, base metals, and uranium mineralization in Horse Prairie are controlled by a Tertiary structural fabric.

FIELD GUIDE/ROAD LOG

The field trip will follow a counter-clockwise loop traverse (fig. 1) starting in Paleozoic rocks of the Leadore mining district, Idaho and ending in Tertiary volcanic strata at the western margin of Horse Prairie, Montana. 4WD vehicles are needed when leaving the highway to visit Stops 2 and 7.

Miles traveled:

0.0 Leadore. Junction Idaho Highway 28 with Idaho Highway 29 (44.680686°N / 113.358147°W). Set odometer to 0.0 and drive eastward toward Railroad Canyon.

3.0 Mine workings visible along the range front at 9 o'clock are part of the Leadville (Junction) mining district which produced silver–lead ore from 1907 to 1954. Mineralization occurs in breccias and shear veins contained within a Tertiary granitic sill (?), which parallels the range front fault zone (Mitchell, 2004 and Cox and Antonioli, this volume). Isolated resistant outcrops on either side of the canyon mouth are augen-like masses enveloped by the range front fault gouge.

4.0 From the mouth of Railroad Canyon to Cruikshank Road, outcrops and roadcuts expose thrust slices of Paleozoic strata.

8.0 Cruikshank Road #130 enters from the right. Continue on Highway 29. Leaving Paleozoic strata and entering subdued topography underlain by Oligocene and Miocene sediments, which are rich in terrestrial fossils. The bed of the G&P Railroad parallels the right side of the highway; some old ties are still in place.

13.5 STOP 1

Bannock Pass (44.814253°N / 113.272236°W).

Overview of Horse Prairie and surrounding Beaverhead and Medicine Lodge Ranges. From here northward, most stretches of the highway (now Montana Highway 324) follow the rail bed of the old G & P Railroad. The railroad tunnel beneath the pass was excavated through Miocene sediments. Take 10 minutes to examine the sandy sediments exposed 100 ft east of the pass. Hills farther east are underlain by unconsolidated gravel: >95% white, green or purple fine-grained quartzite; 2–4% porphyritic volcanics, and a trace of vesicular basalt.

20.26 Junction, Jeff Davis Creek Road 946 (44.901603°N / 113.269661°W). Turn eastward on gravel road and set odometer to 0.0.

0.53 Stay straight (next two roads to the right access the Donovan Ranch).

3.22 Road fork. Bear left, uphill eastward.

3.92 Stay straight at intersection. Road left (uphill) leads to the H & S Mine, which produced silver–lead oxide ore hosted by metamorphic rocks in a clippe or range-front-parallel horst (Geach, 1972).

4.35 Road intersecting from north; stay straight.

4.53 Cross middle fork of Jeff Davis Creek (for this area, see fig. 2 map).

4.40 Cross through gate in fence line.

4.85 Turn right (S), uphill.

4.95 Turn right (W), road curves toward trees on bench.

5.20 STOP 2a

Early ground sluice placer workings (44.881431°N / 113.1784°W).

The cobble and boulder tailing here (fig. 3) appears to be nearly all Archean metamorphic rocks; quartz–feldspar–biotite gneiss, amphibolite, and quartzite. Scattered angular fragments of rhyolite indicate Tertiary volcanic bedrock was the floor of the ground-sluiced area.

5.4 STOP 2b

Jeff Davis Gulch and Chinatown overview (fig. 2 map and fig. 4 photo) (44.881494°N / 113.185675°W)

Placer workings northward from this viewpoint are centered in a rhyolitic flow dome-caldera measuring 1.5 mi east–west, bounded on the east by Archean

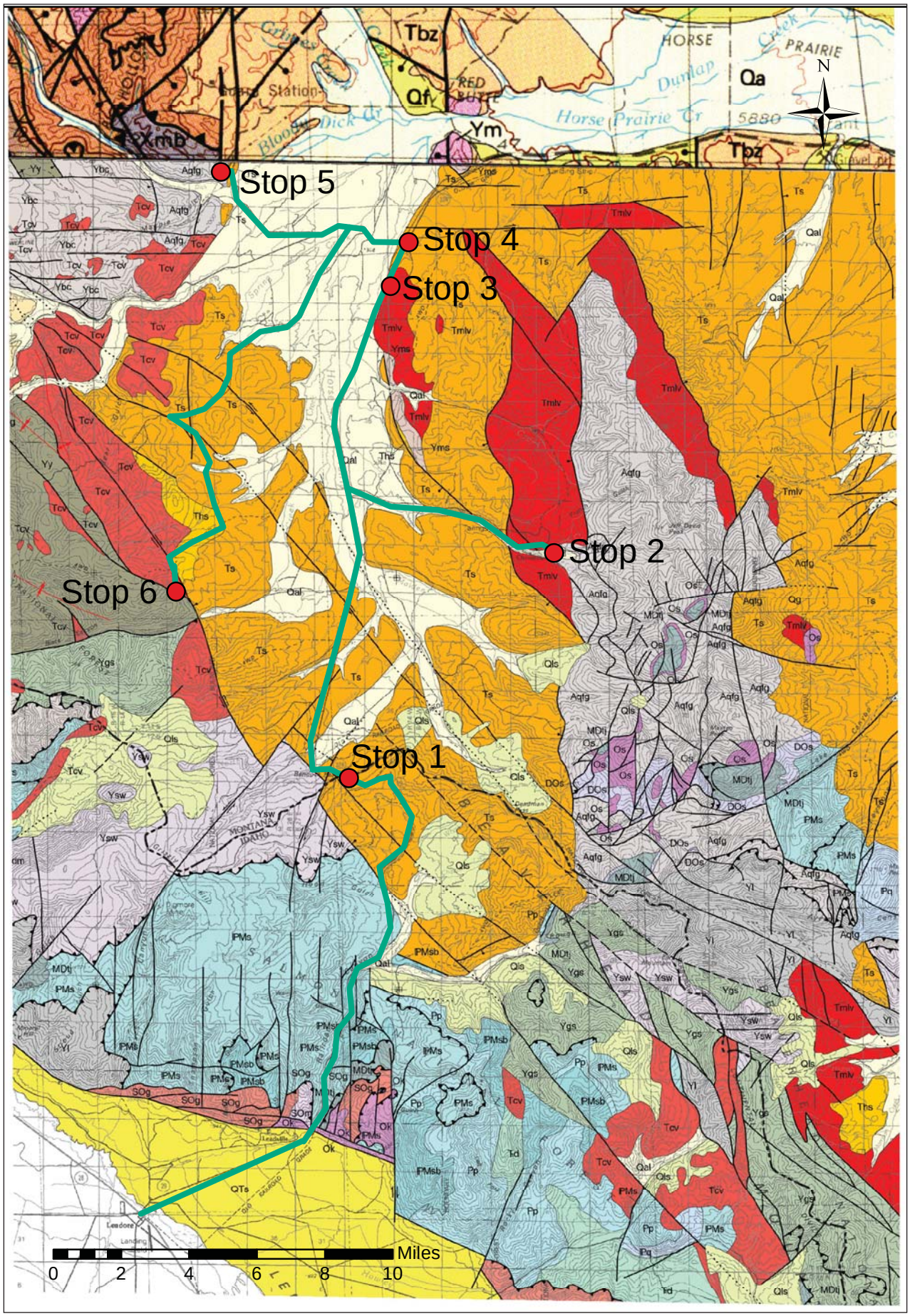

Figure 1. Geologic map of Horse Prairie Basin showing field trip route and stops. Modified from the Leadore (1:100,000-scale) and Dillon (1:250,000-scale) geologic maps, Ruppel (1998), and Ruppel and others (1993), respectively.

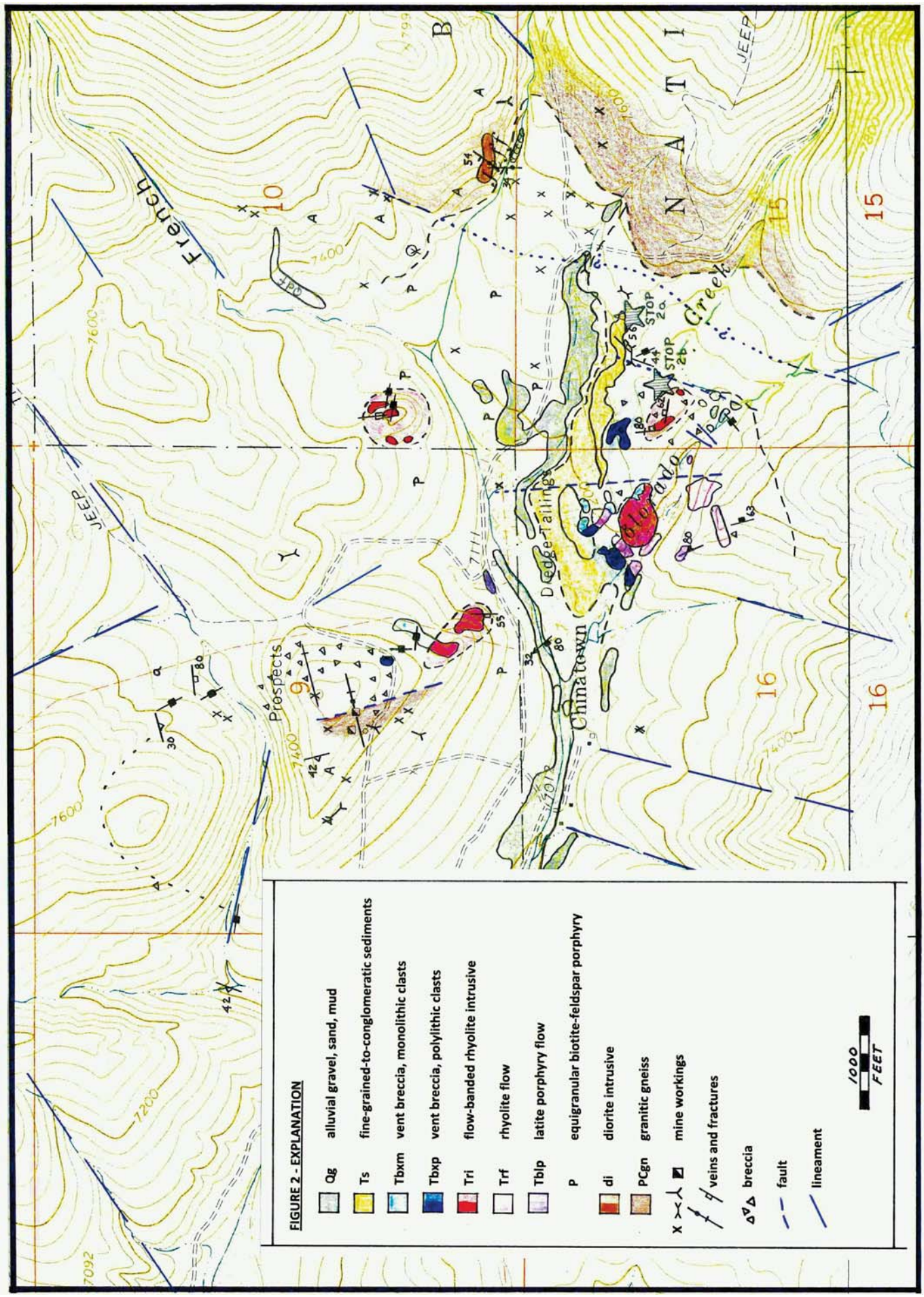

Figure 2. Geologic map of the Chinatown area, Jeff Davis Creek, Beaverhead County, Montana. Map modified from mapping of J. Pearson and J. Jones (1991) for Battle Mountain Exploration Company with additions from mapping of B. Cox (1990) for Earthworks, Inc., both unpublished intracompany reports.

Figure 3. Cobble and boulder tailings in ground sluiced area at Stop 2a.

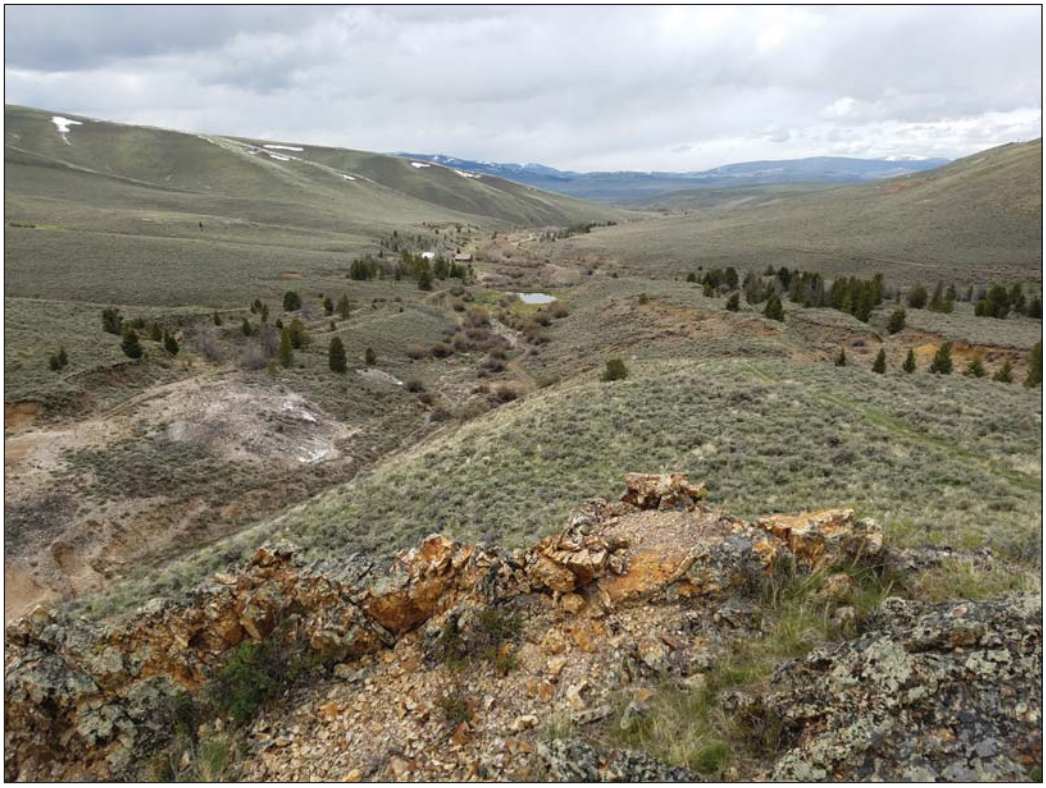

Figure 4. Chinatown gold placer workings, view west. Rhyolite outcrops in foreground.

rocks across a north-trending range front normal fault. The caldera contains a variety of felsic volcanic rocks (fig. 5) including: conglomeratic sediments, rhyolite flows and intrusives, vent breccia, and equigranular biotite–feldspar porphyry. Fracture sets within the caldera are predominately high-angle NNW and WNW. Topographic linears within and surrounding the caldera suggest a radial and concentric fracture pattern.

The bedrock source of the placer gold has been widely debated and was the focus of several exploration programs in the 1980s and 1990s, including work by: Hecla Mining Company, Western Energy Company, Battle Mountain Exploration Company, and self-financed trenching and drilling by Liz Brenner-Younggren. No mineable bedrock gold deposit has yet been defined. Small-scale gold placer mining continues to this day.

Return to the junction of Jeff Davis Creek Road 946 and Highway 324 and reset mileage to 0.0.

0.00 Follow paved Highway 324 northward toward Dillon.

4.63 **STOP 3**

Uranium prospect (reportedly) in Tertiary volcanics (44.965653°N / 113.253203°W).

Pull onto highway shoulder, walk up spur road 100 yd to southeast. The quarry face exposes felsic tuff grading NE to purple intermediate composition lahar/breccia (fig. 6). The prevalent trend of FeOx veins and altered tuff is 310°/80°NE. Check exposures for radioactivity.

5.48 **STOP 4**

Shoshone Ridge Overlook/Interpretive Site and rest stop, i.e., LUNCH (44.977506°N / 113.241631°W).

Geologic discussion: Mesozoic compression and extension, gravity slide/décollement blocks in the Horse Prairie basin. History discussion: Native Ameri-

Figure 5. Rhyolitic lithologies, alterations, and textures at Stop 2b.

Figure 6. Volcanic lithologies, alteration, and textures at Stop 3.

can presence, early prospecting and ranching, and the mystery of the Montague and Winters ditch.

Return to Highway 324, reset mileage to 0.0, and cross highway westward onto County Road 181.

0.00 Follow gravel road westward.

0.16 Cross former route of Highway 324.

0.24 Cross trace of Montague and Winters ditch. The M & W ditch was built prior to the formal survey of Horse Prairie in 1878. Early legal descriptions of the ditch suggest it was designed to convey water to the placer gold mines of "Winters Bar." Today, no one seems to have a clue about the location of Winters Bar, but maybe it is still out there waiting to be (re)found —and rich in gold beyond your wildest dreams!

0.36 Cross Horse Prairie Creek.

0.67 Quaternary alluvial gravels in pit (left) commonly yield 2–3 gold flakes per pan.

0.88 Base of Everson Creek Road 1882. Continue straight; return to this junction after visiting STOP 5.

2.13 Y intersection; make dogleg turn right and follow Brenner Lane westward (do not follow main road that goes SW toward Lemhi Pass).

3.21 Bar TT Middle Ranch, formerly the Lazy E4 Cattle Company and Brenner family homestead.

4.35 Steinbrecher Ranch.

4.49 Cross Bloody Dick Creek.

4.69 Roadcut exposes popcorn weathering typical of bentonitic alteration of tuffs.

4.84 4-way intersection, Kajin/James Ranch on right; bear left around curve onto Bloody Dick Road.

5.19 STOP 5

Geology of the Monument Mine; park off road to the left (44.996783°N / 113.321392°W).

A short walking traverse uphill from the Bloody Dick Road begins in Tertiary sedimentary rocks and crosses into Archean metamorphic rock across a NNW-trending fault with synthetic orientation relative to the Monument fault (see Lonn and Elliot, this volume). A W–NW line of bold siliceous breccia outcrops defines the dominant trend of mineralization (fig. 7).

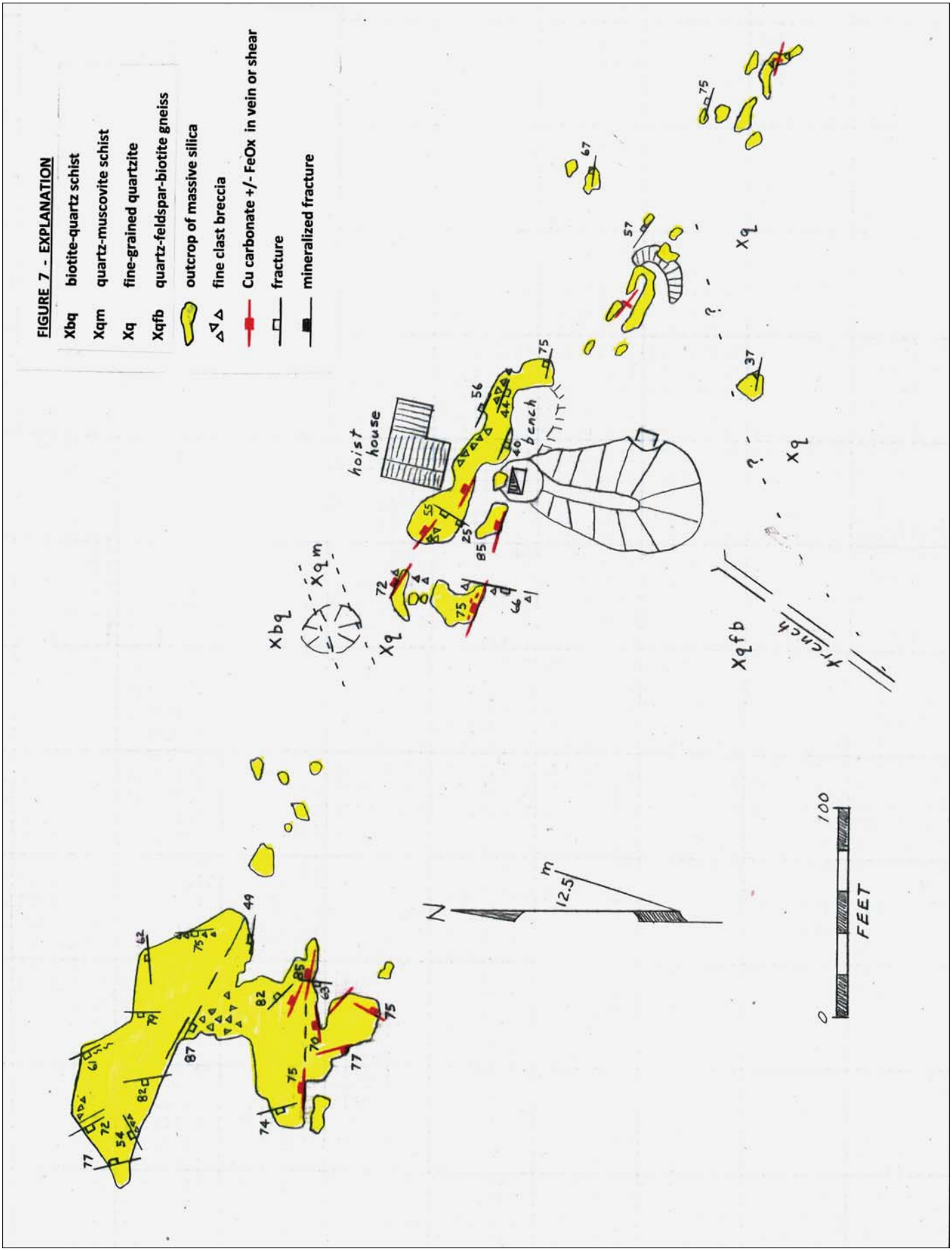

Figure 7. Geologic map of the Monument Mine area, Beaverhead County, Montana. Mapping by Cox and Sherwin, 2012; Cox, 2015–2017.

High-angle quartz veins and silica flooding have replaced metamorphic rocks (mostly quartzites) parallel to the Monument fault. Cross-fractures and brecciated zones typically strike northerly and dip steeply west. The veins host silver–copper-dominant polymetallic mineralization (fig. 8), which was exploited sporadically during the early 1900s (Geach, 1972). Although the mineralizing event(s) has not been dated, the ore mineral assemblage and banded microcrystalline silica of the gangue are typical of Challis-age deposits in nearby districts.

One of the best examples of early 20th Century hoist equipment is still intact in the shaft hoist house. Much if not all of this equipment was transported from St. Louis, Missouri up the Missouri River to Fort Benton and then probably freighted by wagon to Horse Prairie.

Retrace traverse to the base of Everson Creek Road 1882 and reset odometer to 0.0.

0.0 Base of Everson Creek Road 1882 (44.979283°N / 113.261608°W). Follow dirt road SW.

0.1 Y intersection, keep right.

2.0 Entering public lands.

4.17 Fork; follow main track southward.

5.90 Cross ridgeline. Near-horizontal tuff beds are exposed below the road and in bold outcrops along hillside to SE.

6.44 T intersection (44.922211°N / 113.344997°W). Turn left downhill to SE following sign toward "Black Canyon."

7.5 Northernmost (?) evidence of siliceous float in soil and roadcuts (fig. 9).

7.7 Cross North Fork Everson Creek.

8.5 Cross South Fork Everson Creek. Follow road another 100 yd SE across the meadow, through a cattle guard and onto a gentle north-facing slope; park where road levels.

Figure 8. Liz Brenner-Younggren at siliceous breccia outcrop on Monument Mine vein trend, view W–NW. Note pervasive malachite coatings on fractures.

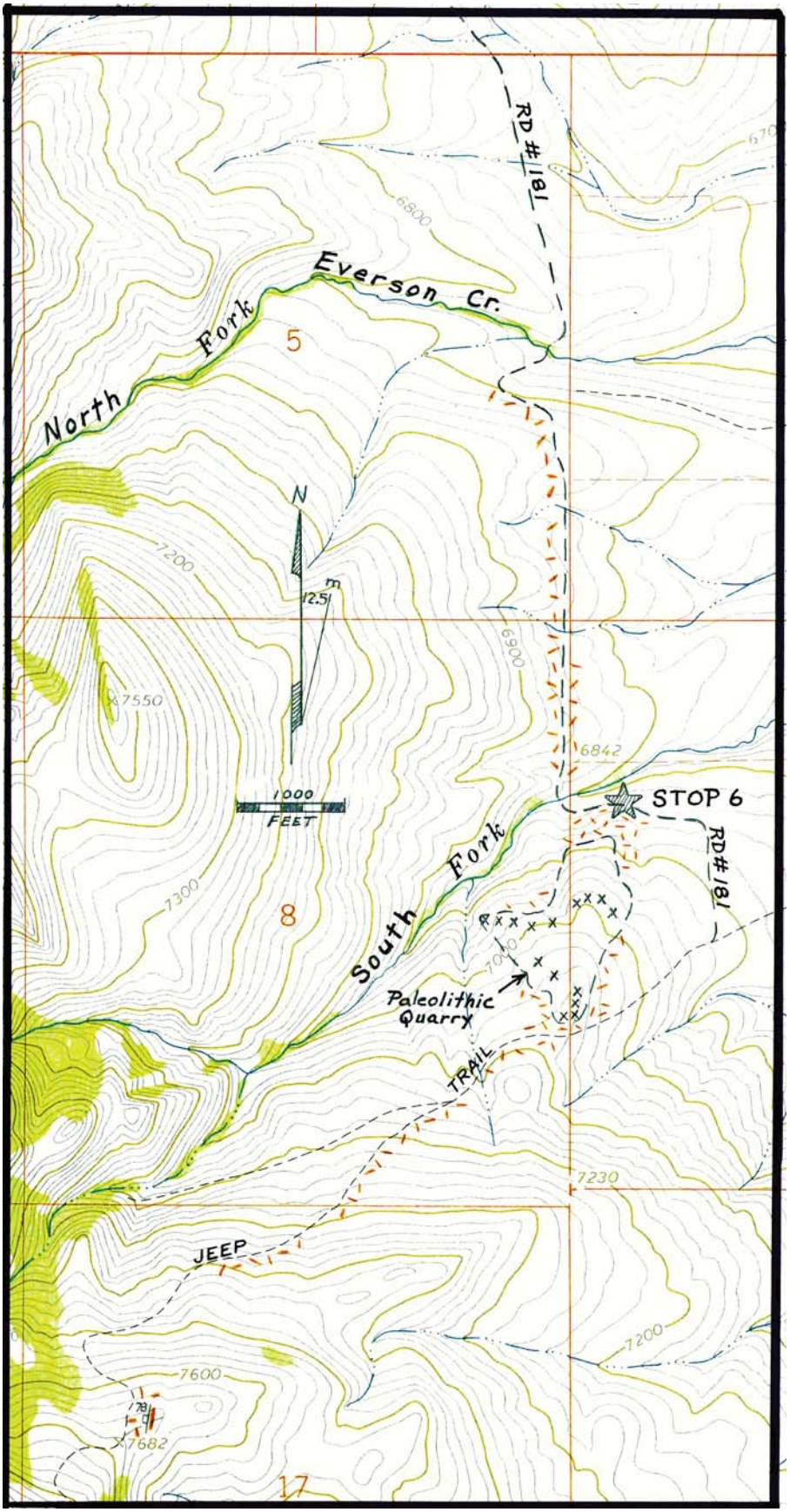

Figure 9. Map showing location of Stop 6 and trend of silicified volcanics (orange lines). Pits associated with the quarry are shown with x's.

8.7 STOP 6

Paleolithic quarry (44.892917°N / 113.32495°W).

This reach of Everson Creek and the surrounding hillsides were rigorously examined by the University of Maine in the late 1980s (Bonnichsen, 1989). Their research documents native mining activity as far back as 11,000 years. The quarry consists of numerous shallow pits (fig. 10) excavated into silicified Tertiary sediments within a 30+ acre area astride the north-plunging ridge. Silicified sediments can be traced for nearly 2 mil along the western margin of the Horse Prairie basin. Some exposures and float contain fossil gastropods, presumably originally living in the mud of fresh water lakes; float of petrified wood is also common. One outcrop located 1 mi southwest from the quarry site shows bedded silica with high-angle, steeply west-dipping fractures.

Much of the silicified volcanics is brightly colored, intricately patterned, and has come to the attention of local gemstone enthusiasts. We encourage visitors to not remove any silicified material or siliceous fragments that might be of archaeological significance.

Return to base of Everson Creek Road.

End of field trip.

Figure 10. Pits and waste rock debris within paleolithic quarry.

REFERENCES CITED

Bonnichsen, Robson, 1989, Archeological and geological investigations in the vicinity of the South Fork of Everson Creek and Black Canyon Creek, southwestern Montana: unpublished 1987–1988 Interim Report for the University of Maine.

Cox, B.E., and Antonioli, Ted, 2017, Ore controls of the Leadville (Junction) and Gilmore mining districts, Lemhi County, Idaho, a field trip guide: Northwest Geology, v. 46, p. 89–96.

Elliott, C., and Lonn, J.D., 2017, Walking tour of the Monument fault near the confluence of Bloody Dick Creek and Horse Prairie Creek, southwestern Montana: Northwest Geology, v. 46, p. 109–114.

Geach, R.D., 1972, Mines and mineral deposits (except fuels) Beaverhead County, Montana: Montana Bureau of Mines and Geology Bulletin 85, 194 p.

Lonn, J.D., Skipp, B., Ruppel, E.T., Janecke, S.U., Perry Jr., W.J., Sears, J.W., Bartholomew, M.J., Stickney, M.C., Fritz, W.J., Hurlow, H.A., and Thomas, R.C., 2000, Geologic map of the Lima 30’ x 60’ quadrangle, southwest Montana: Montana Bureau of Mines and Geology Open-File Report 408, 42 p., 2 sheets, scale 1:100,000.

Mitchell, V.E., 2004, History of the Leadville, Kimmel, and Baby Joe mines, Lemhi County, Idaho: Idaho Geological Survey Staff Report 04-1, 35 p.

Ruppel, E.T., 1998, Geologic map of the eastern part of the Leadore 30’ x 60’ quadrangle, Montana and Idaho: Montana Bureau of Mines and Geology Open-File Report 372, 9 p., 1 sheet, scale 1:100,000.

Ruppel, E.T., O’Neill, J.M., and Lopez, D.A., 1993, Geologic map of the Dillon 1° x 2° quadrangle, Montana and Idaho: U. S. Geological Survey Miscellaneous Geologic Investigations Series I-1803-H, scale 1:250.000.

TENSION FAULTS OF THE CENTENNIAL SHEAR ZONE

Stuart D. Parker

Missoula, Montana 59812, stuart.parker@umconnect.umt.edu

INTRODUCTION

This article is intended as an informal field guide to accompany an informal field trip following the 2017 TRGS field conference. Accessing this locality requires many miles of driving on rough dirt roads and hiking up steep, unconsolidated slopes. For this reason, I have chosen to include this information as an informal field trip. I encourage any and all adventurous field geologists to investigate this location. Accessing these features from the bottom is advised, as there is a considerable risk of falling on the firm, fault-gouged surfaces that define descents from the top.

The primary goal of this guide is to introduce the impressive shear features of the Centennial shear zone. Discussion of the phenomena will be brief. If interested, join me for an informal field trip following the 2017 field conference. For further reading, consult the thesis of Parker (2016), the original geodetic study of Payne and others (2013) and the upcoming article of Parker (in review, 2017).

ABSTRACT

This field guide documents large transtensional faults within the Centennial shear zone along the northern margin of the eastern Snake River Plain. These excellent exposures are located just below the Continental Divide in the southern Beaverhead Mountains, and reveal several meters of pure tension and sinistral offset in a deformed quartzite conglomerate. Cleavage sets occur ~45 degrees counterclockwise to the fault trace, approximately coincident with NE-oriented dextral shear of the Centennial shear zone. Erosion exploits fault-gouged and calcite-cemented zones, forming deeply incised runnels. Linear springs highlight cemented high-angle transtensional fault planes with a variety of orientations. Orientation and slip senses match predicted Riedel shear arrays for a NE-striking right-lateral system. These deformation features document a major transtensional system that borders the eastern Snake River Plain and culminates near the active Yellowstone caldera. Strain is distributed over a broad area, resulting in subtle surface expressions. Brittle deformation resulting from this dextral shear is ongoing and easily apparent in the landscape. Roughly north/south-oriented tension may play an integral role in both explosive caldera and basaltic eruptions within the Yellowstone/Snake River Plain system. The existence of such a shear zone along the boundary of the eastern Snake River Plain challenges previous interpretations regarding the evolution of the eastern Snake River Plain and the driving forces behind the extensive volcanism occurring along the Yellowstone track.

THE CENTENNIAL SHEAR ZONE

Geodetically derived strain rates of the greater Yellowstone/eastern Snake River Plain (ESRP) area highlight NE-oriented dextral motion along the northern boundary of the ESRP at rates of 0.3–1.5 $mmyr^{-1}$ (Payne and others, 2013). Evidence of faults associated with the Centennial shear zone (CSZ) has only recently been documented and is largely limited to a weakly cemented gravel deposit in the southern Beaverhead Mountains (Parker, 2016). The orientations of pressure-solution pits on cobbles provide data to document the paleo-strain field; horizontal, initially E–W resolving to NE–SW, maximum principal stress orientations (Parker, 2016). Dextral shear is distributed across meter-scale high-angle transtensional faults and accommodated as oblique slip on pre-existing fault planes. Both mechanisms of strain accommodation prevent development of major well-defined strike–slip faults (Curren and Bird, 2014). This shear likely accommodates differential modes of Basin and Range extension: brittle deformation and normal faulting to the north and ductile deformation and possibly dike injection within the ESRP (Payne and others, 2013; Parker, 2016; Parsons and others, 1998). Therefore, the CSZ likely immediately postdates formation of the ESRP, which occurred locally in the Pliocene, and is still active today (Rodgers and others, 2002).

TENSION FAULTS OF MIDDLE CREEK

The subject tension faults are exposed in the headwaters of the Middle Creek drainage, just below the Continental Divide. Steep hillsides expose the deformation features in areas of rapid erosion. Aerial photos clearly highlight the E- to ENE-striking features. Linear springs can be seen extending east of the outcrop, tracing a continuation of the faults. These faults display several meters of NNW-oriented tension. Slickensides and deformed and re-cemented cobbles along the fault plane margins record the oblique left-lateral shear sense. ENE orientation and oblique left-lateral tension are predicted for T (P') shear planes for a dextral system oriented NE to NNE (Riedel, 1929). A deeply eroded runnel, striking ESE, has formed in an area of fault gouge. This feature likely corresponds to the R' shear plane. SE-striking linear springs may correspond to X shear planes. Cleavage sets in cobbles bounding the tension fault strike roughly NE, coincident with the orientation of the CSZ. These features likely formed at shallow depths and low pressures in Pliocene or younger time. Faceted spurs and offset topography are common in this drainage, suggesting these features may be active.

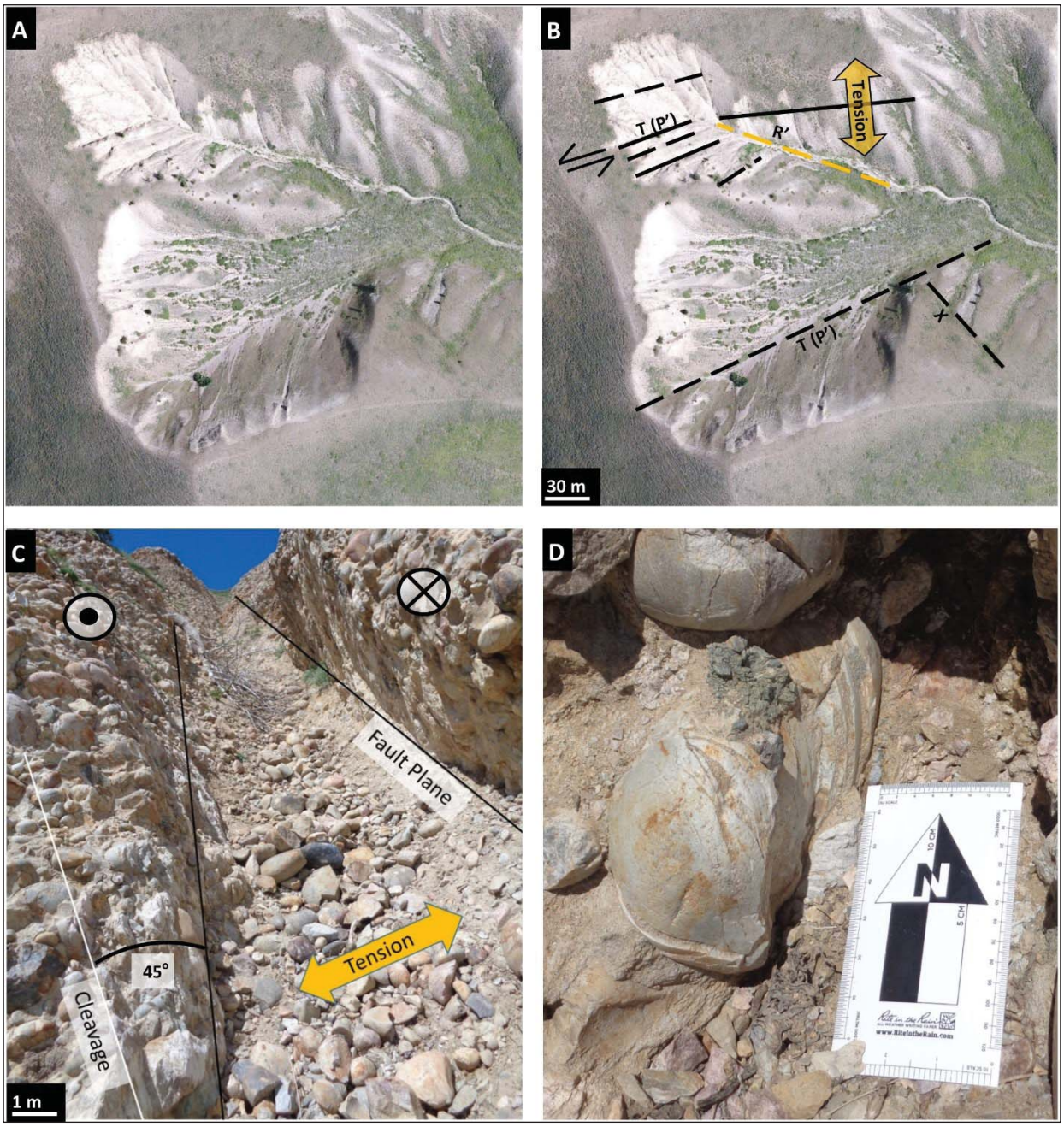

Figure 1. Large-scale shear features in the western area. [A] Aerial photo of fault zone with [B] interpreted shear planes and motions. Solid lines represent exposed faults, dashed represent faults inferred from springs or brecciated zones. Yellow line denotes deep erosion. [C] Kinematics inside a map tension fault showing cleavage 45° counter-clockwise of the fault trace and left-lateral tension. [D] Deformed cobbles along the fault plane show left-lateral strain.

FIELD GUIDE

STOP 1

(44.460950°N, 112.496457°W)

This site is most easily accessed from Dubois, Idaho along I-15. From Dubois, head west along highway ID-22. Take a right on Medicine Lodge Creek Road. Continue straight on Indian Creek Road before quickly turning left on Middle Creek Road. This road becomes FS 204. Continue up the drainage, before taking the last left on FS 1825 near the headwaters of the drainage. The steep and rough "road" will end at a small aspen grove. Hike directly up the drainage from here, heading towards the two prominent eroded headwalls. The described tension faults (figs. 1 and 2) occur in the left zone (44.460950°N, 112.496457°W). Examples of comparable deformation are widespread throughout this area. Accessing the ridgeline provides a good aerial view of linear facets and the linear springs that become prominent in the arid months.

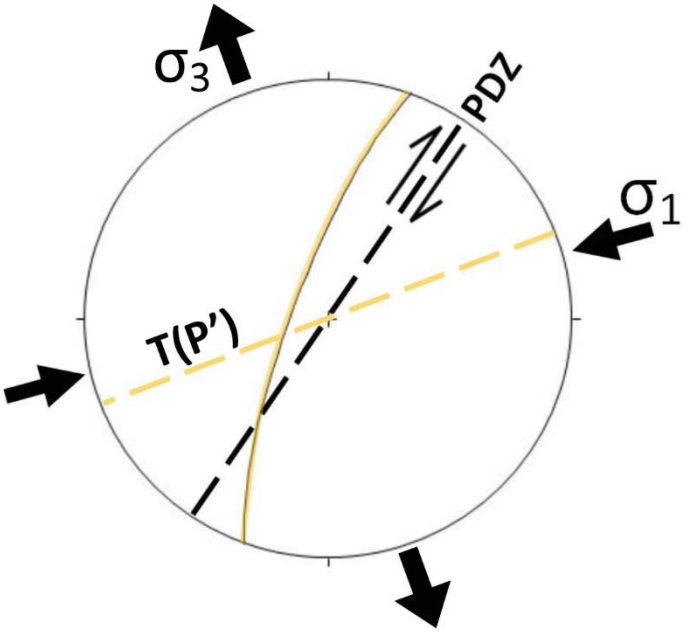

Figure 2. Kinematic interpretation of the study area shown on a lower hemisphere projection. Average strike of tension faults interpreted as T (P') shear planes is shown as yellow dashed line. Average fracture/fault orientation highlighted. Inferred primary deformation zone (PDZ) orientation and shear sense is represented as black dashed line.

REFERENCES CITED

Curren, I.S., and Bird, P., 2014, Formation and suppression of strike–slip fault systems: Pure and Applied Geophysics, v. 171, no. 11, p. 2899–2918.

Parker, S.D., 2016, Tectonic alteration of a major Neogene river drainage of the Basin and Range: Missoula, University of Montana, M.S. thesis, 114 p.

Parker, S.D., in review, More than one way to shear: Rethinking the kinematics of the eastern Snake River Plain and Yellowstone: Lithosphere.

Parsons, T., Thompson, G.A., and Smith, R.P., 1998, More than one way to stretch: A tectonic model for extension along the plume track of the Yellowstone hotspot and adjacent Basin and Range Province: Tectonics, v. 17, no. 2, p. 221–234.

Payne, S.J., McCaffrey, R., and Kattenhorn, S.A., 2013, Extension-driven right-lateral shear in the Centennial shear zone adjacent to the eastern Snake River Plain, Idaho, Lithosphere, v. 5, no. 4, p. 407–419.

Riedel, W., 1929, Zurmechanikgeologischerbruchersscheinungen: Zentralblattfür Mineralogie, Geologie Und Paläontologie B, 1929, p. 354–368.

Rodgers, D.W., Ore, H.T., Bobo, R.T., McQuarrie, N., and Zentner, N., 2002, Extension and subsidence of the eastern Snake River Plain, Idaho: Tectonic and Magmatic Evolution of the Snake River Plain Volcanic Province: Idaho Geological Survey Bulletin, v. 30, p. 121–155.

A train from the Gilmore & Pittsburgh Railroad pauses at the railway's depot in Leadore, Idaho, August 1912. J. Foster Adams, photographer.

A Gilmore & Pittsburgh train ascending the western approach to Bannock Pass, August 1912. J. Foster Adams, photographer.